Autophagy: From Membrane Movement to Nuclear Regulation

by

Melinda Anne Lynch Day

A dissertation submitted in partial fulfillment
of the requirements for the degree of
Doctor of Philosophy
(Molecular, Cellular and Developmental Biology)
in The University of Michigan
2012

Doctoral Committee:

Professor Daniel J. Klionsky, Chair
Professor Laura J. Olsen
Professor Lois S. Weisman
Associate Professor Anuj Kumar

In Memory of Geoff

Whose death drove my desire to study biology, but whose life inspires me to live with conviction and passion.

Acknowledgements

I would first like to thank my wonderful husband, Dave, who has been patiently waiting for me to finish my doctoral studies. His love and encouragement have helped carry me through the last five years. I would also like to thank my parents, whose help has been invaluable. Thank you for teaching me the value of hard work. Appreciation is also due to others of my family including my in-laws and my aunt and uncle, all of whom have provided encouragement through it all.

A special thank you is owed to my advisor, Dan Klionsky. He has been a wonderful mentor and has taught me the critical thinking skills needed to become an independent scientist. He challenged me and encouraged me, and I couldn't have asked for a better mentor. I would also like to thank my committee members, Lois Weisman, Laura Olsen, and Anuj Kumar. Thank you all for your patience and your invaluable advice. I am grateful for all of your support in working with me to finish my dissertation and helping me to find a post-doctoral position.

Lastly, I would like to thank the members of the Klionsky laboratory. It has been a pleasure working and learning with all of you over the last several years. I would especially like to thank Clinton Bartholomew who was always there to offer help and advice when I needed it most, Steven Backues who aided me in my post doctoral search, and Katie Parzych, who was my writing buddy as I put this dissertation together and who didn't think it strange when I would be "gaily tripping" throughout the lab.

Chapter 2 is a review article that I authored on the cytoplasm to vacuole targeting pathway: Melinda A. Lynch-Day and Daniel J. Klionsky. The Cvt pathway as a model for selective autophagy. *FEBS Letters*, 584: 1359-1366, 2010. It has been reprinted here with permission from Elsevier with minor modifications.

Chapter 3 is a primary research article that I co-first authored on the role of Trs85 and Ypt1 in autophagy: Melinda A. Lynch-Day, Deepali Bhandari, Shekar Menon, Ju Huang, Huaqing Cai, Clinton R. Bartholomew, John H. Brumell, Susan Ferro-Novick, and Daniel J. Klionsky. Trs85 directs a Ypt1 GEF, TRAPPIII, to the phagophore to promote autophagy. *Proc Natl Acad Sci USA*, 107: 7811-7816, 2010. It has been reprinted here with permission. I was responsible for figures 3.3, 3.4, 3.5, 3.6, S3.5, S3.6, S3.7, and S3.8B and Table S3.1.

Chapter 4 is a manuscript that has been submitted to *Science.* I was responsible for all of the yeast work in the paper.

Chapter 5 is a first author manuscript that has been submitted to *Science*. I was responsible for all of the figures.

Appendix A is a review article that I first authored on the role of autophagy in Parkinson's Disease: Melinda A. Lynch-Day, Kai Mao, Ke Wang, Mantong Zhao, and Daniel J. Klionsky. The role of autophagy in Parkinson's disease. *Cold Spring Harb Perspect Med,* 2: a009357, 2012. It has been reprinted here with permission from Cold Spring Harbor with minor modifications. I was responsible for the writing of the section "Early discoveries: α-SYNUCLEIN and autophagy", the organization of the section "Recent studies: controversies abound", and general editing.

Appendix B is a research study on mitophagy: Tomotake Kanki, Ke Wang, Misuzu Baba, Clinton R. Bartholomew, Melinda A. Lynch-Day, Zhou Du, Kai Mao, Zhifen Yang, Wei-Lien Yen, and Daniel J. Klionsky. A genomic screen for yeast mutants defective in selective mitochondria autophagy. *Mol Biol Cell*, 20:4730-4738, 2009. It has been reprinted here with permission from The American Society for Cell Biology. I was responsible for the screening of mitophagy defective mutants for defects in the Cvt pathway (Ape1 maturation) and non-specific autophagy (GFP-Atg8 cleavage), figures SB.2B and SB.4.

Appendix C is a research study on the transcriptional inhibition of *ATG8:* Clinton R. Bartholomew, Tsukasa Suzuki, Zhou Du, Steven K. Backues, Meiyan Jin, Melinda A. Lynch-Day, Midori Umekawa, Avani Kamath, Mantong Zhao, Zhiping Xie, Ken Inoki, and Daniel J. Klionsky. Ume6 transcription factor is part of a signaling cascade that regulates autophagy. *Proc Natl Acad Sci USA*, 2012. It has been reprinted here with permission. I was responsible for figure C.2.

Table of Contents

List of Tables

Table

List of Figures

Figure

List of Appendices

CHAPTER 1

The Study of Autophagy is Important for Understanding Human Disease

Introduction

Over the last century life expectancy in western societies has increased dramatically. The US Census Bureau projects that the number of citizens over the age of 65 will double over the next 40 years, and the number of people over the age of 100 will increase eight fold [1]. With such a large elderly population comes a host of age-related diseases such as cancer, type 2 diabetes, cardiovascular disorders, and neurological degeneration. Most of these diseases result from the accumulation of misfolded, damaged, or aggregated proteins and from damaged organelles, as the ability of cells to maintain homeostasis is compromised with age [2,3].

Eukaryotic cells have two main degradative pathways that work together to maintain cellular homeostasis. The first is the ubiquitin-proteasome system, or UPS. The UPS is used to degrade proteins that are damaged or no longer needed; however, this mechanism is used primarily for short-lived proteins. The proteins to be degraded are recognized by the proteasome complex via a covalently attached polyubiquitin chain. The tagged protein is unfolded and then degraded by proteases [4].

The second system used for protein degradation is macroautophagy. Macroautophagy is a ubiquitious, evolutionarily conserved, lysosomal/vacuolar

degradation pathway [5]. Unlike the UPS, macroautophagy has an almost unlimited degradative capacity allowing it to be able to break down a variety of targets such as large protein aggregates, entire organelles, lipids, DNA and RNA[3,6]. As a result, macroautophagy is not just a catabolic process but also a regenerative process; it is able to provide new pools of fatty acids, amino acids, and nucleosides that can be used in a variety of anabolic processes in the cell. In addition to its role in maintaining cellular homeostasis, macroautophagy also acts as an adaptive response to a variety of external and internal stressors such as nutrient deprivation, oxidative stress, hypoxia, and accumulation of damaged or excess organelles [5]. Studies over the last few years have increased our understanding of the molecular mechanisms that underline this pathway and have established a connection between macroautophagy and various disorders. Currently, macroautophagy has been implicated in various aspects of development, tumor suppression, and immune defense, whereas macroautophagic dysfunction is associated with aging, neurodegeneration, cardiomyopathies, diabetes, and other disorders in a variety of tissues [3,7]. Therefore, the study of macroautophagy may shed new light on the processes behind aging-related and other diseases, and potentially lead to improved therapeutic treatments for those diseases.

Autophagy and Disease

There are three main types of autophagy: chaperone-mediated autophagy, microautophagy, and macroautophagy [5]. Chaperone-mediated autophagy uses a chaperone complex that recognizes a specific signaling motif in a target protein to unfold that protein and transport it to the lysosome. Once at the lysosome the protein is transported across the membrane via interaction with the lysosomal membrane protein LAMP2A [8]. This process has only been identified in mammalian cells. Microautophagy involves the direct invagination of the lysosomal/vacuolar membrane, which takes up a small amount of the cytoplasm [9]. As with chaperone-mediated autophagy, uptake occurs directly at the lysosome (or vacuole) limiting membrane, but in this case the substrates are not limited to unfolded proteins. Macroautophagy, hereafter referred to as autophagy, uses a double membrane vesicle called the autophagosome to sequester cytoplasmic proteins and organelles. The autophagosome then travels to the lysosome/vacuole. The outer membrane of the autophagosome fuses with the lysosomal membrane to form an autolysosome (in mammals), or fuses with the vacuole (in plants and yeast) releasing the inner membrane or autophagic body into the lumen. In either case, the autophagosome inner membrane and its contents are degraded [5,8-10]. Autophagy is generally thought of as a bulk, nonselective degradation mechanism, but there are specific forms of autophagy that use receptor and scaffold proteins to target specific cargo. Selective types of autophagy (and their cargo) include the cytoplasm to vacuole targeting pathway (precursor aminopeptidase I, prApe1) [11], mitophagy (mitochondria) [12], pexophagy (peroxisomes) [13], and reticulophagy (endoplasmic reticulum) [5,14] (For more information on selective types of autophagy please refer to

Chapter 2). Defects in most of these types of autophagy can result in disease. In this chapter I will review how defective autophagy contributes to human pathologies.

Autophagy in development and aging

Considering that development and differentiation processes require enhanced degradation and energy consumption in order to achieve extreme cellular and tissue remoldeling, it is no surprise that autophagy is required. Autophagy is uniquely able to degrade large portions of the cytosplasm while providing new nutrient and energy pools to the cell. This dual role of autophagy has made it the evolutionarily favored process to accomplish developmental remodeling in a variety of organisms from fungi to humans.

In yeast, autophagy is required for sporulation. In the autophagy-deficient mutants such as *atg1Δ*, incomplete sporulation is observed. The defect can be partially restored through supplementation of amino acids. The defect in sporulation occurs at different steps in the process, including at the formation of the forespore membrane, chromosome segregation, and nuclear division, suggesting that it is not due to repression of the transcription of sporulation-specific genes [15]. Previous studies have shown by whole-genome microarray analysis that there is an extensive change in gene expression during sporulation, indicating that sporulation requires a large amount of de novo protein synthesis [16-18]. Thus, autophagy may be required to increase the amino acid pool in sporulating cells.

Similarily, in *Dictyostelium,* autophagy is required for fruiting body formation, which is induced by starvation. When autophagy is blocked by mutations in *atg5* or *atg7*, the mutants show normal growth but reduced survival upon nitrogen starvation. In

addition, fruiting body formation is accompanied by a reduction in the number of organelles and vast cytoplasmic degradation, which is not observed in the autophagy mutant cells. Ultimately, autophagy-deficient amoebas fail to produce normal fruiting bodies, suggesting that autophagy is required to provide amino acids for this developmental process and for survivability [19].

Autophagy plays a role in different larval stages in *C. elegans* and *Drosophilia*. In *C. elegans* autophagy is required for dauer formation. Under unfavorable conditions for reproduction, nematode worms can reversibly arrest into an alternative third larvae stage known as the dauer diapause, which allows them to survive inhospitable environments [20]. When autophagy is blocked by inhibiting BEC-1 (ortholog of yeast Vps30 or human BECN1; a subunit of the class III phosphatidylinositol 3-kinase complex) function the mutants show abnormal granules, some binucleated cells, arrested development and abnormal dauer formation [21]. Blocks in dauer formation are also seen in other autophagy deficient mutants including knockdowns of the *C. elegans* homologs of *ATG1, ATG18, ATG7,* and *ATG8.* Autophagy also plays a role in the elimination of paternal mitochondria. Upon fertilization, *C. elegan* spermatozoon trigger autophagy induction of the sperm mitochondria. The mitochondria are degraded by autophagy in the early embryo and this degradation is dependent upon LC3 (homolog of yeast Atg8) and other autophagy proteins. Defective autophagy in the zygote results in the retention of paternal mitochondria through the larval stage [22]. A similar autophagic event has been observed in mouse embryos, suggesting that this might be an evolutionarily conserved method for the selective inheritance of only maternal mitochondrial DNA.

In *Drosphilia* autophagy is required during the transition from the larval to the pupal stage during which several organs are degraded including the salivary glands and the larval midgut. Autophagy is induced just prior to the developmental degradation of salivary glands. Autophagy inhibition blocks degradation, whereas forced autophagy induction promotes premature removal of the glands [23]. Studies on the role of autophagy in the degradation of the larval midgut have been contradictory. Some studies indicate that autophagic cell death is responsible, whereas other studies have shown normal midgut transition in an *Atg7* mutant [24,25]. In addition, autophagy has been shown to regulate neuromuscular junction formation and synaptic development in the fly larvae [26].

In mammals, autophagy plays a role in cell differentiation, embryogenesis, and the neonatal starvation period. Upon fertilization, autophagy is induced, which is important for the removal of maternal macromolecules at the start of embryogenesis [27]. When sperm lacking *Atg5* fertilize autophagy-defective oocytes made by oocyte-specific deletion of *Atg5*, the mouse embryo shows accumulation of LC3 within the nucleus and fails to progress beyond the 8-cell stage. This defect in embryogenesis is rescued when the *Atg5*-deficient oocytes are fertilized with normal sperm [27]. Other autophagy mutants that show early embryonic cell death include *Becn1*, *Rb1cc1/Fip200*, and *Ambra1* [28-30].

After embryogenesis and birth, mouse pups must survive the neonatal starvation period. Immediately after birth the trans-placental nutrient supply is suddenly cut off, causing the new born pups to undergo a period of starvation prior to the start of nursing. Autophagy is induced in the neonates in order to survive this nutritional stress [31]. All

models of autophagy-deficient mice that survive embryogenesis (except *ULK1* and *Atg4C* deletion) fail to survive the neonatal starvation period and die within one day after birth [31-38]. These mice show fatigue and reduced concentrations of amino acids. This result indicates that not only is the degradative properties of autophagy needed to remove specific macromolecules and organelles during development, but that its recycling function is also needed in order for the organism to obtain the nutrients necessary for new protein synthesis and to maintain energy homeostasis.

Autophagy is also important in the regulation of cellular differentiation within an organism. For example, autophagy is required for the clearance of mitochondria during adipocyte, lymphocyte, and erythrocyte differentiation [39-41]. In normal white adipocytes there is a single lipid droplet and few mitochondria, whereas in a mouse model with adipocyte-specific *Atg7* deletion, the morphology is altered with numerous lipid droplets and an increase in the number of mitochondria. The mutant mouse also has increased resistance to obesity but increased sensitivity to insulin [42]. Erthrocytes with autophagy deficiencies due to either *Bnip3l/Nix* or *Atg7* deletion show retention of mitochondria, which leads to erythrocyte cell death. These mice suffer from anemia due to reduced red blood cell counts [39,43]. A similar reduction in cell counts is seen with T-lymphocytes with ATG7 and ULK1 deficiencies [40]. Finally, inhibition of autophagy results in improper differentiation of neuroblastoma cells and glioma stem cells [44,45].

The ability of autophagy to allow cells to adapt to changing environments and to clear out damaging toxins supports cell survival. As such it is no surprise that autophagy plays a role in longevity. Enhancement of autophagy promotes cellular fitness and survival, whereas inhibition of autophagy reverses those effects [46]. Autophagy can be

promoted by several different means including caloric restriction and pharmacological agents. Some of the latter, such as rapamycin, promote autophagy through the inhibition of MTOR, which is a negative regulator of the pathway [47,48]. Others, such as caloric restriction and resveratrol, work to induce autophagy through SIRT1/sirtuin 1 [49]. SIRT1 is an NAD^+-dependent acetylase that is thought to promote autophagy through the deactylation of core autophagy proteins including ATG5 and ATG7. Aging cells show a decrease in the formation and elimination of autophagosomes which can result in a variety of age-related diseases through the accumulation of toxic protein aggregates and damaged organelles. This suggests that promotion of autophagy as an anti-aging regime may increase general life span and quality of life.

Autophagy and immunity

Autophagy is important in both innate and adaptive immunity. In innate immunity there is a selective form of autophagy called xenophagy that helps remove a variety of invading pathogens. Xenophagy has been shown in epithelial cells to be induced upon Group A *Streptococcus* infection, and inhibition of ATG5 allows for improved bacterial survival [50]. Xenophagy is also responsible for the degradation of other bacteria including S. *pyogenes*, *Shigella flexneri*, and *Myobacterium* t*uberculosis*, for the degradation of viruses including the herpes simplex virus, vesicular stomatitis virus, and human immunodeficiency virus 1, and for the degradation of the parasite *Toxoplasma gondii* [50-59]. Xenophagy occurs in both plants and mammals and helps promote host cell survival. In plants with ATG6 deficiencies there is an increase in cell death even in uninfected tissues that surround the site of infection [60]. In mice, when

BECN1 is overexpressed in neurons, there is an observed inhibition in Sindbis virus replication and central nervous system apoptosis [61].

Xenophagy works by using receptor proteins to recognize ubiquitin coated pathogens. Pathogens that have entered the cell and have evaded phagocytosis become ubiquitinated. They are then recognized by receptor proteins such as SQSTM1/p62 and CALCOCO2/NDP52, which recruit the autophagy machinery to the pathogen [62,63]. This pathway is very similar to the one used to recognize misfolded and aggregated proteins.

Autophagy is induced by a variety of immune signals. For example, SQSTM1 is a downstream target of innate defense regulator-1 (IDR-1). IDR-1 is a peptide that acts through different signaling pathways including the mitogen-activated protein kinase. It is productive against both Gram-positive and Gram-negative pathogens and works by enhancing the levels of monocyte chemokines and reduces pro-inflammatory cytokines [64]. Pro-inflammatory Th1 cytokines such as IFNG promote autophagy, whereas the anti-inflammatory Th2 cytokines such as IL4 inhibit autophagy [65]. In contrast, autophagy can regulate cytokine production. In the absence of autophagy there is an observable increase in the production of potent anti-viral factors due to RIG-I receptor activation [66]. When *Atg9* is knocked down using dsRNA in mouse embryonic fibroblasts there is an observed enhancement of IFNB1 production [36]. Finally, there is an increase in IL1B and IL18 production in macrophages deficient for autophagy [37,67]. Autophagy also regulates the inflammatory response through the reduction of reactive oxygen species (ROS) via degradation of impaired mitochondria. When autophagy is inhibited by either *Becn1* or *Atg5* knock down, ROS accumulation occurs and the cells

become sensitive to NLRP3 activation of the inflammasome [68]. Overall, autophagy is induced by pro-inflammatory signals and inhibits their production. Thus, autophagy works to inhibit the inflammasome and prevents necrosis.

Autophagy also serves as a backup mechanism for phagocytosis [69]. Some pathogens are able to disrupt phagocytosis and prevent fusion with the lysosome. These pathogens then use the phagosome as a replicative niche. For example, *M. tuberculosis* inhibits phagosome fusion with the lysosome. Autophagy overcomes this block by aiding in maturation of the phagosome. Autophagy recruits LC3 and then BECN1 to the phagosome membrane, which helps to promote fusion with the lysosome [54]. This maturation signal through LC3 association is prompted by the engagement of Toll-like receptors (TLRs) [70].

The evolution of innate immunity is often referred to as an arms race between the invading pathogen and the host. Autophagy has become one factor in this arms race, and pathogens have developed virulence factors that can inhibit autophagy. The herpes simplex virus is one such pathogen and it secretes ICP34.5, which inhibits autophagy by binding to the host BECN1 [56]. HIV expresses the protein Nef, which also interacts with BECN1 to inhibit autophagosome fusion with the lysosome [71]. Gamma herpes virus and human cytomegalovirus possess BCL2-like proteins that can inhibit BECN1 and activate MTOR signaling to inhibit autophagy induction [72-74]. Some pathogens go even further and use different compartments of the autophagy pathway as replicative niches. *Porphyromonas gingivalis* and *Coxiella burnettii* both use the autophagosome to replicate, and their survival is decreased when autophagosome formation is inhibited with 3-methyladenine (3-MA) [75,76]. *Staphylococcus aureus* hijacks the autophagy

machinery for its own use. It secretes the pore-forming toxin alpha hemolysin (Hlα). Hlα creates a perforated vacuole from an autophagosome, activates autophagy and recruits LC3 to the damaged vacuole. These vacuoles fail to mature and remain non-acidic, serving as a site for bacterial replication [77].

In adaptive immunity, autophagy helps in the presentation of antigens. Adaptive immunity requires the recognition of "non-self" antigens. Invading pathogens are fragmented by the innate immune system and these fragments/antigens are then processed and presented to T-cells in combination with a "self" receptor termed the major histocompatibility complex (MHC) molecule. There are two classes of MHC molecules: class I are used by killer T-cells, and class II are used by helper T-cells [78]. Autophagy aids in both MHC class I and II antigen presentation [79-81]. Autophagy-compromised dendritic cells in mice show impaired $CD4^+$ T-cell priming upon HSV1 infection, suggesting that autophagy is responsible for facilitating the presentation of HSV1 antigens on MHC class I molecules [82,83]. Similar results are seen with the immunization of $CD8^+$ T-cells. Autophagy deficiency decreases the cross-priming efficiency of antigen-specific $CD8^+$ T cells [84].

When it comes to MHC class II antigen presentation, autophagy has a profound influence on the type of class II peptides. Autophagy promotes antigen presentation from intracellular and lysosomal source proteins as compared to membrane and secreted proteins [85]. In addition, autophagosomes have been identified to contain intracellular antigens, and inhibition of autophagy either through pharmacological or genetic means reduces the presence of intracellular antigens in several cell types including lymphoblastoid cells and dendritic cells [83,86]. The opposite has been observed in other

studies; overexpression of the autophagy component LAMP2A increases the presentation of MHC class II antigens [87].

In thymic epithelium cells, the regulation of MHC class II antigens by autophagy is important for the generation of self-tolerant T-cells. These cells are constitutively active for autophagy, and inhibition of autophagy in these cells alters the selection of certain restricted MHC class II T-cell specificities. In the mouse model ATG5 deficiency in the thymus results in severe colitis and multi-organ inflammation due to the increase in self reactive T-cells and autoimmunity [88].

Finally, autophagy aids in the production of type 1 interferons (IFNs) in plasmacytoid dendritic cells (pDCs) [89]. The pDCs use TLRs to detect viruses without direct infection [90]. Viral particles are recognized by TLRs in the endosome which triggers the expression of type 1 IFNs. Autophagy delivers cytosolic viral replication intermediates to the endosomal TLRs, initiating interferon production [89].

One of the better-characterized human diseases associated with the failure of autophagy in the immune response is the inflammatory bowel disorder, Crohn disease. Several studies have identified a link between Crohn disease and a single nucleotide polymorphism (SNP) in *ATG16L1* (corresponding to a mutation of T300A) [91]. Interestingly, this is the only known case of a SNP in a core *ATG* gene that is associated with a human disease. This mutant is incapable of properly sequestering intracellular bacteria that initiate the inflammatory response leading to Crohn disease. In addition, mutations in the immunity related GTPase family M (IRGM) genes, which regulate autophagy during the immune response, and a frame shift mutation in NOD2 that disrupts

the ability of the protein to recruit ATG16L1 to the site of bacterial entry, have also been associated with Crohn disease [92,93]. Moreover, in vivo studies have shown that autophagy is important in maintaining the secretion of antimicrobial proteins by Paneth cells. In mouse models, autophagy deficiencies specific to the intestine results in abnormal granules within Paneth cells, suggesting that autophagy is important for normal vesicle-mediated secretion [94]. Crohn patients who are homozygous for the mutant *ATG16L1*(T300A) show similar abnormalities in their Paneth cells [95]. All this suggests that autophagy is important for the clearance of microbes in the intestine and that those individuals with mutations in key autophagy genes are more susceptible to developing Crohn disease than those with normal autophagic function.

Autophagy and neurodegeneration

The central nervous system is comprised of non-regenerative cells. For that reason maintaining homeostasis is extremely important. Neuronal cells have a constitutively active autophagy pathway that can be additionaly upregulated in response to stressors [96-98] and neuronal injuries including axotomy, excitatory toxicity, and neuronal ischemia [99-101]. Cell death will occur if autophagy fails to be upregulated in those situations. Under certain conditions, however, the upregulation of autophagy can be harmful, especially when inhibition of non-apoptotic cell death is important, and in situations where autophagosome clearance is blocked [102,103]. There are a variety of defects observed in mouse models lacking autophagy in the central nervous system. These mice show the hallmarks of neurodegeneration including the accumulation of protein aggregates and vast neuronal cell death including the loss of pyramidal neurons in the cerebral cortex and the loss of Purkinje cells in the cerebellar cortex [32,104]. The

physical phenotypes include lack of motor coordination, abnormal limb-clasping reflexes, and locomotor ataxia [32,104,105]. In Purkinje cells, specifically, there is observable degeneration of axonal terminals and axonal dystrophy that leads to cell death and behavioral defects when autophagy is diminished [106,107].

Neurodegerative diseases in humans tend to be characterized by the accumulation of protein aggregates and autophagic vacuoles, suggesting that defects in the autophagy pathway contribute to the progression of disease [108]. Since autophagy is responsible for the elimination of protein aggregates it comes as no surprise that there is observed accumulation of SQSTM1 and polyubiquitin proteins in neurons of autophagy-defective brains that increase in size and number with age [32,109]. In mouse models, upregulation of autophagy by pharmacological means is able to reduce the protein aggregates and decrease neurodegenerative symptoms [110]. This system does not always work perfectly. First, not all ubiqutinated protein aggregates are recognixed by the autophagy machinery. AIMP2/p38 inclusions in Parkinson disease (PD) and DES/desmin inclusions in myopathy both fail to be degraded by autophagy [111]. Second, when autophagosomes fail to be cleared via fusion with the lysosome or during periods of ischemia with excessive autophagy, they can become a site for the generation of ROS and thus further promote neurotoxicity [112].

When it comes to human neurodegenerative diseases, a defect in almost every step of autophagy has been characterized. A reduction in autophagy induction has been observed in Alzheimer disease (AD), enhanced autophagy repression is prevalent in Huntington disease (HD), and altered cargo recognition is a hallmark of both Parkinson disease and HD. Inefficient autophagosome elimination has been seen in HD and spinal

muscular atrophy. Finally, inefficient degradation of autophagic cargo in lysosomes is the main cause behind lysosomal storage disorders [113]. Below, I will detail the role autophagy plays in AD and HD. Information regarding the role of autophagy in PD can be found in Appendix A.

AD patients suffer from neuronal atrophy that is preceded by the formation of neurofibrillary tangles composed of MAPT/tau protein aggregates and the accumulation of APP/β-amyloid peptide. Autophagy is blocked at the site of autophagosome fusion with the lysosome, and the accumulated autophagosomes become a site of intracellular production of the APP peptide [114]. The defect in autophagy has been traced back to defective acidification of the lysosome. Mutations in the protein PSEN1/presenilin 1 have been characterized in AD. Wild-type PSEN1 is responsible for the transport from the ER to the lysosome of v-ATPase, the proton pump responsible for acidifying the lysosome. Mutations in PSEN1 block the transport, trapping the proton pump in the ER, leading to the impairment of lysosome/autolysosome acidification and accumulation of autophagosomes [115].

Autophagy failure also prevents the removal of MAPT aggregates. The MAPT protein becomes fragmented and these mutant forms of MAPT aggregate. Specific fragments are targeted by chaperone-mediated autophagy for transport across the lysosomal membrane. However, the F1 fragment fails to completely translocate into the lysosomal lumen, remaining in the membrane. This fragment forms oligomers on the surface of the lysosome and interferes with the organelle's function [116]. Thus, the failure of autophagy in the early stages of AD further induces cellular toxicity and increases autophagy inhibition.

HD is an autosomal dominant genetic disease caused by mutations in the *HTT* gene. Mutant forms of HTT prevent cargo recognition in the autophagy pathway. The mutant protein will bind to the inner surface of the forming autophagosome and will tightly associate with SQSTM1, preventing its ability to recognize cargo [117]. In animal models of HD, pharmacological activation of autophagy reduces the progression of the disease through the reduction of toxic aggregates [118]. Autophagy is able to target mutant HTT for degradation prior to aggregation. Acetylation of mutant HTT at lysine 444 facilitates its inclusion into autophagosomes. In *C. elegans*, this posttranscriptional modification is enough to reverse the toxic effect of mutant HTT in cortical and primary striatal neurons [119].

Other posttranscriptional modifications can also promote the clearance of mutant HTT by chaperone-mediated autophagy. Phosphorylation of the protein by the inflammatory kinase IKBK is able to regulate additional modifications including ubiquitination, acetylation, and SUMOylation. The posttranscriptional modifications promote nuclear localization of the protein where it is recognized by HSPA8/HSC70, cleaved, and degraded by chaperone-mediated autophagy [120]. This system can be used to artificially target mutant HTT for degradation. Fusing the protein to a series of HSPA8 binding motifs is enough to signal clearance of the protein via chaperone-mediated autophagy and reduce the disease phenotype in mouse models of HD [121].

Autophagy and cancer

When it comes to cancer, autophagy can be both anti-oncogenic and oncogenic, depending upon the disease state. Generally, autophagy is thought to be anti-oncogenic

prior to the initiation of cancer, because it can reduce the production of ROS, protein aggregates and other cellular toxins that can cause DNA damage, and which can result in defects in biological processes leading to cancer. During tumorigenesis, autophagy may be oncogenic, providing nutrients and energy to tumor cells in nutrient-poor and hypoxic environments prior to angiogenesis. It is this dual role that makes targeting autophagy in cancer treatment very complex. However, recent studies have shown that the promotion or inhibition (depending on the disease state) of autophagy in conjunction with traditional cancer treatments has enhanced patient outcomes.

Autophagy cell survival properties can be used by cancer cells to survive hypoxic environments that characterize tumors prior to angiogenesis. In pancreatic cancer, primary tumors show increased levels of autophagy. Inhibition of the pathway by pharmacological or genetic means results in robust tumor regression in the genetic mouse model [122]. Increased autophagic activity is not unique to pancreatic cancer. Generally, cancer cells with RAS mutations are heavily dependent upon autophagy for survival and have high levels of basal activity [123]. The coupling of RAS mutation and autophagy in apoptosis-deficient cells can promote adhesion-independent growth, proliferation, and increased glycolysis (increased glycolyssis is a hallmark trait of cancer cells known as the Warburg effect) [124]. When autophagy is disrupted in RAS-mediated tumor cells, cell growth is impaired due to accumulation of damaged mitochondria and reduced oxygen consumption [125]. RAS expression, however, does not always induce autophagy that promotes cell survival. RAS can also upregulate PMAIP1/NOXA and BECN1, resulting in excessive autophagy and subsequently leading to autophagic cell death [126]. Autophagy also promotes cancer by prompting a metabolic change in fibroblasts cells,

which normally prevent cancer metastasis. Autophagy degrades stromal CAV1/caveolin 1, a marker for cancer-associated fibroblasts. Loss of CAV1 promotes oxidative stress and induces inflammation. This further promotes autophagy, which degrades damaged organelles and provides nutrients for aerobic glycolysis. The fibroblasts then provide glycolytic intermediates, which can be used in oxidative metabolism for ATP production, to the neighboring cancer cells [127].

Cancer cells will even use autophagy as a survival mechanism against chemotherapeutic treatments. Autophagy has been observed to be upregulated in hepatocellular carcinoma cells after treatment with the chemotherapy drugs oxaliplatin and sorafenib [128]. Similar increases in atuophagy activity are observed in breast cancer, leukemia, and colon cancer cells [129-131]. Thus, autophagy inhibition in this case will increase the effectiveness of chemotherapeutic drugs.

There is, however, a strong association between autophagy and tumor suppression. In about 40-75% of various cancers including prostate, ovarian and breast cancers, the autophagy genes *BECN1* and *UVRAG* are monoallelically deleted [132-134]. Deletion or inhibition of a variety of genes in addition to *Becn1* and *Uvrag* including *Sh3glb1*, *Atg5* and *Atg4C* results in spontaneous tumor formation and hyperproliferating tumors in mouse models [35,135,136]. When the corresponding proteins are overexpressed they exert a tumor suppressive effect, inhibiting tumorigenesis. In addition, other oncogenes and tumor suppressors regulate autophagy. Tumor suppressors such as TP53 can both promote and inhibit autophagy, whereas proto-oncogenic products such as AKT1/PKB inhibit autophagy [3,30,137]. In non-small cell lung cancer cells AKT1 is constitutively active and promotes cell survival [138]. AKT1 is activated by

PDK1 which then promotes protein synthesis, cell growth, and inhibition of autophagy through the phosphorylation and inhibition of TSC2/tuberin. Inhibition of TSC2 activates RHEB which promotes MTOR [139].

The above indicates that the role autophagy plays in cancer is extremely complex. Autophagy prevents malignant transformation, while it can promote tumor progression. The implications for clinical treatment indicate that the proper regulation of autophagy to treat cancer will be dependent upon the context and stage of the disease.

Autophagy and cardiomyopathies

Cardiomyocytes are another long-lived, non-regenerative cells. Maintaining cellular homeostasis is especially important in the heart, even more so when you consider that the heart is constantly subjected to stressors. The first indication that autophagy is important in cardiomyocyte housekeeping came from *Lamp2* knockout mice. The *Lamp2* knockout mouse is defective in autophagy at the point of autophagosome fusion with the lysosome, and shows an increased accumulation of autophagic vacuoles [140]. This mouse demonstrates a cardiomyopathy that is similar to Danon disease in humans [141]. Danon disease, also known as lysosomal glycogen storage disease, is a rare form of muscular dystrophy that is characterized by hypertrophic cardiomyopathy. One genetic cause of Danon disease is a mutation in the *LAMP2* gene [142]. The exact rate of occurrence of this mutation is, however, unclear with different studies showing that between 1% and 12.5% of patients has a *LAMP2* mutation [143,144].

When looking at other mouse models, it becomes even clearer that autophagy is required for a healthy heart. There is no clear initial phenotype in mice in which

autophagy has been suppressed in the heart since embryogenesis, but upon closer observation defects can be observed. These mice have deformed sarcomere structure and accumulate impaired mitochondria, they mice tend to die after six months of age, and at ten months they exhibit left ventricular hypertrophy and a decrease in left ventricle fractional shortening [145]. An ATG5 deficiency in mice caused by treatment with tamoxifen leads to the accumulation of ubiquitinated proteins and cardiac hypertrophy. Continuous inhibition of ATG5 expression sensitizes the heart to pressure overload causing cardiac dilation and dysfunction [146]. All of these different mouse models indicate that autophagy is important for the proper development and function of the heart.

In addition to its basal activity regulating heart structure and function, autophagy can also be an adaptive response to stressors. For example, autophagy can help prevent cardiomyocyte proteinopathies, such as Desmin disease [147]. Desmin disease is an extremely severe and progressive form of heart failure. Currently, there are no effective treatments for this cardiomyopathy, but recent studies suggest that promoting autophagy may be an effective strategy. Desmin disease is due to the accumulation of DES into protein aggregates that results in defective myofibrillar architecture [147]. These aggregates are caused by mutations in several different proteins including DES, MYOT/myotilin, and DMD/dystrophin [148]. Mutations can inhibit the ability of DES to bind to its chaperone protein CRYAB/αB-crystallin, causing a toxic aggregation of DES [149]. This aggregation leads to myofibrillar disarray, cardiac dysfunction, and cardiac death [150]. Autophagy is increased in response to mutant DES and helps to clear out the toxic protein aggregations, preventing cell death [147].

In other disorders autophagy can be either cytoprotective or harmful, depending upon the disease context. In the pressure overload system, the heart's response to stressors such as hypertension and myocardial injury is to increase in mass by increasing the size of myocardiocytes. This is originally a positive adaptation, however as time progresses without elimination of the stressor the heart becomes dilated and shows reduced performance. Autophagy is originally induced in the heart by the pressure overload process [146]. As the heart moves into this haemodynamic stress-induced hypertrophic growth stage, the genetic upregulation of autophagy becomes maladaptive [151]. In this stage, heterozygous deletion of *Becn1* reduces autophagy activity and increases cardiac performance. Similarily, pharmacological inhibition of autophagy by histone deacetylase inhibitors reduces cardiac hypertrophy [152].

Depending upon the timing, autophagy can be both protective and harmful in ischemia-reperfusion injuries. During the initial ischemic stress when the cells are deprived of oxygen, autophagy is cardioprotective [153,154]. When it is inhibited pharmacologically there is an observed increase in cardiomyocyte death [155,156]. During the reperfusion stage, when blood supply is restored to ischemic tissues, autophagy is maladaptive [157,158]. Studies have shown that both pharmacological and genetic inhibition of autophagy promotes cell survival. Generally, in ischemia-reperfusion injuries, strictly controlled upregulation of autophagy by compounds, including resveratrol, have been useful in treating these injuries [159,160].

Autophagy and other disorders

Autophagy plays a role in maintaining homeostasis in the lung. The deletion of *Atg7* causes severe defects in the phenotype of bronchial epithelial cells including abnormal mitochondria, a loss of rough ER, loss of cilia, and cellular swelling [161]. The cellular swelling phenotype is significant, because the knockout mice suffer from increased airway resistance due to an increase in sensitivity to cholinergic stimuli. These mice also show an accumulation of SQSTM1, and an elevated expression of antioxidant and anti- inflammatory genes that are activated by NFE2L2/Nrf2 [161]. The mouse model shows that autophagy plays a role in the physiology of pulmonary cells.

The pulmonary disorders cystic fibrosis (CF) and chronic obstructive pulmonary disease (COPD) have a link to autophagy. Mouse models of CF show an accumulation of BECN1 into cytoplasmic aggregates, causing a defect in autophagy. Supplementation with additional BECN1 rescues the CF phenotype [162]. Lung epithelial cells from CF patients show a similar defect in autophagy. This has been linked to defects in autophagy caused by the mutant form of the cystic fibrosis transmembrane conductance regulator (CFTR) protein. In CF, mutant forms of CFTR increase the amount of ROS and TGM2/transglutaminase in lung tissues. The increase in TGM2 leads to crosslinked BECN1, sequestering phosphatidylinositol 3-kinase (PtdIns3K) complex II and SQSTM1 into aggresomes. The CF phenotype in the mouse model can be alleviated by restoration of BECN1 and autophagy by both genetic and pharamocological means [162].

COPD is one of the most common lung diseases, and the leading cause of this disease is smoking. Exposure of bronchial epithelial cells and fibroblasts to cigarette

smoke leads to the induction of LC3B-II protein and the accumulation of autophagosomes [163,164]. The clinical severity of COPD in patients has been positively correlated with elevated levels of LC3B-II, suggesting that autophagic flux is disrupted [165]. Indeed, disruption in autophagosome clearance in the alveolar macrophages of COPD patients has been observed [166].

In the pancreas, autophagy helps maintain β-cell homeostasis, preventing type II diabetes. Autophagy is activated in β-cells in response to free fatty acids [167]. When autophagy is disrupted in the pancreas by genetic knockout in mice there is a clear reduction in β-cell mass. The existing cells show severe abnormalities including the accumulation of ubiquitinated protein aggregates and dysfunctional organelles (mitochondria, ER). These knockout mice suffer from symptoms similar to type II diabetes including higher insulin resistance, hypoinsulinemia, and hyperglycemia [168,169].

The study of autophagy in bone is in its infancy, but current studies suggest that it might play a role in proper bone development. One bone disorder is Paget disease, which is characterized by localized areas of enlarged and misshapen bones. Paget disease is a metabolic bone disorder that causes uncontrolled bone turnover. Mutations in the gene encoding the autophagy receptor SQSTM1 are often identified in patients with Paget disease. The mutations tend to be clustered within the ubiquitin-associated (UBA) domain inhibiting the ability of SQSTM1 to recognize and bind to ubiquitinated proteins. These mutations end up increasing the rate of osteoclastogenesis by inhibiting the ability of SQSTM1 to clear out ubiquitinated NFKB1 leading to sustained TRAF6- NFKB1 signaling [170]. Paget disease and frontal temporal dementia are associated with

inclusion body myopathy which is caused by a mutation in valosin-containing protein (VCP/p97). One function of VCP is to aid in the maturation of the autophagosome. In inclusion body myopathy mouse models there occurs an observable accumulation of immature autophagosomes, suggesting that in Paget disease and its associated myopathies there is a failure in the ability of autophagy to recognize and process cargo [171].

The liver, as the detoxification center of the human body, is especially sensitive to disruptions in autophagy. Hepatocyte-specific deletion of *Atg7* causes severe deformities in organelles, including concentric membranous structures made up of ER membrane, increases in the number of peroxisomes, and swollen and defective mitochondria. Lipid droplets and ubiquitinated protein aggregates also accumulate in these cells. In the above mentioned mouse models the mice show an enlarged liver and suffer from hepatitis [33]. These defects have been traced back to abnormal accumulation of SQSTM1, because the additional deletion of *Sqstm1* or its transcription factor *Nfe2l2*, alleviates the phenotype of these mice [109,172].

Autophagy is also an effective target for the treatment of α_1-antitrypsin deficiency in the liver, a disorder that causes protein misfolding and polymerization that resulting in chronic inflammation that ultimately leads to carcinogenesis [173]. Upregulation of autophagy via treatment with carbamazepine, clears out these inclusions bodies leading to a reduction in hepatic fibrosis [174].

Podocytes in the kidney aid in the filtration function of the organ. In general, these cells are constitutively active for autophagy [175]. When *Atg5* is deleted in

podocyte cells in mice, there is an observed increase in ubiquitinated protein aggregates and the animals become susceptible to glomerulosclerosis, the risk of which increases with age [176]. Mice and patients suffering from chronic kidney disease have increased rates of autophagy in their glomeruli cells. In intact podocytes, autophagy is activated in response to glomerular injury by puromycin aminonucleoside and adriamycin to protect against the development of renal disease. Defects in this pathway increase the risk for proteinuric renal disease and kidney failure [176]. In addition, deletion of *Atg5* in the proximal tubules in mice results in increase susceptibility to ischemia-reperfusion injury [177]. Autophagy is required to maintain normal kidney function and works to protect the kidney from serious damage caused by various injuries.

Conclusions

Our knowledge of the autophagy pathway has expanded greatly over the last decade. The autophagy machinery has been identified and the proteins functionally characterized in both yeast and mammals (and various organisms in between). However, we are just beginning to discover the physiological roles that autophagy plays in human disease. Generally, autophagy functions in maintaining cellular homeostasis and prevents disease by degrading toxic protein aggregates and damaged organelles, but autophagy is not always protective against disease, especially in cancer. In cancer, autophagy can aid in tumor cell survival and its inhibition may increase the effectiveness of chemotherapeutics. Recent findings suggest that different types of autophagy, and different signaling events of autophagy in various diseases may determine whether or not the outcome of the pathway is protective or damaging. There has been some suggestion that increased autophagic activity signaled through the upregulation of BECN1 may be damaging (especially in cardiomyopathies), whereas other autophagic signaling pathways are cytoprotective [151,157].

As the above demonstrates, it is important to understand the different regulatory pathways of autophagy and the timing of it in various disease states. We also need to expand our knowledge regarding the basic mechanism of this pathway. There are still many unanswered questions regarding the origin of the membrane for the autophagosome and how the autophagosome is created. This dissertation has used the yeast, *Saccharomyces cerevisiae* to shed more light on some of those questions.

Yeast as a model system

In this dissertation I have used *S. cerevisiae* as a model system for the study of autophagy. Using yeast as my model organism has provided numerous advantages. First, yeast has several properties that make it useful for biological studies. Budding yeast is easily manipulated, has rapid growth, and is non-pathogenic [178]. Second, the yeast genetic system is well-defined, which makes it readily accessible to gene cloning and genetic engineering due to DNA transformation and homologous recombination [179,180]. Finally, the Atg proteins in yeast are non-essential, and, historically, autophagy genes were first cloned from yeast [181,182]. However, the autophagy pathway in yeast is slightly different than the mammalian counterpart. Yeast cells have a vacuole instead of a lysosome in which the final degradation step takes place [183]. Yeasts also have one site adjacent to the vacuole for autophagosome formation called the phagophore assembly site or PAS, which makes it easier to study autophagosome biosynthesis [184,185]. Despite these differences, autophagy work in yeast has been translated back to the mammalian system [11].

In this dissertation I used budding yeast to investigate various aspect of the autophagy pathway that could be used as potential therapeutic targets. I specifically examined the early secretory pathway as a possible membrane source for the autophagosome (Chapter 3), and in collaboration with the lab of Dr. Susan Ferro-Novick (University of California, San Diego) uncovered an autophagy-specific guanine nucleotide exchange factor or GEF, TRAPPIII, that functions with the early secretory Rab GTPase, Ypt1, in the early stages of autophagosome formation. I have also examined nuclear events associated with autophagy. Through collaborative efforts with Dr.

Bertrand Joseph's Lab (Karolinska Institutet, Stockholm, Sweden), an evolutionarily conserved histone modification-associated molecular switch was identified in regulating the outcome of autophagy (Chapter 4). Last, I looked at autophagy regulation through the promotion of *ATG8* transcription by Sas2, a histone acetyltransferase (Chapter 5.)

References

[1] Bureau, U.C. (2008), Vol. Summary Tables (Bureau, U.C., Ed.).

[2] Jiang, H., White, E.J., Conrad, C., Gomez-Manzano, C. and Fueyo, J. (2009) Methods Enzymol 453, 273-86.

[3] Mizushima, N., Levine, B., Cuervo, A.M. and Klionsky, D.J. (2008) Nature 451, 1069-75.

[4] Ciechanover, A. (2005) Nat Rev Mol Cell Biol 6, 79-87.

[5] Yorimitsu, T. and Klionsky, D.J. (2005) Cell Death Differ 12, 1542-52.

[6] Yang, Z. and Klionsky, D.J. Nat Cell Biol 12, 814-22.

[7] Tanno, M., Sakamoto, J., Miura, T., Shimamoto, K. and Horio, Y. (2007) J Biol Chem 282, 6823-32.

[8] Majeski, A.E. and Dice, J.F. (2004) Int J Biochem Cell Biol 36, 2435-44.

[9] Kunz, J.B., Schwarz, H. and Mayer, A. (2004) J Biol Chem 279, 9987-96.

[10] Klionsky, D.J. (2005) J Cell Sci 118, 7-18.

[11] Klionsky, D.J. and Ohsumi, Y. (1999) Annu Rev Cell Dev Biol 15, 1-32.

[12] Lemasters, J.J. (2005) Rejuvenation Res 8, 3-5.

[13] Farre, J.C. and Subramani, S. (2004) Trends Cell Biol 14, 515-23.

[14] Hamasaki, M., Noda, T., Baba, M. and Ohsumi, Y. (2005) Traffic 6, 56-65.

[15] Mukaiyama, H., Kajiwara, S., Hosomi, A., Giga-Hama, Y., Tanaka, N., Nakamura, T. and Takegawa, K. (2009) Microbiology 155, 3816-26.

[16] Chu, S., DeRisi, J., Eisen, M., Mulholland, J., Botstein, D., Brown, P.O. and Herskowitz, I. (1998) Science 282, 699-705.

[17] Mata, J., Lyne, R., Burns, G. and Bahler, J. (2002) Nat Genet 32, 143-7.

[18] Primig, M., Williams, R.M., Winzeler, E.A., Tevzadze, G.G., Conway, A.R., Hwang, S.Y., Davis, R.W. and Esposito, R.E. (2000) Nat Genet 26, 415-23.

[19] Otto, G.P., Wu, M.Y., Kazgan, N., Anderson, O.R. and Kessin, R.H. (2003) J Biol Chem 278, 17636-45.

[20] Melendez, A., Tallóczy, Z., Seaman, M., Eskelinen, E.-L., Hall, D.H. and Levine, B. (2003) Science 301, 1387-91.

[21] Takács-Vellai, K., Vellai, T., Puoti, A., Passannante, M., Wicky, C., Streit, A., Kovács, A.L. and Muller, F. (2005) Curr Biol 15, 1513-7.

[22] Sato, M. and Sato, K. (2011) Science 334, 1141-4.

[23] Berry, D.L. and Baehrecke, E.H. (2007) Cell 131, 1137-48.

[24] Juhasz, G., Erdi, B., Sass, M. and Neufeld, T.P. (2007) Genes Dev 21, 3061-6.

[25] Lee, C.Y., Cooksey, B.A. and Baehrecke, E.H. (2002) Dev Biol 250, 101-11.

[26] Shen, W. and Ganetzky, B. (2009) J Cell Biol 187, 71-9.

[27] Tsukamoto, S., Kuma, A., Murakami, M., Kishi, C., Yamamoto, A. and Mizushima, N. (2008) Science 321, 117-20.

[28] Fimia, G.M. et al. (2007) Nature 447, 1121-5.

[29] Hara, T., Takamura, A., Kishi, C., Iemura, S., Natsume, T., Guan, J.L. and Mizushima, N. (2008) J Cell Biol 181, 497-510.

[30] Yue, Z., Jin, S., Yang, C., Levine, A.J. and Heintz, N. (2003) Proc Natl Acad Sci U S A 100, 15077-82.

[31] Kuma, A. et al. (2004) Nature 432, 1032-6.

[32] Hara, T. et al. (2006) Nature 441, 885-9.

[33] Komatsu, M. et al. (2005) J Cell Biol 169, 425-34.

[34] Kundu, M. et al. (2008) Blood 112, 1493-502.

[35] Marino, G., Salvador-Montoliu, N., Fueyo, A., Knecht, E., Mizushima, N. and Lopez-Otin, C. (2007) J Biol Chem 282, 18573-83.

[36] Saitoh, T. et al. (2009) Proc Natl Acad Sci U S A 106, 20842-6.

[37] Saitoh, T. et al. (2008) Nature 456, 264-8.

[38] Sou, Y.S. et al. (2008) Mol Biol Cell 19, 4762-75.

[39] Mortensen, M., Ferguson, D.J., Edelmann, M., Kessler, B., Morten, K.J., Komatsu, M. and Simon, A.K. (2010) Proc Natl Acad Sci U S A 107, 832-7.

[40] Pua, H.H., Guo, J., Komatsu, M. and He, Y.W. (2009) J Immunol 182, 4046-55.

[41] Singh, R. et al. (2009) J Clin Invest 119, 3329-39.

[42] Zhang, Y., Goldman, S., Baerga, R., Zhao, Y., Komatsu, M. and Jin, S. (2009) Proc Natl Acad Sci U S A 106, 19860-5.

[43] Sandoval, H., Thiagarajan, P., Dasgupta, S.K., Schumacher, A., Prchal, J.T., Chen, M. and Wang, J. (2008) Nature 454, 232-5.

[44] Zeng, M. and Zhou, J.N. (2008) Cell Signal 20, 659-65.

[45] Zhao, Y., Huang, Q., Yang, J., Lou, M., Wang, A., Dong, J., Qin, Z. and Zhang, T. (2010) Brain Res 1313, 250-8.

[46] Madeo, F., Tavernarakis, N. and Kroemer, G. (2010) Nat Cell Biol 12, 842-6.

[47] Bjedov, I., Toivonen, J.M., Kerr, F., Slack, C., Jacobson, J., Foley, A. and Partridge, L. (2010) Cell Metab 11, 35-46.

[48] Toth, M.L. et al. (2008) Autophagy 4, 330-8.

[49] Morselli, E. et al. (2010) Cell Death Dis 1, e10.

[50] Nakagawa, I. et al. (2004) Science 306, 1037-40.

[51] Andrade, R.M., Wessendarp, M., Gubbels, M.J., Striepen, B. and Subauste, C.S. (2006) J Clin Invest 116, 2366-77.

[52] Birmingham, C.L., Smith, A.C., Bakowski, M.A., Yoshimori, T. and Brumell, J.H. (2006) J Biol Chem 281, 11374-83.

[53] Blanchet, F.P. et al. (2010) Immunity 32, 654-69.

[54] Gutierrez, M.G., Master, S.S., Singh, S.B., Taylor, G.A., Colombo, M.I. and Deretic, V. (2004) Cell 119, 753-66.

[55] Ogawa, M., Yoshimori, T., Suzuki, T., Sagara, H., Mizushima, N. and Sasakawa, C. (2005) Science 307, 727-31.

[56] Orvedahl, A. et al. (2007) Cell Host Microbe 1, 23-35.

[57] Shelly, S., Lukinova, N., Bambina, S., Berman, A. and Cherry, S. (2009) Immunity 30, 588-98.

[58] Tallóczy, Z., Virgin, H.W., IV. and Levine, B. (2006) Autophagy 2, 24-9.

[59] Yano, T. et al. (2008) Nat Immunol 9, 908-16.

[60] Liu, Y., Schiff, M., Czymmek, K., Tallóczy, Z., Levine, B. and Dinesh-Kumar, S.P. (2005) Cell 121, 567-77.

[61] Liang, X.H., Kleeman, L.K., Jiang, H.H., Gordon, G., Goldman, J.E., Berry, G., Herman, B. and Levine, B. (1998) J Virol 72, 8586-96.

[62] Thurston, T.L., Ryzhakov, G., Bloor, S., von Muhlinen, N. and Randow, F. (2009) Nat Immunol 10, 1215-21.

[63] Zheng, Y.T., Shahnazari, S., Brech, A., Lamark, T., Johansen, T. and Brumell, J.H. (2009) J Immunol 183, 5909-16.

[64] Yu, H.B. et al. (2009) J Biol Chem 284, 36007-11.

[65] Harris, J., De Haro, S.A., Master, S.S., Keane, J., Roberts, E.A., Delgado, M. and Deretic, V. (2007) Immunity 27, 505-17.

[66] Tal, M.C., Sasai, M., Lee, H.K., Yordy, B., Shadel, G.S. and Iwasaki, A. (2009) Proc Natl Acad Sci U S A 106, 2770-5.

[67] Nakahira, K. et al. (2011) Nat Immunol 12, 222-30.

[68] Zhou, R., Yazdi, A.S., Menu, P. and Tschopp, J. (2011) Nature 469, 221-5.

[69] Rich, K.A., Burkett, C. and Webster, P. (2003) Cell Microbiol 5, 455-68.

[70] Sanjuan, M.A. et al. (2007) Nature 450, 1253-7.

[71] Kyei, G.B. et al. (2009) J Cell Biol 186, 255-68.

[72] Chaumorcel, M., Souquere, S., Pierron, G., Codogno, P. and Esclatine, A. (2008) Autophagy 4, 46-53.

[73] Pattingre, S. et al. (2005) Cell 122, 927-39.

[74] Sinha, S., Colbert, C.L., Becker, N., Wei, Y. and Levine, B. (2008) Autophagy 4, 989-97.

[75] Dorn, B.R., Dunn, W.A., Jr. and Progulske-Fox, A. (2001) Infect Immun 69, 5698-708.

[76] Gutierrez, M.G., Vazquez, C.L., Munafo, D.B., Zoppino, F.C., Beron, W., Rabinovitch, M. and Colombo, M.I. (2005) Cell Microbiol 7, 981-93.

[77] Mestre, M.B., Fader, C.M., Sola, C. and Colombo, M.I. (2010) Autophagy 6, 110-25.

[78] Crotzer, V.L. and Blum, J.S. (2010) Immunology 131, 9-17.

[79] Crotzer, V.L. and Blum, J.S. (2009) J Immunol 182, 3335-41.

[80] Levine, B. and Deretic, V. (2007) Nat Rev Immunol 7, 767-77.

[81] Münz, C. (2006) Cell Microbiol 8, 891-8.

[82] English, L. et al. (2009) Nat Immunol 10, 480-7.

[83] Lee, H.K. et al. (2010) Immunity 32, 227-39.

[84] Uhl, M., Kepp, O., Jusforgues-Saklani, H., Vicencio, J.M., Kroemer, G. and Albert, M.L. (2009) Cell Death Differ 16, 991-1005.

[85] Dengjel, J. et al. (2005) Proc Natl Acad Sci U S A 102, 7922-7.

[86] Paludan, C., Schmid, D., Landthaler, M., Vockerodt, M., Kube, D., Tuschl, T. and Münz, C. (2005) Science 307, 593-6.

[87] Zhou, D., Li, P., Lin, Y., Lott, J.M., Hislop, A.D., Canaday, D.H., Brutkiewicz, R.R. and Blum, J.S. (2005) Immunity 22, 571-81.

[88] Nedjic, J., Aichinger, M., Emmerich, J., Mizushima, N. and Klein, L. (2008) Nature 455, 396-400.

[89] Lee, H.K., Lund, J.M., Ramanathan, B., Mizushima, N. and Iwasaki, A. (2007) Science 315, 1398-401.

[90] Kato, H. et al. (2005) Immunity 23, 19-28.

[91] Prescott, N.J. et al. (2007) Gastroenterology 132, 1665-71.

[92] Rioux, J.D. et al. (2007) Nat Genet 39, 596-604.

[93] Travassos, L.H. et al. (2010) Nat Immunol 11, 55-62.

[94] Cadwell, K. et al. (2008) Nature 456, 259-63.

[95] Cadwell, K. et al. (2010) Cell 141, 1135-45.

[96] Alirezaei, M., Kemball, C.C., Flynn, C.T., Wood, M.R., Whitton, J.L. and Kiosses, W.B. (2010) Autophagy 6, 702-10.

[97] Boland, B., Kumar, A., Lee, S., Platt, F.M., Wegiel, J., Yu, W.H. and Nixon, R.A. (2008) J Neurosci 28, 6926-37.

[98] Young, J.E., Martinez, R.A. and La Spada, A.R. (2009) J Biol Chem 284, 2363-73.

[99] Midorikawa, R., Yamamoto-Hino, M., Awano, W., Hinohara, Y., Suzuki, E., Ueda, R. and Goto, S. (2010) J Neurosci 30, 10703-19.

[100] Piras, A., Gianetto, D., Conte, D., Bosone, A. and Vercelli, A. (2011) PLoS One 6, e22514.

[101] Rodriguez-Muela, N., Germain, F., Marino, G., Fitze, P.S. and Boya, P. (2012) Cell Death Differ 19, 162-9.

[102] Cheng, H.C. et al. (2011) J Neurosci 31, 2125-35.

[103] Russo, R. et al. (2011) Cell Death Dis 2, e144.

[104] Komatsu, M. et al. (2006) Nature 441, 880-4.

[105] Liang, C.C., Wang, C., Peng, X., Gan, B. and Guan, J.L. (2010) J Biol Chem 285, 3499-509.

[106] Komatsu, M. et al. (2007) Proc Natl Acad Sci U S A 104, 14489-94.

[107] Nishiyama, J., Miura, E., Mizushima, N., Watanabe, M. and Yuzaki, M. (2007) Autophagy 3, 591-6.

[108] Nixon, R.A., Yang, D.S. and Lee, J.H. (2008) Autophagy 4, 590-9.

[109] Komatsu, M. et al. (2007) Cell 131, 1149-63.

[110] Fleming, A., Noda, T., Yoshimori, T. and Rubinsztein, D.C. (2011) Nat Chem Biol 7, 9-17.

[111] Wong, E.S. et al. (2008) Hum Mol Genet 17, 2570-82.

[112] Kubota, C., Torii, S., Hou, N., Saito, N., Yoshimoto, Y., Imai, H. and Takeuchi, T. (2010) J Biol Chem 285, 667-74.

[113] Wong, E. and Cuervo, A.M. (2010) Nat Neurosci 13, 805-11.

[114] Yu, W.H. et al. (2005) J Cell Biol 171, 87-98.

[115] Lee, J.H. et al. (2010) Cell 141, 1146-58.

[116] Wang, Y., Martinez-Vicente, M., Kruger, U., Kaushik, S., Wong, E., Mandelkow, E.M., Cuervo, A.M. and Mandelkow, E. (2009) Hum Mol Genet 18, 4153-70.

[117] Martinez-Vicente, M. et al. (2010) Nat Neurosci 13, 567-76.

[118] Ravikumar, B. et al. (2004) Nat Genet 36, 585-95.

[119] Jeong, H. et al. (2009) Cell 137, 60-72.

[120] Thompson, L.M. et al. (2009) J Cell Biol 187, 1083-99.

[121] Bauer, P.O. et al. (2010) Nat Biotechnol 28, 256-63.

[122] Yang, S. et al. (2011) Genes Dev 25, 717-29.

[123] Lock, R., Roy, S., Kenific, C.M., Su, J.S., Salas, E., Ronen, S.M. and Debnath, J. (2011) Mol Biol Cell 22, 165-78.

[124] Koppenol, W.H., Bounds, P.L. and Dang, C.V. (2011) Nat Rev Cancer 11, 325-37.

[125] Guo, J.Y. et al. (2011) Genes Dev 25, 460-70.

[126] Elgendy, M., Sheridan, C., Brumatti, G. and Martin, S.J. (2011) Mol Cell 42, 23-35.

[127] Martinez-Outschoorn, U.E. et al. (2010) Cell Cycle 9, 2423-33.

[128] Ding, Z.B. et al. (2011) Clin Cancer Res 17, 6229-38.

[129] Li, J., Hou, N., Faried, A., Tsutsumi, S. and Kuwano, H. (2010) Eur J Cancer 46, 1900-9.

[130] Shi, Y.H. et al. (2011) Autophagy 7, 1159-72.

[131] Yang, L. et al. (2011) Leuk Lymphoma 53, 315-22.

[132] Aita, V.M. et al. (1999) Genomics 59, 59-65.

[133] Liang, C., Feng, P., Ku, B., Dotan, I., Canaani, D., Oh, B.H. and Jung, J.U. (2006) Nat Cell Biol 8, 688-99.

[134] Liang, X.H., Jackson, S., Seaman, M., Brown, K., Kempkes, B., Hibshoosh, H. and Levine, B. (1999) Nature 402, 672-6.

[135] Takahashi, Y. et al. (2007) Nat Cell Biol 9, 1142-51.

[136] Yousefi, S., Perozzo, R., Schmid, I., Ziemiecki, A., Schaffner, T., Scapozza, L., Brunner, T. and Simon, H.U. (2006) Nat Cell Biol 8, 1124-32.

[137] Levine, B., Sinha, S. and Kroemer, G. (2008) Autophagy 4, 600-6.

[138] Brognard, J., Clark, A.S., Ni, Y. and Dennis, P.A. (2001) Cancer Res 61, 3986-97.

[139] Huang, J. and Manning, B.D. (2009) Biochem Soc Trans 37, 217-22.

[140] Tanaka, Y. et al. (2000) Nature 406, 902-6.

[141] Saftig, P., Tanaka, Y., Lullmann-Rauch, R. and von Figura, K. (2001) Trends Mol Med 7, 37-9.

[142] Lacoste-Collin, L., Garcia, V., Uro-Coste, E., Arne-Bes, M.C., Durand, D., Levade, T. and Delisle, M.B. (2002) Neuromuscul Disord 12, 882-5.

[143] Arad, M. et al. (2005) N Engl J Med 352, 362-72.

[144] Charron, P. et al. (2004) Heart 90, 842-6.

[145] Taneike, M. et al. (2010) Autophagy 6.

[146] Nakai, A. et al. (2007) Nat Med 13, 619-24.

[147] Tannous, P. et al. (2008) Proc Natl Acad Sci U S A 105, 9745-50.

[148] Omary, M.B., Coulombe, P.A. and McLean, W.H. (2004) N Engl J Med 351, 2087-100.

[149] Dalakas, M.C., Park, K.Y., Semino-Mora, C., Lee, H.S., Sivakumar, K. and Goldfarb, L.G. (2000) N Engl J Med 342, 770-80.

[150] Perng, M.D., Wen, S.F., van den, I.P., Prescott, A.R. and Quinlan, R.A. (2004) Mol Biol Cell 15, 2335-46.

[151] Zhu, H. et al. (2007) J Clin Invest 117, 1782-93.

[152] Cao, D.J. et al. (2011) Proc Natl Acad Sci U S A 108, 4123-8.

[153] Hamacher-Brady, A., Brady, N.R. and Gottlieb, R.A. (2006) J Biol Chem 281, 29776-87.

[154] Huang, C., Yitzhaki, S., Perry, C.N., Liu, W., Giricz, Z., Mentzer, R.M., Jr. and Gottlieb, R.A. (2010) J Cardiovasc Transl Res 3, 365-73.

[155] Gurusamy, N., Lekli, I., Gorbunov, N.V., Gherghiceanu, M., Popescu, L.M. and Das, D.K. (2009) J Cell Mol Med 13, 373-87.

[156] Yan, L. et al. (2005) Proc Natl Acad Sci U S A 102, 13807-12.

[157] Matsui, Y., Takagi, H., Qu, X., Abdellatif, M., Sakoda, H., Asano, T., Levine, B. and Sadoshima, J. (2007) Circ Res 100, 914-22.

[158] Valentim, L. et al. (2006) J Mol Cell Cardiol 40, 846-52.

[159] Das, M. and Das, D.K. (2010) Mol Aspects Med 31, 503-12.

[160] Lekli, I. et al. (2010) J Cell Mol Med 14, 2506-18.

[161] Inoue, D., Kubo, H., Taguchi, K., Suzuki, T., Komatsu, M., Motohashi, H. and Yamamoto, M. (2011) Biochem Biophys Res Commun 405, 13-8.

[162] Luciani, A. et al. (2010) Nat Cell Biol 12, 863-75.

[163] Hwang, J.W., Chung, S., Sundar, I.K., Yao, H., Arunachalam, G., McBurney, M.W. and Rahman, I. (2010) Arch Biochem Biophys 500, 203-9.

[164] Kim, H.P., Wang, X., Chen, Z.H., Lee, S.J., Huang, M.H., Wang, Y., Ryter, S.W. and Choi, A.M. (2008) Autophagy 4, 887-95.

[165] Chen, Z.H. et al. (2008) PLoS One 3, e3316.

[166] Monick, M.M., Powers, L.S., Walters, K., Lovan, N., Zhang, M., Gerke, A., Hansdottir, S. and Hunninghake, G.W. (2010) J Immunol 185, 5425-35.

[167] Ebato, C. et al. (2008) Cell Metab 8, 325-32.

[168] Jung, H.S. et al. (2008) Cell Metab 8, 318-24.

[169] Jung, H.S. and Lee, M.S. (2010) Ann N Y Acad Sci 1201, 79-83.

[170] Goode, A. and Layfield, R. (2010) J Clin Pathol 63, 199-203.

[171] Ju, J.S., Fuentealba, R.A., Miller, S.E., Jackson, E., Piwnica-Worms, D., Baloh, R.H. and Weihl, C.C. (2009) J Cell Biol 187, 875-88.

[172] Komatsu, M. et al. (2010) Nat Cell Biol 12, 213-23.

[173] Marciniak, S.J. and Lomas, D.A. (2010) N Engl J Med 363, 1863-4.

[174] Hidvegi, T. et al. (2010) Science 329, 229-32.

[175] Mizushima, N., Yamamoto, A., Matsui, M., Yoshimori, T. and Ohsumi, Y. (2004) Mol Biol Cell 15, 1101-11.

[176] Hartleben, B. et al. (2010) J Clin Invest 120, 1084-96.

[177] Kimura, T. et al. (2011) J Am Soc Nephrol 22, 902-13.

[178] Roman, H. (1981) in: The Molecular and Cellular Biology of the Yeast Saccharomyces Cold Spring Harbor Laboratory Press, Cold spring Harbor, New York.

[179] Gutherie, C. (1991) in: Methods Enzymology, Vol. 194, pp. 1-863.

[180] Johnston, J. (1994) Oxford University Press, Oxfod.

[181] Ohsumi, Y. (1999) Philos Trans R Soc Lond B Biol Sci 354, 1577-80; discussion 1580-1.

[182] Takeshige, K., Baba, M., Tsuboi, S., Noda, T. and Ohsumi, Y. (1992) J Cell Biol 119, 301-11.

[183] Matile, P. and Wiemken, A. (1967) Arch Mikrobiol 56, 148-55.

[184] Kim, J., Huang, W.P., Stromhaug, P.E. and Klionsky, D.J. (2002) J Biol Chem 277, 763-73.

[185] Suzuki, K., Kirisako, T., Kamada, Y., Mizushima, N., Noda, T. and Ohsumi, Y. (2001) EMBO J 20, 5971-81.

CHAPTER 2

The Cvt Pathway as a Model for Selective Autophagy

Abstract

Autophagy is a highly conserved, ubiquitous process that is responsible for the degradation of cytosolic components in response to starvation. Autophagy is generally considered to be non-selective; however, there are selective types of autophagy that use receptor and adaptor proteins to specifically isolate a cargo. One type of selective autophagy in yeast is the cytoplasm to vacuole targeting (Cvt) pathway. The Cvt pathway is responsible for the delivery of the hydrolase aminopeptidase I to the vacuole; as such, it is the only known biosynthetic pathway that utilizes the core machinery of autophagy. Nonetheless, it serves as a model for the study of selective autophagy in other organisms.

Introduction

Autophagy is a ubiquitous process that is highly conserved in all eukaryotes. It is responsible for the degradation of cytosolic components and organelles in response to nutrient deprivation [1, 2]. In addition to playing a role in the cellular response to stress, autophagy also plays a role in development [3], tumor suppression [4], pathogen resistance [5], and aging [6]. We now know that this process is involved in several human pathologies including cancer [7], diabetes [8, 9], cardiomyopathy [10], and neurodegenerative disorders such as Alzheimer and Parkinson diseases [11].

There are three main types of autophagy; chaperone-mediated autophagy, microautophagy, and macroautophagy (Fig. 2.1). Chaperone-mediated autophagy has only been characterized in higher eukaryotes, and currently there is no knowledge of a similar process in yeast. In this process, a chaperone protein binds to a specific target protein, causing it to unfold, allowing for direct transport across the lysosomal membrane[12]. Microautophagy sequesters cytoplasmic components, and delivers them for degradation by the direct invagination or protrusion/septation of the lysosomal or vacuolar membrane [13]. Macroautophagy, hereafter referred to as autophagy, is the most well characterized process of the three. Autophagy was first studied in mammalian cells [14], but the majority of the molecular components were initially elucidated in yeast [15], and this review focuses on the yeast model system.

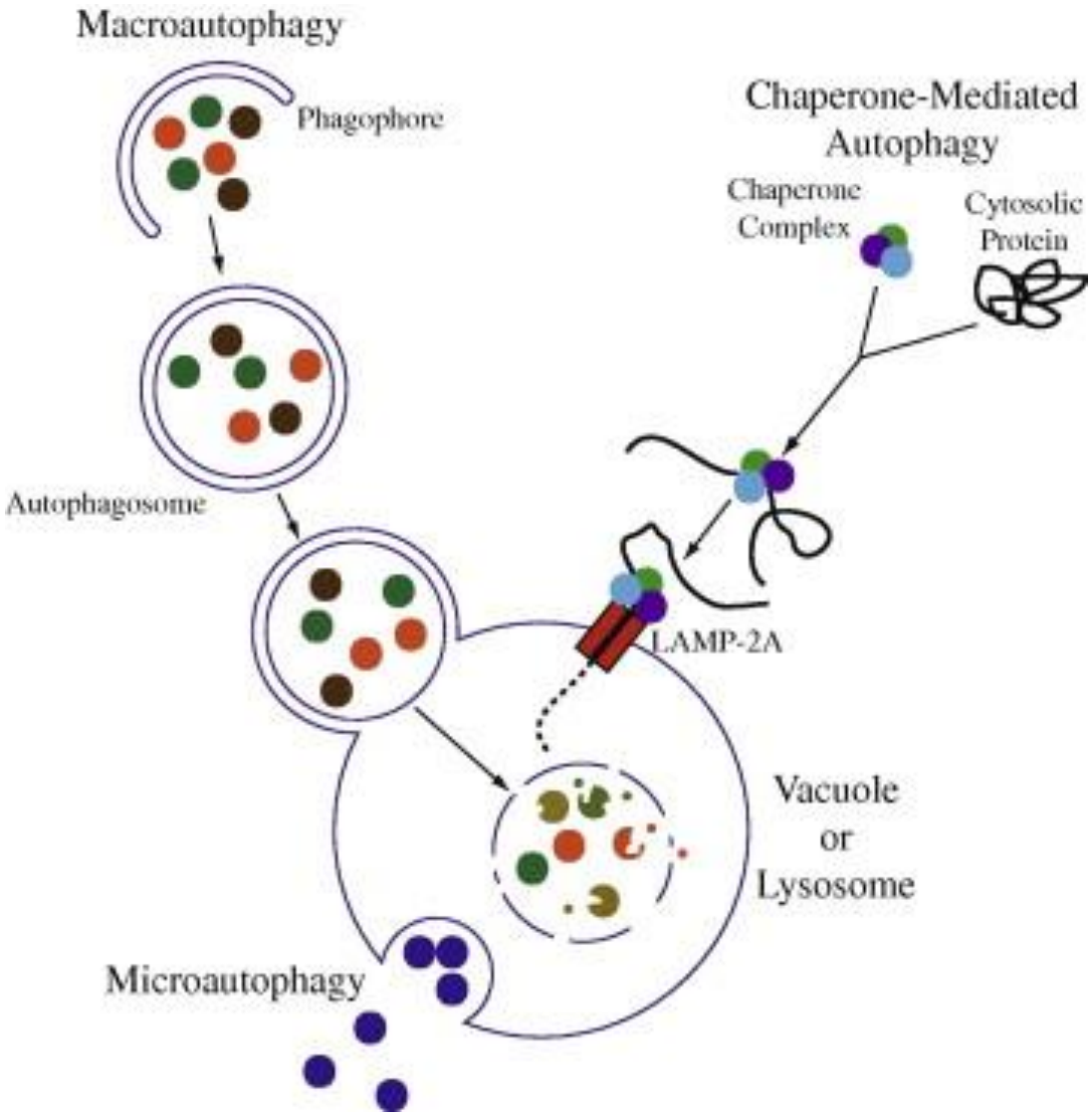

Figure 2.1. Three main types of autophagy. There are three main types of autophagy: chaperone-mediated autophagy, microautophagy, and macroautophagy. The schematic depicts a mixture of these processes in lower and higher eukaryotes. For example, the lysosome is much smaller than the fungal vacuole. Also, chaperone-mediated autophagy has only been characterized in higher eukaryotes, whereas microautophagy and macroautophagy are evolutionarily conserved. Macroautophagy is the best-characterized pathway out of the three and the hallmark of this process is the formation of a double-membrane vesicle that non-selectively sequesters cytoplasmic components and delivers them to the lysosome or vacuole for degradation and recycling of the cargo.

The morphological hallmark of autophagy is the *de novo* formation of the autophagosome, a double-membrane vesicle that sequesters cytosol and organelles. The outer membrane of the autophagosome fuses with the vacuole, releasing the inner membrane, termed the autophagic body, into the lumen where it and its contents are degraded [16]. Although autophagy's primary role in yeast is to respond to cellular stress, homeostatic and biosynthetic functions have also been elucidated. For example, excess peroxisomes are degraded by pexophagy, a selective type of autophagy, when conditions make them superfluous [17]. In addition to pexophagy, there are other organelle-specific autophagy pathways, such as mitophagy for mitochondria [18] (see Appendix B for more information), and reticulophagy for the endoplasmic reticulum [19]. Yeast cells also have the cytoplasm to vacuole targeting (Cvt) pathway. The Cvt pathway is responsible for the delivery of at least two hydrolases, α-mannosidase (Ams1) and aminopeptidase I (Ape1), to the vacuole. Ape1 is synthesized in the cytosol as a proenzyme that is relatively inactive. The Cvt pathway sequesters the precursor Ape1 into a Cvt vesicle at the phagophore assembly site or PAS ("phagophore" is the term that describes the initial sequestering vesicle used in autophagy-related pathways), using much of the same machinery as autophagy, and delivers it into the vacuole where it is activated by the removal of the propeptide[20, 21]. Because of the similarity between autophagy and the Cvt pathway, the Cvt pathway is considered to be a selective type of autophagy. This paper will review the Cvt pathway and its principal cargo, precursor Ape1, in depth.

Ape1 and the Cvt pathway

Ape1 is one of four aminopeptidases that hydrolyze leucine substrates, identified in the yeast*Saccharomyces cerevisiae*[22]. Further characterization of the protein by subcellular fractionation revealed it to be localized to the vacuole [23, 24], and it appeared to be a glycoprotein containing 12% carbohydrate [25]; Metz and Röhm originally concluded from western blot migration patterns that Ape1 was glycosylated and thus transported to the vacuole through a portion of the secretory pathway. However, the presence of carbohydrates on Ape1 was never confirmed and Klionsky et al. show that it is not glycosylated; treatment with the glycosylation inhibitor tunicamycin does not change the migration pattern of Ape1 during SDS–PAGE, and the protein does not bind the lectin concanavalin A [26]. Similar to many other vacuolar hydrolases, Ape1 is synthesized as a zymogen (prApe1) and is processed in a Pep4-dependent manner [22]. Precursor Ape1 maturation is normal in certain *sec* mutants, which block the secretory pathway, further indicating that prApe1 does not enter the endoplasmic reticulum [26]. Yoshihisa and Anraku had indicated that another vacuolar hydrolase, α-mannosidase (Ams1), enters the vacuole directly from the cytosol [27], and subsequent studies show that Ams1 uses the same delivery mechanism as prApe1 [28]. This alternative route is named the cytoplasm to vacuole targeting pathway to distinguish it from the canonical pathway used by most vacuolar hydrolases that transit through a portion of the secretory pathway.

Precursor Ape1 has a half-life of maturation of approximately 45 min, which, coupled with its activation by cleavage of the propeptide in the vacuole, makes it an ideal

marker for the Cvt pathway [26]. A mutagenesis screen used Ape1 to identify components of this alternative vacuole transport pathway by isolating mutants that accumulate prApe1. The authors found two complementation groups that are allelic to the previously identified *vps* class B mutants that lack vacuolar acidification. One complementation group is allelic to the gene encoding proteinase B, which acts along with Pep4 in removal of the prApe1 propeptide, and the remaining five groups were determined to be phenotypically distinct from other known mutants. These mutants show a defect in prApe1 maturation, but no defect in Prc1 maturation. The mutants are named *atg7*, *atg8*, *atg9*, and *atg11* (the original names were *cvt2*, *cvt5*, *cvt6/cvt7* and *cvt3/cvt9*, respectively [29].Cellular fractionation experiments show that in those mutants prApe1 is blocked in delivery to the vacuole, so that it accumulates in the cytosolic fraction [29]. The *cvt* mutants were further analyzed using an in vitro import assay for prApe1 uptake. This assay radiolabels spheroplasts in vivo prior to being lysed, so that the maturation of newly synthesized prApe1 can be followed in vitro. From this assay it is determined that prApe1 maturation is time- and temperature-dependent. It is also shown that the Cvt pathway requires ATP, a functional vacuolar ATPase, and a GTP binding protein [30]. Site-directed mutagenesis of the *APE1* gene indicates an important role for the propeptide region of prApe1 in the proper targeting of the protein to the vacuole [31, 32]. The predicted secondary structure of the propeptide region includes two α-helices separated by a β-turn [33]. The first α-helix is amphipathic with both acidic and basic amino acids [31]. Random and site directed mutations in the first α-helix result in a defect in prApe1 maturation and localization. Mutations in the propeptide region do not prevent proper folding of prApe1, but mutations in the first α-helix do prevent association with a

membrane. The mutagenesis screen identified one key residue, lysine 12, which is especially important for proper vacuolar localization. Mutations in the second α-helix do not affect the kinetics of prApe1 maturation [31]. These data indicate that the first helix is responsible for targeting prApe1 to the vacuole.

Two hypotheses were suggested for the vacuolar import of prApe1. The first suggested that prApe1 is transported across the vacuole membrane in an unfolded or partially unfolded state through a vacuolar pore or channel, similar to the mechanism used in chaperone-mediated autophagy. The problem with this hypothesis is that there is no morphological evidence for a pore complex in the vacuole limiting membrane. The second hypothesis proposed a vesicle-mediated transport mechanism [34]. This hypothesis was supported by a study that examined the oligomeric state of prApe1. Pulse-chase analysis shows that precursor Ape1 rapidly oligomerizes into a homododecamer, which then assembles into a higher order complex composed of multiple dodecamers (the Ape1 complex) [35]. The oligomerization of prApe1 occurs in the cytosol prior to associating with a membrane, and occurs independent of the Atg proteins. Truncations in the C terminus inhibit oligomerization indicating that this region is responsible for generating this higher order structure. Once assembled, the dodecamer is not disassembled, eliminating the possibility of prApe1 entering the vacuole through a small pore in the vacuole membrane, and ruling out translocation of the unfolded protein across the membrane as occurs in chaperone-mediated autophagy [35]. Interestingly, later studies show that Ams1, the other identified cargo of the Cvt pathway, also exists as an oligomer [28], suggesting that one function of this pathway is the transport of hydrolases that assemble into oligomeric complexes.

Vesicle-mediated transport of prApe1 is confirmed using fractionation and immunoelectron microscopy experiments. Subcellular fractionation reveals a pool of prApe1 that is associated with a non-vacuolar membrane compartment [34, 36]. In the *vps18* mutant, that inhibits fusion at the vacuole, prApe1 accumulates in a non-vacuolar membrane compartment, suggesting that prApe1 is transported to the vacuole inside a vesicle [34]. The prApe1^{P22L} mutant is mutated in the β-turn of the propeptide region. This mutant has increased membrane-binding affinity, but inhibits subsequent steps of the transport process. In cells expressing this mutant, prApe1 co-fractionates with membrane that lacks vacuole markers [34]. Immunoelectron microscopy further confirms that prApe1 first binds to, and is then encapsulated by, a double-membrane vesicle before delivery to the vacuole. In *atg15Δ* (originally *cvt17Δ*) cells that are defective in the breakdown of Cvt bodies, cytosolic and subvacuolar prApe1-containing vesicles are visualized [34, 36].

Once prApe1 is oligomerized and bound to a membrane is must be sequestered inside a Cvt vesicle of between 140 and 160 nm in diameter [37]. Electron micrographs illustrate that the Cvt vesicle forms near the vacuole at the PAS and apparently excludes all cytosolic components to selectively isolate prApe1 [36]. The formation of the Cvt vesicle requires the t-SNARE Tlg2 and the Sec1 homolog Vps45 [38]. Baba et al. were able to visualize the steps leading to fusion of the Cvt vesicle with the vacuole membrane using immunoelectron microscopy of *pep4Δ* cells [36]. The Cvt vesicle's outer membrane fuses with the vacuole, leaving the inner membrane exposed to the lumen. Fusion requires the same machinery needed for other vesicle fusion events at the vacuole including the Q-SNAREs Vam3 and Vti1, the docking protein Vps18, and the rab

GTPase Ypt7 [37]. This process is morphologically similar to non-selective autophagy. Both processes require a double-membrane vesicle to sequester cargo and the vesicle fusion machinery to fuse the outer membrane of the sequestering vesicle with the vacuole, which results in the release of the inner membrane and its contents in the vacuole lumen; in the case of autophagy, the contents are degraded and the breakdown products are released back into the cytosol, whereas the cargo of the Cvt pathway are resident hydrolases that function in the vacuole lumen [20]. The genetic screens for autophagy and Cvt pathway mutants reveal substantial overlap between the molecular components [20, 21]. This knowledge changed the direction of study of the Cvt pathway to focus more on the differences and similarities it has with autophagy.

Core machinery required for selective and non-selective autophagy

Several screens were carried out almost simultaneously for mutants defective in selective and non-selective types of autophagy, which resulted in the use of multiple names for the corresponding genes. In 2003, these genes were unified into the autophagy-related (*ATG*) nomenclature [39]. Currently, there are 33 *ATG* genes, with 17 making up the core machinery required for both the Cvt pathway and autophagy. The 17 core *ATG*genes can be classified into four groups based upon their function. The first group includes Atg9 and factors involved in its cycling, which particularly include the Atg1 protein kinase complex [40], the second includes the phosphatidylinositol 3-kinase (PtdIns3K) complex [41], the third group includes the ubiquitin-like (Ubl) protein system [42] and [43], and the fourth group is comprised of proteins that act at the last stages of autophagy, vesicle breakdown and efflux of the cargo degradation products back into the cytosol. The core Atg proteins function at various stages during the autophagy-related pathways, which can be broken down into several steps: (1) The phagophore nucleates at the PAS, a perivacuolar structure that is the site of sequestering vesicle formation in yeast. (2) The phagophore expands to sequester the cargo. (3) The phagophore closes creating the double-membrane autophagosome or Cvt vesicle. (4) The autophagosome or Cvt vesicle fuses with the vacuole, releasing the inner vesicle that is now termed an autophagic body or Cvt body. (5) The autophagic body and its contents are degraded by vacuolar hydrolases, and the products are released into the cytosol by various permeases; the Cvt body is also broken down, and its cargos are matured (in the case of prApe1) and carry out their functions in the vacuole lumen. The differences and

similarities in the Atg proteins needed for autophagy and selective autophagy are shown in Fig. 2.2.

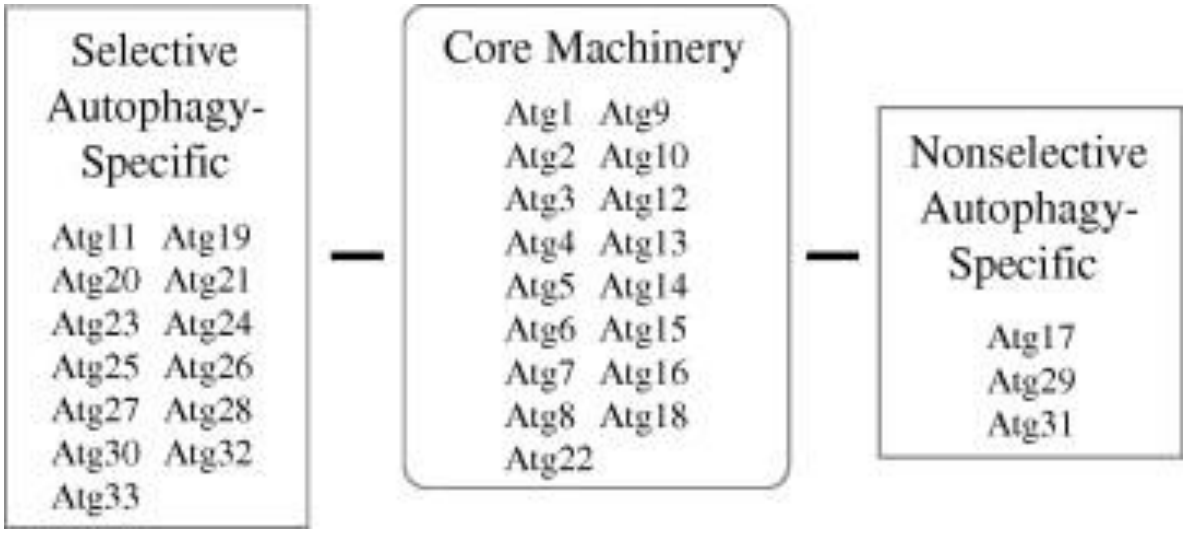

Figure 2.2. Classification of Atg proteins according to function. Autophagy-related (Atg) proteins can be classified according to their role in selective and non-selective autophagy. There are 17 Atg proteins that are required for both types, and these are named the core machinery. Selective autophagy is represented by the cytoplasm to vacuole targeting (Cvt) pathway, mitophagy and pexophagy.

The Atg1 protein kinase complex acts at an initial step of autophagosome formation (and probably at later steps as well). In addition to Atg1, the kinase complex consists of Atg11, Atg13, Atg17, Atg20, Atg24, Atg29, and Atg31, not all of which are considered "core" components. Atg1 is a Ser/Thr kinase whose activity increases upon starvation, and this protein is essential for autophagy [40, 44]. In addition, the Tor signaling pathway negatively regulates autophagy through the Atg1 kinase complex [45]. The Tor complex 1 (TORC1) is a nutrient sensor that is active during periods of readily available nutrients [46]. Parallel to TORC1 is the cyclic AMP (cAMP)-dependent protein kinase A (PKA) [47, 48]. Both are responsible for the hyperphosphorylation of Atg13 during nutrient rich conditions. In response to starvation conditions, TORC1 is inhibited, resulting in the partial dephosphorylation of Atg13, which may allow the protein to associate with Atg1 with greater affinity, subsequently resulting in an increase in Atg1 kinase activity [40, 49, 50]. A second regulatory complex that modulates Atg1 kinase activity is the Atg17–Atg29–Atg31 complex. Atg17, Atg29 and Atg31 form a ternary complex in response to starvation conditions. The Atg17–Atg29–Atg31 complex has dual roles; it associates with Atg1, inducing Atg1 kinase activity, and it is also responsible for recruiting other core Atg proteins to the PAS by acting as an organizing scaffold [51, 52]. The functions of Atg20 and Atg24 are not understood, whereas Atg11 serves as a scaffold protein that is required for most types of selective autophagy [53, 54].

S. cerevisiae has only one phosphatidylinositol 3-kinase, Vps34 [55]. Vps34 associates with two different complexes. The first complex consists of Vps34, Atg6 and Atg14 and is specific for autophagy, whereas the second complex contains Vps38 instead of Atg14, and is required for vacuolar protein sorting by the endosome [41, 56]. Atg14

targets the Vps34 kinase complex to the PAS [56]. Accordingly, Atg14 is responsible for localizing PtdIns(3)P-binding proteins, including Atg18 (which also binds Atg2), to the PAS[57]. Atg18 binds PtdIns(3)P through an FRRY motif. When this motif is mutated to FTTY, Atg18 no longer binds to PtdIns(3)P resulting in a block in both the Cvt pathway and autophagy. This mutant does not affect binding to Atg2, but both Atg2 and the PtdIns(3)P-binding capability of Atg18 are required to localize the complex to the PAS [58]. Relatively little is known about the functions of the Atg18–Atg2 complex, but it is involved in the cycling of Atg9 between peripheral structures and the PAS [59]. Atg9 is a self-associating integral membrane protein that localizes to peripheral (i.e., non-PAS) punctate structures, and cycles to and from the PAS. Atg9 is the only integral membrane protein that is absolutely required for the initial stages of autophagy and the Cvt pathway, and is therefore thought to play a role in trafficking membrane from a donor source(s) to the PAS [60]. Atg9 accumulates at the PAS in *atg1Δ*, *atg2Δ* and *atg18Δ* mutant strains, indicating a role for these proteins in the retrograde (i.e., from the PAS to the peripheral sites) transport of Atg9.

The third group of core Atg proteins is the Ubl protein system. There are two separate yet related conjugation systems that are needed for autophagy. The first is the Atg8 conjugation system. Atg8 is conjugated to phosphatidylethanolamine (PE) and associates with the phagophore and autophagosome [43]. Atg8 expression is increased under starvation conditions [38, 61], and this increase is implicated in regulating the size of the autophagosome; when the expression level of Atg8 is artificially decreased in starvation conditions, the size of the autophagosome is smaller compared to the wild-type phenotype [62]. Atg8 contains a C-terminal arginine residue that is removed by the

cysteine protease Atg4 [38]. Atg8 is then conjugated to PE via the ultimate glycine residue through the actions of an E1 ubiquitin activating enzyme homolog, Atg7, and an E2 ubiquitin conjugating enzyme analog, Atg3 [63, 64]. Atg8–PE is initially located on the inner and outer membranes of the phagophore. Upon completion of the autophagosome or Cvt vesicle, Atg8 is removed particularly from the PE in the outer membrane by a second Atg4-dependent cleavage [38]. The remaining Atg8–PE on the inner membrane is delivered to the vacuole as part of the autophagic (or Cvt) body and is degraded. The association of Atg8 with the inner membrane of the phagophore may play a role in cargo tethering in the Cvt pathway; Atg8 binds the prApe1 receptor Atg19, which may allow the sequestering membrane to enwrap the cargo [64].

The second conjugation system consists of the Atg12—Atg5 complex. Atg12 is conjugated to Atg5 by the formation of an irreversible isopeptide bond between a C-terminal glycine residue of Atg12 and a specific lysine residue of Atg5 [42]. Similar to the Atg8 conjugation system, Atg12 is conjugated to Atg5 through the actions of Atg7, and a different E2-like enzyme, Atg10 [63, 64]. The Atg12-Atg5 complex associates with the multimeric protein Atg16; Atg5 binds non-covalently with the N terminus of Atg16 [65, 66]. Atg16 is responsible for targeting the multimeric complex to the PAS [65]. The Atg12-Atg5–Atg16 complex appears to play some role in Atg8 conjugation to PE in vivo. Atg12-Atg5–Atg16 may act as an E3 enzyme by interacting with Atg3 and enhancing its E2-like activity, and Atg16 appears to dictate in part the location of Atg8 conjugation [67-69].

The last group of core proteins consists of those involved in the final stages of autophagy. At present, there are only two Atg proteins in this group, Atg15 and Atg22.

Atg15 is a putative lipase that is needed for breakdown of the Cvt and autophagic bodies [70, 71], whereas Atg22 is an amino acid permease in the vacuole membrane [72]. These components are critical for some types of autophagy such as starvation-induced non-selective autophagy; the cell cannot survive without degradation of the autophagosome cargo and release of the breakdown products back into the cytosol for reuse.

One question that remains to be answered is how the core machinery is able to switch from creating the smaller, and selective Cvt vesicles to the larger, non-selective autophagosomes upon nutrient starvation. It was first hypothesized that the phosphorylation state of Atg13 may act as the molecular switch to turn off the Cvt pathway and turn on autophagy since Atg13 is hyperphosphorylated during nutrient rich conditions and is rapidly dephosphorylated upon starvation [50]. However, the Cvt pathway and autophagy are not mutually exclusive processes, and therefore the molecular switch must be more complicated than just the dephosphorylation of Atg13 [73]. Another candidate for the molecular switch is the Atg17–Atg29–Atg31 ternary complex, which plays a role along with Atg1 and Atg13 in the nucleation of the PAS under starvation conditions. Cheong et al. show that in the *atg17Δ* mutant pexophagy is completely blocked and autophagy is partially defective while the Cvt pathway is unaffected, suggesting a role for Atg17 in controlling the magnitude of the autophagic response [74]. The Atg17–Atg29–Atg31 autophagy-specific complex could regulate the size of the autophagosome without affecting the Cvt vesicle. In addition, during nutrient rich conditions, Atg11, which is not needed for non-selective autophagy, is responsible for the organization of the PAS [53]. This suggests that the molecular switch between the two

pathways is related to the actions of the Atg1–Atg13–Atg17(–Atg29–Atg31) starvation complex versus the Cvt pathway-specific protein Atg11. More research needs to be done to elucidate the mechanics of this proposed switching complex.

Specificity in the Cvt pathway

Precursor Ape1 is preferentially targeted to the vacuole in both the Cvt pathway and autophagy, suggesting a specific targeting mechanism. A receptor for prApe1 was proposed when it was determined that prApe1 transport to the vacuole by the Cvt pathway is specific and saturable [75]. Two groups simultaneously discovered that Atg19 (originally Cvt19) has all of the characteristics needed to be a receptor for prApe1 in Cvt transport [75, 76]. The protein was first identified in a genome wide yeast two-hybrid screen initiated to identify protein–protein interactions between full-length open reading frames predicted from the *S. cerevisiae* genome sequence [77]. Further characterization of the protein revealed that Atg19 is needed for the stabilization of prApe1 binding to the Cvt vesicle membrane, and that in *atg19Δ* cells prApe1 maturation is inhibited while autophagy is not affected [75]. In addition, Atg19 binds to prApe1 in a propeptide-dependent manner, suggesting that the propeptide region is responsible for the recognition of prApe1 by the Cvt pathway machinery [75]. Finally, Atg19 is a peripheral membrane protein that localizes to the PAS, and its half-life is consistent with that of prApe1 maturation. Atg19 has an expression level stoichiometric with prApe1 and it is delivered to the vacuole along with prApe1 [75]. Consistent with the Cvt pathway transporting both prApe1 and Ams1 to the vacuole, Atg19 is required for Ams1 vacuolar localization [28]. The binding domains for prApe1 and Ams1 on Atg19 are separate and therefore Atg19 is capable of delivering both prApe1 and Ams1 to the vacuole in the same Cvt vesicle [77]. The receptor-mediated Cvt pathway is illustrated in Fig. 2.3.

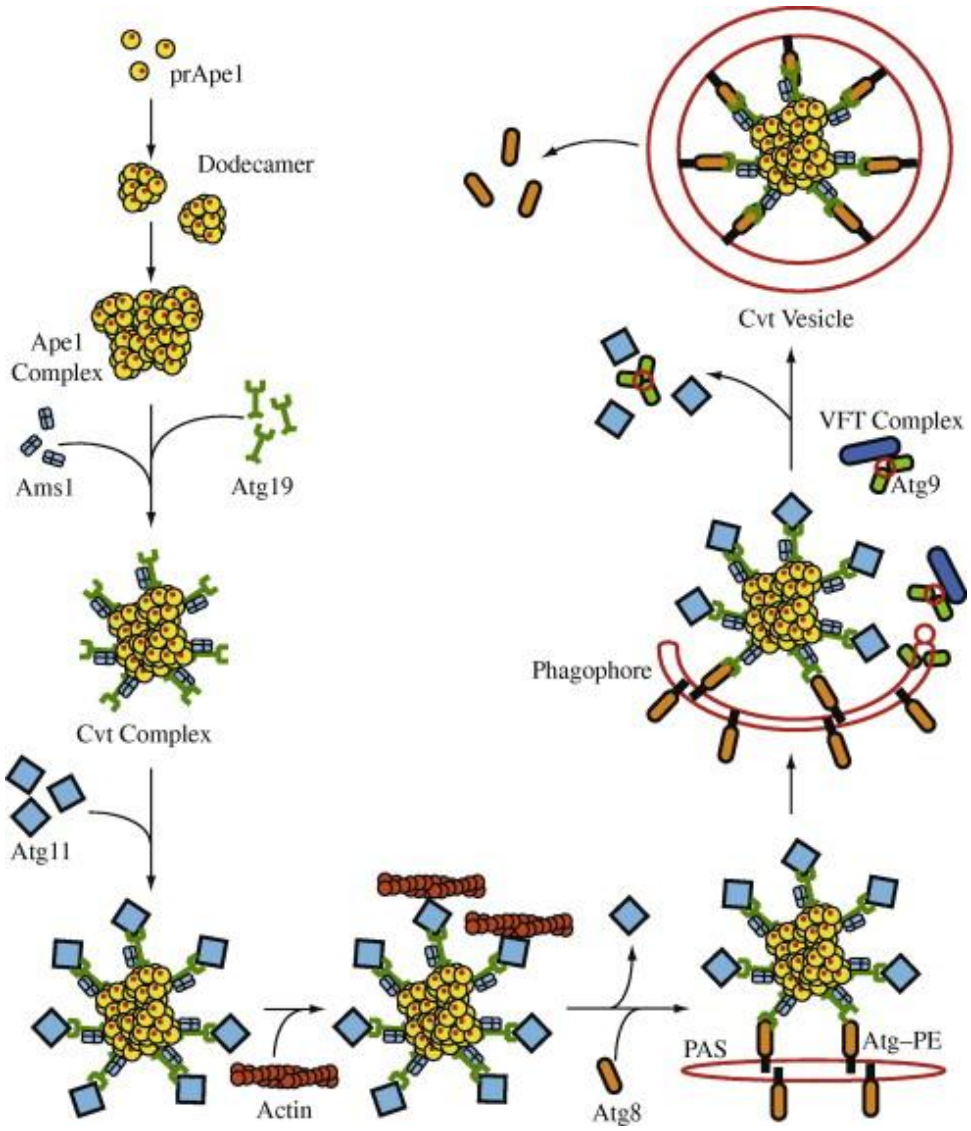

Figure 2.3. Cvt vesicle formation. Precursor Ape1 is a proenzyme that is synthesized in the cytosol, and rapidly oligomerizes to form a homododecamer. The dodecamer further organizes into a higher order structure termed the Ape1 complex. The receptor protein, Atg19, then binds to the Ape1 complex forming the Cvt complex. The Ams1 oligomer is also able to bind Atg19 and can be incorporated into the same Cvt complex. Atg11 binds to Atg9 and transports the Cvt complex to the PAS. At the PAS the Cvt complex binds to the expanding phagophore membrane through an interaction between Atg19 and Atg8–PE. Transport of the Cvt complex to the PAS and the expansion of the phagophore require the actin cytoskeleton and the VFT complex, respectively; delivery of membrane to the expanding vesicle likely involves cycling of Atg9. The phagophore membrane expands around the Cvt complex (excluding bulk cytoplasm) forming the Cvt vesicle.

The prApe1-Atg19 complex (defined as the Cvt complex) is transported to the PAS through a mechanism that is dependent on Atg11 [78]. Atg11 specifically recognizes and binds a C-terminal domain of Atg19 [78], and this interaction is independent of the cargo proteins [79]; immunoprecipitation experiments show that Atg11 and Atg19 coprecipitate both in wild-type and *ape1Δ* cells [79]. The interaction between Atg11 and Atg19 is critical for the proper localization of the Cvt complex to the PAS, because cells lacking Atg11 show mislocalization of prApe1 and Atg19, as well as a defect in prApe1 maturation [78]. In addition, Atg11 localization is dependent upon both Atg19 and prApe1, suggesting that Atg11 associates with the Cvt complex prior to PAS localization [78, 79]. These findings indicate that Atg11 is involved in the transport of the Cvt complex to the PAS. Proper localization of the Cvt complex to the PAS is also dependent upon the Vps53 (VFT) tethering complex [80]. The tethering complex is required for Cvt vesicle formation but not for autophagy, suggesting that the membrane source for Cvt vesicle and autophagosome formation may be, at least in part, different. The VFT complex is composed of four components, Vps51, Vps52, Vps53 and Vps54. This complex works in conjunction with Vps45, and the Q-SNAREs Tlg1 and Tlg2, to mediate Cvt vesicle formation [80]. In cells lacking components of the VFT complex, Atg19 and prApe1 are no longer transported to the PAS, but the defect in prApe1 maturation is reversed upon starvation [80]. Subsequent studies further suggest that the VFT complex plays a role in Cvt vesicle formation by facilitating the transport of Atg9 to the PAS [81].

A role for the actin cytoskeleton has also been elucidated in this process. Actin and the actin-binding complex Arp2/3 are required for the Cvt pathway. Cells treated

with the actin-disrupting drug latrunculin A show a defect in prApe1 maturation, whereas the drug has no affect on autophagy, suggesting that the actin cytoskeleton is only critical for the Cvt pathway [82]. Further analysis by fluorescence microscopy in cell lines with specific actin mutants, suggests that the actin cytoskeleton is required for the localization of the Cvt complex and Atg9 to the PAS; however, disruption of actin does not affect the ability of the Cvt complex to bind to a membrane [82]. It is hypothesized that the actin cytoskeleton acts as a track to guide cargos to the PAS, and that Atg11 is the protein that binds the cargo to actin, whereas the Arp2/3 complex could act as a motor that drives the Cvt complex to the PAS [83].

The localization of the Cvt receptor complex to the PAS is essential for the proper organization of the PAS and Cvt vesicle formation. Without any component of the Cvt complex (and Atg11), other Atg proteins do not efficiently localize to the PAS [54]. Atg11 is the critical component for proper PAS organization during vegetative growth conditions, and the expression level of Atg11 correlates directly with the capacity of the Cvt pathway [84]. Though the C terminus of Atg11 is involved in binding to Atg19, there are other regions in Atg11 that are involved in forming complexes with other Atg proteins including its own self-interaction [79]. For example, Atg11 interacts with Atg9 to allow the delivery of the latter to the PAS [85], and Atg11 interacts with the Atg1–Atg13 kinase complex [79]. Likely as a result of its scaffold properties, the overexpression of Atg11 causes an increase in the amount of Atg8 and Atg9 recruited to the PAS. This results in the formation of more Cvt vesicles during nutrient rich conditions [84]. All of this evidence indicates a critical role for Atg11 in PAS organization and the formation of Cvt vesicles.

Atg19 interacts with Atg11 to transport the Cvt complex to the PAS, once at the PAS Atg19 interacts with Atg8. Atg8 plays two roles in the Cvt pathway; it is responsible for regulating vesicle formation, and is helps mediate the sorting of selective cargo by acting as a tether. The interaction with Atg19 is essential for Atg8's role in tethering the Cvt complex to the phagophore [84]. The Cvt pathway is blocked in *atg8Δ* cells at the step of vesicle formation; precursor Ape1 accumulates and is protease accessible, but can still associate with membranes in the *atg8Δ* mutant [52]. Ho et al. were able to isolate these two functions in the sequence of Atg8. They determined that the residues Arg28, Tyr49 and Leu50 are involved in both vesicle formation and cargo selection, whereas Lys48 and Leu55 are only involved in vesicle formation [86]. It is thought that the binding of Atg19–Atg8 is the anchor that forces the membrane to expand exclusively around the Cvt complex [54].

Atg11 is not required for non-selective autophagy, and hence has been termed Cvt-specific; however, Atg11 is also required for other types of selective autophagy. Other Atg proteins that are not required for non-selective autophagy include Atg20, Atg21, and Atg24. These latter proteins are phosphoinositide-binding proteins. Atg20 and Atg24 bind PtdIns(3)P through a phox homology (PX) domain and are dependent upon Atg14 and the PtdIns3K complex for proper localization [87]. Mutations in the PX domain of either protein prevent their localization at the PAS and partially block prApe1 maturation. Mutations in the PX domains of both proteins result in a complete block of the Cvt pathway. This suggests that the interaction between Atg20 and Atg24 offers partial complementation for a mutation in one of these two components [87]. Atg21 is similar to Atg18 in that it binds PtdIns(3)P, and is required for Cvt vesicle

formation [58]. In *atg21Δ* cells, not only do Atg8 and Atg5 fail to localize to the PAS, there is also an observable decrease in Atg8 lipidation [58]. These proteins provide specificity for the role of the PtdIns3K complex in the Cvt pathway, and presumably other types of selective autophagy.

The CVT pathway and selective autophagy require specificity factors

Selective autophagy is mediated by a cargo receptor and a specificity factor (adaptor) that together connect the cargo to the core autophagy machinery. As discussed previously, the cargo receptor and the specificity factor for the Cvt pathway are Atg19 and Atg11, respectively. Atg19 acts in two capacities; it first binds the cargo and transports it to the PAS through an interaction with Atg11, and second, it interacts with Atg8, a component of the core autophagy machinery, to aid in the formation of the Cvt vesicle. Atg19 interacts with Atg8 through a WXXL motif [88]. The WXXL motif has an extended β conformation and forms an intermolecular parallel β-sheet with β2 of Atg8. The WXXL motif of Atg19 is followed by acidic residues, which, with the motif, are required for binding to Atg8 [88]. The binding pocket for the WXXL motif of Atg8 is crucial only for the Cvt pathway and not non-selective autophagy, indicating that this interaction is specific only for selective autophagy. The WXXL binding pocket of Atg8 is highly conserved in higher eukaryotes[88]. The mammalian adaptor protein p62/SQSTM1, which binds ubiquitin, also contains a WXXL motif that is responsible for binding to the mammalian homolog of Atg8, LC3. These findings suggest a possible fundamental mechanism responsible for selective autophagy. Along these lines, two additional selective autophagy receptors with WXXL motifs have recently been identified in mammalian cells, NBR1 and Nix. Similar to p62, NBR1 contains both a ubiquitin binding domain and the WXXL LC3 binding domain, also termed the LC3-interacting region (LIR). NBR1 is involved in the clearance of ubiquitinated aggregates [89], whereas Nix plays a role in the selective clearance of mitochondria by autophagy (mitophagy) during reticulocyte maturation [90, 91].

In the yeast *S. cerevisiae*, mitophagy is mediated through the receptor protein Atg32. Atg32 was first identified in a genomic screen for yeast mutants defective in mitophagy and it is not required for non-selective autophagy or the Cvt pathway [92]. Atg32 is located in the outer membrane of the mitochondria with its N terminus in the cytosol and the C terminus in the intermembrane space. Similar to Atg19, Atg32 interacts with both Atg11 and Atg8 as confirmed by yeast two-hybrid and co-immunoprecipitation experiments. Atg32 interacts with Atg11 to recruit mitochondria to the PAS. Atg32 also contains a WXXL domain on its N terminus, which is responsible for binding to Atg8, and mutation of the WXXL domain blocks binding to Atg8, but not to Atg11 [93]. The binding of Atg32 to Atg8 is required for the complete sequestration of mitochondria by the phagophore [92, 93]. These observations suggest that Atg32 is a key receptor protein needed for mitophagy.

The selective removal of peroxisomes by autophagy (pexophagy) has mainly been studied in methylotrophic yeast, including *Pichia pastoris*. The *P. pastoris* protein PpAtg30 has been identified as the receptor for pexophagy. It was originally discovered in a screen of a collection of micropexophagy mutants, and was identified as a pexophagy-specific mutant; it is not required for the Cvt pathway or non-selective autophagy. PpAtg30 overexpression is able to stimulate pexophagy even under non-pexophagy inducing conditions. PpAtg30 binds to peroxisomes by interacting with the peroxins, PpPex3 and PpPex14, and it transiently associates with the PAS during pexophagy. PpAtg30 binds to PpAtg11 and PpAtg17, connecting the peroxisome to the core autophagy machinery. However, PpAtg30 does not contain a WXXL domain, and

therefore does not interact with PpAtg8 [94]. It will be interesting to see if future studies can determine if there is an intermediary protein that links PpAtg30 to PpAtg8.

A recurring theme is apparent in selective autophagy. The cargo must first be recognized by a receptor protein, which is Atg19 for the Cvt pathway, Atg32 for mitophagy, and PpAtg30 for pexophagy. The receptor protein must then be able to bind an adaptor protein that connects the cargo to the core autophagy machinery. In yeast, Atg11 (and PpAtg11) acts as the adaptor protein. It binds receptor proteins and uses actin to transport the cargo to the PAS, and is responsible for the organization of the PAS during selective autophagy. Once at the PAS, the cargo protein, at least in the case of the Cvt pathway and mitophagy, is able to bind Atg8 via the receptor. This mechanism appears to be conserved in higher eukaryotes through the WXXL binding domain.

Conclusions

The Cvt pathway is the best-characterized type of selective autophagy and therefore stands as a model for how specific cargos are delivered to the vacuole by the autophagy machinery. The Cvt pathway has only been characterized in yeast, specifically *S. cerevisiae* and *P. pastoris*, and is not evolutionarily conserved [95]. Even in fungi, there are certain differences, in that *P. pastoris* uses the two proteins PpAtg26 and PpAtg28 [96]; *S. cerevisiae* Atg26 is not involved in autophagy, and there is no ortholog of PpAtg28. Despite all of this, the study of the Cvt pathway can be beneficial for identifying and understanding selective types of autophagy in higher eukaryotes.

The study of selective autophagy should provide important information for future research related to human diseases. For example, selective autophagy is implicated in the response to pathogen infection; certain pathogens, including the herpes simplex virus, can be selectively degraded by xenophagy [97]. This process recognizes invading pathogens and sequesters them within autophagosomes, indicating a role for selective autophagy in innate immunity [5, 97]. Little is known about this process, but Thursten et al. show that in human cells the protein NDP52 may act as a receptor by recognizing ubiquitin-coated *Salmonella*, and recruiting LC3 to the bacteria [98]. Selective autophagy also plays a key role in the prevention of neurodegenerative disorders. Huntington, Alzheimer, Parkinson and Creutzfeldt-Jakob diseases are the result of toxic neuropeptides that accumulate and form large protein aggregates [99]. Mouse models show that autophagy can prevent neurodegeneration by degrading aggregate-prone proteins before they can damage neurons. The degradation of these protein aggregates depends on p62, which may act similar to Atg19 as noted above [100, 101]. The basis for specificity in the different

types of selective autophagy requires further study, but certain similarities between the types of selective autophagy occurring in higher eukaryotes and the yeast Cvt pathway are readily apparent. These pathways require both a specificity factor/adaptor and a receptor. The receptor in many cases contains a WXXL or LIR domain that is able to bind Atg8/LC3, connecting the cargo to the core autophagy machinery. Future studies using the Cvt pathway as a model may be able to identify receptors and specificity factors for selective autophagy pathways in higher eukaryotes. Defects in selective autophagy can result in the accumulation of damaged proteins and organelles that are associated with various diseases. Thus, being able to manipulate selective types of autophagy may have therapeutic potential for a range of human pathologies.

References

[1] Reggiori, F. and Klionsky, D.J. (2002) Eukaryot. Cell 1, 11–21.

[2] Klionsky, D.J. (2004) Nature 431, 31–32.

[3] Levine, B. and Klionsky, D.J. (2004) Dev. Cell 6, 463–477.

[4] Gozuacik, D. and Kimchi, A. (2004) Oncogene 23, 2891–2906.

[5] Nakagawa, I. et al. (2004) Science 306, 1037–1040.

[6] Vellai, T., Takacs-Vellai, K., Zhang, Y., Kovacs, A.L., Orosz, L. and Müller, F. (2003) Nature 426, 620.

[7] Qu, X. et al. (2003) J. Clin. Invest. 112, 1809–1820.

[8] Jung, H.S. et al. (2008) Cell Metab. 8, 318–324.

[9] Ebato, C. et al. (2008) Cell Metab. 8, 325–332.

[10] Tanaka, Y. et al. (2000) Nature 406, 902–906.

[11] Yuan, J., Lipinski, M. and Degterev, A. (2003) Neuron 40, 401–413.

[12] Massey, A., Kiffin, R. and Cuervo, A.M. (2004) Int. J. Biochem. Cell Biol. 36, 2420–2434.

[13] Wang, C.-W. and Klionsky, D.J. (2004) Microautophagy in: Autophagy

(Klionsky, D.J., Ed.), pp. 107–114, Landes Bioscience, Georgetown, TX.

[14] Deter, R.L., Baudhuin, P. and de Duve, C. (1967) J. Cell Biol. 35, C11–C16.

[15] Klionsky, D.J. (2007) Nat. Rev. Mol. Cell Biol. 8, 931–937.

[16] Klionsky, D.J. and Ohsumi, Y. (1999) Annu. Rev. Cell Dev. Biol. 15, 1–32.

[17] Hutchins, M.U., Veenhuis, M. and Klionsky, D.J. (1999) J. Cell Sci. 112, 4079–4087.

[18] Kim, I., Rodriguez-Enriquez, S. and Lemasters, J.J. (2007) Arch. Biochem. Biophys. 462, 245–253.

[19] Kraft, C., Reggiori, F. and Peter, M. (2009)

Biochim. Biophys. Acta 1793, 1404–1412.

[20] Harding, T.M., Hefner-Gravink, A., Thumm, M. and Klionsky, D.J. (1996) J. Biol. Chem. 271, 17621–17624.

[21] Scott, S.V., Hefner-Gravink, A., Morano, K.A., Noda, T., Ohsumi, Y. and Klionsky, D.J. (1996) Proc. Natl. Acad. Sci. USA 93, 12304–12308.

[22] Trumbly, R.J. and Bradley, G. (1983) Isolation and characterization of aminopeptidase mutants of Saccharomyces cerevisiae. J. Bacteriol. 156, 36–48.

[23] Matile, P., Cortat, M., Wiemken, A. and Frey-Wyssling, A. (1971) Isolation of glucanase-containing particles from budding Saccharomyces cerevisiae. Proc. Natl. Acad. Sci. USA 68, 636–640.

[24] Frey, J. and Röhm, K.H. (1978) Biochim. Biophys. Acta 527, 31–41.

[25] Metz, G. and Röhm, K.H. (1976) Biochim. Biophys. Acta 429, 933–949.

[26] Klionsky, D.J., Cueva, R. and Yaver, D.S. (1992) J. Cell Biol. 119, 287–299.

[27] Yoshihisa, T. and Anraku, Y. (1990) J. Biol. Chem. 265, 22418–22425.

[28] Hutchins, M.U. and Klionsky, D.J. (2001) J. Biol. Chem. 276, 20491– 20498.

[29] Harding, T.M., Morano, K.A., Scott, S.V. and Klionsky, D.J. (1995) J. Cell Biol. 131, 591–602.

[30] Scott, S.V. and Klionsky, D.J. (1995) J. Cell Biol. 131, 1727–1735.

[31] Oda, M.N., Scott, S.V., Hefner-Gravink, A., Caffarelli, A.D. and Klionsky, D.J. (1996) J. Cell Biol. 132, 999–1010.

[32] Segui-Real, B., Martinez, M. and Sandoval, I.V. (1995) EMBO J. 14, 5476–5484.

[33] Martinez, E., Jimenez, M.A., Segui-Real, B., Vandekerckhove, J. and Sandoval, I.V. (1997) J. Mol. Biol. 267, 1124–1138.

[34] Scott, S.V., Baba, M., Ohsumi, Y. and Klionsky, D.J. (1997) J. Cell Biol. 138, 37–44.

[35] Kim, J., Scott, S.V., Oda, M.N. and Klionsky, D.J. (1997) J. Cell Biol. 137, 609–618.

[36] Baba, M., Osumi, M., Scott, S.V., Klionsky, D.J. and Ohsumi, Y. (1997) J. Cell Biol. 139, 1687–1695.

[37] Noda, T., Kim, J., Huang, W.-P., Baba, M., Tokunaga, C., Ohsumi, Y. and Klionsky, D.J. (2000) J. Cell Biol. 148, 465–480.

[38] Kirisako, T. et al. (2000) J. Cell Biol. 151, 263–276.

[39] Klionsky, D.J. et al. (2003) Dev. Cell 5, 539–545.

[40] Kamada, Y., Funakoshi, T., Shintani, T., Nagano, K., Ohsumi, M. and Ohsumi, Y. (2000) J. Cell Biol. 150, 1507–1513.

[41] Kihara, A., Noda, T., Ishihara, N. and Ohsumi, Y. (2001) J. Cell Biol. 152, 519–530.

[42] Mizushima, N. et al. (1998) Nature 395, 395–398.

[43] Ichimura, Y. et al. (2000) Nature 408, 488–492.

[44] Matsuura, A., Tsukada, M., Wada, Y. and Ohsumi, Y. (1997) Gene 192, 245-250.

[45] Kamada, Y., Yoshino, K., Kondo, C., Kawamata, T., Oshiro, N., Yonezawa, K. and Ohsumi, Y. (2010) Mol. Cell Biol. 30, 1049–1058.

[46] Noda, T. and Ohsumi, Y. (1998) J. Biol. Chem. 273, 3963–3966.

[47] Budovskaya, Y.V., Stephan, J.S., Reggiori, F., Klionsky, D.J. and Herman, P.K. (2004) J. Biol. Chem. 279, 20663–20671.

[48] Yorimitsu, T., Zaman, S., Broach, J.R. and Klionsky, D.J. (2007) Mol. Biol. Cell 18, 4180–4189.

[49] Funakoshi, T., Matsuura, A., Noda, T. and Ohsumi, Y. (1997) Gene 192, 207–213.

[50] Scott, S.V. et al. (2000) J. Biol. Chem. 275, 25840–25849.

[51] Kawamata, T., Kamada, Y., Kabeya, Y., Sekito, T. and Ohsumi, Y. (2008) Mol. Biol. Cell 19, 2039–2050.

[52] Cheong, H., Nair, U., Geng, J. and Klionsky, D.J. (2008) Mol. Biol. Cell 19, 668–681.

[53] Kim, J. et al. (2001) J. Cell Biol. 153, 381–396.

[54] Shintani, T. and Klionsky, D.J. (2004) J. Biol. Chem. 279, 29889–29894.

[55] Schu, P.V., Takegawa, K., Fry, M.J., Stack, J.H., Waterfield, M.D. and Emr, S.D. (1993) Science 260, 88–91.

[56] Obara, K., Sekito, T. and Ohsumi, Y. (2006) Mol. Biol. Cell 17, 1527–1539.

[57] Dove, S.K. et al. (2004) EMBO J. 23, 1922–1933.

[58] Stromhaug, P.E., Reggiori, F., Guan, J., Wang, C.-W. and Klionsky, D.J. (2004) Mol. Biol. Cell 15, 3553–3566.

[59] Suzuki, K., Kubota, Y., Sekito, T. and Ohsumi, Y. (2007) Genes Cells 12, 209–218.

[60] Reggiori, F., Tucker, K.A., Stromhaug, P.E. and Klionsky, D.J. (2004) Dev. Cell 6, 79–90.

[61] Nakatogawa, H., Ichimura, Y. and Ohsumi, Y. (2007) Cell 130, 165–178.

[62] Xie, Z., Nair, U. and Klionsky, D.J. (2008) Mol. Biol. Cell 19, 3290–3298.

[63] Mizushima, N. et al. (2001) J. Cell Biol. 152, 657–668.

[64] Kirisako, T., Baba, M., Ishihara, N., Miyazawa, K., Ohsumi, M., Yoshimori, T., Noda, T. and Ohsumi, Y. (1999) J. Cell Biol. 147, 435–446.

[65] Mizushima, N., Noda, T. and Ohsumi, Y. (1999) EMBO J. 18, 3888- 3896.

[66] Kuma, A., Mizushima, N., Ishihara, N. and Ohsumi, Y. (2002) J. Biol. Chem. 277, 18619–18625.

[67] Ichimura, Y., Imamura, Y., Emoto, K., Umeda, M., Noda, T. and Ohsumi, Y. (2004) J. Biol. Chem. 279, 40584–40592.

[68] Hanada, T., Noda, N.N., Satomi, Y., Ichimura, Y., Fujioka, Y., Takao, T., Inagaki, F. and Ohsumi, Y. (2007) J. Biol. Chem. 282, 37298–37302.

[69] Sou, Y.S., Tanida, I., Komatsu, M., Ueno, T. and Kominami, E. (2006) J. Biol. Chem. 281, 3017–3024.

[70] Epple, U.D., Suriapranata, I., Eskelinen, E.-L. and Thumm, M. (2001) J. Bacteriol. 183, 5942–5955.

[71] Teter, S.A., Eggerton, K.P., Scott, S.V., Kim, J., Fischer, A.M. and Klionsky, D.J. (2001) J. Biol. Chem. 276, 2083–2087.

[72] Yang, Z., Huang, J., Geng, J., Nair, U. and Klionsky, D.J. (2006) Mol. Biol. Cell 17, 5094–5104.

[73] Khalfan, W.A. and Klionsky, D.J. (2002) Curr. Opin. Cell Biol. 14, 468–475.

[74] Cheong, H., Yorimitsu, T., Reggiori, F., Legakis, J.E., Wang, C.-W. and Klionsky, D.J. (2005). Mol. Biol. Cell 16, 3438–3453.

[75] Scott, S.V., Guan, J., Hutchins, M.U., Kim, J. and Klionsky, D.J. (2001) Mol. Cell 7, 1131–1141.

[76] Leber, R., Silles, E., Sandoval, I.V. and Mazon, M.J. (2001) J. Biol. Chem. 276, 29210–29217.

[77] Uetz, P. et al. (2000) Nature 403, 623–627.

[78] Shintani, T., Huang, W.-P., Stromhaug, P.E. and Klionsky, D.J. (2002) Dev. Cell 3, 825–837.

[79] Yorimitsu, T. and Klionsky, D.J. (2005) Mol. Biol. Cell 16, 1593–1605.

[80] Reggiori, F., Wang, C.-W., Stromhaug, P.E., Shintani, T. and Klionsky, D.J. (2003) J. Biol. Chem. 278, 5009–5020.

[81] Reggiori, F. and Klionsky, D.J. (2006) J. Cell Sci. 119, 2903–2911.

[82] Reggiori, F., Monastyrska, I., Shintani, T. and Klionsky, D.J. (2005) Mol. Biol. Cell 16, 5843–5856.

[83] Monastyrska, I., Reggiori, F. and Klionsky, D.J. (2008) Autophagy 4, 914–916.

[84] Geng, J. and Klionsky, D.J. (2008) Autophagy 4, 955–957.

[85] Chang, C.Y. and Huang, W.-P. (2007) Mol. Biol. Cell 18, 919–929.

[86] Ho, K.H., Chang, H.E. and Huang, W.-P. (2009) Autophagy 5, 461–471.

[87] Nice, D.C., Sato, T.K., Stromhaug, P.E., Emr, S.D. and Klionsky, D.J. (2002) J. Biol. Chem. 277, 30198–30207.

[88] Noda, N.N. et al. (2008) Genes Cells 13, 1211–1218.

[89] Kirkin, V. et al. (2009) Mol. Cell 33, 505–516.

[90] Schweers, R.L. et al. (2007) Proc. Natl. Acad. Sci. USA 104, 19500–19505.

[91] Novak, I. et al. (2010) EMBO Rep. 11, 45–51.

[92] Kanki, T., Wang, K., Cao, Y., Baba, M. and Klionsky, D.J. (2009) Dev. Cell 17, 98–109.

[93] Okamoto, K., Kondo-Okamoto, N. and Ohsumi, Y. (2009) Dev. Cell 17, 87–97.

[94] Farre, J.C., Manjithaya, R., Mathewson, R.D. and Subramani, S. (2008) Dev. Cell 14, 365–376.

[95] Meijer, W.H., van der Klei, I.J., Veenhuis, M. and Kiel, J.A.K.W. (2007) Autophagy 3, 106–116.

[96] Farre, J.C., Vidal, J. and Subramani, S. (2007) Autophagy 3, 230–234.

[97] Tallóczy, Z., Virgin IV, H.W. and Levine, B. (2006) Autophagy 2, 24–29.

[98] Thurston, T.L., Ryzhakov, G., Bloor, S., von Muhlinen, N. and Randow, F. (2009) Nat. Immunol. 10, 1215–1221.

[99] Landles, C. and Bates, G.P. (2004) EMBO Rep. 5, 958–963.

[100] Bjørkøy, G., Lamark, T., Brech, A., Outzen, H., Perander, M., Øvervatn, A., Stenmark, H. and Johansen, T. (2005) J. Cell Biol. 171, 603–614.

[101] Pankiv, S. et al. (2007) J. Biol. Chem. 282, 24131–24145.

CHAPTER 3

Trs85 Directs a Ypt1 GEF, TRAPPIII, to the Phagophore to Promote Autophagy

Preface

The autophagy pathway uses a large amount of membrane. Currently, the source of the membrane is unknown [1]. Today, there is no evidence that shows the autophagosome budding off of an existing organelle, so it must form de novo. The mobilization of membrane for this process must occur quickly, because an autophagosome is formed and degraded in about 10 minutes [2]. A likely source of membrane for this process is the secretory pathway [3]. The organelles in the secretory pathway are excellent candidates since there is a constant movement of membrane between them. Autophagy could use the secretory pathway's ability to bud off membrane bound vesicles and reroute those vesicles to the phagophore assembly site (PAS).

Previous studies have indicated that the secretory pathway is required for autophagy. Functional impairment of the ER and Golgi complexes inhibits autophagy [4] and when ER to Golgi transport is inhibited there is an observed block in autophagy [5]. The NSF/SNARE complex is needed for the fusion of the autophagosome with the vacuole, and two COPII coat subunits, Sec23 and Sec24, are required for autophagosome formation [6]. Last, subunits of the conserved oligomeric Golgi (COG) complex also play

a role in autophagosome formation. The COG complex is involved in tethering and is responsible for the retrograde trafficking within the Golgi complex. The COG complex has been shown to interact with various autophagy-related proteins and to localize to the PAS. Disruption of the complex results in mislocalization of Atg8 and Atg9, inhibiting autophagosome formation [7]. Together, these data clearly show that autophagy is dependent upon a functional secretory pathway, and it uses certain components to aid in autophagosome formation and fusion.

Rab GTPases are the key players in the trafficking of secretory vesicles [8,9]. Rab proteins are involved in the docking of transport vesicles to target membranes by aiding in the formation of the v/t-SNARE complex [10,11]. They are found in two states: a GDP-bound form, which is cytosolic, and a GTP-bound form, which associates with membranes [10]. The protein must be in the GTP bound state in order to deliver vesicles to target membranes [11]. In mammalian cells, studies have shown that Rab proteins associate with the autophagosome. Rab24, an ER protein, becomes associated with the autophagosome after starvation [12,13]. Rab7 is envolved in late endosomal trafficking, and is recruited to the autophagosome during the late stages of formation, aiding in the fusion between the autophagosome and the lysosome [14,15]. Rab11 plays a role in the fusion of multivesicular bodies to autophagosomes [16]. Finally, Rab33, a Golgi-localized protein, plays a role in autophagy as well. It has been determined that Rab33 interacts with the coiled-coil domain of Atg16 (a protein essential for autophagosome formation); the Atg16 coiled-coil domain co-localizes with the Golgi, and the GTPase-deficient mutant *rab33-Q92L* blocks autophagy [16-18].

The yeast Rab GTPase, Ypt1, is essential for early vesicular transport between the ER and the Golgi, and for early intra-Golgi transport [19-21]. *YPT1* was the first rab gene identified in 1983 [22]. It is a member of the Rab/Ypt family, which includes key players in vesicular transport, and is the largest subfamily of the p21 ras superfamily [9]. Ypt1 influences the docking of transport vesicles by aiding in the formation of the v/t-SNARE complex [20,23,24]. This is accomplished by interacting with its target t-SNARE, resulting in the displacement of a negative regulator. Ypt1's role in vesicle docking is mediated by its guanine nucleotide exchange factor (GEF) TRAPPI [25,26]. TRAPPI is a complex of seven proteins that mediates vesicle tethering by exchanging the guanine nucleotide on Ypt1 [25,26]. The TRAPP complex associates with the cis-Golgi where it binds Ypt1, exchanges the nucleotide, and allows for the interaction of Ypt1 with its t-SNARE [27-29].

This chapter presents a research study into the role Ypt1 and its GEF, Trs85, play in autophagy. You will be presented with data that shows that Trs85 is an autophagy specific subunit of the TRAPP complex, forming TRAPP III. Trs85 and Ypt1 both localize to the PAS. Disruption of their function leads to mislocalized Atg8, suggesting that the two play a role in autophagosome formation.

Abstract

Macroautophagy (hereafter autophagy) is a ubiquitous process in eukaryotic cells that is integrally involved in various aspects of cellular and organismal physiology. The morphological hallmark of autophagy is the formation of double-membrane cytosolic vesicles, autophagosomes, which sequester cytoplasmic cargo and deliver it to the lysosome or vacuole. Thus, autophagy involves dynamic membrane mobilization, yet the source of the lipid that forms the autophagosomes and the mechanism of membrane delivery are poorly characterized. The TRAPP complexes are multimeric guanine nucleotide exchange factors (GEFs) that activate the Rab GTPase Ypt1, which is required for secretion. Here we describe another form of this complex (TRAPPIII) that acts as an autophagy-specific GEF for Ypt1. The Trs85 subunit of the TRAPPIII complex directs this Ypt1 GEF to the phagophore assembly site (PAS) that is involved in autophagosome formation. Consistent with the observation that a Ypt1 GEF is directed to the PAS, we find that Ypt1 is essential for autophagy. This is an example of a Rab GEF that is specifically targeted for canonical autophagosome formation.

Introduction

Autophagy is a catabolic process in which damaged or superfluous cytoplasmic components are degraded in response to stress conditions; it is evolutionarily conserved in eukayotes and is integrally involved in development and physiology [30,31]. The morphological hallmark of autophagy is the formation of double-membrane cytosolic vesicles, autophagosomes, which sequester cytoplasm. The autophagosomes then fuse with the lysosome, resulting in the degradation of the cargo. The mechanism of autophagosome formation is distinct from that used for vesicle formation in the secretory or endocytic pathways and is said to be de novo in that it does not occur by direct budding from a preexisting organelle. Instead, a nucleating structure, the phagophore, appears to expand by the addition of membrane possibly through vesicular fusion. One consequence of this mechanism is that it allows the sequestration of essentially any sized cargo, including intact organelles or invasive microbes, and this capability is critical to autophagic function. When autophagy is induced there is a substantial demand for membrane, and a major question in the field concerns the membrane origin; nearly every organelle has been implicated in this role [32]. The early secretory pathway is likely one such membrane source for autophagy [4,5].

Rab GTPases are key regulators of membrane traffic that mediate multiple events including vesicle tethering and membrane fusion. These molecular switches cycle between an inactive (GDP-bound) and active (GTP-bound) conformation. The yeast Rab Ypt1, which is essential for ER-Golgi and Golgi traffic [33], is activated by the multimeric guanine nucleotide exchange factor (GEF) called TRAPP [25,26]. Two forms of the TRAPP complexes have been identified [29]. These two complexes share several

subunits, including four (Bet3, Bet5, Trs23, and Trs31) that are essential to activate Ypt1. How each of these subunits contributes to nucleotide exchange activity has recently been described [34]. The first and smaller form of the complex, TRAPPI, mediates ER-Golgi traffic [35]. The second and larger complex, TRAPPII, mediates Golgi traffic [36,37]. Both complexes are tethering factors that are needed to tether vesicles to their acceptor compartment. The TRAPPI complex recognizes the coat (COPII) on ER-derived vesicles [35], whereas the TRAPPII complex recognizes the coat (COPI) on Golgi-derived vesicles [36,37]. Subunits specific to TRAPPII, bind to the COPI coat complex [37]. We have proposed that TRAPPII-specific subunits mask the COPII binding site on TRAPPI to convert this GEF into a tethering factor that recognizes a new class of vesicles [34,37].

The TRAPP complexes include three nonessential subunits, Trs33, Trs65, and Trs85 [29,38]. Previous studies demonstrate that Trs85 is required for the cytoplasm to vacuole targeting (Cvt) pathway, a specific type of autophagy, and macroautophagy, the nonspecific autophagy of cytoplasm [39,40]. These earlier studies did not resolve if a free pool of Trs85 or TRAPP was required for the Cvt pathway and autophagy. Here, we show that Trs85 is part of a third TRAPP complex, TRAPPIII, which specifically acts in autophagy. TRAPPIII is a Ypt1 GEF that is targeted to the PAS by the Trs85 subunit. Consistent with this proposal, we also show that Ypt1 is required for both specific and nonspecific types of autophagy.

Results

Trs85 Is a Component of a Third TRAPP Complex That Is a Ypt1 GEF.

The finding that Trs85 is required for autophagy in yeast [39,40] raised the possibility that there may be a separate pool of Trs85 that functions in autophagy-related processes. To begin to address this possibility, we fractionated cytosol on a Superdex-200 column and blotted the column fractions for Trs85, Trs65, and Trs33. Trs33 and Trs65 (TRAPPII-specific subunit) marked the location of the TRAPPI and TRAPPII complexes in these fractions (Fig. 3.1*A*,*Middle* and *Bottom*). There are 10 TRAPP subunits (Trs130, Trs120, Trs85, Trs65, Trs33, Trs31, Trs23, Trs20, Bet5, and Bet3). Three of these subunits (Trs130, Trs120, and Trs65) are unique to TRAPPII [29,38]. Trs33 peaked in fractions 8, 9 (TRAPPII), and 12 (TRAPPI) (Fig. 3.1*A*), whereas Trs65-myc was largely found in fractions 8 and 9 (TRAPPII). The location of Trs85 in these fractions was determined by monitoring an epitope tagged version of Trs85 (Trs85-myc) that was shown to be functional (Fig. S3.1 *A* and *B*). Trs85-myc trailed more than Trs65-myc on the Superdex-200 column and was primarily present in column fractions 8–10 (Fig. 3.1*A*, *Top* and *Middle*).

The fractionation of Trs85-myc suggested there may be a pool of Trs85 that is not present in either TRAPPI or TRAPPII. To begin to address this possibility, we immunoprecipitated Trs85-myc from lysates and compared the precipitated TRAPP subunits to precipitates of Trs33-myc and Trs65-myc. These data showed that Trs85 coprecipitated with Trs33-myc and Trs20 but not Trs65-myc, Trs130, or Trs120 (or a breakdown product of Trs120, see starred band in Fig. 3.1*B* and ref.[29]) (Fig. 3.1*B*).

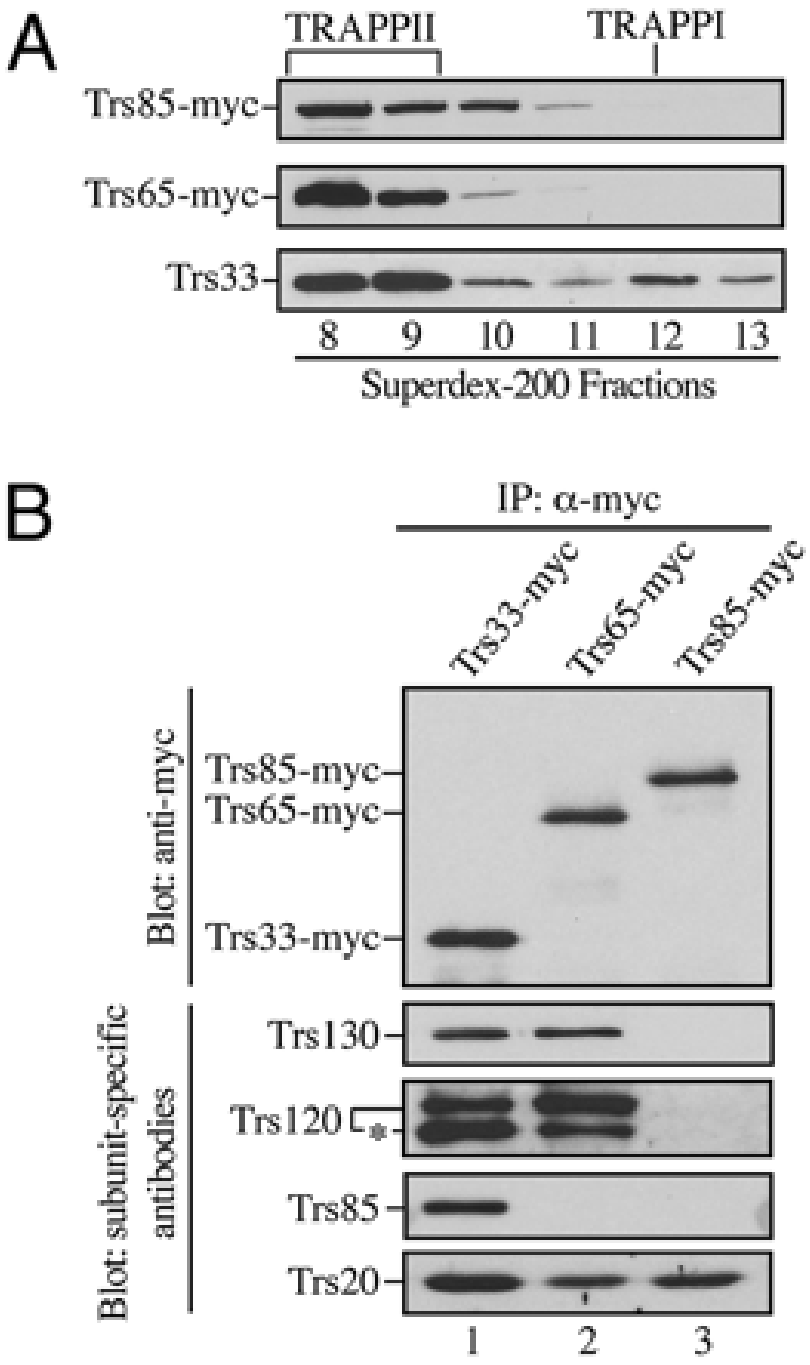

Figure 3.1. Trs85 does not coprecipitate with Trs130, Trs120, and Trs65. (*A*) Trs85 is found in Superdex-200 column fractions 8–10. Cleared lysates (from strains SFNY1295 and SFNY1302) were fractionated and analyzed by Western blot analysis with anti-myc antibody (*Top* and *Middle*) or anti-Trs33 antibody (*Bottom*). (*B*) Trs130, Trs120, and Trs65 do not coprecipitate with Trs85 from lysates. Cleared lysates were immunoprecipitated with anti-myc antibody and immunoblotted for the presence of the indicated TRAPP subunits. *Top* was blotted with anti-myc antibody and *Lower* with subunit-specific antibodies as indicated. The asterisk marks a degradation product of Trs120.

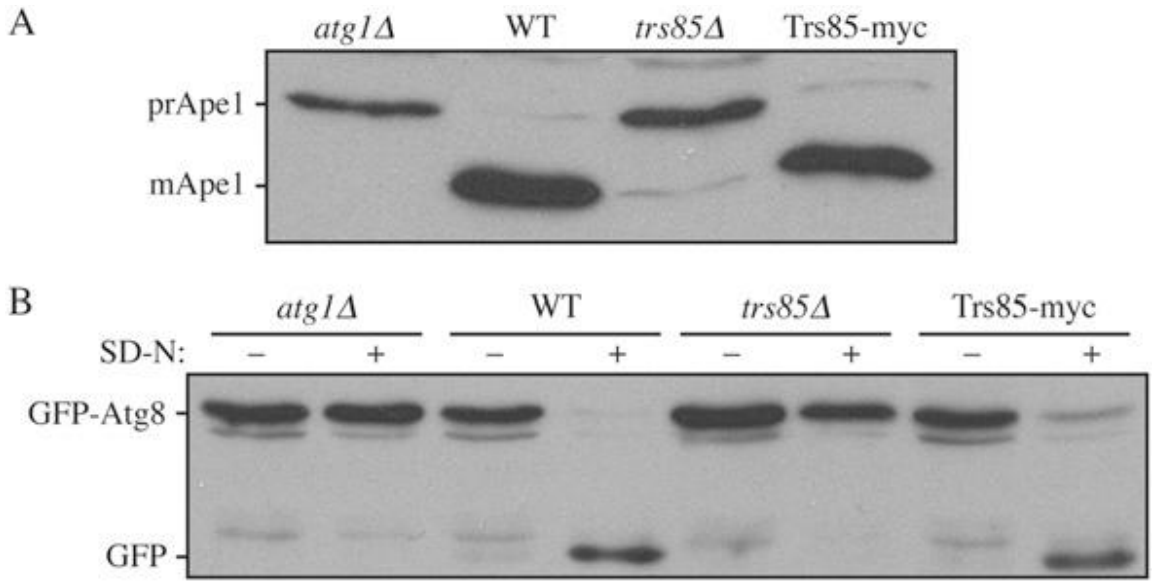

Figure S3.1. Epitope tagging Trs85 does not interfere with autophagy function. The presence of a myc tag on Trs85 does not interfere with the Cvt pathway (A) or nonspecific autophagy (B). Wild-type (WT), atg1Δ, trs85Δ, and WT cells with a 13×-myc epitope integrated at the C terminus of TRS85 were analyzed for the Cvt pathway (A) and nonspecific autophagy (B) by monitoring the processing of prApe1 or GFP-Atg8, respectively

To identify the other TRAPP subunits that coprecipitate with Trs85, we fractionated a radiolabeled lysate prepared from the Trs85-myc strain and precipitated Trs85 from Superdex-200 column fraction 8; contaminating proteins in the precipitate were identified by fractionating an untagged lysate. This analysis revealed that Trs85-myc coprecipitates with Trs33, Trs31, Trs23, Bet3, Trs20, and Bet5 (Fig. 3.2*A*, compare lane 1 to untagged control in lane 2). The identity of these coprecipitating bands was confirmed by precipitating Trs85-myc from fraction 8 and blotting for Trs33, Trs31, Trs23, Bet3, Trs20, and Bet5 (Fig. 3.2*B*). The TRAPPII-specific subunits Trs65, Trs130, Trs120, and a breakdown product of Trs120 (see starred band in Fig. 3.2*C*) were not detected in the Trs85-myc precipitate from fraction 8 (compare lane 2 with the Trs120-myc precipitate in lane 1 in Fig. 3.2*C*). Together, these findings show that Trs85 is not a component of the TRAPPII complex. Additionally, none of the small TRAPP subunits could be precipitated from fraction 12 (TRAPPI) when a Trs85-myc-containing lysate was fractionated (Fig. 3.2*D*, compare the TRAPPI complex in lane 2 with lane 1 and the untagged control in lane 3), and Trs85 was not detected when Bet3-myc was precipitated from fraction 12 (Fig. S3.2). Together, these findings indicate that Trs85 is not a component of the TRAPPI or TRAPPII complexes, which are required for ER-Golgi and Golgi traffic [29,36]. Consistent with this observation, we observed no significant delay in the trafficking of the vacuolar protease Prc1 from the ER through the Golgi complex in *trs85*Δ cells (Fig. S3.3*A*) or an effect on cell growth (Fig. S3.3*B*). Although an earlier study suggested that Trs85 is a subunit of the TRAPPI and TRAPPII complexes [29], the data we report here imply this is not the case. Instead, Trs85 appears to be a specific component of a third TRAPP complex, called TRAPPIII, which is required for autophagy

and the Cvt pathway (see Fig. S3.4 for a summary of the subunits in the different TRAPP complexes). Earlier characterization of the TRAPP complexes was done by precipitating Bet3-myc from Superdex-200 column fractions [29]; because Bet3 is present in all three TRAPP complexes, we speculate that TRAPPIII was not resolved from TRAPPI and TRAPPII in the earlier study.

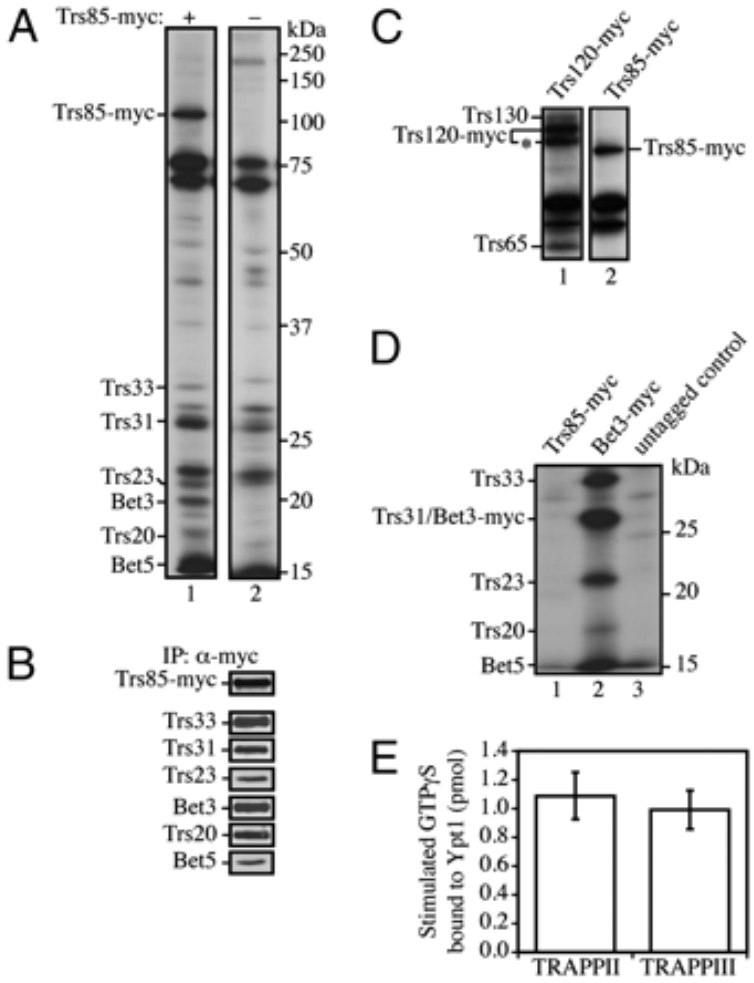

Figure 3.2. Identification of a third TRAPP complex that activates Ypt1. (*A*) Trs85-myc coprecipitates with Trs33, Trs31, Trs23, Bet3, Trs20, and Bet5. Radiolabeled lysates (from strains SFNY1295 and NY915, respectively) were fractionated, and fraction 8 was immunoprecipitated as described in *Materials and Methods*. (*B*) Confirmation of TRAPP subunits that coprecipitate with Trs85. A lysate prepared from strain SFNY1295 was fractionated on a Superdex-200 column. Fraction 8 was immunoprecipitated with anti-myc antibody and analyzed by Western blot analysis using antibody to the indicated TRAPP subunit. (*C*) Trs130, Trs120, and Trs65 do not coprecipitate with Trs85 from fraction 8. Radiolabeled lysates (from strains SFNY1301 and SFNY1295) were fractionated, and fraction 8 was immunoprecipitated. The two dark bands that appear above Trs65 are contaminants (see the untagged control in *A* lane 2). The asterisk marks a degradation product of Trs120. (*D*) Trs85 is not a component of the TRAPPI complex. Radiolabeled lysates (from strains SFNY1295, SFNY656, and NY915) were fractionated, and fraction 12 was immunoprecipitated. (*E*) TRAPPIII is a Ypt1 GEF. TRAPPII was purified from a strain containing TAP-tagged Trs65 (SFNY1075), and TRAPPIII was purified from a strain expressing TAP-tagged Trs85 (SFNY1080) by incubating lysate with IgG-Sepharose beads as described previously (8). The beads were then used to assay for the uptake of GTPγS onto Ypt1. The data shown are normalized to the amount of Trs33 present on IgG-Sepharose beads.

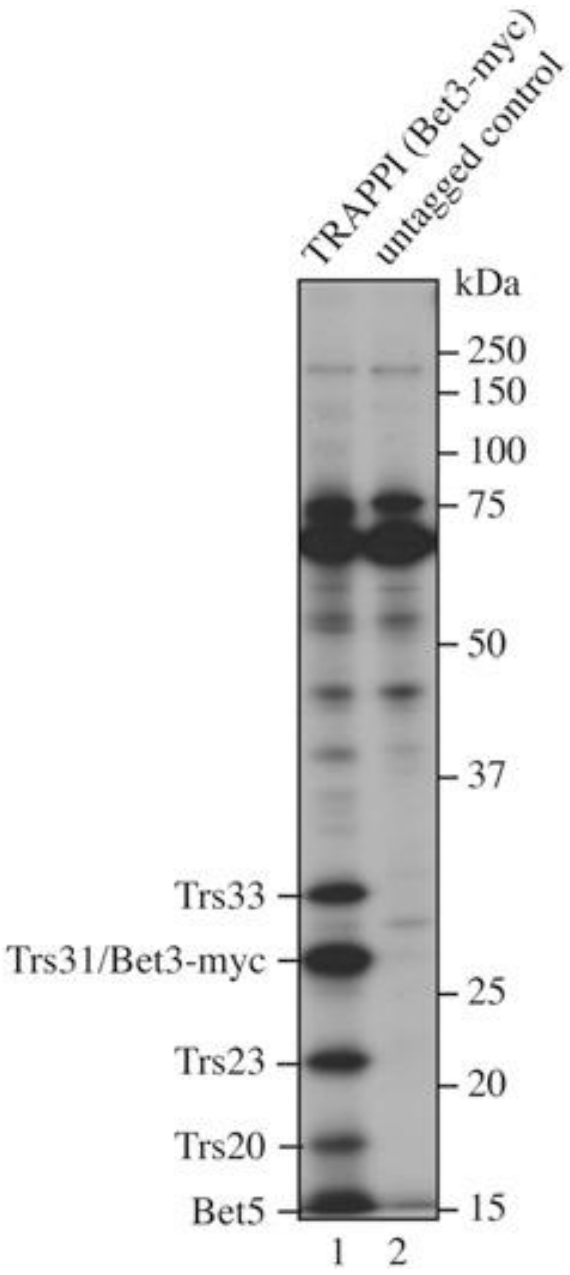

Figure S3.2. Trs85 is not a component of the TRAPPI complex. Radiolabeled lysates were fractionated on a Superdex 200 column and the fractions were immunoprecipitated with anti-myc antibody. Shown are autoradiograms of immunoprecipitates of fraction 12 from strains SFNY656 and NY915 (the untagged control).

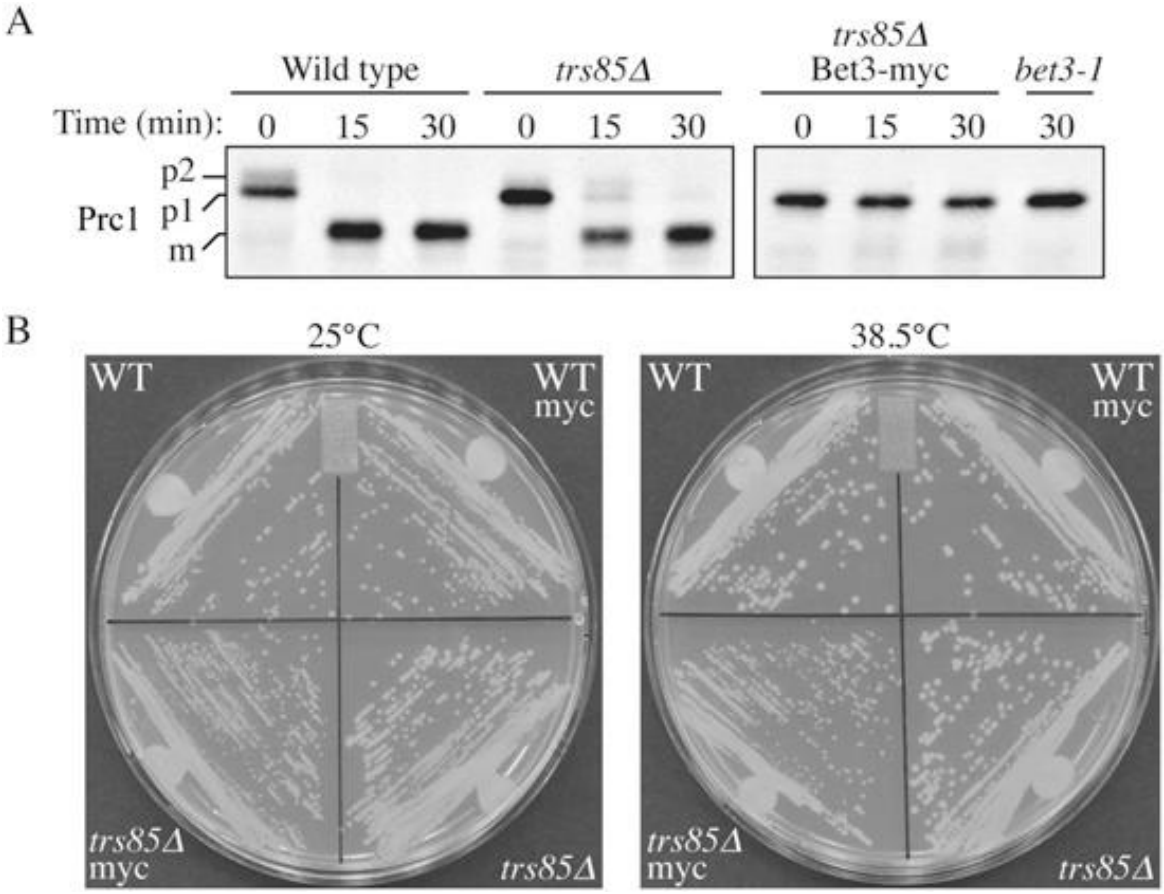

Figure S3.3. Loss of Trs85 does not block ER-Golgi traffic. (A) Wild-type (SFNY26-3a) and trs85Δ (SFNY1040) cells or trs85Δ cells that also contain a myc tag on Bet3 (SFNY996) were pulse-labeled for 4 min (0 time point) and chased for 15 and 30 min. Prc1 in the bet3-1 mutant (SFNY596) lysate marks the ER form, called p1 (30-min time point). The addition of the myc tag on Bet3 in the trs85Δ strain disrupted ER-Golgi traffic, which leads to the accumulation of the p1 form. We speculate that the previously reported block in ER-Golgi traffic [29] in this strain is an indirect consequence of tagging Bet3 in a TRAPP complex that lacks Trs85, however, Trs85 itself does not appear to be required for ER-Golgi traffic. (B) The presence of a myc tag on Bet3 in trs85Δ cells leads to a growth defect. The growth of wild type without (WT, SFNY26-3a) or with a myc tag on Bet3 (SFNY656) was compared after two days to trs85Δ cells with (SFNY996) and without (SFNY1040) a myc tag on Bet3. A YPD plate grown at 25 °C (Left) and 38.5 °C (Right) is shown.

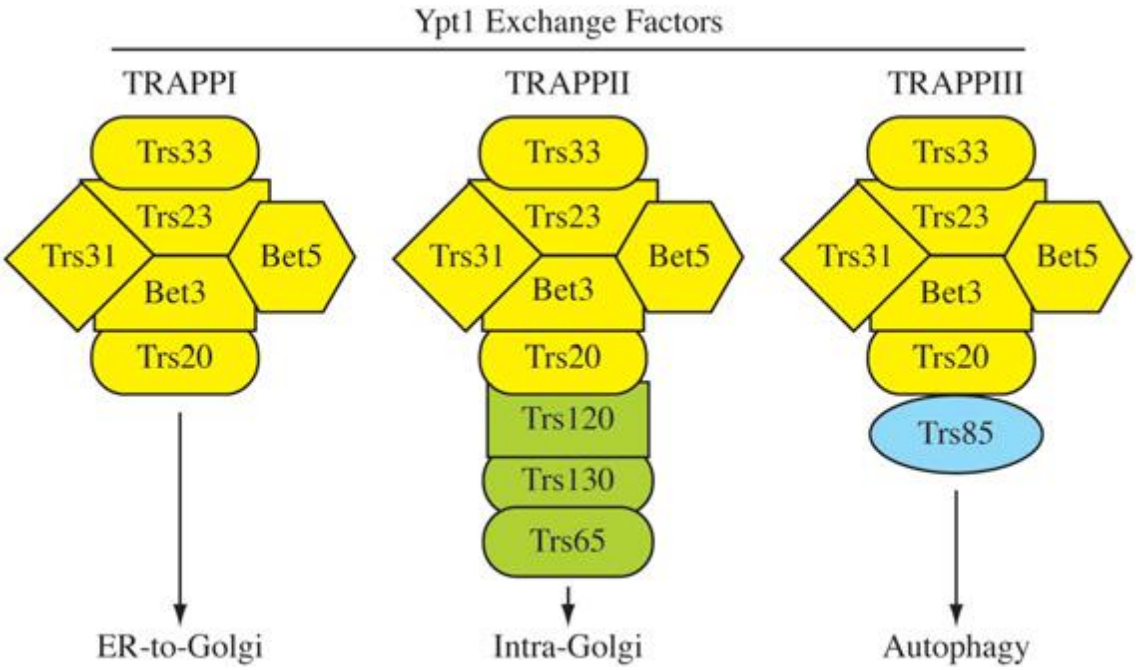

Figure S3.4. Subunit composition of the three TRAPP complexes. The three TRAPP complexes share the core GEF machinery (Bet3, Trs31, Bet5, and Trs23) plus two additional subunits Trs33 and Trs20 (shown in yellow). In addition to these subunits, the TRAPPII complex contains three specific subunits (Trs120, Trs130 and Trs65, shown in green), whereas the Trs85 subunit (shown in blue) is specific to the TRAPPIII complex. The specific subunits determine the localization of the complex and, as indicated in the cartoon, where Ypt1 is activated.

The TRAPPIII complex contains all of the subunits that are required for Ypt1 GEF activity [34]. To determine if Trs85 is a component of a functional Ypt1 GEF, we immobilized TAP-tagged Trs85 on IgG-Sepharose beads and assessed its ability to stimulate the uptake of GTPγS onto Ypt1. As a control, we also assayed TRAPPII (TAP-tagged Trs65), which has comparable Ypt1 GEF activity to TRAPPI [34]. Both TAP-tagged Trs85 and Trs65 stimulated the uptake of GTPγS onto Ypt1 to approximately the same level (Fig. 3.2*E*). These findings show that Trs85 is a component of a Ypt1 GEF that is distinct from TRAPPI and TRAPPII.

Ypt1 Is Required for Nonspecific Autophagy.

The observation that a component of a Ypt1 GEF is required for autophagy [39,40] suggests that Ypt1 may also be required for this event. To address this possibility, the role of this GTPase in autophagy was examined. Ypt1 is an essential component of the ER-Golgi trafficking machinery, and its loss leads to cell death [33,41]. To circumvent this problem, we used conditional *ypt1* mutants. The *ypt1-1*, *ypt1-3* and $ypt1^{A136D}$ mutants are temperature-conditional partial loss-of-function alleles of *YPT1* that block ER-Golgi traffic at the nonpermissive temperature [42]. To begin our analysis, we used the Pho8Δ60 (vacuolar alkaline phosphatase lacking the N-terminal 60 amino acids) assay, which provides a quantitative method to measure autophagic activity [43]. In wild-type yeast, nitrogen-starvation induces autophagy and delivery of Pho8Δ60 from the cytosol into the vacuole lumen, resulting in activation of Pho8. The *ypt1-1* mutant, which grows poorly at all temperatures, was defective in Pho8Δ60 activation at the permissive (30 °C) and nonpermissive (14 °C) temperatures (Fig. 3.3*A*). The $ypt1^{A136D}$ mutant showed some reduction in activity at the permissive (25 °C)

temperature relative to the isogenic parental strain and essentially a complete block in Pho8Δ60 activity at 37 °C (Fig. S3.5*A*), whereas *ypt1-3* was essentially normal at the permissive (25 °C) temperature, but blocked at 37 °C (Fig. 3.3*A*), indicating impaired autophagy in both cases. These results also suggest that the defect was not allele-specific.

As a second method to analyze autophagy, we examined translocation of the autophagy protein Atg8 (fused to GFP) to the vacuole. In wild-type cells, GFP-Atg8 is localized to the PAS and the cytosol. Rapamycin treatment induces autophagy and results in delivery of GFP-Atg8 into the vacuole. This process is evidenced by a GFP signal in the vacuole lumen. At the permissive or nonpermissive temperature, all of the wild-type strains showed GFP-Atg8 localization at the PAS and/or in the vacuole lumen (Fig. 3.3*B* and Fig. S3.5*B*). In contrast, the *ypt1-3* and $ypt1^{A136D}$ mutants at the nonpermissive temperature, and the*ypt1-1* strain at either temperature, displayed blocks in GFP-Atg8 transport, as shown by a lack of GFP signal in the vacuole lumen of the mutant cells after rapamycin treatment (Fig. 3.3*B* and Fig. S3.5*B*).

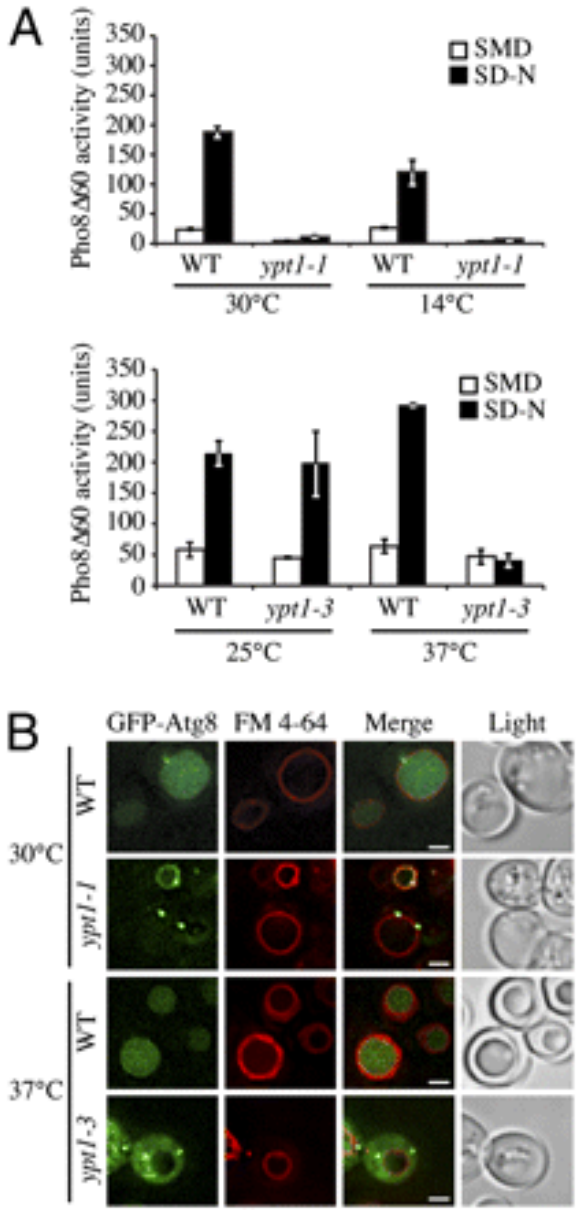

Figure 3.3. Ypt1 is involved in nonspecific autophagy in yeast. (*A*) Isogenic wild-type (WT) and the indicated *ypt1* mutant strains were cultured in growth medium (SMD) at the permissive temperature (30 °C or 25 °C), to exponential phase and then shifted to a nonpermissive temperature (14 °C or 37 °C); the *ypt1-1*mutant is cold sensitive for growth and was analyzed at 14 °C. In parallel, cells were switched to nitrogen starvation (SD-N) medium for 4 h at each temperature. Cell lysates from each condition were collected and assayed for Pho8Δ60 activity. Error bars indicate SE. (*B*) The isogenic wild-type and *ypt1*mutant strains were transformed with GFP-Atg8, grown to exponential phase as in *A* and then shifted to the nonpermissive temperature for 30 min. Rapamycin (0.2 μM) was added for 4 h. Shown are epifluorescent images of GFP-Atg8 and the vacuolar limiting membrane (stained with FM 4–64). (Scale bars, 2.5 μm.)

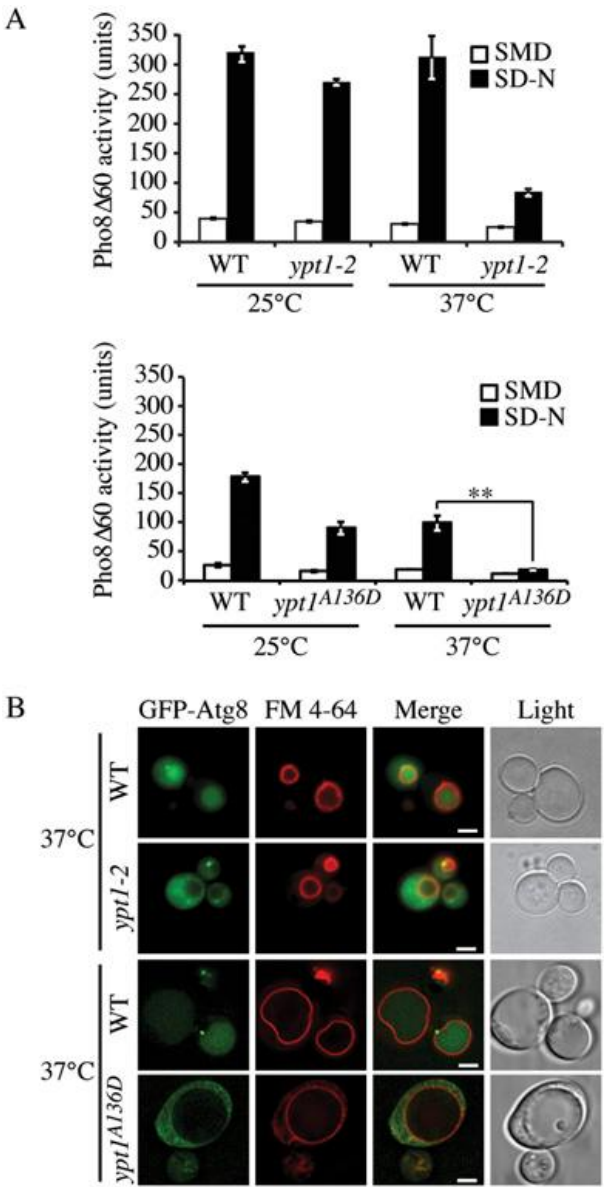

Figure S3.5. Ypt1 is involved in nonspecific autophagy in yeast. (A) Isogenic wild-type (WT) and the indicated ypt1 mutant strains were cultured in growth medium (SMD) at the permissive temperature (25 °C), to exponential phase and then shifted to a nonpermissive temperature (37 °C); the ypt1-2 mutant is not temperature sensitive for growth, but displays a temperature-sensitive phenotype for autophagy. In parallel, cells were switched to nitrogen starvation (SD-N) medium for 4 h at each temperature. Cell lysates from each condition were collected and assayed for Pho8Δ60 activity. Error bars indicate SE. Double asterisks indicate a significant reduction from the WT level, $P < 0.01$. (B) The isogenic wild-type and ypt1 mutant strains were transformed with GFP-Atg8, grown to exponential phase as in (A) and then shifted to 37 °C for 30 min. Rapamycin (0.2 μM) was added for 4 h. Shown are epifluorescent images of GFP-Atg8 and the vacuolar limiting membrane (stained with FM 4–64). (Scale bars, 2.5 μm.)

Membrane flow through the secretory pathway is required for autophagy [4,5], leaving open the possibility that any defect in autophagy that we observe may be an indirect consequence of blocking secretion. For this reason, we also analyzed the *ypt1-2* mutant, which is not temperature-sensitive for growth and blocks membrane traffic in vitro but not in vivo [41]. The *ypt1-2* mutant displayed a defect in Pho8Δ60 activity (Fig. S3.5*A*) and in the delivery of GFP-Atg8 to the vacuole at elevated temperatures (Fig. S3.5*B*). Although we observed occasional GFP fluorescence in the vacuole lumen with the *ypt1-2* mutant, the percentage of cells exhibiting vacuolar GFP-Atg8 localization was 17% for the *ypt1-2* strain compared to 90% for wild type at 37 °C.

Previous studies indicate that the *trs85*Δ mutant is defective in autophagosome formation [40] and in GFP-Atg8 localization to the PAS [39]. To place Ypt1 and Trs85 within the autophagy pathway we examined GFP-Atg8 localization in two different *ypt1* alleles. We found an approximately 24%, 47%, and 26% reduction in GFP-Atg8 puncta at the PAS in the *trs85*Δ, *ypt1-2*, and *ypt1-3* mutants, respectively (Fig. S3.6*A*). In addition, when compared to wild type, these mutants displayed a substantial increase in the number of cells with more than one GFP-Atg8 punctum per cell (Fig. S3.6*B*), suggesting a defect in both the recruitment and localization of Atg8 to the PAS. Combined with the previous data, these results imply that Ypt1 and Trs85 play a role in autophagosome biogenesis.

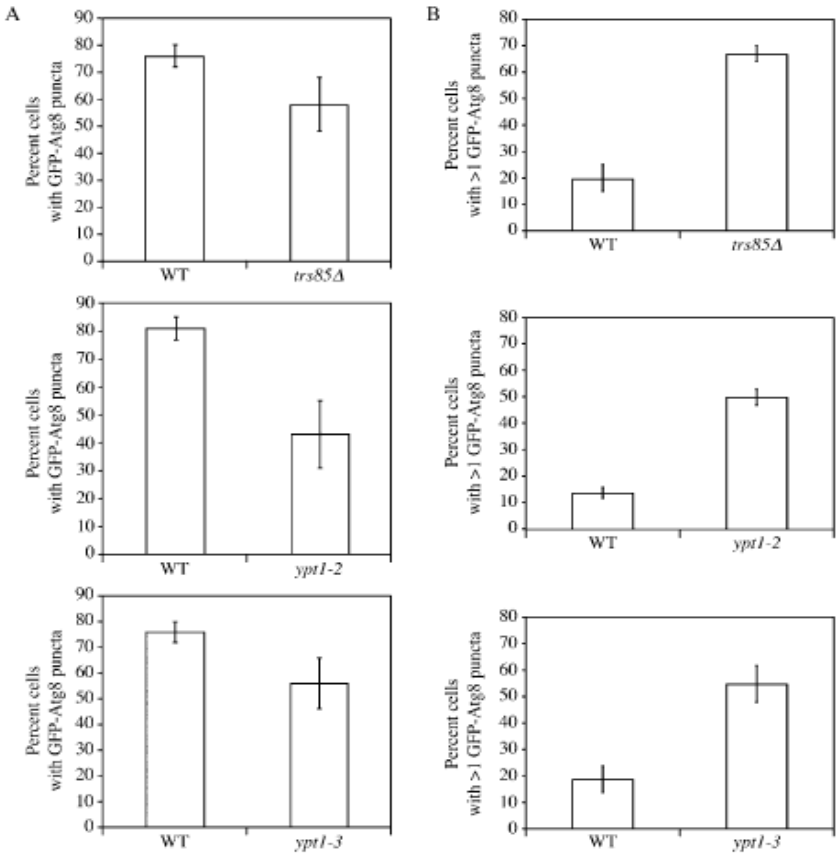

Figure S3.6. Ypt1 and Trs85 function at the stage of autophagosome formation. The *trs85Δ*, *ypt1-2* and *ypt1-3* mutants and the corresponding isogenic wild-type strains transformed with GFP-Atg8 were grown to exponential phase at 30 °C and kept at that temperature (*trs85Δ*) or shifted to 37 °C for 30 min (*ypt1-2* and *ypt1-3*) and then treated with rapamycin as described in Fig. S3.5. (A) The percent of cells with GFP-Atg8 puncta were quantified. (B) The percent of cells with more than one GFP-Atg8 punctum were quantified. Error bars represent the standard deviation

Ypt1 Is Required for Specific Autophagy.

To extend our analysis of the role of Ypt1 in autophagy, we examined a selective type of autophagy, the Cvt pathway, which delivers the precursor form of the resident hydrolase aminopeptidase I (prApe1) to the vacuole, where it is proteolytically activated. As expected, *atg1*Δ mutant cells that are defective in the Cvt pathway accumulated prApe1 (Fig. 3.4). In contrast, wild-type cells contained primarily the mature form of Ape1 (Fig. 3.4). The *ypt1* mutant strains displayed variable defects in the processing of prApe1, ranging from partial (*ypt1-1*, *ypt1-2*, and *ypt1-3*) to complete blocks ($ypt1^{A136D}$). In general, equivalent defects were seen at the permissive and nonpermissive temperatures, suggesting that the Cvt pathway was particularly sensitive to the functional status of Ypt1. It is likely that the mutant protein does not retain complete function even at the permissive temperatures. These results indicate a role for Ypt1 in specific autophagy.

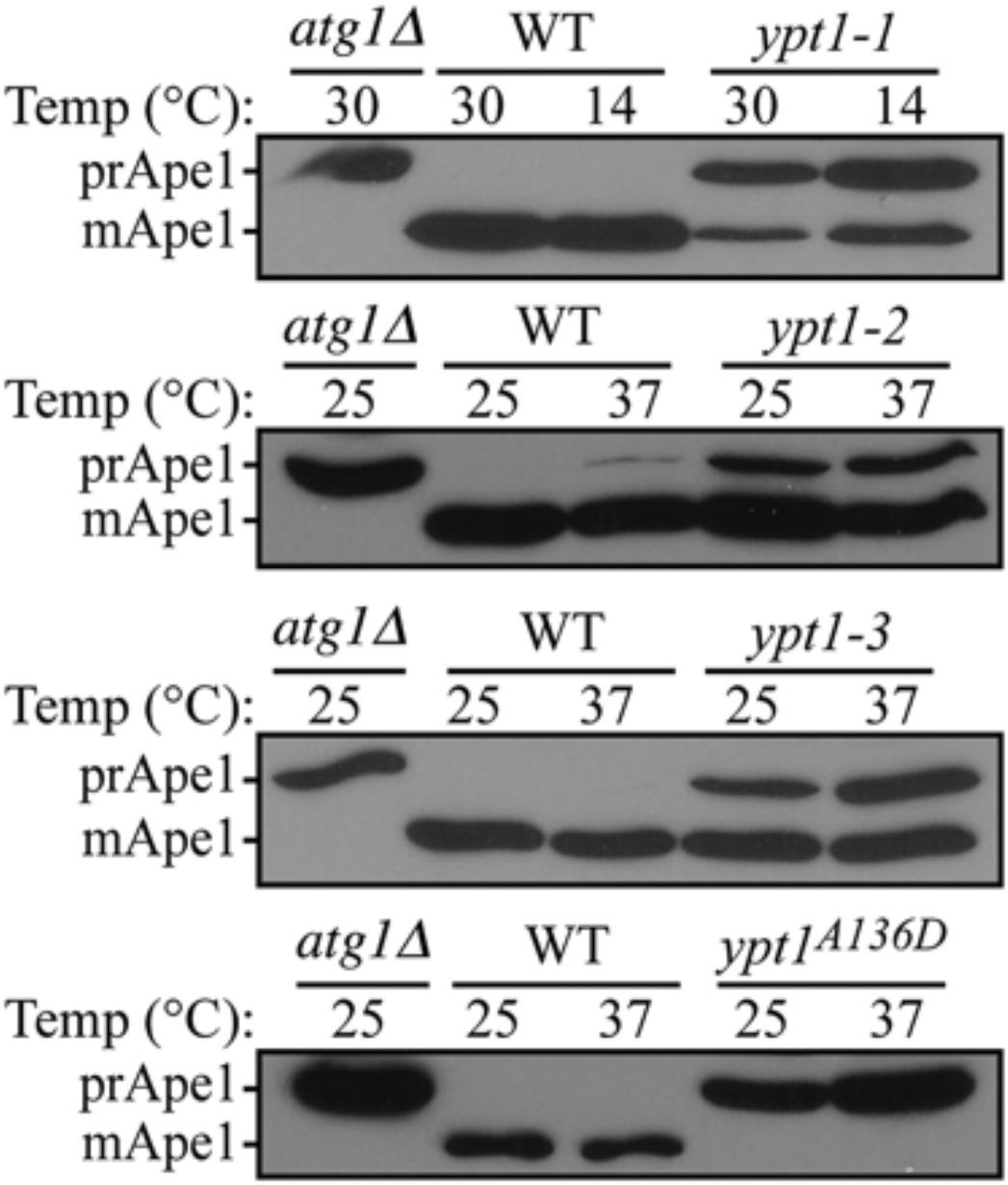

Figure 3.4. The *ypt1* mutants are defective for the Cvt pathway. The isogenic wild-type and *ypt1* mutant strains used in Fig. 3.3 and an *atg1*Δ control strain were cultured in rich medium (SMD) at the indicated permissive temperature to exponential phase and then shifted to the indicated nonpermissive temperature for 60 min. Protein extracts were resolved by SDS/PAGE and Western blot analysis was performed with anti-Ape1 antiserum. The positions of prApe1 and mature Ape1 are as indicated.

A Constitutively Active *ypt1* Mutant Suppresses the *trs85*Δ Defect.

If Ypt1 is involved in directing membrane flow to the autophagy pathway, we hypothesized that elevated expression of Ypt1 might display enhanced autophagic activity. Therefore, we overexpressed Ypt1 and examined autophagy using the Pho8Δ60 assay. There was no change in autophagy activity in rich medium; however, following starvation we observed an approximately 30% increase in Pho8Δ60 activity (Fig. 3.5*A*), suggesting that Ypt1 is a limiting factor for the autophagy process.

We extended our analysis by determining whether a constitutively active (i.e., GTP-bound) form of Ypt1 affected autophagy. First, we expressed the *ypt1*^{Q67L}mutant under the control of the *GAL1* promoter and examined the effect on nonspecific autophagy. Even under basal conditions (nutrient-rich medium) there was an elevation in Pho8Δ60 activity in the presence of *ypt1*^{Q67L} (Fig. 3.5*B*). A similar increase in activity was seen when autophagy was induced by starvation (Fig. 3.5*B*). Second, to further examine the role of the Trs85-containing TRAPPIII complex as an autophagy-specific GEF for Ypt1, we expressed the constitutively active *ypt1*^{Q67L} mutant in a strain deleted for *TRS85* and monitored the effect on the Cvt pathway. As seen previously, the *trs85*Δ mutant accumulated only the precursor form of Ape1 similar to the *atg1*Δ control strain (Fig. 3.5*C*, lanes 1 and 3). Overexpression of wild-type Ypt1 in the *trs85*Δ mutant had no effect on prApe1 processing (Fig. 3.5*C*, lane 4). In contrast, overexpression of the *ypt1*^{Q67L} mutant resulted in complete maturation of prApe1, indicating efficient delivery to the vacuole (Fig. 3.5*C*, lane 5). Thus, the constitutively active form of Ypt1 suppressed the defect in the Cvt pathway that resulted from the loss of Trs85.

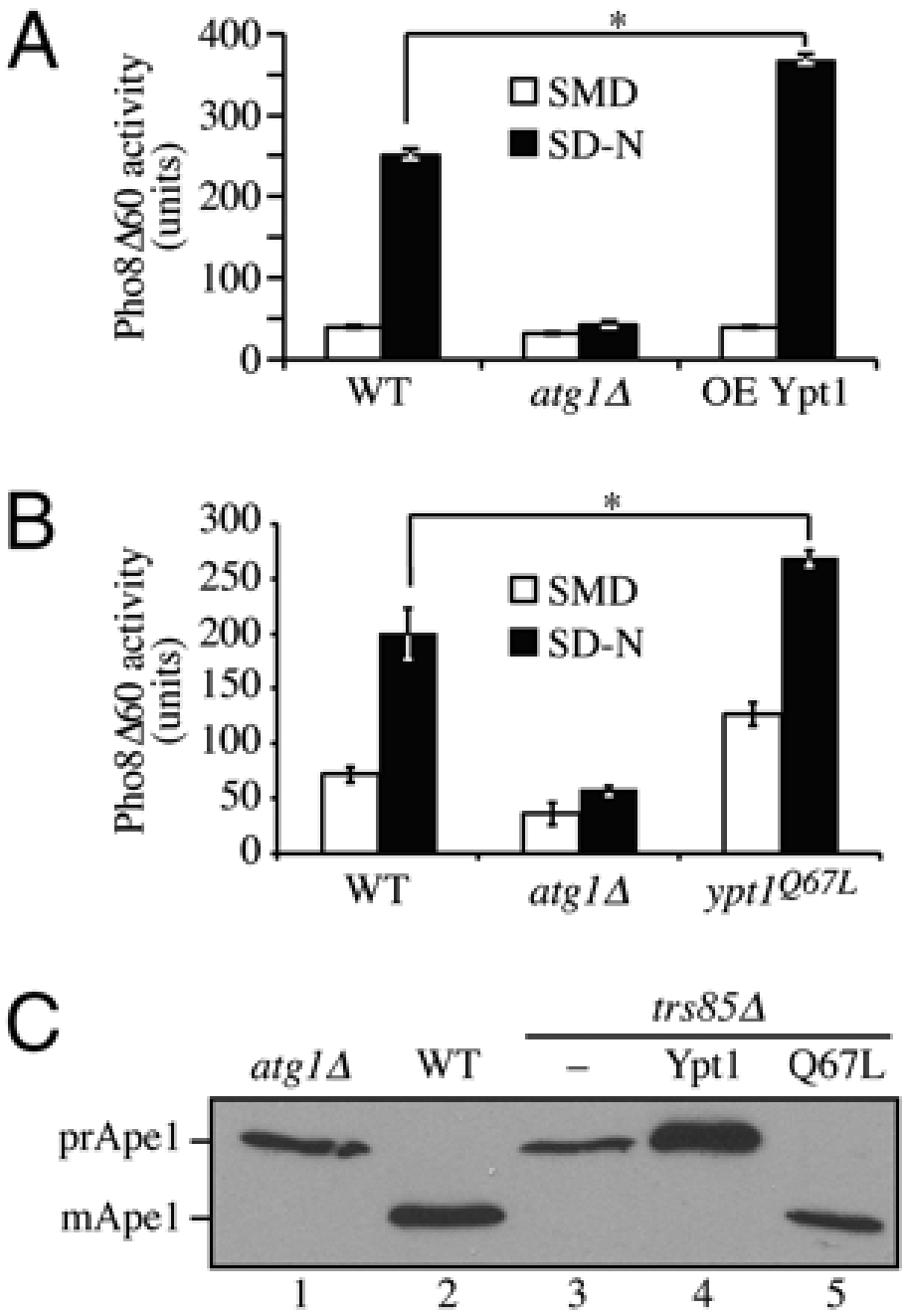

Figure 3.5. Ypt1 overexpression enhances autophagy and constitutively active Ypt1 bypasses the requirement for its GEF. (*A*) Wild-type (WT; TN124), *atg1*Δ, and Ypt1 overexpressing (OE Ypt1) cells were grown at 30 °C and shifted to SD-N medium for 4 h. Protein extracts were analyzed by the Pho8Δ60 assay. Error bars indicate SE. The asterisk indicates a significant difference from the WT level, $P < 0.05$. (*B*) WT, *atg1*Δ, and *ypt1*^{Q67L} cells were grown and analyzed as in *A*. (*C*) WT, *atg1*Δ, and *trs85*Δ cells harboring an empty vector or a plasmid encoding Ypt1 or Ypt1^{Q67L} were grown in rich medium to exponential phase. Protein extracts were resolved by SDS/PAGE and Western blot analysis was performed with anti-Ape1 antiserum.

Trs85 Directs Ypt1 to the PAS.

The observation that Trs85 is required for autophagy [39,40] and is part of an autophagy-specific GEF for Ypt1 raised the possibility that TRAPPIII is targeted to the PAS. To address this point, we examined the localization of Trs85 and Ypt1. In yeast, autophagosomes are thought to form at the PAS. Thus, Ypt1 and Trs85 should localize to the PAS if they play a direct role in autophagy. Because of this, we compared the localization of Ypt1 and Trs85 to Trs65 and Trs130. Trs65 and Trs130 are only present in the TRAPPII complex, and Trs65 is not required for the Cvt pathway or autophagy [39,40]. All proteins were tagged with GFP and expressed in cells with RFP-Ape1, a marker for the PAS. The cells were grown to midlog phase and then starved for 45 min before determining the extent of colocalization between RFP-Ape1 and the GFP tagged proteins. Both Ypt1 and Trs85 colocalized to the PAS at a much higher rate than Trs65 or Trs130 (approximately 44%, 34%, 4%, and 10%, respectively) (Fig. 3.6 and Table S3.1). Cells lacking *atg1*Δ are defective in autophagosome formation, which leads to the accumulation of autophagic proteins at the PAS [44]. Therefore, we examined the localization of Ypt1 and the TRAPP subunits in an *atg1*Δ strain. We found an increase in colocalization in the absence of Atg1, which was most apparent for Trs85 (Fig. 3.6 and Table S3.1); however, even in the*atg1*Δ background, Trs65 and Trs130 did not display significant colocalization with the PAS marker. To verify that the punctate appearance of Trs85 was not due to multimerization of the triple-GFP tag, we expressed Trs85-3xGFP in the multiple-knockout (MKO) strain. The MKO strain lacks the 24 *ATG* genes that are known to be required for autophagosome formation in *Saccharomyces cerevisiae* [45]. When expressed in the MKO strain, Trs85-3xGFP

displayed occasional puncta along with diffuse cytosolic staining (Fig. S3.7). The few Trs85-3xGFP puncta observed did not colocalize with RFP-Ape1 in either rich medium or starvation conditions, indicating that this chimera did not aggregate and did not colocalize with prApe1 in the absence of the Atg proteins. These findings indicate that Trs85, but not Trs65 or Trs130, localizes to the PAS and that this localization is dependent on Atg proteins. Consistent with the notion that Trs85 and Trs65 are in separate TRAPP complexes, we found a larger cytoplasmic pool of Trs85 (Fig. 3.6 and Fig. S3.8*A*).

We also examined localization of these subunits in the *atg9*Δ and *atg11*Δ strains. The absence of either Atg9 or Atg11 caused a decrease in the level of Trs85 or Ypt1 that colocalized with RFP-Ape1 relative to the *atg1*Δ strain, but neither deletion had a significant effect on the low level of colocalization seen with Trs65 or Trs130 (Table S3.1). Atg11 is required for the movement of Atg9, a putative membrane carrier for autophagy-related pathways [46,47], to the PAS. Decreased colocalization of Trs85 and Ypt1 in the *atg9*Δ and *atg11*Δ mutants relative to the*atg1*Δ strain is consistent with the hypothesis that Ypt1 and its GEF tethers Atg9-containing membranes needed for the biogenesis of autophagic sequestering vesicles. In agreement with this proposal, we found that the peripheral pools of Atg9, which are thought to mark the donor membranes involved in autophagosome biogenesis, colocalize with Ypt1 (85% ± 6 of the cells have at least one overlapping punctum, n = 211 cells; Fig. S3.8*B*). Finally, we monitored the localization of Ypt1 in the absence of Trs85. GFP-Ypt1 colocalization with RFP-Ape1 dropped from approximately 44% in the wild-type strain to 12% in the*trs85*Δ background

(Fig. 3.6 and Table S3.1). Together, these findings imply that Trs85 plays a role in directing Ypt1 to the PAS.

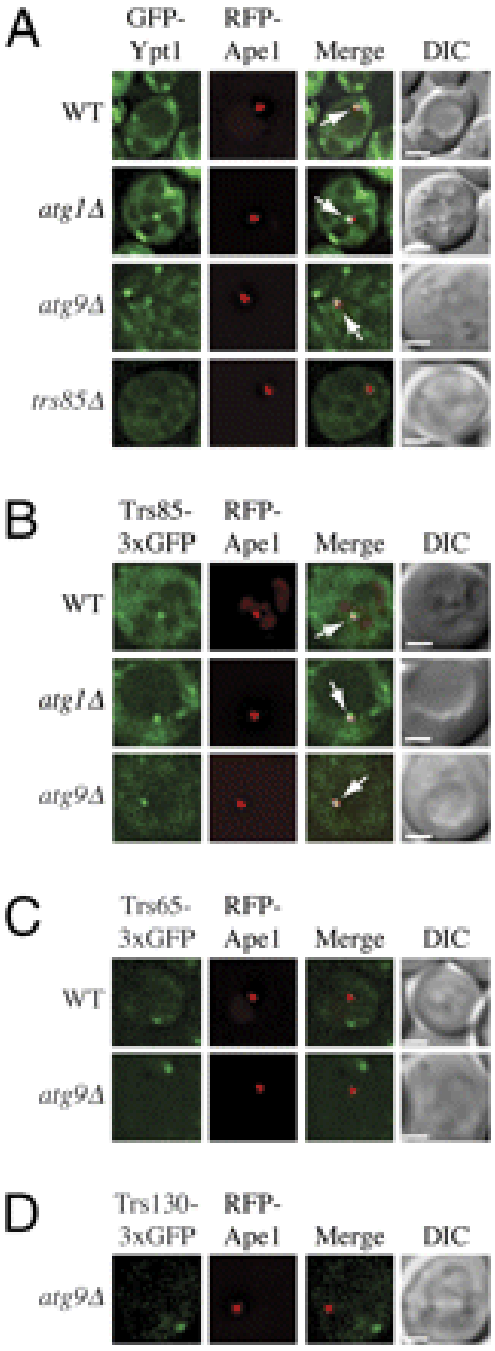

Figure 3.6. Ypt1 and Trs85 localize to the PAS. (*A*) Wild-type (WT, SEY6210), *atg1*Δ (WHY1), *atg9*Δ (JKY007), and *trs85*Δ (YJH3) cells transformed with plasmids expressing RFP-Ape1 and GFP-Ypt1; (*B*) WT (YJH9), *atg1*Δ (YCB151), and *atg9*Δ (MDY15) cells expressing integrated RFP-Ape1 and Trs85-3xGFP; (*C*) WT (SFNY1573) and *atg9*Δ strains expressing Trs65-3xGFP (MDY12); or (*D*) the *atg9*Δ strain expressing Trs130-3xGFP (MDY10) were cultured in SMD medium to exponential phase before being transferred to SD-N medium for 45 min. The cells were then analyzed by fluorescence microscopy. Arrows mark overlapping GFP-Ypt1 and RFP-Ape1 puncta, and overlapping Trs85-3xGFP and RFP-Ape1 puncta. (Scale bar, 2.5 μm.)

Table S3.1. Summary of localization data.

Strain	Total RFP-Ape1 puncta	Total RFP-Ape1 puncta colocalized with GFP	Percentage	SE
GFP-Ypt1	202	88	43.6	5.3
GFP-Ypt1 *atg1*Δ	267	138	51.7	3.5
GFP-Ypt1 *atg11*Δ	231	75	32.5	1.9
GFP-Ypt1 *atg9*Δ	212	59	27.8	4.5
GFP-Ypt1 *trs85*Δ	234	29	12.4	1.5
Trs85-3xGFP	227	77	33.9	3.1
Trs85-3xGFP *atg1*Δ	322	191	59.3	7.6
Trs85-3xGFP *atg11*Δ	302	130	43.0	1.3
Trs85-3xGFP *atg9*Δ	203	110	54.2	2.7
Trs130-3xGFP	208	20	9.6	3.2
Trs130-3xGFP *atg1*Δ	212	33	15.6	1.5
Trs130-3xGFP *atg11*Δ	216	31	14.3	3.1
Trs130-3xGFP *atg9*Δ	240	23	9.6	0.5
Trs65-3xGFP	201	8	4.0	1.8
Trs65-3xGFP *atg1*Δ	241	14	5.8	0.6
Trs65-3xGFP *atg11*Δ	214	13	6.1	1.5
Trs65-3xGFP *atg9*Δ	207	12	5.8	2.1

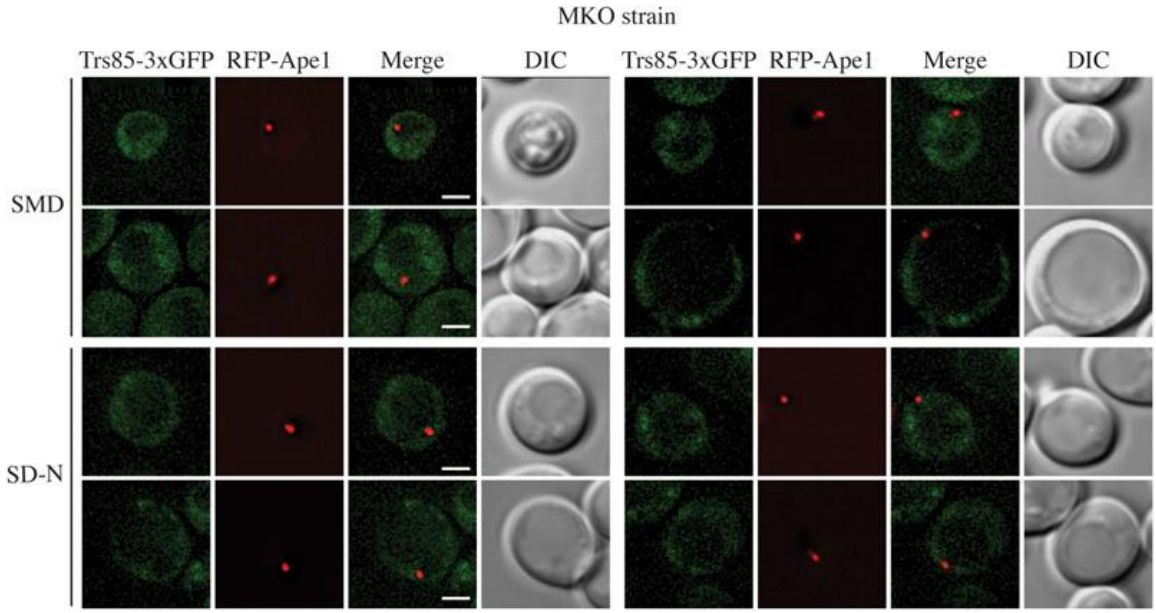

Figure S3.7. The GFP tag on Trs85 does not result in aggregate formation. Trs85-3xGFP was integrated into the MKO strain (MDY14) that expressed RFP-Ape1. Cells were grown in rich medium to exponential phase and shifted to SD-N for 45 min before microscopy. (Scale bars, 2.5 μm.) DIC, differential interference contrast.

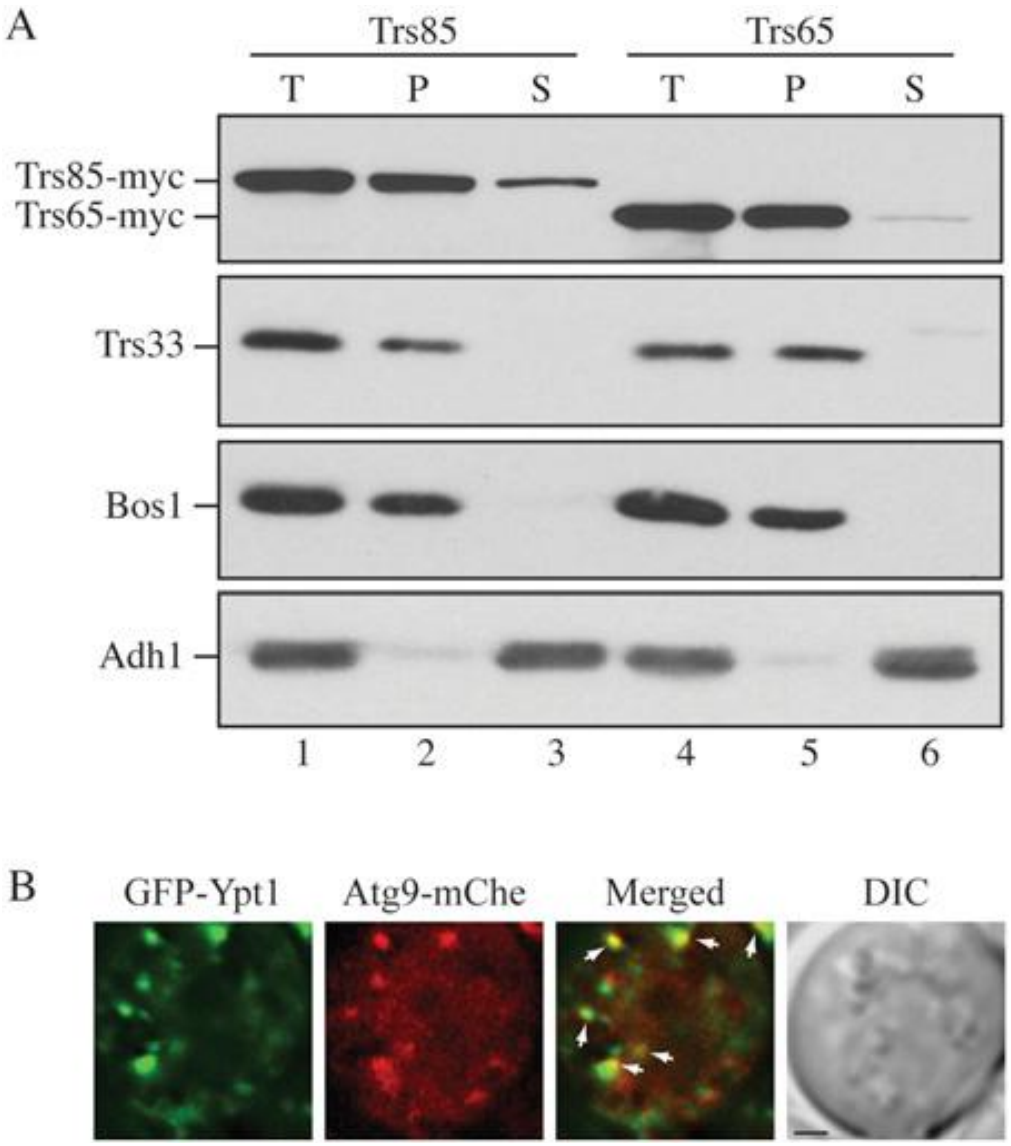

Figure S3.8. Subcellular fractionation and localization of Trs85. (A) Total cell lysates (T) of the Trs85-13xmyc (SFNY1295; lanes 1–3) and Trs65-13xmyc (SFNY1302; lanes 4–6) strains were centrifuged at 132,000 × g and the supernatant (S) and pellet (P) fractions were collected. Equal volumes of the lysate, supernatant and pellet fractions were analyzed by Western blot analysis. Bos1 and Adh1 were used as controls for the membrane and soluble fractions, respectively. (B) Wildtype (SEY6210) cells expressing Atg9-mCherry (Atg9-mChe; integrated at the LEU2 locus) and transformed with a plasmid expressing GFP-Ypt1, were grown to midlog phase in selective SMD medium at 30 °C. The cells were then analyzed by fluorescence microscopy. Arrows mark sites of overlap between Atg9-mCherry and GFP-Ypt1. (Scale bar, 2.5 μm.) DIC, differential interference contrast.

Discussion

Here we describe a third form of the TRAPP complex, TRAPPIII, which contains Trs85 and is a GEF for Ypt1. Additionally, we show that TRAPPIII and Ypt1 are required for the Cvt pathway and nonselective autophagy. The defect in autophagy-related processes in the *ypt1* mutants we analyzed is not an indirect consequence of blocking ER-to-Golgi traffic because these phenotypes are seen under conditions where secretory traffic is normal. Similarly, the loss of Trs85 has no effect on the secretory pathway but disrupts specific and nonspecific autophagy. We also found that Trs85 and Ypt1, and not the TRAPPII-specific subunits Trs65 and Trs130, localize to the PAS. Although previous studies implicated Trs85 in these processes [39,40], the relationship between Trs85, TRAPP and autophagy has remained unclear until now. The findings we report here indicate that TRAPPIII and Ypt1 play a direct role in the Cvt pathway and autophagy. Additionally, they imply that Trs85 directs the Ypt1 GEF, TRAPPIII, to the phagophore to promote autophagy.

Our experiments show that Ypt1 is essential for both specific and nonspecific autophagy (Fig. 3.3–3.5). Based on the results we report here and previous findings, we propose that TRAPPIII and Ypt1 are required for a membrane tethering event that is needed for Cvt vesicle and autophagosome formation. It was recently reported that the Ypt1 effector COG is also needed for the Cvt pathway and autophagy [7]. The COG complex contains two lobes, A and B [48]. The A lobe, but not the B lobe, is required for autophagosome formation [7]. Consistent with the proposal that TRAPPIII and Ypt1 are required for Cvt vesicle formation, prApe1 is sensitive to exogenously added protease in *trs85*Δ cells [39,40] and Atg8 is mislocalized in *trs85*Δ and *ypt1* mutants [39,40] (Fig.

S3.6). No defect in the localization of Atg9 was previously reported in *trs85*Δ cells [39]. Together, these results imply that TRAPPIII and Ypt1 are needed after Atg9 is recruited to the PAS but before or at the stage of Atg8 recruitment.

Our findings show that yeast cells contain three GEFs for Ypt1: TRAPPI, TRAPPII and TRAPPIII. The TRAPP complexes act in ER-Golgi traffic (TRAPPI) [29,35], Golgi traffic (TRAPPII) [29,36], and autophagy (TRAPPIII). All three complexes share several subunits (Bet3, Trs23, Bet5, and Trs31) that are essential for Ypt1 GEF activity, as well as Trs20 and Trs33. Trs65 (not present in higher eukaryotes), Trs120, and Trs130 are specific to TRAPPII, whereas Trs85 is only in TRAPPIII (Fig. S3.4). We previously postulated that the TRAPPII-specific subunits Trs120 and Trs130 target Ypt1/Rab1 GEF activity to COPI coated vesicles [34,37]. Here we show that the TRAPP subunit Trs85 targets Ypt1 GEF activity to the PAS. Thus, certain TRAPP subunits act as adaptors to bring core GEF components to different parts of the cell [34,37]. The cellular components that interact with Trs85 at the PAS are the focus of current studies.

Materials and Methods

Strains and Media.

Yeast strains used in this study are listed in Table S3.2. Strains were grown in media (SMD, YPD, YPL, and YTO) as described previously [44,49]. For autophagy induction, cells were shifted to SD-N or treated with rapamycin [44].

Immunoblotting and Quantitative Analysis.

Protein samples for Western blot analysis were analyzed as described previously [44].

Fluorescence Microscopy.

Cells were cultured in SMD selective medium to midlog phase. For starvation experiments, cells were shifted to SD-N for 45 min. Fluorescence signals were visualized on a DeltaVision system using an Olympus IX71 fluorescence microscope (Olympus). The images were captured by a Photometrics CoolSNAP HQ camera (Roper Scientific, Inc.) and deconvolved using softWoRx software (Applied Precision).

Nucleotide Exchange Assay.

TRAPP was purified from strains SFNY1080 and SFNY1075 and the uptake of GTPγS was measured as described previously [26].

Gel Filtration Analysis and Immunoprecipitation.

Yeast cells were radiolabeled as described previously [29]. An aliquot (200×10^6 cpm) of radiolabeled lysate or 10 mg of cleared lysate was applied to a Superdex 200 gel filtration column and fractions of 1 mL were collected. Fractions [26,36], or 2 mg of cleared lysate, were immunoprecipitated with anti-myc antibody and analyzed by SDS-polyacrylamide gel electrophoresis.

Other Assays.

The Pho8Δ60 assay was done as previously described [40].

SI Materials and Methods

Yeast Strains and Cultures. The ypt1-3 allele was isolated previously [50] and integrated into BY4742 by PCR as follows: ypt1-3 was amplified from Y6938 and the kanR MX4 cassette from pUCKanMX6 (Rosetta) with the primers F1: ATGAATAGCGAGTACGATTACCTGTTCAAACT , R2: GACCCGGCGGGGACGAGGCAAGCTAAACAGATCTAAATGTTGTGCATTAATT GCTGTGGCAG (for ypt1-3), F3: AGATCTGTTTAGCTTGCCTCGTCC, and R4:TAGTTATTATATTATATGGGTCTGCAAGGTAGAGGCGCGCTTGTGAATTCG AGCTCGTTTTCGACACTG (for the kanR MX4 cassette). The two PCR products were cotransformed into strain BY4742, and the transformants were selected on YPD containing G418. To induce the mutant phenotype in the ypt1-3 mutant, cell cultures were shifted from 25 °C to 37 °C for 30 min. For the ypt1A136D mutant, cells were shifted from 30 °C to 37 °C. Where indicated, cells were treated with rapamycin (0.2 μM) to induce autophagy. The lipophilic dye FM 4–64 was from Molecular Probes/Invitrogen.

Plasmids. The plasmid pCuGFPATG8, which expresses Atg8 with an N-terminal GFP fusion, and RFP-Ape1 were described previously [51]. The Ypt1 overexpression plasmid CUP1p-YPT1-HA (426) was created as follows: the YPT1 ORF fused to HA-coding DNA was amplified from yeast genomic DNA with primers Fwd: ATATCGCGCGGATCCATGAATAGCGAGTACGATTAC (including a BamHI site) and Rev:

ATATCTCGAGCTAAGCATAGTCAGGCACATCATAGGGGTATCTAGAACAGCA GCCCCCACCGGTGT (including HA-coding sequence, and a Xho1 site). The YPT1-HA fragment was cloned into pCu426 [52]. Western blot analysis verified that the expression level of Ypt1 was higher under the control of the CUP1 promoter than the endogenous YPT1 promoter. GFP-Ypt1 contains YPT1 from S. cerevisiae N-terminally fused to eGFP in YCplac33 and was a gift from Dr. Benjamin Glick (University of Chicago, Chicago, IL). Immunoprecipitation. Pulse-chase labeling and immunoprecipitation of Prc1 was carried out as described previously [53,54]. GFP-Atg8 Processing. The GFP-Atg8 processing assay to monitor nonspecific autophagy was carried out as described previously [44]. Differential Fractionation. One hundred OD600 units of cells of strains SFNY1295 and SFNY1302 were converted to spheroplasts and lysed in lysis buffer (20 mM Hepes, pH 7.4, plus protease inhibitors) by dounce homogenization. The cell debris was removed after centrifugation at 500 × g for 2 min, and the supernatant fraction (T, total cell lysate) was centrifuged at 132,000 × g. The resulting pellet (P) fraction was resuspended in the same volume as the new supernatant (S) fraction. For Western blot analysis, 30 μg of lysate was loaded on the gel.

Table S3.2. Strains.

Strain	Genotype	Source
AHY001	SEY6210 *atg11Δ::HIS3*	(1)
atg1Δ	BY4742 *atg1Δ::KAN*	ResGen
BY4742	*MATα his3Δ1 leu2Δ0 lys2Δ0 ura3Δ0*	ResGen
CBY474	*MATα his3Δ1 leu2Δ0 lys2Δ0 ura3Δ0 ypt1-3*	(2)
DBY1034	*MATa ypt1-1 (T40K) his4-539 lys2-801 ura3-52*	(3)
DBY1803	*MATa his4-539 lys2-801 ura3-52*	(3)
HAY572	TN124 *atg1Δ::URA3*	(4)
JKY007	SEY6210 *atg9Δ::HIS3*	(5)
MDY1	DBY1803 *pho8::pho8Δ60 (TRP1) pho13Δ::KAN*	This study
MDY2	NSY161 *pho8::pho8Δ60 (TRP1) pho13Δ::KAN*	This study
MDY3	NY2304 *pho8::pho8Δ60 (URA3) pho13Δ::KAN*	This study
MDY4	CBY474 *pho8::pho8Δ60 (HIS3) pho13Δ::LEU2*	This study
MDY5	DBY1034 *pho8::pho8Δ60 (TRP1) pho13Δ::KAN*	This study
MDY6	NSY160 *pho8::pho8Δ60 (TRP1) pho13Δ::KAN*	This study
MDY7	NY1211 *pho8::pho8Δ60 (URA3) pho13Δ::KAN*	This study
MDY8	BY4742 *pho8::pho8Δ60 (HIS3) pho13Δ::LEU2*	This study
MDY9	JKY007 *TRS85-3xGFP::URA3*	This study
MDY10	YJH17 *atg9Δ::HIS3*	This study
MDY11	AHY001 *TRS65-3xGFP::URA3*	This study
MDY12	JKY007 *TRS65-3xGFP::URA3*	This study
MDY13	WHY1 *TRS65-3GFP::URA3*	This study
MDY14	YCY123 *TRS85-3xGFP::URA3*	This study
MDY15	YJH9 *atg9Δ::HIS3*	This study
NSY160	*MATα his4-539 ura3-52*	(6)
NSY161	*MATa his4-539 ura3-52 ypt1*^{A136D}	(6)
NSY222	NSY160 *ypt1*^{A136D}	(6)
NY915	*MATα his3Δ200 leu2-3,112 trp1 ura3-52*	Peter Novick
NY1211	*MATα his3Δ200 leu2-3,112 ura3-52*	(7)
NY2304	NY1211 *ypt1-2*	(7)
SEY6210	*MATα leu2-3,112 ura3-52 his3Δ200 lys2-801 suc2-Δ9 trp1Δ905*	(8)
SFNY26-3a	*MATa ura3-52*	(9)
SFNY596	*MATa bet3-1 ura3-52 leu2-3,112*	(10)
SFNY656	*MATa ura3-52 BET3-3x-c-myc*	(11)
SFNY996	*MATa trs85Δ BET3-3x-c-myc*	(9)
SFNY1040	*MATa trs85Δ*	This study
SFNY1075	*MATα leu2-3,112 trp1 ura3-52 L-A-o TRS65-TAP::TRP1*	
SFNY1080	*MATα leu2-3,112 trp1 ura3-52 L-A-o TRS85-TAP::TRP1*	This study
SFNY1295	*MATα his3Δ200 leu2-3,112 trp1 ura3-52 TRS85-13xmyc::HIS3*	This study
SFNY1296	*MATα his3200Δ leu2-3,112 trp1 ura3-52 TRS33-13xmyc::HIS3*	This study
SFNY1301	*MATα his3200Δ leu2-3, 112 trp1 ura3-52 TRS120-13xmyc::HIS3*	This study
SFNY1302	*MATα his3200Δ leu2-3,112 trp1 ura3-52 TRS65-13xmyc::HIS3*	This study
SFNY1573	NY1210 *TRS65-3xGFP::URA3*	This study
TN124	*MATa leu2-3,112 trp1 ura3-52 pho8::pho8Δ60 pho13Δ::LEU2*	(12)
trs65Δ	BY4742 *trs65Δ::KAN*	ResGen
trs85Δ	BY4742 *trs85Δ::KAN*	ResGen
WHY1	SEY6210 *atg1Δ::HIS3*	(13)
YCB151	NY1211 *RFP-APE1::LEU2 atg1Δ::KAN TRS85-3xGFP::URA3*	This Study
YCB152	YJH17 *atg1Δ::KAN*	This Study
YCB155	NY1211 *RFP-APE1::LEU2 atg1Δ::KAN TRS130-3xGFP::URA3*	This Study
YCB156	YJH17 *atg11Δ::HIS3*	This Study
YCY123	SEY6210 *atg1Δ 2Δ 3Δ 4Δ 5Δ 6Δ 7Δ 8Δ 9Δ 10Δ 11Δ 12Δ 13Δ 14Δ 16Δ 17Δ 18Δ 19Δ 20Δ 21Δ 23Δ 24Δ 27Δ 29Δ*	(14)
YJH3	SEY6210 *trs85Δ::URA3*	This study
YJH9	NY1211 *RFP-APE1::LEU2 TRS85-3xGFP::URA3*	This study
YJH17	NY1211 *RFP-APE1::LEU2 TRS130-3xGFP::URA3*	This study
YJH36	YJH9 *atg1Δ::HIS3*	This study
YJH37	YJH9 *atg11Δ::HIS3*	This study

1. Scott SV, Nice DC 3rd, Nau JJ, Weisman LS, Kamada Y, Keizer-Gunnink I, Funakoshi T, Veenhuis M, Ohsumi Y, Klionsky DJ. (2000) J Biol Chem 275:25840–25849.

2. Cao X, Ballew N, Barlowe C (1998) EMBO J 17:2156–2165.

3. Segev N, Mulholland J, Botstein D (1988) Cell 52:915–924.

4. Abeliovich H, Zhang C, Dunn WA, Jr, Shokat KM, Klionsky DJ (2003) Mol Biol Cell 14:477–490.

5. Noda T, Kim J, Huang WP, Baba M, Tokunaga C, Ohsumi Y, Klionsky DJ. (2000) J Cell Biol 148:465–480.

6. Jedd G, Richardson C, Litt R, Segev N (1995) J Cell Biol 131:583–590.

7. Du LL, Novick P (2001) Mol Biol Cell 12:1215–1226.

8. Robinson JS, Klionsky DJ, Banta LM, Emr SD (1988) Mol Cell Biol 8:4936–4948.

9. Wang W, Sacher M, Ferro-Novick S (2000) J Cell Biol 151:289–296.

10. Kim DW, Sacher M, Scarpa A, Quinn AM, Ferro-Novick S (1999) Mol Biol Cell 10:3317–3329.

11. Sacher M, Jiang Y, Barrowman J, Scarpa A, Burston J, Zhang L, Schieltz D, Yates JR 3rd, Abeliovich H, Ferro-Novick S. (1998). EMBO J 17:2494–2503.

12. Noda T, Matsuura A, Wada Y, Ohsumi Y (1995) Biochem Biophys Res Commun 210:126–132.

13. Shintani T, Huang W-P, Stromhaug PE, Klionsky DJ (2002) Dev Cell 3:825–837.

14. Cao Y, Cheong H, Song H, Klionsky DJ (2008) J Cell Biol 182:703–713.

References

[1] Axe, E.L., Walker, S.A., Manifava, M., Chandra, P., Roderick, H.L., Habermann, A., Griffiths, G. and Ktistakis, N.T. (2008) J Cell Biol 182, 685-701.

[2] Xie, Z., Nair, U. and Klionsky, D.J. (2008) Mol Biol Cell 19, 3290-8.

[3] Dunn, W.A., Jr. (1990) J Cell Biol 110, 1923-33.

[4] Reggiori, F., Wang, C.W., Nair, U., Shintani, T., Abeliovich, H. and Klionsky, D.J. (2004) Mol Biol Cell 15, 2189-204.

[5] Hamasaki, M., Noda, T. and Ohsumi, Y. (2003) Cell Struct Funct 28, 49-54.

[6] Ishihara, N. et al. (2001) Mol Biol Cell 12, 3690-702.

[7] Yen, W.L. et al. (2010) J Cell Biol 188, 101-14.

[8] Lazar, T., Gotte, M. and Gallwitz, D. (1997) Trends Biochem Sci 22, 468-72.

[9] Martinez, O. and Goud, B. (1998) Biochim Biophys Acta 1404, 101-12.

[10] Bourne, H.R., Sanders, D.A. and McCormick, F. (1990) Nature 348, 125-32.

[11] Macara, I.G., Lounsbury, K.M., Richards, S.A., McKiernan, C. and Bar-Sagi, D. (1996) FASEB J 10, 625-30.

[12] Egami, Y., Kiryu-Seo, S., Yoshimori, T. and Kiyama, H. (2005) Biochem Biophys Res Commun 337, 1206-13.

[13] Munafo, D.B. and Colombo, M.I. (2002) Traffic 3, 472-82.

[14] Gutierrez, M.G., Munafo, D.B., Beron, W. and Colombo, M.I. (2004) J Cell Sci 117, 2687-97.

[15] Jager, S., Bucci, C., Tanida, I., Ueno, T., Kominami, E., Saftig, P. and Eskelinen, E.L. (2004) J Cell Sci 117, 4837-48.

[16] Fader, C.M., Sanchez, D., Furlan, M. and Colombo, M.I. (2008) Traffic 9, 230-50.

[17] Fukuda, M., Kanno, E., Ishibashi, K. and Itoh, T. (2008) Mol Cell Proteomics 7, 1031-42.

[18] Itoh, T., Fujita, N., Kanno, E., Yamamoto, A., Yoshimori, T. and Fukuda, M. (2008) Mol Biol Cell 19, 2916-25.

[19] Becker, J., Tan, T.J., Trepte, H.H. and Gallwitz, D. (1991) EMBO J 10, 785-92.

[20] Clague, M.J. (1998) Biochem J 336 (Pt 2), 271-82.

[21] Lafourcade, C., Galan, J.M., Gloor, Y., Haguenauer-Tsapis, R. and Peter, M. (2004) Mol Cell Biol 24, 3815-26.

[22] Gallwitz, D., Donath, C. and Sander, C. (1983) Nature 306, 704-7.

[23] Cao, X., Ballew, N. and Barlowe, C. (1998) EMBO J 17, 2156-65.

[24] Lupashin, V.V. and Waters, M.G. (1997) Science 276, 1255-8.

[25] Jones, S., Newman, C., Liu, F. and Segev, N. (2000) Mol Biol Cell 11, 4403-11.

[26] Wang, W., Sacher, M. and Ferro-Novick, S. (2000) J Cell Biol 151, 289-96.

[27] Barrowman, J., Sacher, M. and Ferro-Novick, S. (2000) EMBO J 19, 862-9.

[28] Kim, Y.G. et al. (2006) Cell 127, 817-30.

[29] Sacher, M., Barrowman, J., Wang, W., Horecka, J., Zhang, Y., Pypaert, M. and Ferro-Novick, S. (2001) Mol Cell 7, 433-42.

[30] Huang, J. and Klionsky, D.J. (2007) Cell Cycle 6, 1837-49.

[31] Mizushima, N., Levine, B., Cuervo, A.M. and Klionsky, D.J. (2008) Nature 451, 1069-75.

[32] Reggiori, F. (2006) Curr Top Dev Biol 74, 1-30.

[33] Segev, N., Mulholland, J. and Botstein, D. (1988) Cell 52, 915-24.

[34] Cai, Y. et al. (2008) Cell 133, 1202-13.

[35] Cai, H. et al. (2007) Nature 445, 941-4.

[36] Cai, H., Zhang, Y., Pypaert, M., Walker, L. and Ferro-Novick, S. (2005) J Cell Biol 171, 823-33.

[37] Yamasaki, A. et al. (2009) Mol Biol Cell 20, 4205-15.

[38] Sacher, M., Barrowman, J., Schieltz, D., Yates, J.R., 3rd and Ferro-Novick, S. (2000) Eur J Cell Biol 79, 71-80.

[39] Meiling-Wesse, K., Epple, U.D., Krick, R., Barth, H., Appelles, A., Voss, C., Eskelinen, E.L. and Thumm, M. (2005) J Biol Chem 280, 33669-78.

[40] Nazarko, T.Y., Huang, J., Nicaud, J.M., Klionsky, D.J. and Sibirny, A.A. (2005) Autophagy 1, 37-45.

[41] Bacon, R.A., Salminen, A., Ruohola, H., Novick, P. and Ferro-Novick, S. (1989) J Cell Biol 109, 1015-22.

[42] Jedd, G., Richardson, C., Litt, R. and Segev, N. (1995) J Cell Biol 131, 583-90.

[43] Klionsky, D.J., Cuervo, A.M. and Seglen, P.O. (2007) Autophagy 3, 181-206.

[44] Cheong, H., Yorimitsu, T., Reggiori, F., Legakis, J.E., Wang, C.W. and Klionsky, D.J. (2005) Mol Biol Cell 16, 3438-53.

[45] Cao, Y., Cheong, H., Song, H. and Klionsky, D.J. (2008) J Cell Biol 182, 703-13.

[46] He, C., Song, H., Yorimitsu, T., Monastyrska, I., Yen, W.L., Legakis, J.E. and Klionsky, D.J. (2006) J Cell Biol 175, 925-35.

[47] Reggiori, F., Shintani, T., Nair, U. and Klionsky, D.J. (2005) Autophagy 1, 101-9.

[48] Ungar, D. et al. (2002) J Cell Biol 157, 405-15.

[49] Kanki, T. and Klionsky, D.J. (2008) J Biol Chem 283, 32386-93.

[50] Wuestehube, L.J., Duden, R., Eun, A., Hamamoto, S., Korn, P., Ram, R. and Schekman, R. (1996) Genetics 142, 393-406.

[51] Kim, J., Huang, W.P. and Klionsky, D.J. (2001) J Cell Biol 152, 51-64.

[52] Labbe, S. and Thiele, D.J. (1999) Methods Enzymol 306, 145-53.

[53] Rossi, G., Kolstad, K., Stone, S., Palluault, F. and Ferro-Novick, S. (1995) Mol Biol Cell 6, 1769-80.

[54] Scott, S.V., Baba, M., Ohsumi, Y. and Klionsky, D.J. (1997) J Cell Biol 138, 37-44.

CHAPTER 4

The histone acetyltransferase hMOF regulates the outcome of autophagy

Preface

DNA in eukaryotic cells is packaged into chromosomes. The basic unit of the chromosome is the nucleosome. The nucleosome consists of 147 base pairs of DNA wrapped around an octamer of histone proteins. The octamer is made up of two histone 3 (H3) - histone 4 (H4) dimers, which are flanked on either side by an histone 2A (H2A) - histone 2B (H2B) dimer [1,2]. Each histone has an N-terminal tail which is largely unstructured outside of the core nucleasome complex, making them readily accessible for posttranslational modifications [1,3,4]. Histone tail modifications are thought to contribute to chromatin structure and gene expression. For example, hyperacetylation allows for an increase in association of transcription factors to sequence specific genomic sites promoting gene expression [5-8]. The interplay between different modifications can be complex. Existing modifications can promote further specific modifications: ie H4 lysine 16 (H4K16) acetylation promotes H3 lysine 4 (H3K4) trimethylation [9], which then works to recruit different proteins/protein complexes that can alter chromatin functions [10]. This interplay idea is known as the histone code hypothesis.

Histone modifications work with signal transduction pathways to control gene expression. For example, the mitogen-activated protein kinase (MAPK) pathway

component Hog1 interacts in a complex that recruits the SAGA histone acetyltransferase complex to activate osmotic stress genes [11]. Hog1 also recruits the Rpd3-Sin3 histone deacetylase complex to the promoters of osmoresponsive genes, resulting in reduced transcription [12]. Signaling kinases can also act to modify histones. AMP-activated kinase (AMPK) is able to phosphorylate H2B serine 36 (H2BS36) to promote gene transcription. When H2BS36 is mutated there is an observed reduction in the expression of AMPK target genes [13]. AMPK is also able to induce autophagy through the inhibition of mTOR which is cytoprotective during ischemia [14].

Another histone modifying protein that can regulate autophagy is the deacetylase, SIRT1. In yeast, resversatrol is able to promote lifespan extension via the upregulation of autophagy by Sir2 (the yeast homolog of SIRT1) [15]. This is done by deacetylating Atg5, Atg7 and Atg8 and allowing them to form the proper autophagic complexes [16]. In addition, SIRT1 deacetylates and inhibits the cytoplasmic autophagy repressor TP53/p53 [17]. In yeast Sir2 has been shown to promote cellular life-span by removing H4K16 acetylation. As the cells age there is a decrease in Sir2 protein and an increase in H4K16 acetylation, leading to a loss of transcriptional silencing at heterochromatin [18]. Sas2, the H4K16 acetylase, and Sir2 are antagonists that together regulate lifespan. Since autophagy is known to promote cell survival, and the efficacy of the pathway decreases with age, we hypothesized that Sas2/KAT8 (hMOF/MYST1), Sir2/SIRT1 and H4K16 acetylation act with autophagy to promote cell survival. This chapter describes a histone modification molecular switch that regulates the outcome of autophagy.

Abstract

Autophagy is an evolutionarily conserved process in eukaryotes by which cytoplasmic components including macromolecules and organelles are degraded by the lysosome[19,20]. Paradoxically, although autophagy is primarily a protective process for the cell, it can also play a role in cell death [21,22]. Although controversial, there is little question that dysregulated autophagy can be lethal. However, it is not clear what distinguishes the life or death decision in autophagic cells [23]. Here we report that an epigenetic covalent modification of histones regulate the outcome of autophagy. Induction of autophagy, in mammalian cells and in yeast, is coupled to autophagy-related (ATG)5- and ATG7-dependent reduction of histone H4 lysine 16 acetylation (H4K16ac) through downregulation of the histone acetyltransferase hMOF/KAT8/MYST1. H4K16ac chromatin immunoprecipitation (ChIP-Seq) and global run-on sequencing (GRO-Seq) reveal on a genome-wide level that H4K16 deacetylation is associated with the regulation of autophagy-related genes. Overexpression of hMOF or antagonizing the activity of SIRT1, a H4K16ac deacetylase, resulted in an upregulation of H4K16ac, inhibition of the conversion of LC3-I to LC3-II and the induction of apoptotic cell death. Our findings establish a feedback loop by which specific alteration in histone posttranslational modifications during autophagy, critically alternates a program, including actions of autophagy genes, serving as a key transcriptional determinant of survival versus death responses upon autophagy induction.

Introduction

Macroautophagy, often referred to as autophagy, is a catabolic process that results in the autophagosome-dependent lysosomal degradation of bulk cytoplasmic contents, abnormal protein aggregates, and excess or damaged organelles. This process involves a series of dynamic membrane-rearrangements mediated by a core set of autophagy-related (ATG) proteins [24]. Autophagy is activated by conditions of nutrient deprivation and by other types of stress. The kinase mechanistic target of rapamycin (MTOR) is a critical regulator of autophagy induction, with activated MTOR suppressing autophagy, and inhibition of MTOR by rapamycin or nutrient deprivation promoting it. Interestingly, autophagy is also associated with physiological as well as pathological processes such as development, differentiation, neurodegenerative diseases, infection and cancer [19]. Understanding the pathways regulating the autophagic life and death decision and its cellular long-term effects might help to improve autophagy-based clinical treatments [25].

Autophagy is commonly seen as a set of cytoplasmic events, and, hitherto, no changes in the epigenome have been recognized upon the induction of autophagy. However, it is worth noting that accumulating evidence has established sirtuin 1 (SIRT1), a NAD^+-dependent deacetylase, as a key player in the starvation-induced autophagic process. SIRT1 downregulation inhibits starvation-induced autophagy, whereas its upregulation is sufficient to stimulate basal rates of autophagy [26]. However, SIRT1 is not always required for the autophagic process to occur; *e.g.*, autophagy induced by rapamycin does not require SIRT1 [26,27]. SIRT1 can form molecular complexes with several essential components of the autophagy machinery, namely ATG5, ATG7, and

ATG8, and *in vitro* can directly deacetylate these components [26]. SIRT1 shuttles between the nucleus and cytoplasm, and is therefore found expressed in both cell compartments [28]. SIRT1 has a wide range of non-histone targets but lysine 16 on histone H4 (H4K16) is its primary histone target [29,30]. Whereas many histone acetyltransferases show either little substrate specificity or preference for other residues, the product of the human orthologue of the *Drosophila melanogaster MOF* gene, hMOF/KAT8/MYST1, has been reported to be necessary and sufficient for the bulk of H4K16 acetylation and thereby antagonize the enzymatic activity of SIRT1 [30-32]. This single histone modification is not only responsible for the modulation of higher order chromatin structure but also for functional interactions between non-histone proteins and the chromatin fiber [33]. Since SIRT1 has been linked to both the autophagic process and epigenetic chromatin changes, this encouraged us to investigate whether epigenetic covalent modifications of histones contribute to autophagy. As SIRT1 preferentially deacetylates H4K16ac, we hypothesized that this histone modification could be altered upon induction of autophagy.

Results

Autophagy is associated with decreased H4K16 acetylation

We induced autophagy in mouse embryonic fibroblast (MEF) cells by amino acid starvation, which acts in a SIRT1-dependent fashion, and observed a pronounced decrease in acetylation of H4K16, as early as 3 h after starvation was initiated (Fig. 4.1A). To elucidate whether the observed effect on H4K16ac was linked to the role of SIRT1 during starvation-induced autophagy, or if the deacetylation of H4K16 is a general feature of the autophagic process, rapamycin treatment was used to induce SIRT1-independent autophagy. Remarkably, 48 h after rapamycin treatment, the global level of H4K16ac was robustly reduced in MEF cells (Fig. 4.1B, E). Whereas SIRT1 is not required for rapamycin-induced autophagy *per se*, its knockout reduces the endogenous level of autophagy, as seen in *Sirt1*-deficient MEF cells (Fig. 4.1C). Interestingly, in the SIRT1 null MEF cells, rapamycin treatment, but not starvation, induced the downregulation of H4K16ac, confirming that SIRT1 is not required for the repression of this histone modification upon autophagy induction (Fig. 4.1C and Fig. S4.1) and suggesting that either the rapamycin-induced repression of H4K16ac was achieved by other deacetylases, or alternatively by an active attenuation of certain acetyltransferase activity. Rapamycin-induced downregulation of H4K16ac was not restricted to MEF cells, but also occurred in various human cancer cell types, *i.e.*, non-small cell lung carcinoma U1810 cells, osteosarcoma U2OS cells, and cervical cancer HeLa cells (Figure 4.1D-F) and was even found to occur in yeast (Figure 4.1G), revealing the conservation of this process through evolution. Rapamycin treatment did not affect histone H4 levels

(Fig. S4.2). Of note, the rapamycin- and starvation-induced changes in histone covalent posttranslational modifications were linked to the occurrence of autophagy as established by an increased lipidation of the autophagic marker LC3, resulting in an increased ratio of the lipidated form (LC3-II) to the unlipidated form (LC3-I) (Fig. 4.1A-D). Similarly, in yeast this treatment resulted in increased lipidation of Atg8 (yeast homolog of LC3) and both cleavage and vacuolar localization of GFP-Atg8, which suggest complete flux through the autophagy pathway (Fig. S4.3).

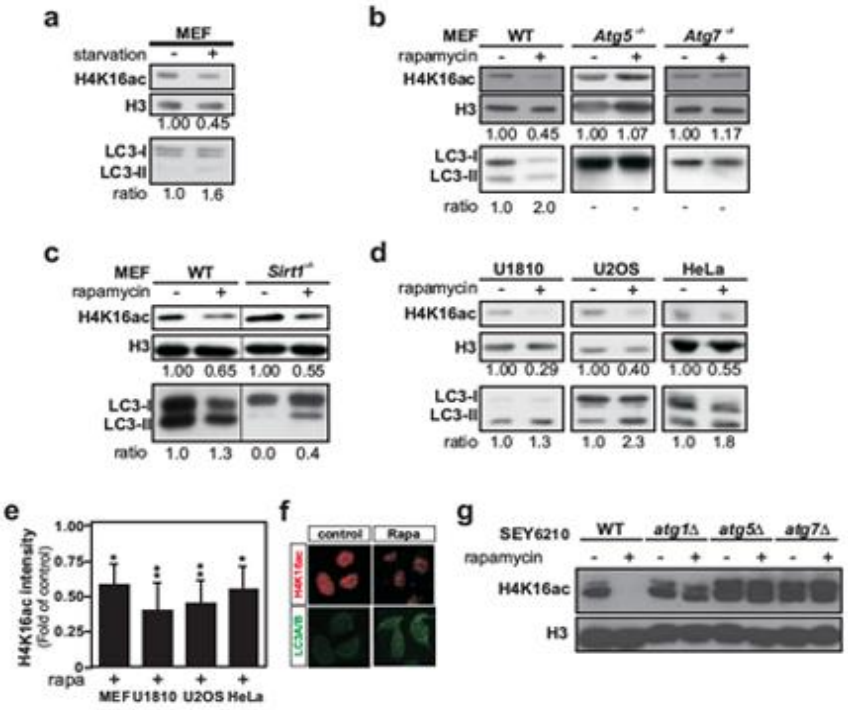

Figure 4.1 SIRT1-dependent and -independent autophagy is associated with a reduced acetylation of histone H4 lysine 16. (A) Amino acid starvation (3 h)-induced autophagy, as distinguished by the lipidation and cleavage of LC3-I and consequent increase of the LC3-II/LC3-I ratio, results in a global downregulation of H4K16ac in a histone extract of wild-type (WT) MEF cells. (B) Upon rapamycin treatment (300 nM) LC3-I was lipidated to form LC3-II in WT MEF cells. In the autophagy-deficient cell lines (*Atg5*$^{-/-}$ and *Atg7*$^{-/-}$ MEFs), LC3-I was not converted into LC3-II. In parallel, major downregulation of H4K16ac was observed exclusively in a histone extract derived from WT MEF cells upon rapamycin treatment. (C) Rapamycin treatment increased the LC3-II/LC3-I ratio and promoted H4K16ac decrease in *Sirt1*$^{-/-}$ and WT MEF cells. (D) Rapamycin-induced autophagy, as distinguished by the increase of the LC3-II/LC3-I ratio, led to downregulation of H4K16ac at 48 h in histone extracts of cervical adenocarcinoma HeLa and osteosarcoma U20S cells, and after 6 h in non-small cell carcinoma U1810 cells. (E) A quantification of H4K16 acetylation expression level by immunobloting is depicted for rapamycin-treated MEF, U1810, U2OS and HeLa cells. H4K16ac expression levels are reported as fold expression over untreated control cells. Histone 3 is used as a standard for equal loading of protein. Statistical evaluations were performed by Student's t-test (*Pvalue<0.01; **Pvalue<0.001). (F) Rapamycin-induced *punctate LC3 staining (in green),* was *associated with a reduction of* H4K16ac (in red) *in HeLa cells as* seen by confocal imaging after immunostaining with LC3A/B and H4K16ac antibodies. (G) WT, and autophagy-deficient *atg1Δ*, *atg5Δ* and *atg7Δ* SEY6210 yeast cells were treated with rapamycin to investigate the effect of autophagy on H4K16ac. Only the WT, but not the autophagy-deficient cells, displayed a massive downregulation of H4K16ac upon rapamycin treatment.

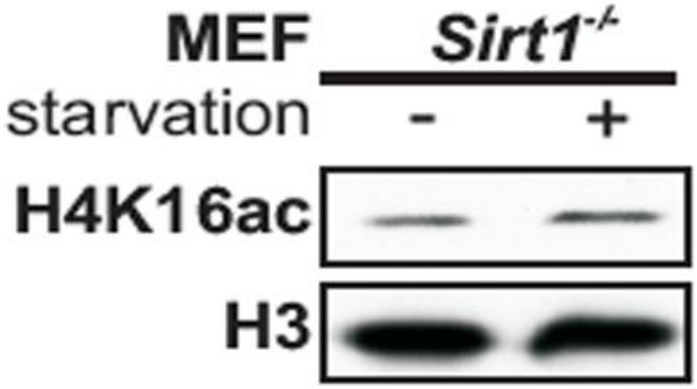

Figure S4.1. Starvation does not induce H4K16ac downregulation in *Sirt1*$^{-/-}$ MEF cells. Starvation for 4 h did not reduce the H4K16ac level in *Sirt1* knockout MEF cells. Histone 3 is used as a loading control.

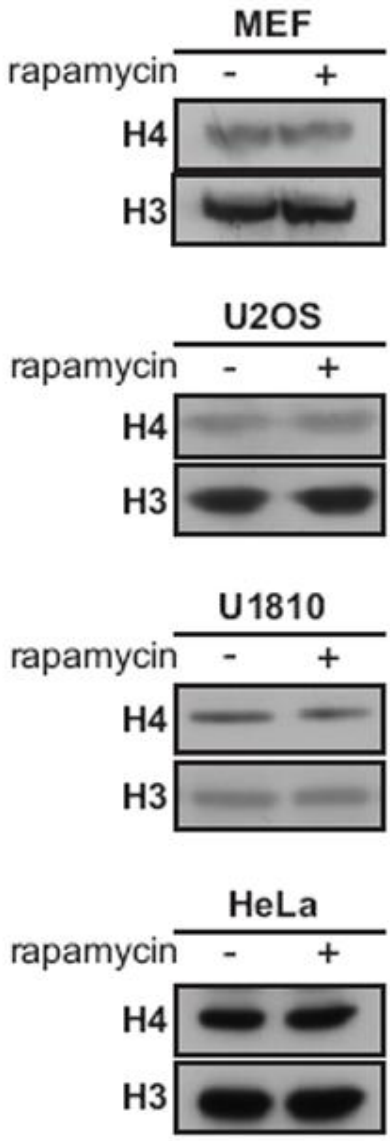

Figure S4.2. **Rapamycin treatment does not affect histone H4 levels.** Rapamycin treatment for 48 h did not reduce the expression levels of histone H4 in MEF, U1810, U2OS and HeLa cells. Histone H3 is used as a loading control.

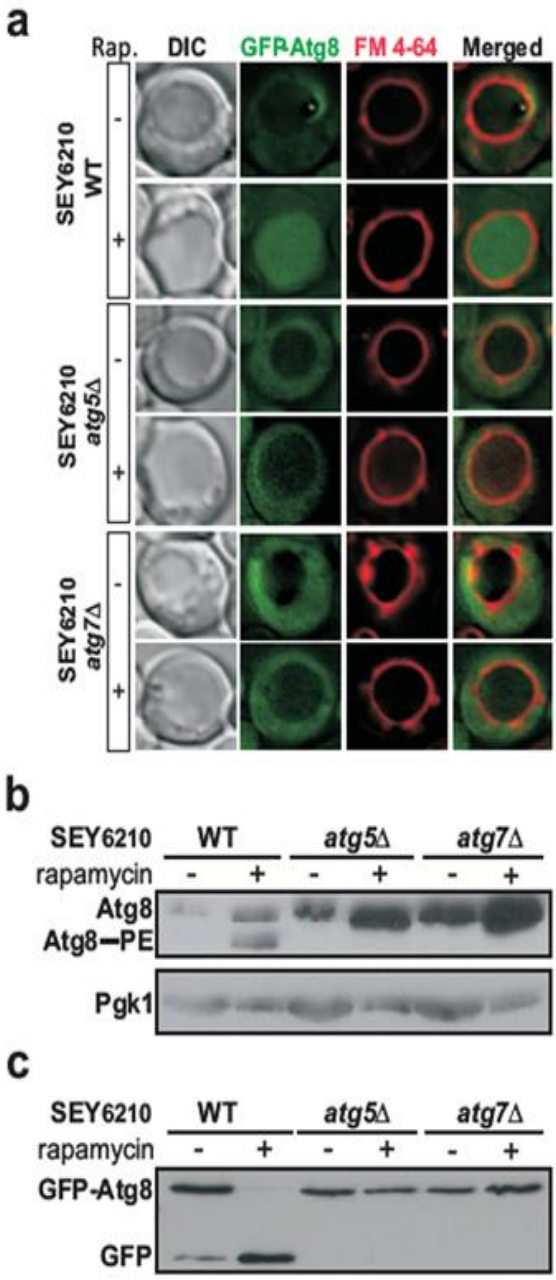

Figure S4.3. Autophagy can only be induced in the WT, but not *atg5*Δ and *atg7*Δ mutant yeast cells. (A) WT, and *atg5Δ* and *atg7Δ* mutant SEY6210 cells were transformed with a plasmid expressing GFP-Atg8 and stained with FM 4-64, which marks the vacuole membrane; autophagy is monitored by the appearance of GFP fluorescence within the vacuole lumen. (B) Rapamycin only induces the formation of Atg8–phosphatidylethanolamine (Atg8–PE) when Atg5 and Atg7 are present. Phosphoglycerate kinase 1 (Pgk1) is used as a loading control. (C) Additionally, rapamycin induced cleavage of GFP-Atg8 only occurs in WT, but not in *atg5*Δ and *atg7*Δ SEY6210 cells. Upon autophagy-dependent cleavage, the GFP-Atg8 band disappears and a free GFP band is observed.

H4K16 acetylation is associated with the transcription of ATG genes

We next addressed the central association between H4K16 acetylation state and the regulation of autophagy. Dynamic histone modifications are known to play a pivotal role in cell regulatory events [34] and the H4K16 residue is of particular interest as acetylation of this residue influences higher order chromatin structure [33] and plays an important role in transcription [35]. The observed decline in the level of acetylation of H4K16 during autophagy prompted us to perform chromatin immunoprecipitation (ChIP) targeting H4K16ac, followed by high-throughput sequencing (ChIP-Seq) to elucidate the genome-wide occurrence of this histone mark in U1810 cells undergoing rapamycin-induced autophagy (Fig. 4.2A). Remarkably, H4K16ac ChIP-Seq data analysis reveal 3422 called peaks in untreated U1810 cells which subsequently show reduced H4K16ac occupancy after 8 h rapamycin treatment (Fig. 4.2A). To gain insight into the role of this induced H4K16 acetylation in the regulation of gene expression during autophagy, we performed a global run-on-sequencing (GRO-Seq) assay [36,37] to generate a genome-wide view of the location, orientation, and density of nascent transcripts engaged by RNA polymerases at high resolution in rapamycin-treated versus untreated U1810 cells (Fig. 4.2B and Fig. S4.4A). This approach unveiled a significant alteration of the U1810 transcriptome with the identification of 1622 significantly (*FC>1.5 or <0.75 and Pvalue<0.001*) up- or down-regulated genes relative to the control condition already after 8 h rapamycin treatment (Fig. 4.2B,C and Fig. S4.4A). An unexpectedly large fraction of the identified genes (*141 genes; 8.7%*) were found to be related to the autophagic process as documented in PubMed and available autophagy gene databases *(http://tp-apg.genes.nig.ac.jp/autophagy/; http://autophagy.lu/)* (Fig. 4.2C and Fig. S4.4B).

Interestingly, there is an overall coincidence across the autophagy-related genes between the alteration of the GRO-Seq signal and the absence of H4K16 acetylation. Indeed 55 genes, *i.e.* 39% of the autophagy-related genes identified by GRO-Seq analysis, were found to exhibit reduced H4K16ac tag counts upon rapamycin treatment (Fig. 4.2C and Fig. S4.5A,B). These data are consistent with the reported elevated H4K16 acetylation in the promoter and transcribed regions of active genes [32,35]. Collectively, these genome-wide deep-sequencing analyses indicate that the observed deacetylation of lysine 16 of histone H4 during rapamycin-induced autophagy results in transcriptional regulation of autophagy-related genes.

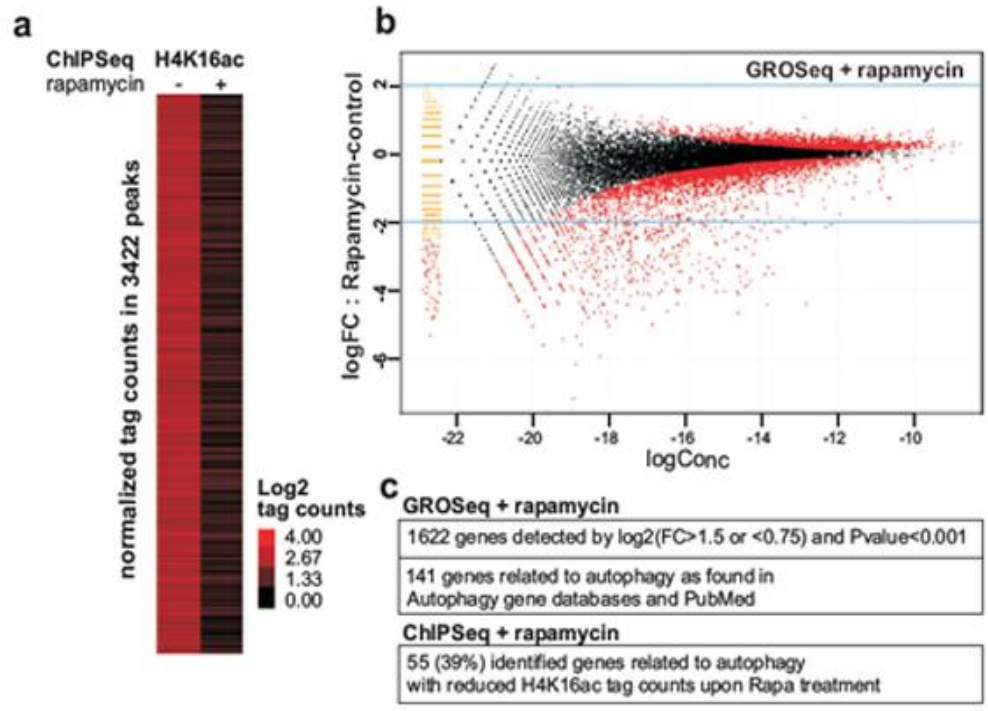

Figure 4.2. Deacetylation of H4K16 by rapamycin treatment is associated with transcriptional regulation of autophagy-related genes. (A) Heat map of H4K16Ac ChIP-Seq performed in U1810 cells without treatment or with 8 h rapamycin treatment. Data are shown as log2 values of tag counts in the 3422 regions defined as peaks in the no treatment sample. (B) De novo detection of transcripts using GRO-Seq analysis was performed in 8 h rapamycin-treated U1810 cells and compared to untreated U1810 cells. Groseq data can be visualized as 'MA' plots(log ratio versus abundance). The plot shows Groseq gene expression for pair-wise comparison between rapamycin treated cell vs control cell. The red points denote for the differentially expressed genes. The smear of points on the left side denotes that genes were observed in only one group of comparison samples. (C) 55 autophagy-related genes identified as regulated with a FC<1.5 or FC<0.75 by rapamycin in the GRO-Seq data analysis display in the ChIP-Seq data analysis reduced H4K16ac tag counts upon rapamycin treatment.

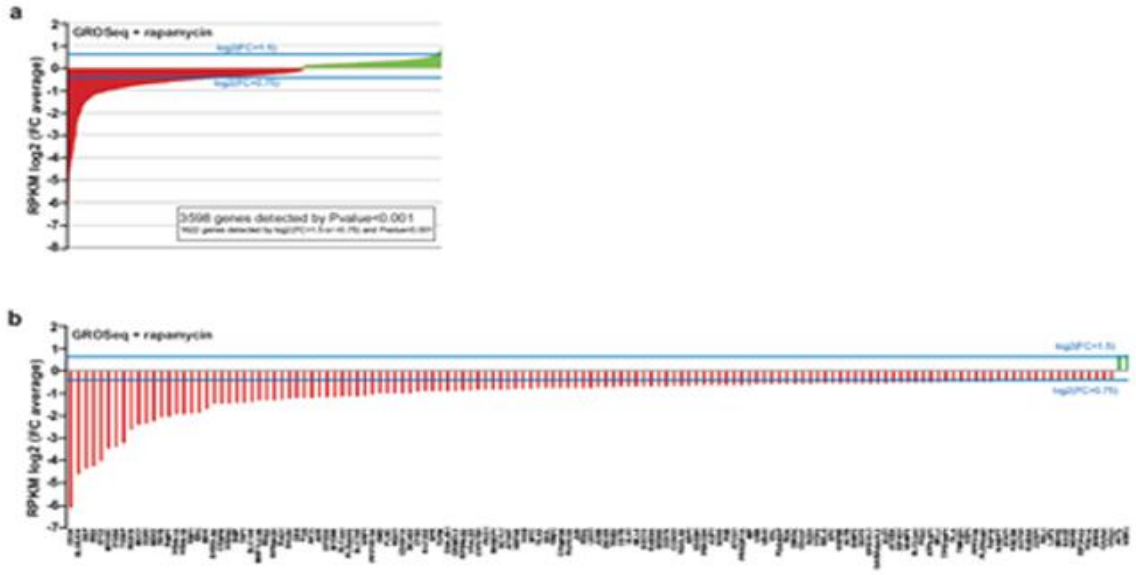

Figure S4.4. Rapamycin treatment is associated with transcriptional regulation of autophagy-related genes. De novo detection of transcripts using GRO-Seq analysis was performed in 8 h rapamycin-treated U1810 cells and compared to untreated U1810 cells. (A) An illustration of the *RPKM* (reads per kilobase and million mappable reads) log2 fold-change values for 3598 rapamycin-regulated genes detected by Pvalue>0.001 is depicted. (B) An illustration of the *RPKM* (reads per kilobase and million mappable reads) log2 fold-change values for 141 rapamycin-regulated autophagy-related genes is depicted.

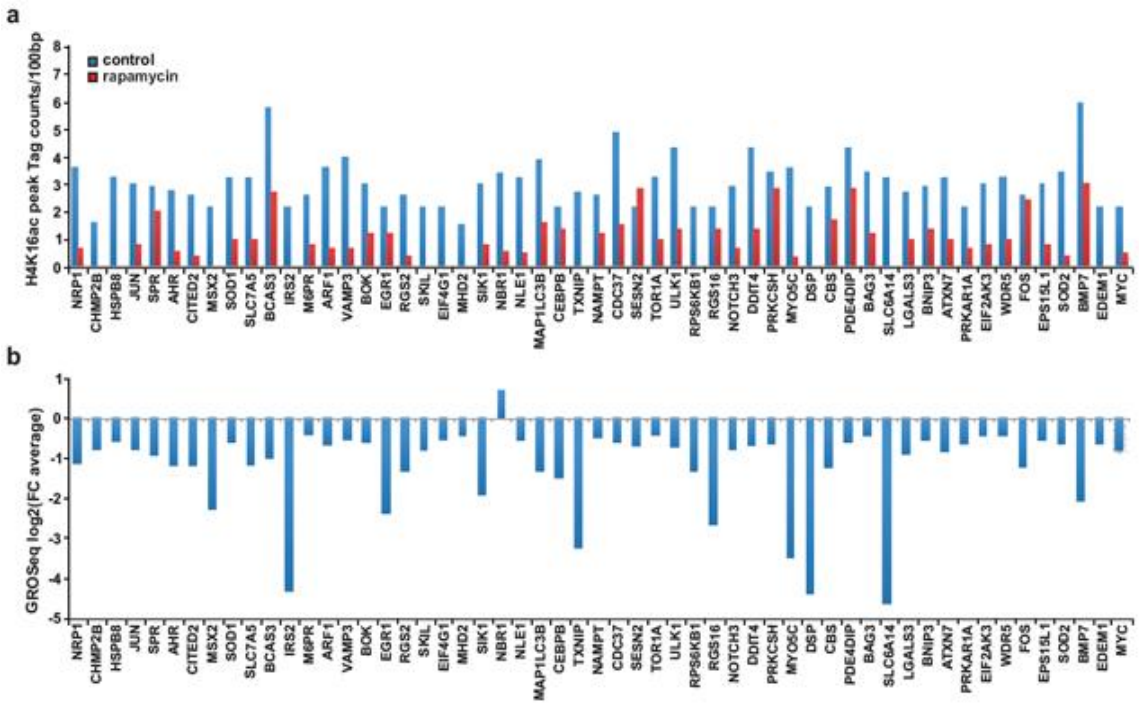

Figure S4.5 H4K16 deacetylation in autophagy annotated genes. (A) H4K16 deacetylation presented as tag counts per 100 bp in 55 regions defined as peaks in the no treatment sample and where the peaks have been annotated to an autophagy-related gene. (B) 55 rapamycin-regulated autophagy-related genes sorted by H4K16ac peak distance to TSS.

Since MTOR is involved in a wide variety of signaling pathways, treating cells with rapamycin could cause the observed epigenetic changes by mechanisms unrelated to autophagy. To exclude this possibility, we tested the effect of rapamycin on H4K16ac histone modification in *Atg5*- and *Atg7*-deficient MEF cells. These genes encode two ATG proteins that are essential for the canonical autophagy pathway, and no lipidation of LC3 takes place in these cells upon rapamycin treatment (Fig. 4.1B). Supporting the conclusion that the H4K16ac histone modification is directly linked to the autophagic process, treatment of *Atg7*$^{-/-}$ or *Atg5*$^{-/-}$ MEFs, *i.e.*, autophagy-deficient cells, with rapamycin, did not lead to a similar degree of downregulation of H4K16ac (Fig. 4.1B). Identical effects were observed in yeast, where rapamycin failed to reduce H4K16ac levels in *atg1*Δ, *atg5*Δ and *atg7*Δ strains. Consistent with the mammalian system, only the WT yeast cells showed massive downregulation of H4K16ac upon rapamycin treatment (Fig. 4.1G and Fig. S4.3).

hMOF downregulation promotes H4K16 deacetylation upon autophagy induction

Thus, the process of autophagy, independent of whether its induction required a SIRT1-dependent signaling pathway, was associated with global deacetylation of H4K16. Collectively, these data suggest that alteration in another histone modifying enzyme should be responsible for the observed modification in the acetylaytion status of H4K16 during autophagy. This observation prompted us to examine the status of the H4K16 histone acetyltransferase hMOF during autophagy. hMOF activity is responsible for the maintenance of H4K16 acetylation levels in mammalian cells [30,31]. Interestingly, while SIRT1 expression was not significantly altered upon rapamycin treatment (Fig.

S4.6A), hMOF expression was effectively downregulated upon autophagy induction in mammalian cells (Fig. 4.3A-C). Interestingly, in yeast cells engineered to express an HA-tagged version of the yeast homolog of hMOF, Sas2, rapamycin treatment induced a nearly complete loss of the HA signal within 2 h (Fig. 4.3H). H4K16ac is thought to play an important role in active transcription, presumably by facilitating chromatin decondensation [9,33,38-41]. H3K4me3, occurring at transcription start sites, is also correlated with active transcription [9,39-41]. Genome-wide investigations provide the compeling evidence that these H4K16ac and H3K4me3 histone marks reside within single nucleosomal units in human cells [40,41]. The coexistence of H4K16ac with H3K4me3 marks is consistent with the identification of multiple molecular interactions between the enzymes that are responsible for installing these marks [9,39,40]. In agreement with the established molecular link between H4K16ac and H3K4me3, rapamycin-induced autophagy was associated with a significant reduction in H3K4me3 in human cancer cell lines (Fig. 4.3J,K). The joint downregulation of the H4K16ac and the H3K4me3 histone modifications was also observed upon rapamycin treatment in WT yeast, but not *atg1Δ, atg5Δ* and *atg7Δ* autophagy-deficient yeast or Sas2-overexpressing yeast (Fig. 4.3I and L). The observed downregulation of the levels of both H4K16ac and H3K4me3 in response to autophagy further strengthens our findings with regard to the activation of an epigenetic feedback loop that governs specific gene expression in response to autophagy induction, specifically a transcriptional down-regulation of a cohort of key autophagy genes.

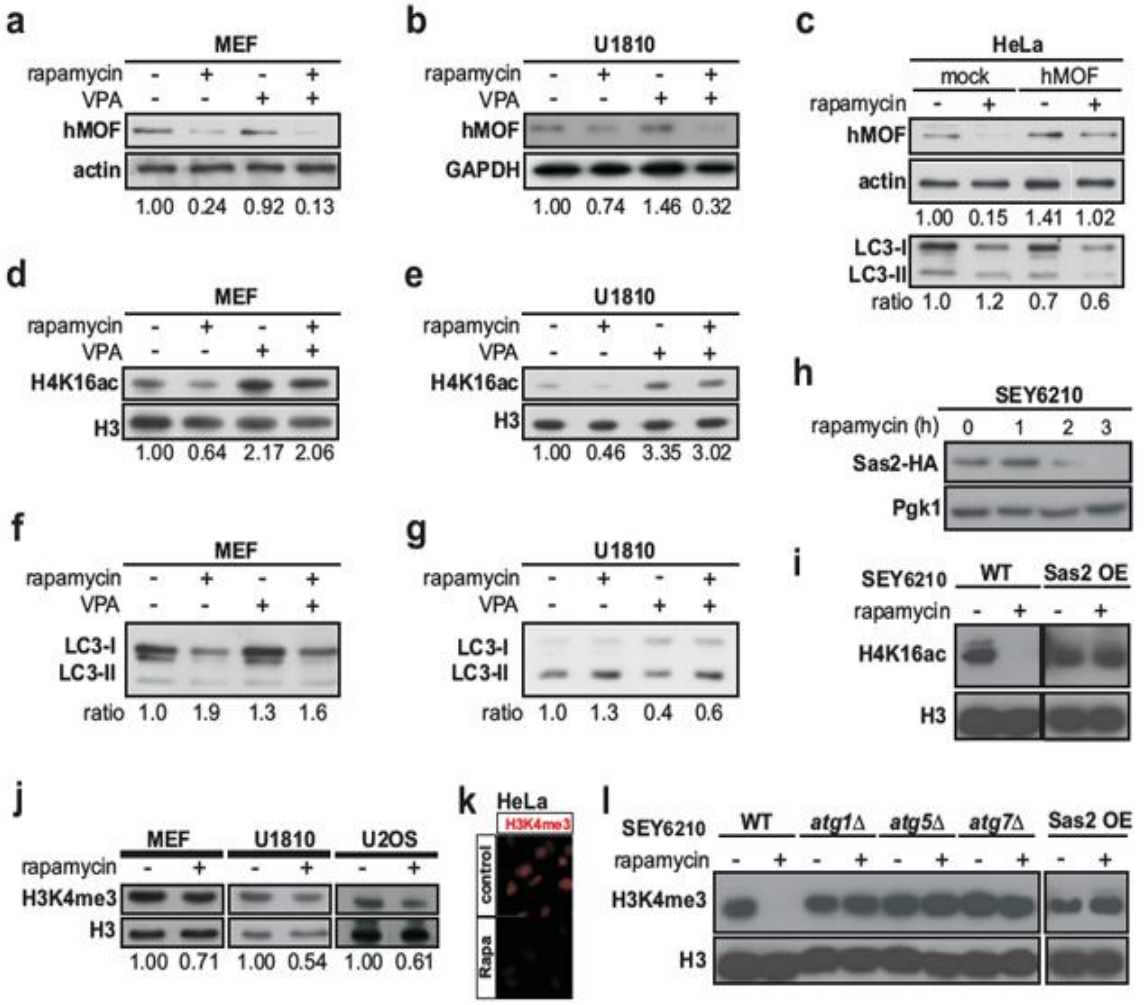

Figure 4.3. Rapamycin-induced hMOF downregulation promotes deacetylation of H4K16. (A-C) Rapamycin treatment (48 h) promoted the downregulation of the H4K16 histone acetyltransferase hMOF expression level in (A) MEF cells, (B) U1810 cells and (C) mock transfected HeLa cells. (C) Overexpression of hMOF reduced rapamycin-induced LC3-I to LC3-II conversion in HeLa cells. VPA treatment in (D,F) MEF and (E,G) U1810 cells counteracted rapamycin-induced H4K16ac downregulation (D,E) and inhibited the conversion of LC3-I to LC3-II (F,G). GAPDH, beta-actin, and histone 3 (H3) are used as standards for equal loading of protein. (H) The yeast homolog of hMOF, Sas2, was chromosomally tagged with 3xHA in strain SEY6210. Upon autophagy induction, the HA signal vanished over time, leading to a complete disappearance after 3 h. The signal was not recovered after 3 days. Phosphoglycerate kinase 1 (Pgk1) is used as a standard for equal loading of protein. (I) Overexpression of Sas2 repressed the downregulation of H4K16ac upon rapamycin treatment in SEY6210 yeast cells. (J,K) The H4K16ac-associated histone posttranslational modification H3K4me3 is downregulated upon rapamycin induction of autophagy. (L) This downregulation occurred in rapamycin-treated WT SEY6210 yeast cells, but not the autophagy-deficient or Sas2-overexpressing yeast cells.

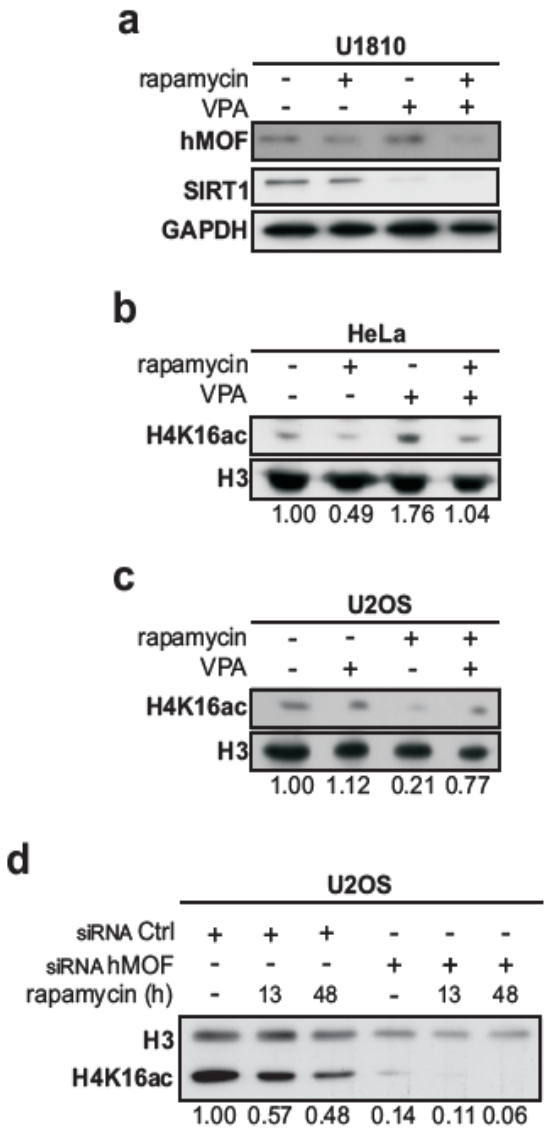

Figure S4.6. Rapamycin treatment reduces hMOF expression levels. (A) Rapamycin treatment (48 h) promoted the downregulation of the histone acetyltransferase hMOF expression level, but left SIRT1 protein expression unaffected in U1810 cells. VPA (1 mM) treatment reduced SIRT1 expression. GAPDH is used as a standard for equal loading of protein. VPA treatment counteracted rapamycin-induced H4K16ac downregulation in (B) HeLa cells and (C) U2OS cells. (D) U20S cells were transfected with either non-targeting siRNA (Ctrl) or siRNA targeting *hMOF*. The baseline H4K16ac level was greatly reduced when siRNA against *hMOF* was used. Rapamycin treatment reduced the H4K16ac level over time. Histone 3 (H3) is used as a standard for equal loading of protein.

The observed dramatic changes in levels of H4K16 acetylation and associated transcriptional gene regulation suggested that there may be a functional role for this epigenetic change during autophagy. It has only recently become clear how histone modifications can play a regulatory role in apoptosis and how they can influence the decision between life and death (reviewed in [42]). A similar regulatory role for histone modifications could be present during autophagy, and influence the life and death decision during this process. Shifting the equilibrium of *hMOF* and *SIRT1* expression in favor of *SIRT1*, leads to a decrease in acetylation of H4K16 [30]. Therefore, e*ven in a SIRT1-independent type of autophagy*, i.e. *rapamycin-induced autophagy, the inhibition of SIRT1* should be able to counteract the loss of H4K16ac observed during autophagy. Treatment with VPA increased the acetylation status of H4K16 in mammalian cells (Fig. 4.3D,E and Fig. S4.6B,C) by reducing SIRT1 levels [30]. Treatment with VPA was not only able to reverse rapamycin-induced downregulation of the H4K16ac histone modification (Fig. 4.3D,E), but also the conversion of LC3-I to LC3-II was greatly reduced (Fig. 4.3F,G). Accordingly, hMOF *overexpression in HeLa* cells correlated with decreased conversion of LC3-I to LC3-II upon rapamycin induction of autophagy (Fig. 4.3C).

Downregulation of H4K16 acetylation during autophagy is cytoprotective.

We extended our analysis by examining the effect of VPA or the SIRT1-specific inhibitor Ex527 on cell death [30]. We observed a significant increase in apoptotic cell death in human-derived cell lines co-treated with rapamycin and VPA, or with rapamycin and Ex527 (Fig. 4.4A-C). Indeed, while neither rapamycin, VPA nor Ex527 alone

induced a significant increase in apoptosis, rapamycin+VPA and rapamycin+Ex527 co-treatments induced apoptotic cell death as demonstrated upon nuclear Hoechst staining by the appearance of condensed or fragmented nuclei. These results were further confirmed by FACS analysis of the loss of mitochondrial transmembrane potential or appearance of a sub-G_1 hypodiploid DNA peak (Fig. S4.7A-C). To investigate whether the observed cell death upon abrogation of H4K16 deacetylation after rapamycin treatment is a consequence of autophagy induction, we performed an additional set of experiments with the autophagy inhibitor chloroquine. We noted that co-treatment with chloroquine abrogated both rapamycin+VPA- and rapamycin+Ex527-induced cell death in human cancer cells (Fig. 4.4D,E). Furthermore, we investigated the link between hMOF activity and the outcome of autophagy. In agreement with the discovery that the perturbation of H4K16 acetylation status regulate the outcome of autophagy, we observed a significant increase in apoptotic cell death in hMOF-overexpressing HeLa cells upon rapamycin treatment (Fig. 4.4F). Collectively, these data indicate that the downregulation of hMOF, the associated reduction in H4K16 acetylation level, and transcriptional regulation of autophagy-related genes are required for the proper progression of the autophagic process and that disturbance of this epigenetic program results in cell death.

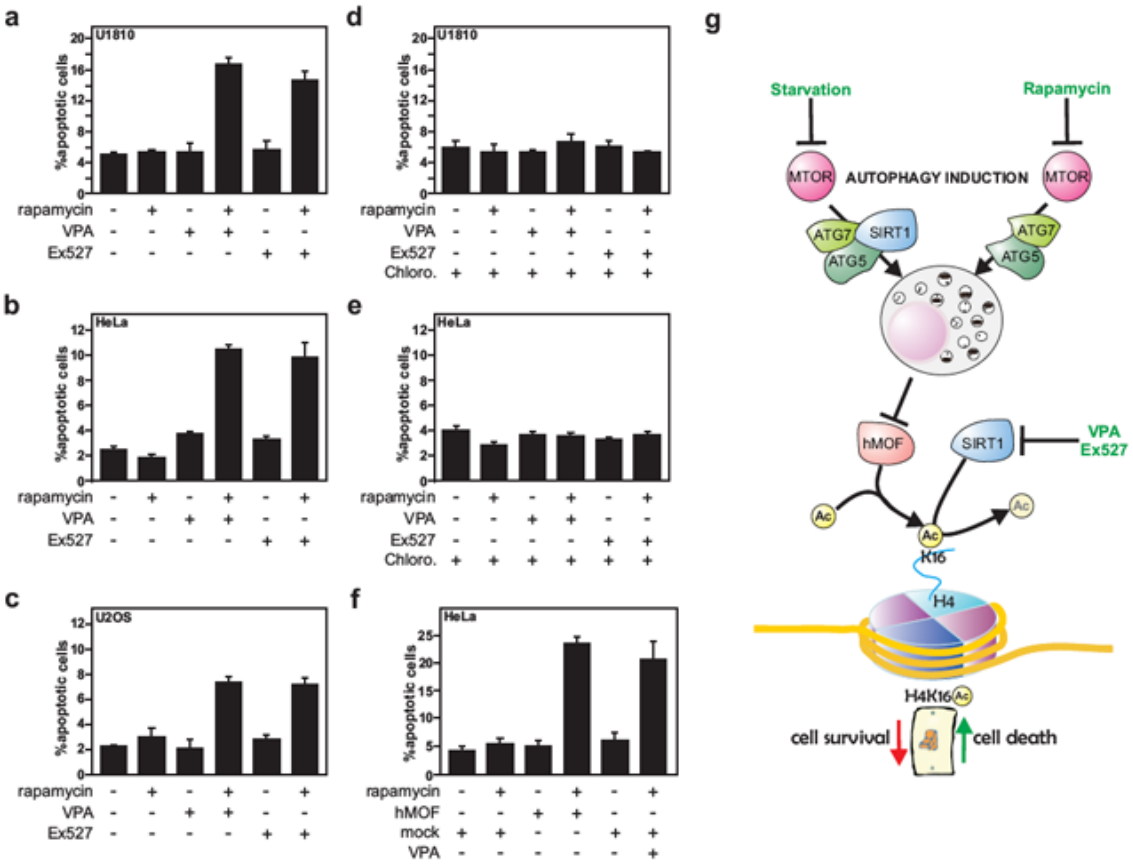

Figure 4.4. Inhibition of H4K16ac downregulation upon autophagy induction results in cell death. (A-C) Neither rapamycin (300 nM), VPA (1 mM) nor Ex527 (10 µM) treatment alone promoted cell death of U1810 (A), HeLa (B) or U2OS cells (C), as shown by scoring of condensed or fragmented nuclei upon nuclear Hoechst staining. However, co-treatment with VPA and rapamycin or with Ex527 and rapamycin led to increased cell death in all cell types tested. Data are expressed as mean ± SEM (n=3). (D,E) Co-treatment with chloroquine (10 µM), an autophagy inhibitor, abrogated both VPA+rapamycin- and EX527+rapamycin-induced cell death in all tested cell lines. (F) Overexpression of hMOF promoted cell death upon rapamycin treatment, and mimics the effect of VPA+rapamycin co-treatment in HeLa cells. (G) Scheme illustrating the potential epigenetic pathways regulating the autophagic life and death decision via the hMOF-SIRT1 control of H4K16 acetylation.

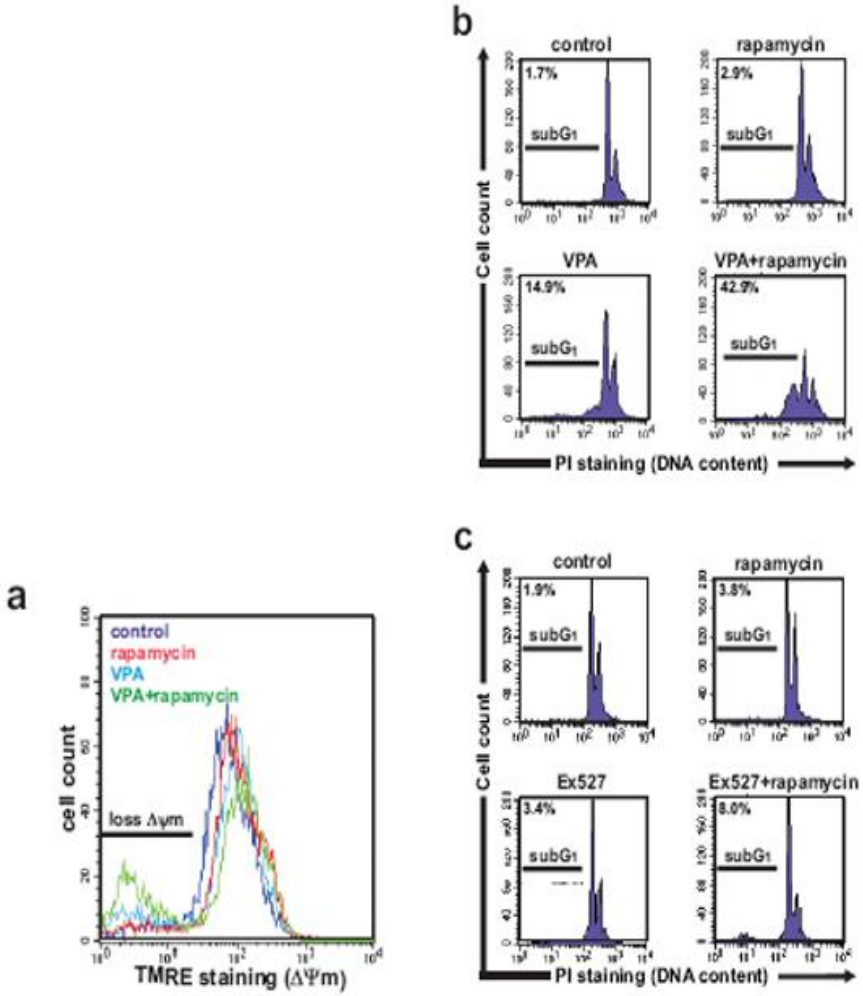

Figure S4.7. Inhibition of H4K16ac downregulation upon autophagy induction results in cell death. (A) Neither rapamycin (300 nM) nor VPA (1 mM) treatment alone caused a significant drop in mitochondrial transmembrane potential (ΔΨm) in U1810 cells, as measured by FACS analysis upon TMRE staining. However, co-treatment with VPA and rapamycin induced a drop in mitochondrial membrane potential indicating cell death. Co-treatments with VPA and rapamycin (B) or with Ex527 (10 μM) and rapamycin (C) promoted the appearance of a hypodiploid sub-G_1 peak in HeLa cells, as monitored by FACS analysis upon propidium iodide (PI) staining. Percentages of cells in sub-G_1 are displayed. Results are representative for at least 3 independent experiments.

Discussion

In conclusion, while until now, nuclear events have not been considered of primary importance for autophagy, as enucleated cells are still able to accumulate GFP-LC3 puncta in response to autophagic stimuli [27]. Our data unveil a critical linkage of the induction of autophagy and the activation of a transcriptional feedback loop. Thus, we demonstrate that the autophagic process is associated with covalent histone modifications in the chromatin that alters the global transcriptional program. Deep sequencing analyses on a genome-wide scale revealed a direct association between H4K16ac histone modifications and alteration of autophagy-related gene expression, and GRO-seq analysis established this link to altered gene activation programs, including the regulation of key genes in the autophagy program.Our findings imply a molecular histone switch, where the balancing effects of hMOF and SIRT1 on H4K16 acetylation therefore regulates autophagic survival and death decisions in concert with their opposing regulation of specific histone modifications (Fig. 4.4G). Our results shown here do not oppose the findings about functionality of the autophagic process in enucleated cells, but add a new feedback regulatory network influencing the outcome of autophagy with respect to cell death/survival. An autophagy long-term memory has recently been speculated to explain the long-lasting effect of autophagy, for example following calorie restriction and during life span extension [43], and accumulating evidence has linked life span extension to autophagy [43,44]. Thus, any persistent non-genetic alterations in chromatin, so-called epigenetic/epigenomic changes, including histone post-translational modifications that control long-lasting effects in cells, may also regulate subsequent events [45]. The identification of tightly regulated histone modifications associated with the autophagic

process offer an attractive conceptual framework both to understand the short term transcriptional response to stimuli eliciting autophagy, as well as constituting a potential aspect of long-term responses to autophagy.

Material and Methods

Antibodies and reagents used in this study are listed in Table S4.1 and S4.2. ON-TARGET plus SMARTpools siRNAs were purchased from Dharmacon (Table S4.3). Experiments were performed on U1810, U2OS and HeLa human cancer cells and wild-type, *Atg5*$^{-/-}$, *Atg*7$^{-/-}$ and *Sirt1*$^{-/-}$ mouse embryonic fibroblasts as well as *wild-type, atg1Δ*, *atg5Δ*, and *atg*7Δ *SEY6210 yeast cells*. Histone protein extracts, total protein extracts and immunoblotting were performed as reported previously [30,46,47]. ChIP-Seq and GRO-Seq analyses were executed as described in [36,37]. Cell death quantification methods have been described [47]. Bars and error bars represent mean with SEM. Statistical evaluations were performed by Student's t-test.

Cell culture

Non-small cell lung carcinoma U1810 cells, osteosarcoma U2OS cells, cervical cancer HeLa cells and wild-type, *Atg5*$^{-/-}$, *Atg*7$^{-/-}$ and *Sirt1*$^{-/-}$ mouse embryonic fibroblasts were cultured using standard procedures [30,48]. The *Atg*5$^{-/-}$ and WT MEF cell lines were gifts from Dr. Gerald McInerney, the A*tg*7$^{-/-}$ MEF cell line was a gift from Dr. Masaaki Komatsu [48] and the *Sirt1*$^{-/-}$ MEF cell line was a gift from Dr. Xiaoling Li. *SEY6210 wild-type, atg1Δ*, *atg5Δ*, and *atg*7Δ *yeast cells were grown* as described previously [49]. Transfection of cells was carried out with Lipofectamine 2000 (Invitrogen) in U2OS cells and with Lipofectamine and Lipofectamine reagent in HeLa cells.

Histone extracts and immunoblotting

Histone protein extracts were performed as described elsewhere [30,46] using TCA precipitation and H_2SO_4 extraction or using the Histone Purification Mini Kit (Active Motif). Total protein extracts and immunoblotting were performed as reported previously [47]. Densitometry was done using ImageJ.

Yeast procedures

The GFP-Atg8 processing assay and fluorescence microscopy were carried out as described previously [50].

Immunofluorescence and confocal microscopy

For confocal microscopy analysis, the adherent mammalian cells were grown on coverslips. Paraformaldehyde-fixed cells were blocked in HEPES, 3% bovine serum albumin, 0.3% Triton X-100 and incubated with primary (4°C, overnight) and secondary (room temperature, 1 h) antibodies. Samples were mounted with Vectashield (Vector Laboratories) and analyzed with Zeiss 510 META confocal laser scanning microscopy (Zeiss) [47].

Cell death quantification

After treatment, cells were fixed in 4% paraformaldehyde, harvested and cytospins were prepared. Subsequently, DNA was stained with Hoechst 33342 (0.1 mg/ml; Molecular Probes/Invitrogen). The number of dying cells was measured quantitatively by assessing the percentage of cells with fragmented, damaged or condensed nuclei.

Fluorescence-activated cell sorting (FACS) analysis

Quantification of PI (Sigma) and TMRE (Molecular Probes/Invitrogen) staining was performed with a FACSCalibur flow cytometer (Becton Dickinson) using standard procedures [47].

ChIP assays and ChIP-sequencing

ChIP was performed following the High Cell Chip kit protocol from Diagenode (Cat no: kch-mahigh-A16). 5 μg of the anti-acetyl histone H4 (Lys16) antibody was used in each IP. For ChIP-Seq analysis, 5 μg of chromatin was used in two separate IP's and combined in one elution for each condition. Subsequently, the DNA sequencing library was made using a kit from Illumina (Cat no 1003473) except that Illumina TruSeq adaptors (to enable multiplexing) were used. The library was analyzed by Solexa/Illumina Hi-seq. After pre-filtering the raw data by removing sequenced adapters and low quality reads, the sequence tags were aligned to the human genome (assembly hg19) with the Bowtie alignment tool [51]. To avoid any PCR-generated spikes we allowed only one read per chromosomal position, thus eliminating PCR bias. From the filtered raw data, 8 million unique reads per sample were used for peak detection. Peak detection was performed using the CisGenome program [52] with a two-sample analysis where sequenced input (1%) was used as a negative control. Peaks were called with a window statistic cutoff of 3 and a log2 fold change of 2. Using the defined chromosomal peak regions from the no treatment condition, the number of tags were counted in the corresponding rapamycin-treated sample and heat maps were generated using Java Treeview [53].

GRO-Sequencing

GRO-Seq experiments were performed as previously reported [36,37]. Briefly, cells were washed with cold 1X PBS buffer and swelled in swelling buffer (10mM Tris-Cl pH7.5, 2mM MgCl2, 3mM CaCl2) for 5min on ice and harvested. Cells were lysed in lysis buffer (swelling buffer with 0.5% NP-40, 2u/ml Superase In and 10% glycerol) and finally re-suspended in 100uL of freezing buffer (50mM Tris-Cl pH8.3, 40% glycerol, 5mM MgCl2, 0.1mM EDTA). For the run-on assay, resuspended nuclei were mixed with an equal volume of reaction buffer (10mM Tris-Cl pH 8.0, 5mM MgCl2, 1mM DTT, 300mM KCL, 20 units of SUPERase In, 1% sarkosyl, 500uM ATP, GTP, and Br-UTP, 2uM CTP) and incubated for 5 min at 30 Celsius degree. The nuclear-run-on RNA (NRO-RNA) was then extracted with TRIzol LS reagent (Invitogen) following manufacturer's instructions. NRO-RNA was then subjected to base hydrolysis on ice for 40min and followed by treatment with DNase I and antarctic phosphatase. To purify the Br-UTP labeled nascent RNA, the NRO-RNA was immunoprecipitated with an anti-BrdU argarose beads (Santa Cruz Biotech) in binding buffer (0.5XSSPE, 1mM EDTA, 0.05% tween). To repair the end, the immunoprecipitated BrU-RNA was re-suspended in 50uL reaction (45uL DEPC water, 5.2uL T4 PNK buffer, 1uL SUPERase In and 1uL T4 PNK [NEB]) and incubated at 370C for 1hr. The RNA was extracted and precipitated using acidic phenol-chloroform. The cDNA synthesis was performed basically as in Ingolia et al., (2009) with few minor modifications. First, RNA fragments were subjected to poly-A tailing reaction by poly-A polymerase (NEB) for 30 min at 370C. Subsequently, reverse transcription was performed using oNTI223 primer (5'-pGATCGTCGGACTGTAGAACTCT;

CAAGCAGAAGACGGCATACGATTTTTTTTTTTTTTTTTTTTVN). Second, tailed RNA (8.0uL) was subjected to reverse transcription using superscript III (Invitrogen). The cDNA products were separated on a 10% polyacrylamide TBE-urea gel and the extended first-strand product (100-500bp) was excised and recovered by gel extraction. After that, the first-strand cDNA was circularized by CircLigase (Epicentre) and relinearized by Ape1 (NEB). Relinearized single strand cDNA (sscDNA) was separated on a 10% polyacrylamide TBE gel and the product of needed size was excised (~120-320bp) for gel extraction. Finally, sscDNA template was amplified by PCR using the Phusion High-Fidelity enzyme (NEB) according to the manufacturer's instructions with two oligonucleotide primers oNTI200 (5'- CAAGCAGAAGACGGCATA) and oNTI201 (5'-
AATGATACGGCGACCACCGACAGGTTCAGAGTTCTACAGTCCGACG). DNA was then sequenced on the Illumina HiSeq2000 according to the manufacturer's instructions, using small RNA sequencing primer 5'-CGACAGGTTCAGAGTTCTACAGTCCGACGATC.

Table S4.1: Primary antibodies used in this study.

Primary Antibodies	*Companies*
β-actin (mouse monoclonal anti-)	Sigma Aldrich (A-3853)
Atg5 (rabbit polyclonal anti-)	Cell Signaling (#2630)
Atg8 (rabbit polyclonal anti-)	See reference [54]
cleaved caspase-3(Asp175) (rabbit polyclonal anti-)	Cell Signaling (#9661)
G3PDH (rabbit polyclonal anti-)	Trevigen (#2275)
H3 C-terminal (rabbit polyclonal anti-)	Active Motif 39164
H3 (rabbit polyclonal anti-)	Active Motif (#39164)
H3K4me3 (rabbit polyclonal anti-)	LP Bio (AR-0169)
H3K4me3 (rabbit polyclonal anti-)	Active Motif (#39159)
H4 (rabbit polyclonal anti-)	Active Motif (#61199)
H4K16ac (rabbit polyclonal anti-)	Millipore (#07-329)
H4K16ac (rabbit polyclonal anti-)	Active Motif (#39167)
HA (mouse monoclonal anti-)	Sigma Aldrich(H-3663)
hMOF (mouse monoclonal anti-)	GeneTex Inc. (8C4C4)
hMOF (rabbit polyclonal anti-)	GeneTex Inc. (GTX104587)
LC3B (rabbit polyclonal anti-)	Sigma Aldrich (L-7543)
LC3A/B (rabbit polyclonal anti-)	Cell Signaling (#4108)
PGK-1 (rabbit polyclonal anti-)	Dr. Jeremy Thorner
SIRT1 (mouse monoclonal anti-)	Sigma Aldrich (WHOO23411)

Table S4.2: Reagents used in this study.

Reagents	*Companies*
Chloroquine	Sigma Aldrich
Ex527	Tocris
Hoechst	Molecular Probes/Invitrogen
2-propylpentanoic acid (VPA)	Sigma Aldrich
Rapamycin	LC Laboratories

Table S4.3: ON-TARGETplus SMART pool small interfering RNAs used in this study. This technology is based on the use of four duplex siRNA's targeting four different regions of the mRNA to be targeted (SMARTpool). This technology is also based on dual-strand modification (ON-TARGETplus) proven to reduce off target effects caused by both strands.

ON-TARGET plus SMARTpools siRNAs	Companies
hMOF (human, MYST1 NM_032188)	Dharmacon (L-014800)
Non-targeting siRNA #1	Dharmacon (D-001810)

References

[1] Dutnall, R.N. and Ramakrishnan, V. (1997) Structure 5, 1255-9.

[2] Luger, K., Mader, A.W., Richmond, R.K., Sargent, D.F. and Richmond, T.J. (1997) Nature 389, 251-60.

[3] Fletcher, T.M. and Hansen, J.C. (1996) Crit Rev Eukaryot Gene Expr 6, 149-88.

[4] Luger, K. and Richmond, T.J. (1998) Curr Opin Genet Dev 8, 140-6.

[5] Juan, L.J., Utley, R.T., Adams, C.C., Vettese-Dadey, M. and Workman, J.L. (1994) EMBO J 13, 6031-40.

[6] Lee, D.Y., Hayes, J.J., Pruss, D. and Wolffe, A.P. (1993) Cell 72, 73-84.

[7] Vettese-Dadey, M., Grant, P.A., Hebbes, T.R., Crane- Robinson, C., Allis, C.D. and Workman, J.L. (1996) EMBO J 15, 2508-18.

[8] Vettese-Dadey, M., Walter, P., Chen, H., Juan, L.J. and Workman, J.L. (1994) Mol Cell Biol 14, 970-81.

[9] Katoh, H. et al. (2011) Mol Cell 44, 770-84.

[10] Strahl, B.D. and Allis, C.D. (2000) Nature 403, 41-5.

[11] Proft, M. and Struhl, K. (2004) Cell 118, 351-61.

[12] De Nadal, E., Zapater, M., Alepuz, P.M., Sumoy, L., Mas, G. and Posas, F. (2004) Nature 427, 370-4.

[13] Bungard, D. et al. (2010) Science 329, 1201-5.

[14] Sarbassov, D.D., Ali, S.M. and Sabatini, D.M. (2005) Curr Opin Cell Biol 17, 596-603.

[15] Howitz, K.T. et al. (2003) Nature 425, 191-6.

[16] Geng, J. and Klionsky, D.J. (2008) EMBO Rep 9, 859-64.

[17] Vaziri, H., Dessain, S.K., Ng Eaton, E., Imai, S.I., Frye, R.A., Pandita, T.K., Guarente, L. and Weinberg, R.A. (2001) Cell 107, 149-59.

[18] Dang, W. et al. (2009) Nature 459, 802-7.

[19] Levine, B. and Kroemer, G. (2008) Cell 132, 27-42.

[20] Mizushima, N., Levine, B., Cuervo, A.M. and Klionsky, D.J. (2008) Nature 451, 1069-75.

[21] Levine, B. and Klionsky, D.J. (2004) Dev Cell 6, 463-77.

[22] Levine, B. and Yuan, J. (2005) J Clin Invest 115, 2679-88.

[23] Chen, Y. and Klionsky, D.J. (2011) J Cell Sci 124, 161-70.

[24] Yang, Z. and Klionsky, D.J. (2010) Nat Cell Biol 12, 814-22.

[25] Jiang, H., White, E.J., Conrad, C., Gomez-Manzano, C. and Fueyo, J. (2009) Methods Enzymol 453, 273-86.

[26] Lee, I.H. et al. (2008) Proc Natl Acad Sci U S A 105, 3374-9.

[27] Morselli, E. et al. (2011) J Cell Biol 192, 615-29.

[28] Tanno, M., Sakamoto, J., Miura, T., Shimamoto, K. and Horio, Y. (2007) J Biol Chem 282, 6823-32.

[29] Vaquero, A., Sternglanz, R. and Reinberg, D. (2007) Oncogene 26, 5505-20.

[30] Hajji, N., Wallenborg, K., Vlachos, P., Fullgrabe, J., Hermanson, O. and Joseph, B. (2010) Oncogene 29, 2192-204.

[31] Taipale, M., Rea, S., Richter, K., Vilar, A., Lichter, P., Imhof, A. and Akhtar, A. (2005) Mol Cell Biol. 25, 6798-810.

[32] Smith, E.R., Cayrou, C., Huang, R., Lane, W.S., Cote, J. and Lucchesi, J.C. (2005) in: Mol Cell Biol, Vol. 25, pp. 9175-88, United States.

[33] Shogren-Knaak, M., Ishii, H., Sun, J.M., Pazin, M.J., Davie, J.R. and Peterson, C.L. (2006) Science 311, 844-7.

[34] Kouzarides, T. (2007) Cell 128, 693-705.

[35] Kind, J., Vaquerizas, J.M., Gebhardt, P., Gentzel, M., Luscombe, N.M., Bertone, P. and Akhtar, A. (2008) Cell 133, 813-28.

[36] Core, L.J., Waterfall, J.J. and Lis, J.T. (2008) Science 322, 1845-8.

[37] Wang, D. et al. (2011) Nature 474, 390-4.

[38] Robinson, P.J., An, W., Routh, A., Martino, F., Chapman, L., Roeder, R.G. and Rhodes, D. (2008) J Mol Biol 381, 816-25.

[39] Dou, Y. et al. (2005) Cell 121, 873-85.

[40] Ruthenburg, A.J. et al. (2011) Cell 145, 692-706.

[41] Wang, Z., Zang, C., Cui, K., Schones, D.E., Barski, A., Peng, W. and Zhao, K. (2009) Cell 138, 1019-31.

[42] Fullgrabe, J., Hajji, N. and Joseph, B. (2010) Cell Death Differ 17, 1238-43.

[43] Marino, G. et al. (2011) Autophagy 7, 6.

[44] Melendez, A., Talloczy, Z., Seaman, M., Eskelinen, E.L., Hall, D.H. and Levine, B. (2003) Science 301, 1387-91.

[45] Fullgrabe, J., Kavanagh, E. and Joseph, B. (2011) Oncogene 30, 3391-403.

[46] Shechter, D., Dormann, H.L., Allis, C.D. and Hake, S.B. (2007) Nat Protoc 2, 1445-57.

[47] Burguillos, M.A. et al. (2011) Nature 472, 319-24.

[48] Komatsu, M. et al. (2005) J Cell Biol 169, 425-34.

[49] Cao, Y., Cheong, H., Song, H. and Klionsky, D.J. (2008) J Cell Biol 182, 703-13.

[50] Shintani, T. and Klionsky, D.J. (2004) J Biol Chem 279, 29889-94.

[51] Langmead, B., Trapnell, C., Pop, M. and Salzberg, S.L. (2009) Genome Biol 10, R25.

[52] Ji, H., Jiang, H., Ma, W., Johnson, D.S., Myers, R.M. and Wong, W.H. (2008) Nat Biotechnol 26, 1293-300.

[53] Saldanha, A.J. (2004) Bioinformatics 20, 3246-8.

[54] Huang, W.P., Scott, S.V., Kim, J. and Klionsky, D.J. (2000) J Biol Chem 275, 5845-51.

Chapter 5

Histone Acetylation Regulates Autophagy by Controlling Atg8 Expression

Preface

Atg8, a ubiquitin like protein, is a core machinery component of autophagy, and is required for both nonselective autophagy and the cytoplasm to vacuole targeting pathway [1,2]. Atg8 is conjugated to phosphatidylethanolamine (PE) after its terminal cysteine residue is cleaved off by Atg4 [3-5]. This exposes a glycine residue that is then conjugated to PE by Atg7 (E1-like activating enzyme), Atg3 (E-2 like conjugating enzyme), and the Atg12-Atg5-Atg16 complex (E3 like enzyme) [1,6-10]. During autophagy, Atg8 localizes to the PAS where it becomes associated with the phagophore membrane. This localization is dependent upon Atg9 and the phosphatidylinositol 3-kinase (PI3K) complex [4,5,7,11-14]. Atg8 lines the inner and outer membrane of the expanding phagophore and aids in the fusion of membranes comprising the autophagosome [15-17]. Upon completion of the autophagosome, Atg8 on the outer membrane is cleaved from PE by Atg4, releasing it back into the cytoplasm [5]. The cleavage step is critical for the completion of the autophagosome [18]. The Atg8 on the inside of the autophagosome is transported to the vacuole where it is degraded [15,16,19,20]. Each round of autophagosome formation requires first the transport of Atg8 to the PAS and then release of the protein [18].

Upon nitrogen starvation, *ATG8* expression increases over 10-fold. This increase in expression occurs quickly with peak mRNA levels occurring 30 minutes after starvation [16,21]. This increase in expression is critical for the regulation of autophagy. When *ATG8* expression is not induced upon nitrogen starvation due to alterations in the promoter, the autophagosomes remain abnormally small, but the number of autophagosome remains the same as compared to the wild-type cell [18]. This indicates that Atg8 expression regulates the size of the autophagosome, but not the number. This phenomenon is observed during Group A *Streptococcus* infection. Upon infection, Atg8 expression is increased to a greater extent than during starvation conditions, resulting in the larger autophagosome needed to degrade the bacterium [22]. This suggests that Atg8 is an important regulatory site for autophagosome formation.

Recent studies have looked into the regulation of *ATG8* transcription. The *ATG8* promoter contains an URS1 site where the transcription factor Ume6 binds and suppresses transcription. Ume6 recruits the histone deacetylase complex containing Rpd3 and Sin3. This leads to the deacetylation of H3 and H4, repressing transcription [23]. During meiosis, Ume6 is phosphorylated and degraded, releasing the transcriptional inhibition [24]. This does not happen at the *ATG8* promoter. Ume6 remains bound after nitrogen starvation, leaving unanswered how the transcriptional inhibition is removed (for more information see Appendix C) [23]. In this chapter, I explored how *ATG8* transcription is promoted upon induction of autophagy. I discovered that the acetyltransferase, Sas2, promotes *ATG8* transcription and Sas2 expression regulates autophagy activity.

Abstract

Autophagy, an evolutionarily conserved, primarily degradative pathway, is important to the maintenance of cellular homeostasis, and its dysfunction is implicated in several different physiological and pathological processes including aging, cancer, and neurodegeneration. Autophagy is generally cytoprotective, allowing cells to survive periods of nutrient deprivation and other stressors. Global changes in histone modifications control the outcome of autophagy. Here we have discovered that locus specific histone modifications regulate autophagy through the transcription of an essential autophagy gene, *ATG8*. The level of Atg8 expression controls the magnitude of autophagy, and thus its regulation is key to modulating the overall pathway. We have identified a histone acetyltransferase, Sas2, which regulates Atg8 expression through the acetylation of histone 4 lysine 16 at the *ATG8* promoter, whereas degradation of Sas2 prevents excessive autophagy.

Introduction

Macroautophagy, hereafter referred to as autophagy, is a ubiquitous and evolutionarily conserved process used by eukaryotic cells to survive periods of cellular stress and nutrient deprivation [25]. Autophagy results in the degradation of cytoplasmic components including proteins, macromolecules, and organelles [26]. This process requires the vast mobilization of large amounts of membrane to engulf portions of the cytoplasm into a double-membrane vesicle called the autophagosome. The autophagosome then fuses with the vacuole in yeast cells or the lysosome in mammalian cells where its contents are degraded and the resulting macromolecules are released back into the cytoplasm [27]. Autophagy helps maintains cellular homeostasis and as such plays a role in a variety of physiological and pathological processes such as development and aging, immune defense, cancer, and neurodegeneration [28,29]. Therefore, it is important to understand the regulation of autophagy in order to improve current, and develop new, therapeutic treatments.

The focus of the autophagy field has mainly centered on the cytoplasmic apects of this process, such as cargo recognition and autophagosome formation; however, there are specific nuclear events that are associated with the induction of autophagy. For example, in mammalian cells, several studies have examined the role of histone modifying proteins in autophagy regulation. For example, SIRT1/sirtuin 1, a NAD^+ -dependent deacetylase, regulates starvation-induced autophagy but not rapamycin induced autophagy [30,31]. SIRT1 overexpression increases the basal autophagy activity, whereas its down regulation inhibits starvation-induced autophagy. SIRT1 shuttles between the nucleus and the cytoplasm and has a variety of targets [32]. In the cytoplasm, SIRT1 can form

complexes with the autophagy components ATG5, ATG7, and LC3 (the homolog of yeast Atg8) and deacetylates them in vitro [30]. In the nucleus, SIRT1 specifically targets lysine 16 on histone 4 (H4K16) for deacetylation [33,34]. So far, however, most of the studies on the role of histone acetyltransferases and deacetylases in regulating autophagy have focused on non-histone targets [30,35-37].

Recently, we examined the role of specific histone modifications, including acetylation of H4K16, on the outcome of autophagy. We found that there is a global loss of H4K16 acetylation when autophagy is induced (our unpublished data). When those histone modifications are maintained after the induction of autophagy either through the inhibition of SIRT1 or through the forced retention of the acetyltransferase hMOF (KAT8/MYST1), the outcome of the autophagic process is cell death rather than cell survival. The regulatory components that control this conversion from cytoprotection to cell death are evolutionarily conserved from yeast to mammalian cells (our unpublished data).

Other studies show that autophagy is also regulated through the transcription of an essential autophagy gene *ATG8* in yeast or *MAP1LC3* in mammalian cells. Atg8 plays an important role in controlling the formation of the autophagosome and specifically regulates its size[18,38]. Upon the induction of autophagy, *ATG8* transcription increases dramatically leading to increased levels of the Atg8 protein in the cell. Atg8 conjugated to phosphatidylethanolamine (Atg8-PE) plays a central role in regulating the formation of the autophagosome. A large pool of Atg8 protein is needed to maintain normal autophagy levels and cells with reduced Atg8 expression form abnormally small autophagosomes [18]. Therefore, understanding *ATG8* regulation is important for the understanding of the

regulation of autophagy and thus for the creation of new therapeutic targets. Today, little is known regarding how *ATG8* transcription is upregulated upon induction of autophagy.

Although there is a role for specific histone modifications in autophagy (our unpublished data), to date no studies have linked epigenetic modifications with transcriptional changes at a specific locus corresponding to an autophagy-related protein. In the present paper we examined the role of Sas2, the yeast homolog of hMOF, on autophagy through the regulation of *ATG8* correspond with alterations in Atg8 levels and autophagy activity.

Results

Sas2 deletion delays induction of autophagy

In order to investigate the role of epigenetic modifications in regulating autophagy we first decided to examine the effect of modulating H4K16Ac on autophagy induction in yeast. *SAS2* encodes the yeast homolog of mammalian hMOF. Therefore, we knocked out *SAS2* and used the quantitative Pho8Δ60-dependent alkaline phosphatase assay to measure autophagy activity. *PHO8* encodes a vacuolar alkaline phosphatase, which normally is delivered to the vacuole through a portion of the secretory pathway. The modified version of this protein, Pho8Δ60, lacks the N-terminal transmembrane domain and is thus unable to enter the endoplasmic reticulum; it can only enter the vacuole through nonspecific autophagy [39]. In the wild-type strain there was a clear increase in autophagy activity following induction by the addition of rapamycin to the growth medium (Fig. 5.1A). In contrast, there was no increase seen in an *atg1Δ* strain that is defective for autophagy. In the *sas2Δ* strain, autophagy activity was reduced as compared to the wild-type strain (Fig. 5.1A). The difference between the two strains was largely eliminated within 4 h of rapamycin treatment. These results suggest that Sas2 plays a role in the initial induction of autophagy, but that the absence of this protein does not block the formation of autophagosomes per se. The delay in induction was abolished when Sas2 was reintroduced into the knockout strain via expression on a plasmid (Fig. S5.1). These results are specific to Sas2 and not histone acetyltransferases in general, because a delay in autophagy induction was not observed in a *gcn5Δ* strain, which lacks a different histone acetyltransferase (Fig. 5.1B). In addition, the deletion of *SIR2*, which encodes a deacetylase that targets H4K16 [33,34], resulted in an increase in the basal

levels of autophagy (Fig. 5.1C, black bars). These data indicate that acetylation of H4K16 by Sas2 regulates an early step in autophagy induction.

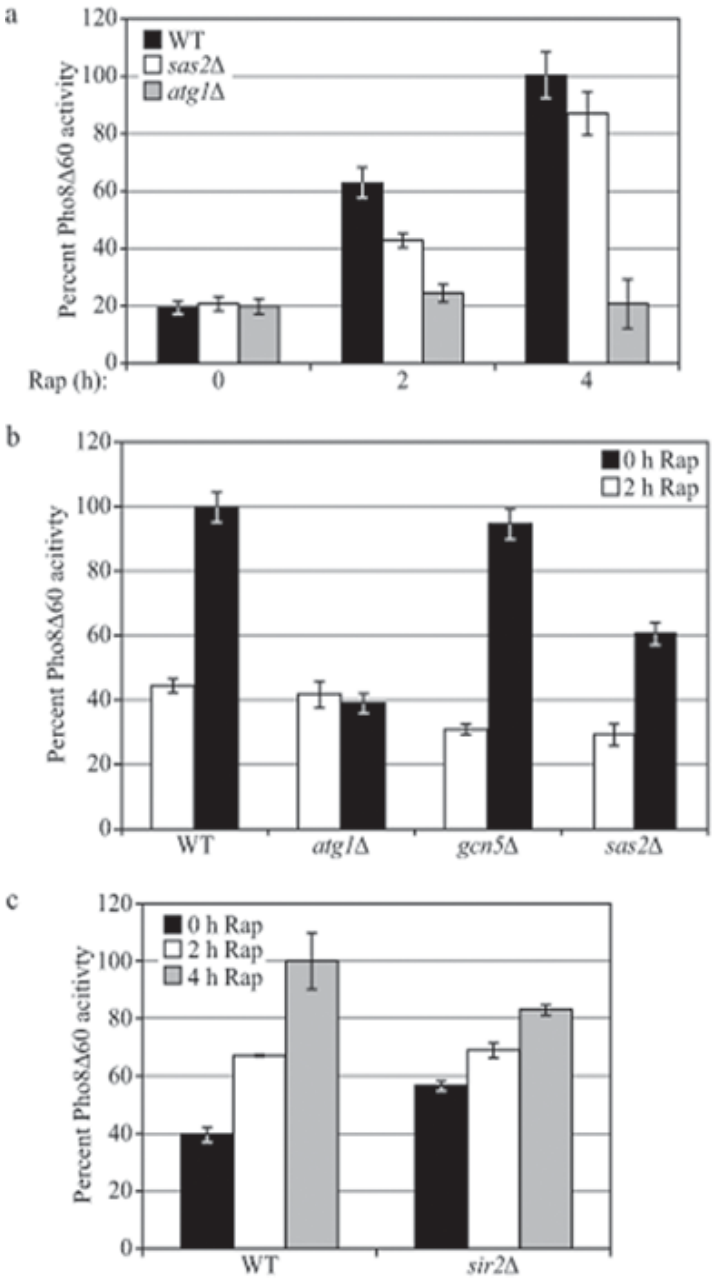

Figure 5.1. *SAS2* deletion delays induction of autophagy. (A) Autophagy as measured by the Pho8Δ60 assay was decreased in *sas2Δ* cells after 2 h of rapamycin treatment. Results were normalized to wild-type cells after 4h rapamycin treatment which was set to 100%. Error bars represent the SEM of three independent experiments. (B) Autophagy was unchanged in the *gcn5Δ* strain. Error bars represent the SEM of three independent experiments. (C) Basal autophagy (time 0) activity was increased in the *sir2Δ* strain. Error bars represent the SEM of three independent experiments.

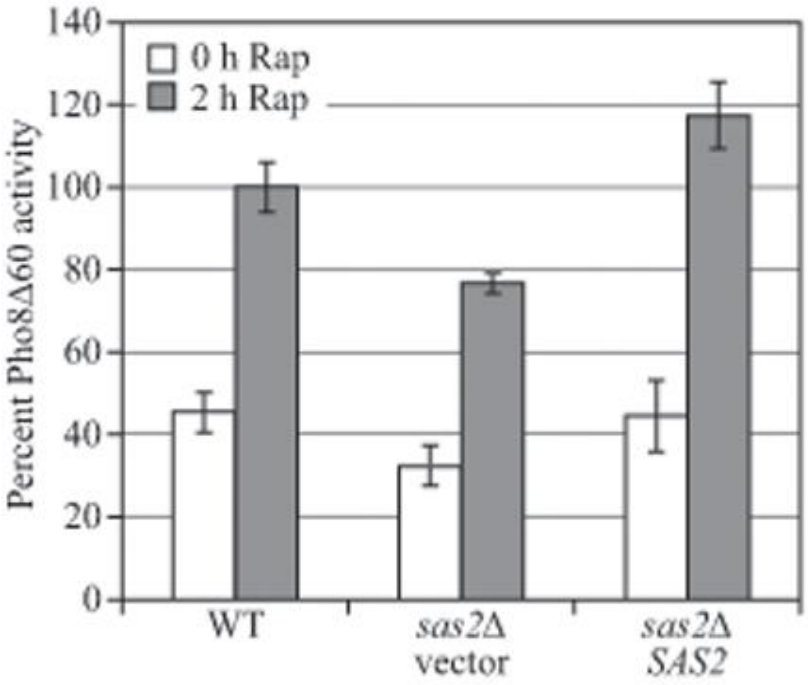

Figure S5.1. A plasmid expressing Sas2 complements the *sas2Δ* strain. Autophagy activity as measured by the Pho8Δ60 assay was restored in the *sas2Δ* when transformed with pSAS2(416). pSAS2(416) and empty vector were transformed into the TN124, *atg1Δ*, and *sas2Δ* strain. Cells were grown to mid-log phase and then treated with rapamycin for 2 h. The Pho8Δ60 assay was performed as described in the Methods Summary. Results were normalized to wild-type cells after 4 h rapamycin treatment, which was set to 100%. Error bars represent the SEM of three independent experiments.

Sas2 regulates *ATG8* expression

One of the earliest events in the induction of autophagy in yeast is the increased transcription of *ATG8;* the corresponding gene product shows the greatest increase in amount of any of the autophagy-related proteins, increasing up to 40-fold relative to basal levels [16,40]. Previously, we showed that Atg8 expression controls the size of the autophagosome [18]. Since Sas2 is needed for the early induction of autophagy we hypothesized that it regulates *ATG8* transcription by acetylating histone 4 at lysine 16 in the promoter region of the *ATG8* gene. Accordingly, we first examined Atg8 protein levels in the presence and absence of Sas2. In the wild-type strain, Atg8 was present at basal levels prior to autophagy induction (i.e., in the absence of rapamycin), and then rapidly increased, reaching a plateau by approximately 2 h (Fig. 5.2A). In the *sas2Δ* strain, there was also an increase in the level of Atg8 following autophagy induction, but to a substantially lower level. To ensure that this phenotype was not dependent on the strain background we repeated this analysis in a second strain, and observed a similar result (Fig. 5.2B).

Atg8 is one of the few autophagy-related proteins that remain associated with the completed autophagosome. As a result, the Atg8 that is conjugated to PE on the inner surface of the autophagosome is delivered to the vacuole and degraded [41]; loss of the Atg8/Atg8-PE signal could in theory reflect elevated autophagic flux. In order to look at the total amount of Atg8, we deleted the *PEP4* gene, which encodes one of the major vacuolar hydrolases [42]. In the wild-type strain lacking Pep4, there was an increase in Atg8 and in particular Atg8-PE, following autophagy induction (Fig. 5.2C). In contrast, the deletion of *PEP4* had no effect on the Atg8 levels in the absence of Sas2. Once again,

the defect in Atg8 expression was specific to the deletion of *SAS2*, because it was not observed in a strain lacking *GCN5* (Fig. S5.2). Since the absence of Sas2 resulted in decreased levels of Atg8, we decided to extend our analysis by examining the effect of overexpressing Sas2, Accordingly, we introduced a plasmid expressing *SAS2* under the control of the *CUP1* promoter. Overexpression of Sas2 resulted in much higher levels of Atg8 compared to the wild-type strain (Fig. 5.2D). Furthermore, expression was increased even prior to autophagy induction.

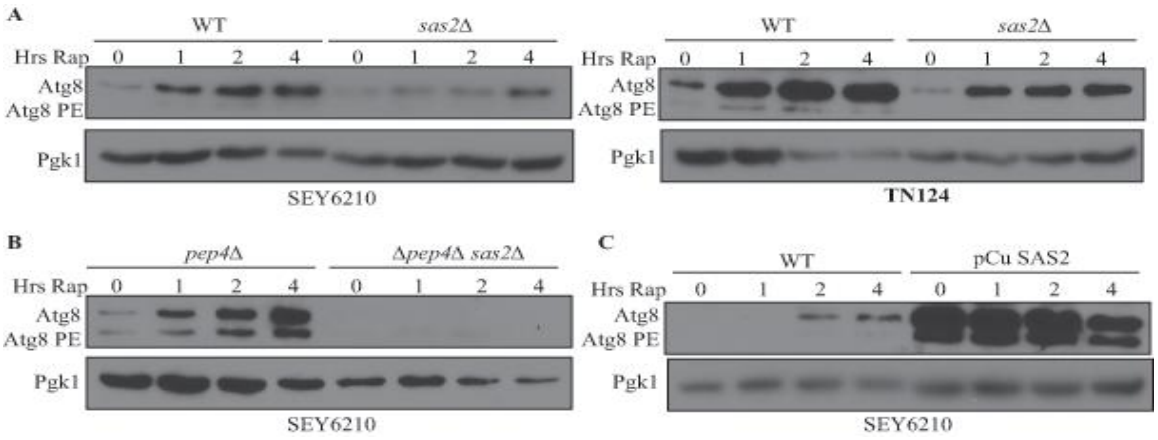

Figure 5.2. Sas2 regulates Atg8 protein levels. (A-D) Atg8 protein levels in the (A) WT (SEY6210) and *sas2Δ*, (B) WT (TN124) and *sas2Δ*, (C) WT (SEY6210, *pep4Δ*) and *sas2Δ*, and (D) WT (SEY6210, empty pCu426 vector) and SAS2 overexpression (pCUSAS2(426)) strains following rapamycin addition. Protein extracts were analyzed with anti-Atg8 and anti-Pgk1 (loading control) antisera.

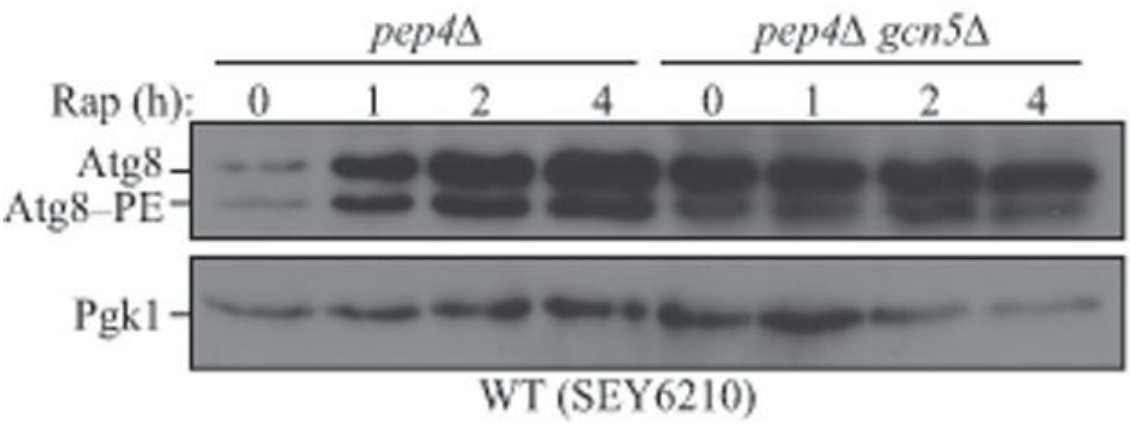

Figure S5.2. The Atg8 expression defect is specific to *sas2Δ*. No defect in Atg8 expression was observed in the *gcn5Δ* strain. Wild-type (SEY6210) and *gcn5Δ* cells were grown to mid-log phase and then treated with rapaymcin to induce autophagy. Cells were collected at 0, 1, 2, and 4 h rapamycin treatment. Protein extracts were analyzed with anti-Atg8 and anti-Pgk1 (loading control) antisera.

We used reverse transcriptase PCR to confirm that Sas2 regulates Atg8 expression by increasing transcription using. We isolated total RNA from *sas2Δ* cells and wild-type cells after 1 h of rapamycin treatment. Gene specific cDNA was then made, followed by amplication using primers to target *ATG8*. In the wild-type strain *ATG8* mRNA was greatly upregulated after 1 h of autophagy induction by rapamycin, whereas in the *sas2Δ* strain *ATG8* mRNA transcription was not upregulated (Fig. 5.3A). These data indicate that Sas2 increases Atg8 expression by promoting *ATG8* transcription.

Considering the function of Sas2 as a H4K16 acetyltransferase, we next wanted to determine if the effect on Atg8 protein levels corresponded with the acetylation of H4K16 at the *ATG8* promoter. To determine this we performed a chromatin immunoprecipitation (ChIP) experiment, wherein we looked at cultures of cells before and after autophagy induction by rapamycin. Genomic DNA fragments were prepared and immunoprecipitated with an antibody that specifically recognized H4K16 acetylation. We then amplified the DNA using a primer set against the *ATG8* promoter just upstream from the start codon. We observed a 6-fold increase in the DNA precipitated upon induction of autophagy (Fig. 5.3B). As controls, we examined *DUR1,2* and *PDA1*. *DUR1,2* transcription is induced upon rapamycin treatment[43] whereas *PDA1* transcription is unchanged[44]. We saw a slight increase (approximately 2 fold) of H4K16 acetylation in the promoter of *DUR1,2*, and no change in acetylation in the *PDA1* promoter. When looking at the acetylation of H4K16 in the deacetylase mutant, *sir2Δ*, we saw an increase in acetylation at the *ATG8* locus prior to autophagy induction as compared to the wild-type (Fig. 5.3C). Together, these results suggest that Sas2 regulates

autophagy by controlling the transcription of *ATG8* through H4K16 acetylation at the *ATG8* promoter.

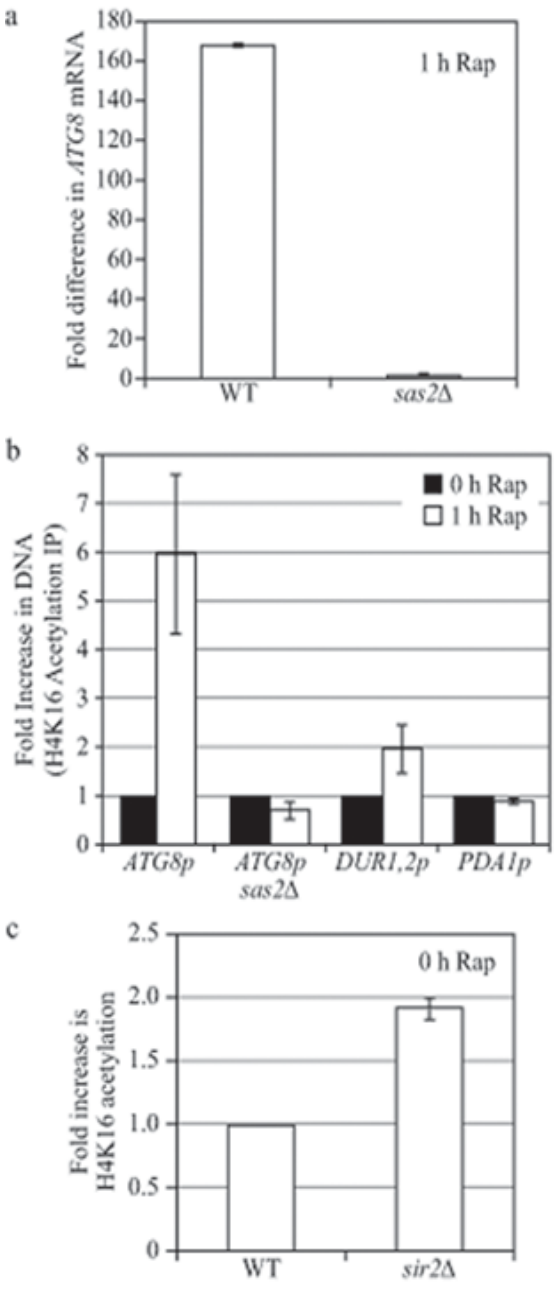

Figure 5.3. Sas2 regulates *ATG8* expression (A) *ATG8* transcription lower in the *sas2Δ* strain. qPCR results of *ATG8* RNA from Wild-type (SEY6210) and *sas2Δ* cells. (B-C) H4K16 acetylated by Sas2 at the *ATG8* promoter upon autophagy induction. ChIP analysis of the *ATG8* promoter upon autophagy induction. ChIP analysis of the *ATG8* promoter in the (B) wild-type strain, *sas2Δ* and (C) *sir2Δ* strain. Controls were the *DUR1,2* and the *PDA1* promoters. Results normalized to the input DNA and then to control conditions. H4K16 acetylated prior to autophagy induction in the *sir2Δ* strain. (A-C) Error bars represent the SEM of three independent reactions.

Sas2 is increased upon autophagy induction and then degraded by the proteasome

Our results suggest that Sas2-dependent histone modifications affect autophagy induction in part by controlling the Atg8 protein levels; thus Sas2 acetyltransferase activity would positively correlate with autophagy. Excessive autophagy, however, would be deleterious to cell physiology. An obvious question then is how Sas2-dependent regulation is itself controlled. Sas2 tagged with 3xhemagglutinin (3HA) is detectable by western blot for 2 h after the induction of autophagy and is almost completely degraded by 3 h (Fig. 5.4A). There are two main pathways through which proteins can be degraded, autophagy and the ubiquitin-proteasome system (UPS) [45]. To determine whether autophagy is involved in Sas2 degredation, we chromosomally integrated a 3HA tag at the *SAS2* locus in wild-type and autophagy mutant strains. Cells were grown to midlog phase and then treated with rapamycin for 3 h. In the *atg1Δ*, *atg5Δ*, and *atg7Δ* strains, Sas2 was rapidly degraded similar to the wild-type strain, suggesting that autophagy was not required for the turnover of this protein (Fig. 5.4A). Next, we examined the potential role of the proteasome using the temperature sensitive *pre1-1* mutant. Compared to the isogenic wild-type strain, the *pre1-1* mutant grown at a non-permissive temperature displayed stabilization of Sas2-3HA (Fig. 5.4B).

The loss of Sas2 following rapamycin treatment led us to hypothesize that although Sas2 may play a role in the early induction steps of autophagy, it is degraded to prevent excessive autophagy activity. We first examined this possibility by looking at Sas2 expression in the early stages of autophagy induction. By examining samples at shorter time points we saw a consistent upregulation of Sas2 expression immediately after autophagy induction followed by degradation, suggesting that there is a biphasic

effect with regard to Sas2 protein levels (Fig. 5.4C). This biphasic effect was also observed in mammalian cells (data not shown); in U2OS cells, hMOF was upregulated 8 h after autophagy induction and was mostly degraded within 48 h. Together these data suggest that Sas2/hMOF is initially upregulated after autophagy induction to induce Atg8/LC3 expression and is then degraded to turn the process off.

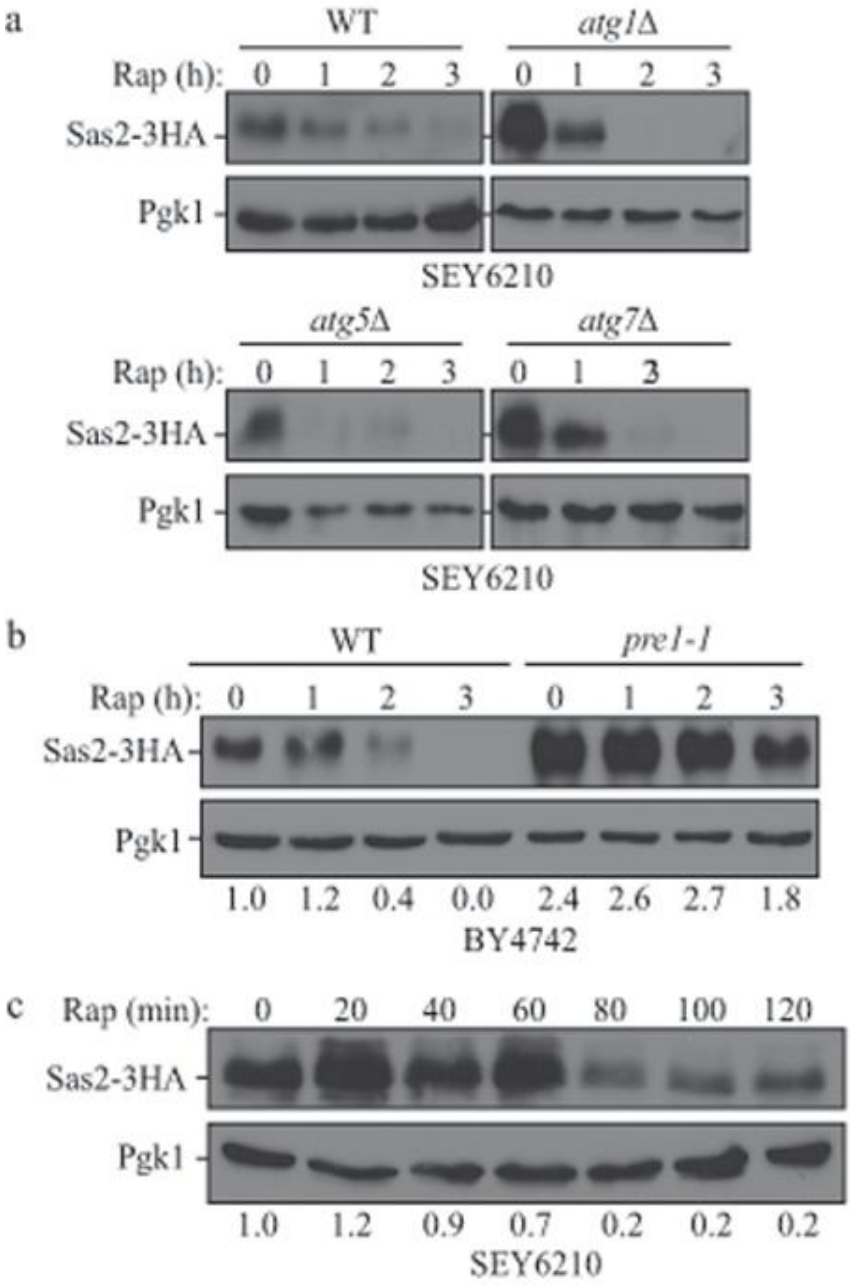

Figure 5.4. Sas2 protein is increased upon autophagy induction and then degraded by the proteosome. (A) Sas2 was degraded in wild-type cells and in autophagy mutants by 3 h post rapamycin. Wild-type (SEY6210), *atg1Δ*, *atg5Δ*, and *atg7Δ SAS2-3HA* protein extracts were analyzed with anti-HA and anti-Pgk1 (loading control) antisera. (B) Sas2 expression is maintained in a proteosome mutant strain. Cell extracts from the *pre1-1* mutant and its isogenic wild-type strain (BY4742) were analyzed as in (A). (C) Sas2 expression is biphasic after autophagy induction; showing an increase in expression before degredation. Wild-type *SAS2-3HA* cell extracts were analyzed as in (A).

Sas2 regulation of Atg8 expression promotes autophagic cell survival

Sas2 promotes the transcription of *ATG8*, but is then degraded after the induction of autophagy, possibly to serve as a guard against overactive autophagy. To determine whether excessive levels of Sas2 are deleterious, the protein was overexpressed by placing it under the control of the *CUP1* promoter at its chromosomal locus. Cultures were grown in copper-limiting medium and then switched to copper-rich medium upon induction of autophagy by nitrogen depletion. The cultures were starved for 96 h and cell viability was determined at 48, 72, and 96 h via serial dilutions and colony counts (Fig. 5.5A-C). There was a clear defect in cell viability after nitrogen starvation when Sas2 was overexpressed as compared to wild-type expression. At a 10^{-4} dilution (with colonies numbering between 10 and 300 per plate) the Sas2 overexpression strain grown in the presence of copper had only about 4% of the number of colonies as the wild-type strain at all three time points. To ensure that the cytotoxicity seen when Sas2 was overexpressed was due to autophagy we looked at cell viability during growing conditions. In this case, we did not observe a loss of cell viability in the Sas2 overexpression strain (Fig. 5.5D). This suggests that the loss of cell viability with Sas2 overexpression during nitrogen starvation was due to autophagy and not just a general cytotoxicity from copper or overexpressed Sas2.

We examined Sas2 expression in the wild-type and overexpressing stains by western blot (Fig. 5.5E). In the wild-type strain, Sas2 was only observed in growing conditions and was completely degraded by 48 h of nitrogen starvation. In the Sas2 overexpression strain, we saw extended Sas2 expression through the 96 h time course.

Together, these data suggest that Sas2 expression must be reduced upon, or following, autophagy induction to promote cell survival.

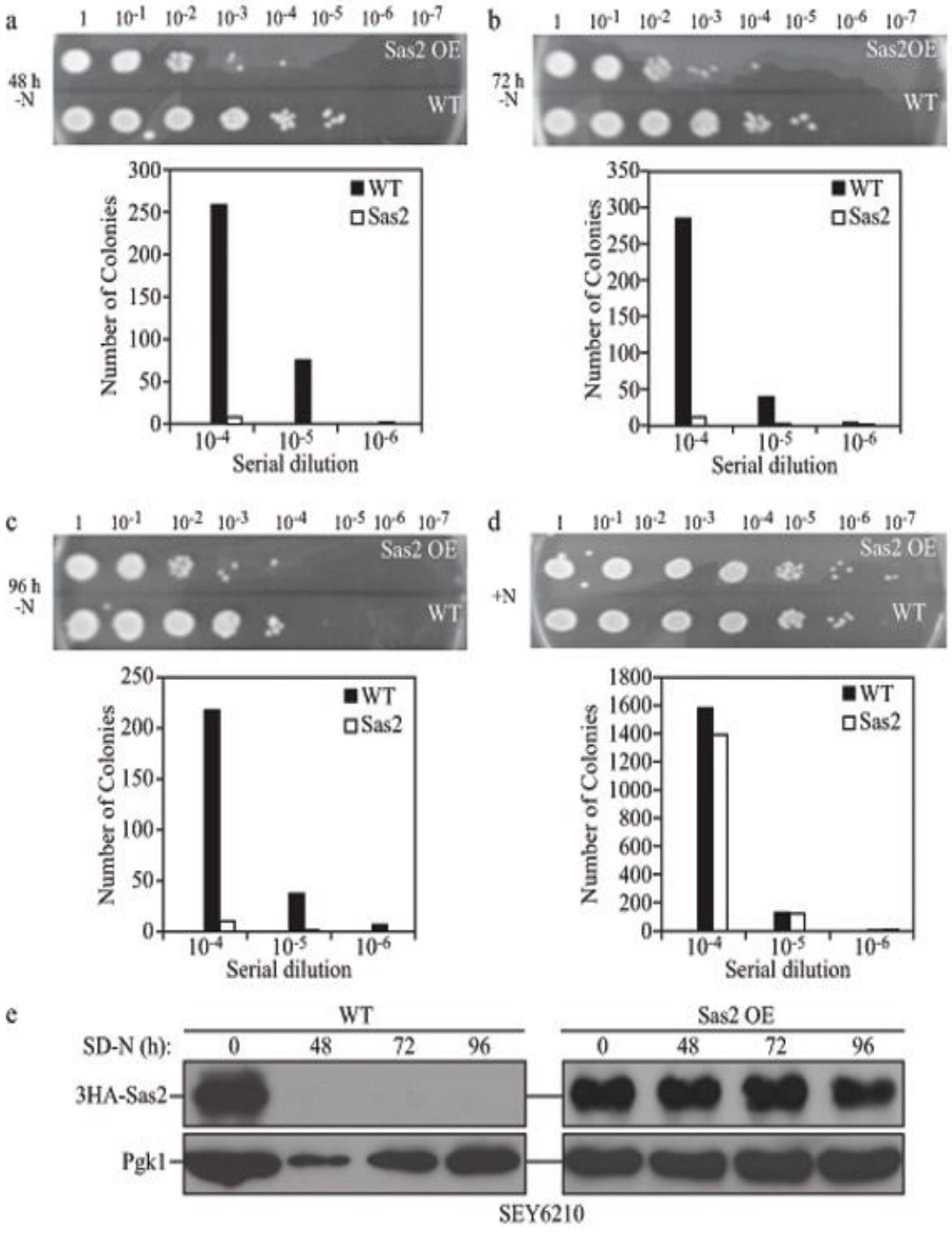

Figure 5.5. Sas2 regulation of Atg8 promotes autophagic cell survival. (A-D) Sas2 overexpression reduces cell survival after prolonged nutrient deprivation. *CUP1*p SAS2 (Sas2 OE), and *SAS2*p SAS2 (WT) cultures were starved for (A) 48 h, (B) 72 h, and (C) 96 h. 1:10 serial dilutions were spotted (image) and spread plated (graph). (D) Cytotoxicty of Sas2 overexpression is due to autophagy. Non-starved cells were plated as in (A-C) (E) Western blot analysis of Sas2 expression for WT and Sas2 OE for each of the starvation time points examined in A-D. Cell extracts were analyzed with anti-HA and anti-Pgk1 (loading control) anti-sera.

Discussion

Our results illustrate the role that the histone acetyltransferase, Sas2 plays in the regulation of autophagy. When autophagy is induced, Sas2 acetylates H4K16 at the *ATG8* promoter leading to activation of transcription. This facilitates maximal autophagy by increasing the pool of Atg8 protein needed to form the autophagosome. Sas2 is then degraded allowing Sir2 to deacetylate the histone. This combination of Sas2 degradation and Sir2-dependent deacetylation limits the expression of Atg8 and acts as an off-switch for autophagy. The degredation of Sas2 by the proteosome therefore limits Atg8 expression level, which in turn dictates the activity of the pathway, preventing hyper activation of autophagy. Thus, this process both induces and limits the autophagic pathway allowing for cytoprotective autophagy. When this regulatory process is disrupted by the continued expression of Sas2 cell viability is reduced. This is a very simple, yet efficient regulatory mechanism.

Sas2 degradation is mediated by the proteasome upon induction of autophagy. The proteasome and autophagy are the two main degredative pathways in the cell [45]. Previous studies have shown that there is crosstalk between the two systems. First, the UPS and autophagy are in balance with one another in the cell. When the UPS is inhibited, autophagy activity increases to compensate, and when autophagy is activated there is a decrease in proteasomal activity and protein [46-49]. A second point of cross talk is in the use of ubiquitin. Originally it was thought that ubiquitin tags were exclusive to the UPS [50,51]. However, recent studies have shown that ubiquitin tags are used during autophagy to recognize cargo in selective forms of the pathway. Both autophagy and the proteasome share some of the ubiquitin recognizing molecules including

SQSTM1/p62 and UBQLN/ubiquilin [52,53]. Third, the proteasome is a favored substrate of autophagy, and all proteins of the 20S proteasome have been observed in association with the autophagosome [46]. In this study we provide an additional example of crosstalk between autophagy and the UPS; Sas2, a regulatory protein of autophagy, is degraded by the proteasome. This data demonstrates a role for the proteasome in providing a direct regulatory function in autophagy.

The appropriate induction of autophagy depends on the ability of the cell to sense various extracellular and intracellular signals, and initiate a corresponding response. The associated signal transduction pathways clearly include nuclear events, but the details of the regulatory process are poorly understood. Here we have established a clear link between a specific histone modification (H4K16 acetylation) and the responsible acetyltransferase (Sas2) and the regulation of autophagy. This is the first demonstration of specific histone modifications at a specific gene locus regulating autophagy. Furthermore, elements of the regulatory mechanism include a means of downregulating autophagy even if cells remain exposed to inducing conditions. Thus, these data provide a new site of regulation that could be targeted by specific therapeutics for the purpose of modulating autophagy to treat disease.

Materials and Methods

Yeast strains used in this study are listed in Table S5.1. Gene disruptions and HA tag integrations were performed using a standard method [54]. Introduction of the *CUP1* promoter was done by excising the *GAL1* promoter of pFA6a-kanMX6-pGAL1-3HA with BglII and PacI and ligating in the *CUP1* promoter. Similar methods with the *SAS2* promoter were employed to N-terminally tag *SAS2*. Protein extraction, immunoblot, and alkaline phosphatase (Pho8Δ60) assays were performed as previously described [39,41,55]. Chromatin immunoprecipitation was performed as previously described with antibody against the H4K16ac epitope [56]. Strains were grown in medium as previously described [56]. Autophagy induction was done by either shifting cells to SD-N, or by treating cell cultures with 0.2µg/ml final concentration rapamycin [57]. RNA extraction was performed with hot acid phenol and RT-PCR was done as previously described [58,59]. Survivability during prolonged autophagy was measured by serial dilutions starting with 1.0 OD_{600} of cells that were then diluted in a series of 1:10 dilutions. The pRS416 plasmid carrying *SAS2* (pSAS2(416)) was made by cloning *SAS2* and its promoter into the pRS416 vector by restriction enzyme digestion with SacI and XbaI. pCuSAS2(426) expressing SAS2 under the control of the *CUP1* promoter was made by cloning *SAS2* into the pCu426 vector by restriction enzyme digestion with ClaI and XmaI.

TABLE S1. Strains

Strain	Genotype	Source
BY4741	*MATa his3Δ1 leu2Δ0 lys2Δ0 ura3Δ0*	ResGen™
BY4742	*MATα his3Δ1 leu2Δ0 lys2Δ0 ura3Δ0*	ResGen™
HAY572	TN124; *atg1Δ::URA3*	[1]
MDY16	TN124; *sas2Δ::TRP1*	This study
MDY17	TN124; *gcn5Δ::TRP1*	This study
MDY18	TN124; *sir2Δ::TRP1*	This study
MDY19	SEY6210; *sas2Δ::TRP1*	This study
MDY20	TVY1; *sas2Δ::TRP1*	This study
MDY21	TVY1; *gcn5Δ::TRP1*	This study
MDY22	SEY6210; *sir2Δ::HIS3*	This study
MDY23	SEY6210; *SAS2-3HA::KAN*	This study
MDY24	WHY1; *SAS2-3HA::KAN*	This study
MDY25	MGY101; *SAS2-3HA::KAN*	This study
MDY26	VDY101; *SAS2-3HA::KAN*	This study
MDY27	*pre1-1; SAS2-3HA::KAN*	This study
MDY28	BY4742; *SAS2-3HA::KAN*	This study
MDY29	SEY6210; *pCu3HA-SAS2::KAN*	This study
MDY30	SEY6210; *3HA-SAS2::KAN*	This study
MGY101	SEY6210; *atg5Δ::LEU2*	[2]
pre1-1	BY4741; *pre1-1::KAN*	This study
SEY6210	*MATα leu2-3,112 ura3-52 his3Δ200 lys2-801 suc2-Δ9 trp1Δ905*	[3]

TN124	*MATa leu2-3,112 ura3-52 trp1 pho8::pho8Δ60 pho13Δ::LEU2*	[4]
TVY1	SEY6210; *pep4Δ::LEU2*	[5]
VDY101	SEY6210; *atg7Δ::LEU2*	[6]
WHY1	SEY6210; *atg1Δ::HIS5 S.p.*	[7]

References

1 Abeliovich, H., Zhang, C., Dunn, W. A., Jr., Shokat, K. M. & Klionsky, D. J. Chemical genetic analysis of Apg1 reveals a non-kinase role in the induction of autophagy. *Mol Biol Cell* **14**, 477-490 (2003).

2 George, M. D. *et al.* Apg5p functions in the sequestration step in the cytoplasm-to-vacuole targeting and macroautophagy pathways. *Mol Biol Cell* **11**, 969-982 (2000).

3 Robinson, J. S., Klionsky, D. J., Banta, L. M. & Emr, S. D. Protein sorting in *Saccharomyces cerevisiae*: isolation of mutants defective in the delivery and processing of multiple vacuolar hydrolases. *Mol Cell Biol* **8**, 4936-4948 (1988).

4 Noda, T., Matsuura, A., Wada, Y. & Ohsumi, Y. Novel system for monitoring autophagy in the yeast *Saccharomyces cerevisiae*. *Biochem Biophys Res Commun* **210**, 126-132 (1995).

5 Gerhardt, B., Kordas, T. J., Thompson, C. M., Patel, P. & Vida, T. The vesicle transport protein Vps33p is an ATP-binding protein that localizes to the cytosol in an energy-dependent manner. *J Biol Chem* **273**, 15818-15829 (1998).

6 Kim, J., Dalton, V. M., Eggerton, K. P., Scott, S. V. & Klionsky, D. J. Apg7p/Cvt2p is required for the cytoplasm-to-vacuole targeting, macroautophagy, and peroxisome degradation pathways. *Mol Biol Cell* **10**, 1337-1351 (1999).

7 Shintani, T., Huang, W.-P., Stromhaug, P. E. & Klionsky, D. J. Mechanism of cargo selection in the cytoplasm to vacuole targeting pathway. *Dev Cell* **3**, 825-837 (2002).

References

[1] Ichimura, Y. et al. (2000) Nature 408, 488-92.

[2] Paz, Y., Elazar, Z. and Fass, D. (2000) J Biol Chem 275, 25445-50.

[3] Hemelaar, J., Lelyveld, V.S., Kessler, B.M. and Ploegh, H.L. (2003) J Biol Chem 278, 51841-50.

[4] Kim, J., Huang, W.P. and Klionsky, D.J. (2001) J Cell Biol 152, 51-64.

[5] Kirisako, T. et al. (2000) J Cell Biol 151, 263-76.

[6] Hanada, T., Noda, N.N., Satomi, Y., Ichimura, Y., Fujioka, Y., Takao, T., Inagaki, F. and Ohsumi, Y. (2007) J Biol Chem 282, 37298-302.

[7] Suzuki, K., Kirisako, T., Kamada, Y., Mizushima, N., Noda, T. and Ohsumi, Y. (2001) EMBO J 20, 5971-81.

[8] Tanida, I., Mizushima, N., Kiyooka, M., Ohsumi, M., Ueno, T., Ohsumi, Y. and Kominami, E. (1999) Mol Biol Cell 10, 1367-79.

[9] Tanida, I., Tanida-Miyake, E., Komatsu, M., Ueno, T. and Kominami, E. (2002) J Biol Chem 277, 13739-44.

[10] Tanida, I., Tanida-Miyake, E., Ueno, T. and Kominami, E. (2001) J Biol Chem 276, 1701-6.

[11] Kametaka, S., Okano, T., Ohsumi, M. and Ohsumi, Y. (1998) J Biol Chem 273, 22284-91.

[12] Reggiori, F., Shintani, T., Nair, U. and Klionsky, D.J. (2005) Autophagy 1, 101-9.

[13] Suzuki, K., Kubota, Y., Sekito, T. and Ohsumi, Y. (2007) Genes Cells 12, 209-18.

[14] Young, A.R. et al. (2006) J Cell Sci 119, 3888-900.

[15] Huang, W.P., Scott, S.V., Kim, J. and Klionsky, D.J. (2000) J Biol Chem 275, 5845-51.

[16] Kirisako, T., Baba, M., Ishihara, N., Miyazawa, K., Ohsumi, M., Yoshimori, T., Noda, T. and Ohsumi, Y. (1999) J Cell Biol 147, 435-46.

[17] Nakatogawa, H., Ichimura, Y. and Ohsumi, Y. (2007) Cell 130, 165-78.

[18] Xie, Z., Nair, U. and Klionsky, D.J. (2008) Mol Biol Cell 19, 3290-8.

[19] Kabeya, Y. et al. (2000) EMBO J 19, 5720-8.

[20] Tanida, I., Minematsu-Ikeguchi, N., Ueno, T. and Kominami, E. (2005) Autophagy 1, 84-91.

[21] Gasch, A.P., Spellman, P.T., Kao, C.M., Carmel-Harel, O., Eisen, M.B., Storz, G., Botstein, D. and Brown, P.O. (2000) Mol Biol Cell 11, 4241-57.

[22] Nakagawa, I. et al. (2004) Science 306, 1037-40.

[23] Bartholomew, C.R. et al. (2012) Proc Natl Acad Sci U S A.

[24] Mallory, M.J., Cooper, K.F. and Strich, R. (2007) Mol Cell 27, 951-61.

[25] Yorimitsu, T. and Klionsky, D.J. (2005) Cell Death Differ 12 Suppl 2, 1542-52.

[26] Xie, Z. and Klionsky, D.J. (2007) Nat Cell Biol 9, 1102-9.

[27] Yang, Z. and Klionsky, D.J. (2010) Nat Cell Biol 12, 814-22.

[28] Mizushima, N., Levine, B., Cuervo, A.M. and Klionsky, D.J. (2008) Nature 451, 1069-75.

[29] Jiang, H., White, E.J., Conrad, C., Gomez-Manzano, C. and Fueyo, J. (2009) Methods Enzymol 453, 273-86.

[30] Lee, I.H. et al. (2008) Proc Natl Acad Sci U S A 105, 3374-9.

[31] Morselli, E. et al. (2011) J Cell Biol 192, 615-29.

[32] Tanno, M., Sakamoto, J., Miura, T., Shimamoto, K. and Horio, Y. (2007) J Biol Chem 282, 6823-32.

[33] Vaquero, A., Sternglanz, R. and Reinberg, D. (2007) Oncogene 26, 5505-20.

[34] Hajji, N., Wallenborg, K., Vlachos, P., Fullgrabe, J., Hermanson, O. and Joseph, B. (2010) Oncogene 29, 2192-204.

[35] Lee, I.H. and Finkel, T. (2009) J Biol Chem 284, 6322-8.

[36] Lin, S.Y. et al. (2012) Science 336, 477-81.

[37] Yi, C. et al. (2012) Science 336, 474-7.

[38] Weidberg, H., Shvets, E., Shpilka, T., Shimron, F., Shinder, V. and Elazar, Z. (2010) EMBO J 29, 1792-802.

[39] Noda, T., Matsuura, A., Wada, Y. and Ohsumi, Y. (1995) Biochem Biophys Res Commun 210, 126-32.

[40] Lang, T., Schaeffeler, E., Bernreuther, D., Bredschneider, M., Wolf, D.H. and Thumm, M. (1998) EMBO J 17, 3597-607.

[41] Shintani, T. and Klionsky, D.J. (2004) J Biol Chem 279, 29889-94.

[42] Woolford, C.A., Daniels, L.B., Park, F.J., Jones, E.W., Van Arsdell, J.N. and Innis, M.A. (1986) Mol Cell Biol 6, 2500-10.

[43] Erdman, S., Lin, L., Malczynski, M. and Snyder, M. (1998) J Cell Biol 140, 461-83.

[44] Wenzel, T.J., Teunissen, A.W. and de Steensma, H.Y. (1995) Nucleic Acids Res 23, 883-4.

[45] Ciechanover, A. (2005) Nat Rev Mol Cell Biol 6, 79-87.

[46] Becker, A.C., Bunkenborg, J., Eisenberg, T., Harder, L.M., Schroeder, S., Madeo, F., Andersen, J.S. and Dengjel, J. (2012) Autophagy 8.

[47] Ding, W.X., Ni, H.M., Gao, W., Yoshimori, T., Stolz, D.B., Ron, D. and Yin, X.M. (2007) Am J Pathol 171, 513-24.

[48] Iwata, A., Riley, B.E., Johnston, J.A. and Kopito, R.R. (2005) J Biol Chem 280, 40282-92.

[49] Pandey, U.B. et al. (2007) Nature 447, 859-63.

[50] Chastagner, P., Israel, A. and Brou, C. (2008) PLoS One 3, e2735.

[51] Kraft, C., Peter, M. and Hofmann, K. (2010) Nat Cell Biol 12, 836-41.

[52] Douglas, P.M., Summers, D.W. and Cyr, D.M. (2009) Prion 3, 51-8.

[53] Waters, S., Marchbank, K., Solomon, E., Whitehouse, C. and Gautel, M. (2009) FEBS Lett 583, 1846-52.

[54] Longtine, M.S., McKenzie, A., 3rd, Demarini, D.J., Shah, N.G., Wach, A., Brachat, A., Philippsen, P. and Pringle, J.R. (1998) Yeast 14, 953-61.

[55] Yorimitsu, T., Zaman, S., Broach, J.R. and Klionsky, D.J. (2007) Mol Biol Cell 18, 4180-9.

[56] Aparicio, O., Geisberg, J.V., Sekinger, E., Yang, A., Moqtaderi, Z. and Struhl, K. (2005) Curr Protoc Mol Biol Chapter 21, Unit 21 3.

[57] Cheong, H., Yorimitsu, T., Reggiori, F., Legakis, J.E., Wang, C.W. and Klionsky, D.J. (2005) Mol Biol Cell 16, 3438-53.

[58] Collart, M.A. and Oliviero, S. (2001) Curr Protoc Mol Biol Chapter 13, Unit13 12.

[59] Del Aguila, E.M., Dutra, M.B., Silva, J.T. and Paschoalin, V.M. (2005) BMC Mol Biol 6, 9.

[60] Robinson, J.S., Klionsky, D.J., Banta, L.M. and Emr, S.D. (1988) Mol Cell Biol 8, 4936-48.

[61] Shintani, T., Huang, W.P., Stromhaug, P.E. and Klionsky, D.J. (2002) Dev Cell 3, 825-37.

[62] Gerhardt, B., Kordas, T.J., Thompson, C.M., Patel, P. and Vida, T. (1998) J Biol Chem 273, 15818-29.

[63] Abeliovich, H., Zhang, C., Dunn, W.A., Jr., Shokat, K.M. and Klionsky, D.J. (2003) Mol Biol Cell 14, 477-90.

[64] Kim, J., Dalton, V.M., Eggerton, K.P., Scott, S.V. and Klionsky, D.J. (1999) Mol Biol Cell 10, 1337-51.

[65] George, M.D., Baba, M., Scott, S.V., Mizushima, N., Garrison, B.S., Ohsumi, Y. and Klionsky, D.J. (2000) Mol Biol Cell 11, 969-82.

CHAPTER 6

Summary and Perspectives

Summary of Results

The autophagy pathway was first reported approximately fifty years ago when Clark and Novikoff observed mitochondria within a membrane-bound vesicle in mouse kidney. They termed these compartments "dense bodies" [1,2]. Shortly thereafter, similar structures were observed in hepatocytes of rats [3], and it was discovered that they contained lysosomal hydrolases [4]. In 1963, the term autophagy was coined by de Duve, and this field of study was officially established [5].

For the next thirty years, studies on autophagy focused on the morphology of the autophagosome. Scientists examined the contents of the autophagosomes, and discovered that the pathway was not just used for bulk degradation, but could also digest specific substrates such as the ER [6], mitochondria [7,8], and peroxisomes [9]. Then, in the late nineties, a genetic approach was taken using the yeast *Saccharomyces cerevisiae* as a model system. Three separate genetic screens identified the core machinery of the autophagy pathway, as well as the genes required for the specific autophagy pathways of pexophagy and cytoplasm to vacuole targeting (Cvt) [10-12]. In the past few years, specific components of the mitophagy pathway have also been uncovered [13] (Appendix B). These genetic studies have lead to a basic understanding of how the pathway works.

We know the basic steps and the basic protein mechanisms of autophagy. We also have some knowledge about the regulation of this pathway. However, much remains to be discovered. For example, we still do not know the exact function of all the autophagy-associated proteins. We do not know the source of the autophagosomeal membrane. We do not understand how the pathway is regulated by different signaling events and how those events control the magnitude of the response. In this dissertation, I have presented the work I have contributed to the field to help shed some light on these questions.

In the first chapter I have described the role autophagy plays in a variety of human disorders. Autophagy prevents diseases by maintaining cellular homeostasis through the removal of damaged organelles and toxic protein aggregates. However, autophagy can also promote disease. In cancer, autophagy contributes to tumor cell survival by providing nutrients to the cancer cells to overcome the hypoxic tumor environment. As such, the inhibition of autophagy in conjunction with chemotherapy treatments can improve patient outcomes. In cardiomyopathies, autophagy is cytoprotective during ischemia, but detrimental during reperfusion. When it comes to regulating autophagy in disease it is important to keep in context the timing of the disease state and the involved regulatory pathways.

In the second chapter I have gone into detail to describe selective autophagy, using the Cvt pathway as an example. Even though the Cvt pathway is not evolutionarily conserved it can still serve as a model for the study of other types of selective autophagy. In the Cvt pathway a receptor protein, Atg19, recognizes the cargo protein prApe1. Then a scaffold protein, Atg11, connects the receptor and its cargo to the main autophagy machinery by binding to both Atg19 and Atg8. The same is true for all specific types of

autophagy; they all require a receptor and a scaffold that links the receptor with the autophagy machinery. Generally, the receptor contains an LIR domain that allows it to bind to Atg8 or LC3 in mammalian cells. Although I have focused my own research on yeast, it is obviously important to continue the study of selective types of autophagy in mammalian cells, because defects in these pathways have been observed in human diseases.

The third chapter focuses on the early secretory pathway as a source of membrane for the autophagosome. In collaboration with the Ferro-Novick and Brumell laboratories we discovered a new guanine nucleotide exchange factor, TRAPPIII, for the early secretory pathway Rab, Ypt1. In the early secretory pathway there are two TRAPP complexes; TRAPPI regulates ER-to-Golgi traffic, whereas TRAPPII regulates intra-Golgi and endosome-to-Golgi traffic [14-17]. The two complexes are composed of the same core subunits: Bet3, Bet5, Trs20, Trs23, Trs31, and Trs33 [18]. The TRAPPII complex contains three additional specificity factors: Trs65, Trs120, and Trs130 [17]. Previously it was thought that Trs85 was one of the core components of the TRAPP complexes; however we discovered that Trs85 is actually the specificity factor for its own TRAPP complex, TRAPPIII.

Prior to this study it was shown that Trs85 is required for both the Cvt pathway and autophagy [19,20]. This earlier study did not uncover the mechanism of involvement of Trs85 in autophagy. We first identified a separate pool of Trs85 that was distinct from the TRAPPI and TRAPII complexes using a combination of fractionation and immunoprecipitation experiments. Trs85 eluted on a Superdex-200 column in fraction 10, independently of the other TRAPP components. We then identified the components that

were precipitated with Trs85 and discovered that this protein co-precipitates with the TRAPPI components but not with those that are specific to TRAPPII. When looking at isolates of the TRAPPI complex, however, Trs85 was not present. In addition, Trs85 deletion did not disrupt the secretory pathway. Together, these data indicated that Trs85 is not a component of the TRAPPI and TRAPPII complexes and is not involved in the secretory pathway. We named this new complex containing the specificity factor Trs85, TRAPPIII. We then determined that TRAPPIII was a GEF for the Rab Ypt1 by measuring GTPγS uptake onto Ypt1 in the sole presence of TRAPPIII.

The identification of this new GEF required for autophagy suggested that Ypt1 may be involved in this pathway as well. I then looked at the role Ypt1 plays in autophagy using four different temperature sensitive (ts) mutants. I discovered that Ypt1 is required for both the Cvt pathway and autophagy using assasys for Pho8Δ60-dependent alkaline phosphatase activity and GFP-Atg8 processing, and the Cvt assay that monitors prApe1 maturation. At first I was concerned that the defect seen in these mutants was due to a defect in the secretory pathway because it had been shown that functional ER-to-Golgi trafficking is required for autophagy [21]. Thus, I examined the secretory pathway for functionality in the ts mutants. The secretory pathway showed normal function in the *ypt1-2* mutant, indicating that the autophagy and Cvt defect seen in this mutant was due solely to a defect in its function in the autophagy pathway and not due to a disruption in ER-to-Golgi trafficking.

I then examined the role Ypt1 and Trs85 play in autophagy using fluorescence microscopy. Both Trs85 and Ypt1 colocalize with the PAS, whereas the TRAPPII-specific components do not. The colocalization is dependent upon the autophagy

machinery, because in the multiple knockout strain, in which the genes encoding the majority of the autophagy machinery have been deleted, Trs85 fails to colocalize with the PAS. The rate of co-localization increased in the *atg1Δ* mutant. This mutant arrests the autophagy machinery at the PAS, and thus the increase in localization suggests that Trs85 and Ypt1 play a role in autophagosome formation. Consistent with this hypothesis, Atg8 failed to properly localize to the PAS upon autophagy induction in the Ypt1 and Trs85 mutant strains, indicating that Ypt1 and Trs85 play a role in the proper recruitment and localization of Atg8 to the PAS.

I also examined the localization of Ypt1 and Trs85 to the PAS in the *atg9Δ* and *atg11Δ* mutants. Both of these strains showed lower colocalization than what was seen in the *atg1Δ* strain. This suggested that Ypt1 and its GEF transport Atg9-containing membranes to the forming autophagosome. Consistent with this hypothesis, I discovered that Ypt1 and Atg9 colocalize at peripheral sites during growing conditions.

The Ypt1 colocalization to the PAS is dependent upon Trs85; Ypt1 remains at the ER membrane in the *trs85Δ* strain. This indicates that the involvement of Ypt1 in the autophagy pathway is dependent upon its GEF, TRAPPIII. This was confirmed using a constitutively active mutant form of Ypt1 that is constantly bound to GTP and no longer requires a GEF. The autophagy defect seen in the *trs85Δ* strain is rescued by the presence of the constitutively active mutant of Ypt1.

All of this together indicated a direct role for Ypt1 and Trs85 in autophagy. From these data we developed the model that Ypt1 and its GEF, TRAPPIII, are involved in the

direct transport of ER membrane to the PAS using Atg9 to mark the membrane and Atg11 to help transport it. Further study needs to be done to confirm this model.

Chapter four was a collaborative effort with the Joseph laboratory at the Karolinska Institutet to study the nuclear regulation of autophagy. In this study we looked at the role of histone modifications in regulating the outcome of autophagy. Upon induction of autophagy there is a global loss of H4K16 acetylation. This loss of acetylation upon induction of autophagy by either amino acid starvation or rapamycin treatment was observed by western blot in mouse embryonic fibroblasts (MEFs), non-small cell lung carcinoma U1810, osteosarcoma U2OS, and cervical cancer HeLa cells. H4K16 acetylation is targeted for removal by the deacetylase SIRT1. Rapamycin induces autophagy independent of SIRT1. Rapamycin treatment is able to decrease H4K16 acetylation, which suggested the decrease in H4K16 acetylation was occurring independent of SIRT1 through the use of other deacetylases or by attenuating acetyltransferase activity. That hypothesis was confirmed when the loss of H4K16 acetylation was observed in *Sirt1* deletion cells upon rapamycin treatment. I was able to show that the loss of H4K16 acetylation was evolutionarily conserved by showing the same results in yeast.

The loss of H4K16 acetylation is associated with the autophagy pathway. In autophagy-deficient yeast strains, *atg1Δ*, *atg5Δ*, and *atg7Δ*, the modification remains visible by western blot after autophagy induction. Similar results were seen in the same mutants in mammalian cells. The H4K16 acetylation mark is associated with H3K4 trimethylation and both promote gene transcription. During autophagy induction, H3K4 trimethylation is also reduced and the reduction is dependent upon a functioning

autophagy pathway. Together, this suggests that there is a global repression of gene transcription upon autophagy induction.

H4K16 acetylation is associated with the regulation of autophagy-associated genes. Using ChIP-Seq and Gro-Seq assays, we discovered that 1,622 genes are either up- or downregulated after 8 hours of rapamycin treatment. Of those genes identified 8.7% are associated with atuophagy and a little less than half of those genes showed reduced H4K16 acetylation. This suggests that the loss of H4K16 acetylation during autophagy induction regulates the transcription of autophagy genes.

The downregulation of H4K16 during autophagy is also associated with the degradation of the acetyltransferase protein KAT8/hMOF in mammalian cells and Sas2 in yeast. Both Sas2 and KAT8 are degraded upon autophagy induction. When Sas2 is overexpressed in yeast, H4K16 acetylation is retained after rapamycin treatment, indicating that the loss of H4K16 acetylation is due to the degradation of the acetyltransferase.

The global loss of H4K16 acetylation and H3K4 trimethylation is important to the outcome of autophagy. When H4K16 acetylation is maintained after autophagy induction by using deacetylase inhibitors there is an increase in apoptotic cell death. These cells show increased nuclear condensation and fragmentation and loss of mitochondrial transmembrane potential, all hallmark signs of cell death. When autophagy is inhibited by chloroquine in these cells in addition to the rapamycin and deacetylase inhibitors, cell death is prevented. In addition, when KAT8 is overexpressed in HeLa cells there is a similar increase in cell death upon autophagy induction.

These findings show that there is an evolutionarily conserved molecular histone switch. In cells, the balance of KAT8/Sas2, and SIRT1/Sir2 regulate H4K16 acetylation. Upon autophagy induction, H4K16 acetylation is removed due to the degradation of KAT8/Sas2 which then promotes autophagic cell survival. When this molecular switch is disrupted the cells undergo apoptosis.

In Chapter 5, I continued to investigate the nuclear regulation of autophagy. In Chapter 4, it was suggested that H4K16 acetylation regulates the transcription of autophagy-associated genes. I decided to examine whether or not Sas2 can promote *ATG8* transcription through the acetylation of H4K16 at the promoter of this gene. I discovered that Sas2 is required for autophagy. When *SAS2* is deleted, there is a reduction in autophagy activity as measured by the alkaline phosphatase assay after two hours of rapamycin treatment as compared to the wild-type strain. This defect was specific to Sas2 and not acetyltransferases in general, because it was not seen in the *gcn5Δ* strain. The block in autophagy was gone after four hours of rapamycin treatment. This suggests that Sas2 is important for the induction of autophagy.

Since Sas2 is involved at the induction step of autophagy, I next looked to determine if it could regulate *ATG8* expression. In the *sas2Δ* strain, there is a failure in the induction of Atg8 expression upon autophagy induction, unlike in the wild-type strain where Atg8 is upregulated. This defect was observed in several different strain backgrounds indicating that it was not strain dependent. Atg8 is degraded during autophagy so I accounted for autophagic flux by examining Atg8 expression in the *pep4Δ* strain. Again, there was a defect in Atg8 induction with Sas2 deleted. When Sas2 is

overexpressed there is an increase in the basal levels of Atg8. Together this indicates that Sas2 does promote Atg8 expression.

To confirm that this was occurring through increased transcription of the gene due to H4K16 acetylation at the promoter, I performed a series of chromatin immunoprecipitation (ChIP) assays and reverse transcriptase PCR (RT-PCR). The ChIP assays indicated that the *ATG8* promoter does show increased H4K16 acetylation upon autophagy induction by rapamycin treatment. When *SAS2* is deleted, the increase in acetylation is not observed. The RT-PCR experiments indicated that *ATG8* transcription is increased upon autophagy induction and that there is less mRNA present in the *sas2Δ* strain as compared to the wild-type strain. Taken in combination, this indicates that Sas2 is responsible for the promotion of *ATG8* transcription upon autophagy induction, and that autophagy induction is inefficient when *SAS2* is deleted.

From chapter four I knew that Sas2 is degraded during autophagy, so I hypothesized that degradation of Sas2 might act as a regulatory mechanism to control the magnitude of the autophagy response. I looked first at Sas2 stability in a variety of autophagy mutants. Sas2 was degraded faster in the autophagy mutants as compared to the wild-type strain; this indicated that autophagy was not required for Sas2 turnover. This result suggested that Sas2 might be degraded by the proteasome system and that the increased rate of degradation was due to an uptick in proteasome activity in response to a defective autophagic pathway. To confirm that Sas2 is degraded by the proteasome, I looked at Sas2 stability in the proteasome ts mutant *pre1-1*. Sas2 expression was maintained after autophagy in the mutant at non-permissive temperature, confirming that the proteasome does degrade Sas2. This is interesting, because it suggests that the

proteasome may help regulate autophagy activity. Previous studies have shown crosstalk between the two systems, but none have shown the proteasome taking a regulatory role in autophagy [22-26].

I hypothesized that Sas2 is degraded to prevent overinduction of autophagy. Dysregulated autophagy is just as problematic as defective autophagy and can result in cell death. I tested this hypothesis by overexpressing Sas2 through copper induction of the gene. This allowed for sustained Sas2 expression through 96 hours of nitrogen starvation, whereas in wild-type cells Sas2 is degraded immediately after autophagy induction. Overexpression of Sas2 decreased cell survival during nitrogen starvation confirming that Sas2 is degraded to promote autophagic cell survival.

This chapter illustrated a unique regulatory mechanism of autophagy. It showed that a histone acetyltransferase regulates autophagy by promoting the transcription of *ATG8*. This pathway is involved in both induction and inhibition of autophagy by modifying acetylation and deacetylation (or trimethylation) of the histones at least at the *ATG8* locus. To my knowledge, this is the first study to look at histone modifications at a specific gene locus with regard to their affect on autophagy. Most epigenetic studies focus on global changes; however, here I have shown that modifications at specific gene loci may be contrary to what is seen globally. This study also indicated that the proteasome can regulate autophagy.

The appendices represent other work that I have been involved in over the last four years. Appendix A is an examination of the role autophagy plays in Parkinson disease. It is clear that both selective and nonselective autophagy play an important role

in maintaining neuronal homeostasis, and defects in those pathways contribute to the progression of the disease. Appendix B is the genetic screen performed to identify genes involved in mitophagy. This screen identified several different genes as playing a role in this process. One gene identified in the screen had no previously-identified function and was named Atg33. This screen will provide the foundation for future studies of mitophagy. Lastly, inhibition of *ATG8* transcription by Ume6 is characterized in Appendix C. Ume6 inhibits *ATG8* transcription by binding to the URS1 site in the promoter of the gene. Ume6 recruits Sin3 and Rpd3, which deacetylate the histones. This provides further insight into the regulation of Atg8 expression.

Future Perspectives

Much work still needs to done to identify the membrane source for the autophagosome. This can be done in two ways; first, by looking for the transport of membrane from different sources to the autophagosome and second, by looking at the contents of the autophagosomal membrane. In following up on the identification of the TRAPPIII complex, I have used two methods to determine if Trs85 and Ypt1 are able to transport ER membrane directly to the PAS. I have used the multiple knockout strain to reintroduce the autophagy machinery one component at a time to determine the proteins required to localize Trs85 and Ypt1 to the PAS. Recently, the Segev laboratory has shown that Atg11 is a downstream effector of Ypt1, and that Trs85 and Ypt1 interact on Atg9 containing membranes [27]. The next step would be to determine if the Atg9 transport proteins are required for localization to the PAS.

The second method has been to follow ER maker proteins to the vacuole. I have used the ER membrane protein Yop1 as a marker for the ER and preliminary results indicate that it is degraded in the vacuole upon autophagy induction (Fig. 6.1). Similar studies can be done using Atg9 as a marker for membrane flow, but there is at least one large hurdle that will have to be overcome; Atg9 is at a variety of peripheral spots prior to autophagy induction, which makes it difficult to follow a single source.

Isolating the autophagosomal membrane may also provide us with significant information making it easier to identify the source of the autophagosome. Once its protein and lipid compositions known we might be able to trace those components back to the membrane source. There are, however, several issues with this approach. First,

organelle markers may be excluded from the source vesicle. Second, there could be a variety of sources so that there might not be enough organelle-specific components to identify a specific source. Last, it may be difficult to remove all other membrane when isolating the autophagosome, resulting in contamination.

The nuclear regulation of autophagy is a growing research field. Several autophagy genes are induced upon the initiation of autophagy including *ATG8* and *ATG19*. The research I have presented here has focused on the regulation of *ATG8* transcription. We have discovered both a transcription inhibitor, Ume6, and a transcription activator, Sas2, but there are probably several other components involved. RNA-Seq, ChIP-Seq, and Gro-Seq can be used to determine the transcription profile of cells after autophagy induction. By looking at these in a variety of conditions that promote autophagy we might be able to elucidate different signaling pathways for each induction event. That could enable us to target autophagy in a context specific manner, thereby eventually leading to better therapeutic treatments in human disease.

More needs to be done to follow up on the role that Sas2 plays in autophagy. First, work needs to be done to delve into the possible regulatory role the proteasome exerts on autophagy. I would begin by looking at how Sas2 is degraded by first identifying the sites of ubiquitination and then determine the ubiquitination pattern of the protein. This could then help to identify other autophagy proteins that might be degraded by the proteasome. I would also look to determine if Sas2 is able to regulate the transcription of other autophagy genes in a manner similar to how it regulates *ATG8* transcription.

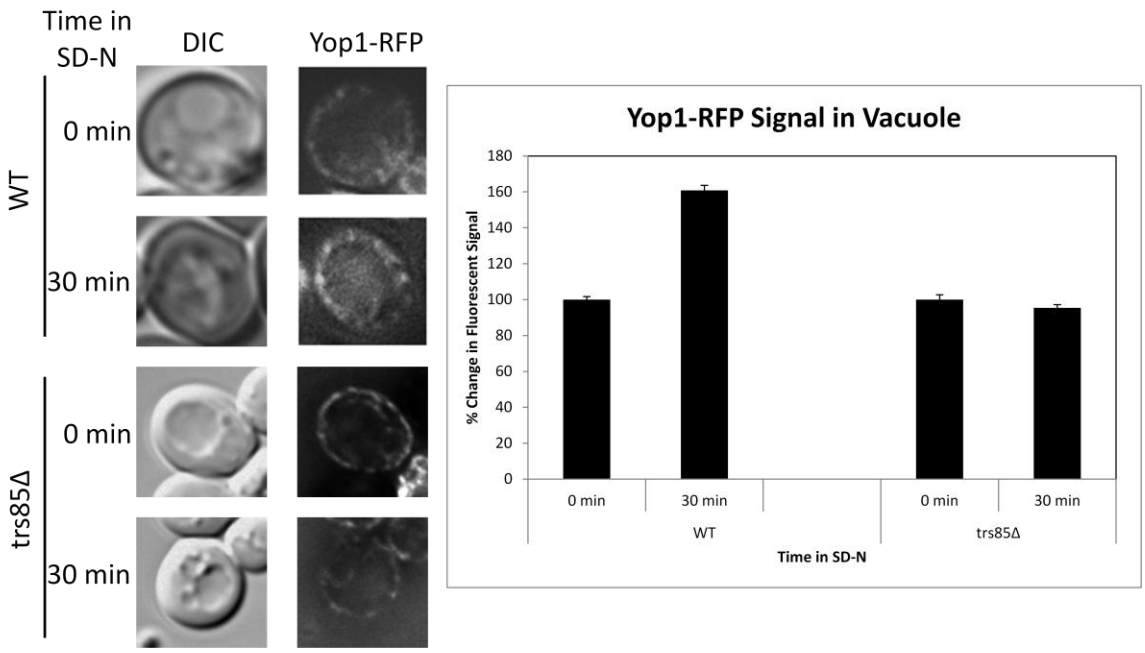

Figure 6.1. Yop1 may be a marker for membrane flow from the ER to the PAS during autophagy. Yop1 is an ER-specific transmembrane protein. Upon autophagy induction it is transported from the ER into the vacuole. Transport of Yop1 to the vacuole is inhibited in the *trs85Δ* strain.

Concluding Remarks

Overall, this dissertation has provided insight into the regulation of autophagy. The work presented here furthers our understanding of the membrane source for the autophagosome. This work also delves into the nuclear regulation of what has mostly been considered a cytoplasmic event. Interestingly, it appears that the nuclear events are also evolutionarily conserved indicating that work in the yeast *Saccharomyces cerevisiae* will continue to be relevant to our understanding of the pathway in higher eukaryotes.

Much remains to be discovered and the work here presents more questions than answers. Autophagy plays a large role in maintaining cellular physiology and both inadequate and excessive autophagy can be harmful. By increasing our knowledge of how autophagy is regulated we can better target it therapeutically to improve patient outcomes in the treatment of various diseases.

References

[1] Clark, S.L., Jr. (1957) J Biophys Biochem Cytol 3, 349-62.

[2] Novikoff, A.B. (1959) J Biophys Biochem Cytol 6, 136-8.

[3] Ashford, T.P. and Porter, K.R. (1962) J Cell Biol 12, 198-202.

[4] Novikoff, A.B. and Essner, E. (1962) J Cell Biol 15, 140-6.

[5] Yang, Z. and Klionsky, D.J. (2010) Nat Cell Biol 12, 814-22.

[6] Bolender, R.P. and Weibel, E.R. (1973) J Cell Biol 56, 746-61.

[7] Beaulaton, J. and Lockshin, R.A. (1977) J Morphol 154, 39-57.

[8] Lemasters, J.J. et al. (1998) Biochim Biophys Acta 1366, 177-96.

[9] Veenhuis, M., Douma, A., Harder, W. and Osumi, M. (1983) Arch Microbiol 134, 193-203.

[10] Harding, T.M., Morano, K.A., Scott, S.V. and Klionsky, D.J. (1995) J Cell Biol 131, 591-602.

[11] Titorenko, V.I., Keizer, I., Harder, W. and Veenhuis, M. (1995) J Bacteriol 177, 357-63.

[12] Tsukada, M. and Ohsumi, Y. (1993) FEBS Lett 333, 169-74.

[13] Kanki, T. et al. (2009) Mol Biol Cell 20, 4730-8.

[14] Cai, H. et al. (2007) Nature 445, 941-4.

[15] Cai, H., Zhang, Y., Pypaert, M., Walker, L. and Ferro-Novick, S. (2005) J Cell Biol 171, 823-33.

[16] Sacher, M., Barrowman, J., Wang, W., Horecka, J., Zhang, Y., Pypaert, M. and Ferro-Novick, S. (2001) Mol Cell 7, 433-42.

[17] Yamasaki, A. et al. (2009) Mol Biol Cell 20, 4205-15.

[18] Cai, Y. et al. (2008) Cell 133, 1202-13.

[19] Meiling-Wesse, K., Epple, U.D., Krick, R., Barth, H., Appelles, A., Voss, C., Eskelinen, E.L. and Thumm, M. (2005) J Biol Chem 280, 33669-78.

[20] Nazarko, T.Y., Huang, J., Nicaud, J.M., Klionsky, D.J. and Sibirny, A.A. (2005) Autophagy 1, 37-45.

[21] Reggiori, F., Wang, C.W., Nair, U., Shintani, T., Abeliovich, H. and Klionsky, D.J. (2004) Mol Biol Cell 15, 2189-204.

[22] Chastagner, P., Israel, A. and Brou, C. (2008) PLoS One 3, e2735.

[23] Ding, W.X., Ni, H.M., Gao, W., Yoshimori, T., Stolz, D.B., Ron, D. and Yin, X.M. (2007) Am J Pathol 171, 513-24.

[24] Iwata, A., Riley, B.E., Johnston, J.A. and Kopito, R.R. (2005) J Biol Chem 280, 40282-92.

[25] Kraft, C., Peter, M. and Hofmann, K. (2010) Nat Cell Biol 12, 836-41.

[26] Pandey, U.B. et al. (2007) Nature 447, 859-63.

[27] Lipatova, Z., Belogortseva, N., Zhang, X.Q., Kim, J., Taussig, D. and Segev, N. (2012) Proc Natl Acad Sci U S A 109, 6981-6.

APPENDIX A

The Role of Autophagy in Parkinson's Disease

Abstract

Great progress has been made toward understanding the pathogenesis of Parkinson's disease (PD) during the past two decades, mainly as a consequence of the discovery of specific gene mutations contributing to the onset of PD. Recently, dysregulation of the autophagy pathway has been observed in the brains of PD patients and in animal models of PD, indicating the emerging role of autophagy in this disease. Indeed, autophagy is increasingly implicated in a number of pathophysiologies, including various neurodegenerative diseases. This article will lead you through the connection between autophagy and PD by introducing the concept and physiological function of autophagy, and the proteins related to autosomal dominant and autosomal recessive PD, particularly α-synuclein and PINK1-PARKIN, as they pertain to autophagy.

Introduction

There seem to be various causes of Parkinson's disease (PD), yet the pathogenesis of this disease appears to be converging on common themes—oxidative stress, mitochondrial dysfunction, and protein aggregation—all of which are tightly linked to autophagy, a highly conserved cellular homeostatic process essential for bulk degradation of cytoplasmic contents. In particular, the recent identification of autosomal dominant and autosomal recessive mutations in familial PD has revealed the involvement of the corresponding gene products in autophagy. Although autophagy has commonly been regarded as an adaptive response to nutrient deprivation, increasing evidence indicates that basal, constitutive autophagy is essential for neuronal survival and that its dysregulation leads to neurodegeneration.

Autophagy

Main Types of Autophagy

Autophagy is an evolutionarily conserved catabolic process that mediates the degradation of long-lived proteins and dysfunctional or superfluous organelles in eukaryotic cells. Autophagy is induced by various adverse conditions such as limited nutrients, low oxygen levels, and decreased energy supply, and its action results in the release of degradation products, especially amino acids, back into the cytoplasm to be used in essential biosynthetic pathways.

According to the different pathways by which cargo is delivered to the lysosome or vacuole, autophagy can be divided into three main types (Fig. A.1): macroautophagy, microautophagy, and chaperone-mediated autophagy (CMA). CMA involves direct translocation of unfolded proteins across the lysosome membrane. Chaperone proteins mediate this process by binding to cytosolic substrates that enter the lysosome through interaction with a receptor/channel on the lysosomal membrane [1]. Microautophagy describes the process of direct uptake of cytoplasmic materials at the lysosome surface by invagination of the lysosome membrane. After vesicles containing the cytosolic substrates pinch off into the lysosomal lumen, they are rapidly degraded [2]. In contrast, during macroautophagy, portions of the cytoplasm are engulfed by a double-membrane phagophore that expands into a cytosolic vesicle called an autophagosome; the completed autophagosome is targeted to the lysosome in mammalian cells or the vacuole in yeast [3]. The outer membrane of the autophagosome subsequently fuses with the lysosomal/vacuolar membrane, allowing hydrolases access to the inner autophagosome

membrane and its cargo, which is degraded and recycled. In contrast to the ubiquitin-26S proteasome system, macroautophagy can mediate nonselective and bulk degradation of cytoplasmic contents, including entire organelles [4,5]. Among the three main types of autophagy, macroautophagy is the best characterized process and will hereafter be referred to as autophagy.

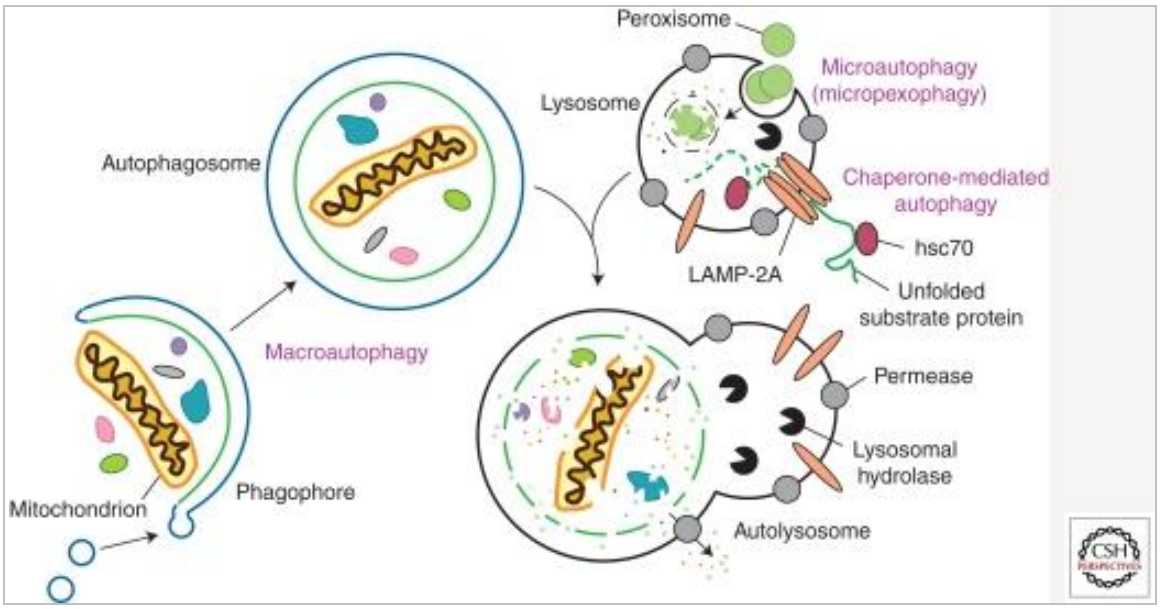

Figure A.1. Schematic model of the three main types of autophagy. The modes of autophagy differ depending on the nature of the substrate and the site of sequestration. In chaperone-mediated autophagy, the substrates contain a KFERQ-consensus motif, are unfolded by HSC70 chaperones, and translocate directly across the lysosome membrane via interaction with a LAMP-2A oligomer. There are various types of microautophagy-like processes including micropexophagy and micromitophagy, the selective degradation of peroxisomes and mitochondria, respectively. Again, sequestration occurs at the lysosome-limiting membrane, but the substrates do not have to be unfolded. Macroautophagy uses a double-membrane phagophore to sequester the cargo. Essentially any cytoplasmic component can be enwrapped by a phagophore, which expands into an autophagosome. Fusion with the lysosome allows the cargo to be degraded, and the resulting macromolecules are released into the cytosol through permeases, allowing them to be reused for anabolic processes.

Selective Autophagy

In some cases, autophagy displays substrate specificity, even though autophagy is often considered to be a nonselective pathway for the degradation of bulk cytoplasmic components. Indeed, the unique feature of the autophagy process where the initial sequestering compartment expands into an autophagosome allows for flexible cargo selection. For example, in the cytoplasm to vacuole targeting (Cvt) pathway, autophagy fulfills a biosynthetic role by delivering three vacuolar hydrolases, α-mannosidase (Ams1) [6], aminopeptidase I (Ape1) [7], and aspartyl aminopeptidase (Ape4) [8] to their final destination, the vacuole. In addition, superfluous or damaged organelles and misfolded or aggregated proteins are selectively targeted for degradation by autophagy. Different terms are used depending on the cargo, for example, "mitophagy" for selective autophagic degradation of mitochondria, "pexophagy" for peroxisomes, "reticulophagy" for the endoplasmic reticulum (ER), and "ribophagy" for ribosomes [9]. Among them, mitophagy has been increasingly implicated in the pathogenesis of PD through the PINK1-PARKIN-mediated pathway.

Molecular Mechanisms of Autophagy

The molecular understanding of autophagy was initiated by pioneering work in yeast utilizing genetic screens that led to the discovery of autophagy-related (*ATG*) genes, followed by the identification of homologs in higher eukaryotes. The corresponding Atg proteins can be divided into four major groups: the Atg1/unc-51-like kinase (ULK) complex, two ubiquitin-like protein (Atg12 and Atg8/LC3) conjugation systems, the class III phosphatidylinositol 3-kinase (PtdIns3K)/Vps34 complex I, and the Atg9/mATG9

transmembrane protein system [10]. The target of rapamycin (TOR), a master regulator of nutrient and growth factor signaling, is one of the critical components involved in controlling the induction of autophagy [11]. In most cell types, TOR activity is necessary and sufficient to suppress autophagy under favorable growth conditions, primarily in response to nitrogen. Other kinases, including protein kinase A, AMPK/Snf1, and Pho85, modulate autophagy in response to various types of stress.

Both the Atg1/ULK complex and the membrane protein Atg9 function early in the process of autophagosome formation. Atg1 is a target of the Tor signaling pathway and acts in part by regulating the localization of other Atg proteins such as Atg9, an integral membrane protein that cycles back and forth between the site of phagophore nucleation/autophagosome formation, termed the phagophore assembly site (PAS), and other peripheral locations [12]. Due to its subcellular itinerary and its characterization as a membrane protein, Atg9 is thought to be responsible for the transport of donor membrane that contributes to autophagosome formation.

The main product of the ubiquitin-like conjugation systems is the covalent attachment of Atg8 to phosphatidylethanolamine (PE) [13]. Atg8–PE becomes associated with both the inner and outer membrane of the phagophore. Once the autophagosome is complete, Atg8 is cleaved off of PE from the outer membrane, whereas the Atg8 on the inner membrane remains associated with PE and is degraded in the vacuole. Atg8 controls the size of the forming autophagosome [14], and is also involved in cargo recognition during selective autophagy [5,15].

Physiological Functions and Connections to PD

Although autophagy is primarily a starvation response in yeast, in higher eukaryotic organisms, autophagy is involved in a wide range of physiological and pathological processes, including responses to nutrient deprivation, development, intracellular clearance, suppression of tumor formation, aging, cell death and survival, and immunity [16]. As a primary protective mechanism that maintains nutrient and energy homeostasis in response to stress, dysregulation of autophagy underlies the pathophysiologies of many diseases. Increasing evidence suggests that dysregulation of autophagy results in the accumulation of abnormal proteins and/or damaged organelles, which is commonly observed in neurodegenerative diseases, such as Alzheimer, Huntington's, and Parkinson's diseases [17]. Of note, autophagy is the only known mechanism that eukaryotic cells possess to degrade protein aggregates and damaged organelles that cannot be processed by the proteasome. Recent studies from transgenic mice, animal, and cell models of PD suggest the involvement of proteins genetically linked to autosomal dominant PD, particularly α-synuclein and LRRK2, in the autophagy pathway [18,19]. In addition, proteins related to recessive PD, such as PINK1 and PARKIN, have an important role in the process of mitophagy.

Early Discoveries: α-Synuclein and Autophagy

α-Synuclein and PD

α-Synuclein was found to localize to the presynaptic terminals in the central nervous system and is involved in vesicular release [20-22]. It is a natively unfolded protein, but can be found in several aberrant conformational states including an oligomer, a protofibril, and an amyloid fibril [23]. α-Synuclein was identified as a component of Lewy bodies, cytosolic inclusions that are a pathological trait of PD [24,25]. Studies of familial cases of autophagy reveal two separate autosomal dominant mutations in the α-synuclein gene: A53T and A30P [26]. In addition to the point mutations, several posttranslational modifications such as phosphorylation, ubiquitination, nitration, oxidation, and dopamine-dependent adduct formation also create toxic forms of the protein [23].

Chaperone-Mediated Autophagy

α-Synuclein in its native form is degraded by chaperone-mediated autophagy [27]. The protein contains a 15 amino acid sequence that consists of imperfect yet overlapping variations of the KFERQ CMA recognition motif. The chaperone protein HSC70 recognizes the pentapeptide sequence motif and binds to α-synuclein. α-Synuclein then binds to the lysosomal-associated membrane protein type 2A (LAMP-2A) at the lysosomal membrane. This CMA receptor with the aid of a lysosomal lumenal HSC70 transports α-synuclein into the lysosome where it is degraded by proteases. Mutant forms of the protein prevent its degradation by the CMA pathway resulting in toxic aggregation in the cytoplasm as was seen in cell culture and postmortem tissues [23]. Autophagy can

partially compensate for the lack of CMA-mediated degradation, but may cause autophagic cell death under stress conditions. Cells expressing mutant α-synuclein can be characterized by an increase in cell death, accumulation of autophagosomes, and a loss of ability to store catecholamine along with a failure to release dopamine [28].

All mutant forms of α-synuclein vary in the degree to which they hamper the lysosomal/CMA degradation pathway and thus have different levels of toxicity. In cell culture studies, the A53T and A30P mutants of the protein bind more strongly to the LAMP-2A receptor than the wild-type form, but fail to be transported across the lysosomal membrane [23]. The mutants act as receptor inhibitors, preventing other CMA targets from binding. This leads to a complete block in CMA resulting in a higher degree of toxicity. Overexpression of the wild-type protein is matched by an increase in expression of the CMA receptor protein LAMP-2A, but high levels of protein expression lead to the formation of oligomeric forms that cannot be degraded by CMA [29,30]. This results in a toxicity level that is lower than the familial point mutant forms. Similar intermediate levels of toxicity are seen in certain posttranslationally modified versions of α-synuclein as was illustrated in cell and post-mortem tissues. Phosphorylated, ubiquitinated, nitrated, and oxidized forms are less susceptible to CMA degradation than the nonmodified protein, but they do not block CMA in its entirety. It is thought that these modifications promote higher-order oligomers that cannot be broken down and degraded. This is reflected in the observation of all of these modifications in cytosolic aggregates.

Modification of the protein with dopamine gives a phenotype that more closely resembles the point mutations. α-Synuclein can be modified with oxidized dopamine

through a noncovalent interaction. Dopamine α-synuclein (DA-α-syn) inhibits not only its own degradation, but it also blocks CMA activity in general. This defect can be seen in a variety of experimental conditions including isolated lysosomes, dopaminergic cell lines, and visceral motor neurons. The CMA defect results from DA-α-syn expression because it is not seen in α-synuclein deletion cells, it is not observed with the dopamine insensitive form of α-synuclein, and it is reproduced with isolated lysosomes when presented with DA-α-syn. The complete blockage of CMA creates a high level of toxicity [23]. What is interesting about the DA-α-syn modification is that it is the dopaminergic substantia nigra and the norepinephrine-releasing locus coeruleus neurons that are killed first in the progression of PD. Both of these types of neurons contain cytosolic dopamine and produce neuromelanin (a product of dopamine modifications). The toxic DA-α-syn form of the protein may explain why those two types of neurons are particularly sensitive.

The blockage of CMA activity with mutant forms of α-synuclein not only results in the direct buildup of toxicity in the neuron through the formation of aggregates, but it also prevents the protective activity of the protein myocyte enhancer factor 2D (MEF2D). MEF2D, a transcription factor, is an important player in neuronal survival. Patients with PD show an increase of this protein in brain neurons, and a genetic polymorphism of a related protein (MEF2A) has been linked to Alzheimer disease. CMA-dependent degradation regulates MEF2D activity. MEF2D is continuously shuttled to the cytosol from the nucleus where it interacts with hsc70. In cells, when CMA is inhibited, an inactive form of the protein accumulates in the cytosol and the amount of protein in the nucleus drops. This inactive form can no longer bind DNA. Wild-type and mutant forms

of α-synuclein prevent binding between HSC70 and MEF2D [31]. This suggests that not only does α-synuclein promote neuronal death through the formation of aggregates, but it also promotes cell death by inhibiting cell survival proteins.

α-Synuclein and Autophagy

As noted previously, inhibition of CMA by aberrant α-synuclein leads to an increase in autophagy. This appears to be a compensatory response, but rather than leading to cell survival, the induction of autophagy can be detrimental causing autophagic cell death. Blocking autophagy by knocking down the autophagy protein Atg5 in cells expressing the A53T α-synuclein mutant can rescue the cell from toxicity-induced cell death [30]. However, autophagy-induced neuronal death is not always the outcome. One study suggests that the signaling pathway for activation of autophagy may be important as to whether or not autophagy will be protective or detrimental. Autophagy is mainly initiated through the mTOR signaling pathway either directly or indirectly through the autophagy protein Atg1. An additional signaling pathway for initiation of autophagy is the Vps34-Beclin 1 complex. It is this secondary signaling pathway that appears to promote cell survival. For example, a reduction in α-synuclein accumulation is seen when Beclin 1 is overexpressed. In addition, Beclin 1 overexpression decreases cell death and increases autophagy activity observed through enhanced lysosomal degradation [22].

Not only does aberrant α-synuclein inhibit CMA, but it also inhibits autophagy through RAB1A and omegasome formation as seen in both cell and mouse models [32]. RAB1A is a GTPase involved in the early secretory pathway, specifically ER-to-Golgi transport. The early secretory pathway is important for autophagy, and inhibition of the secretory pathway blocks autophagy. Furthermore, RAB proteins can play a role in

autophagy independent of the secretory pathway, as seen with Ypt1 in yeast [33] and RAB1A in mammalian cells [34]. α-Synuclein overexpression blocks autophagosome formation, inhibits secretion, and increases Golgi fragmentation. Overexpression of RAB1A rescues this defect. The block in autophagy due to α-synuclein overexpression occurs early in the pathway, before autophagosome formation, suggesting an effect on ATG9, which is the only transmembrane protein required for autophagy. It is thought that ATG9 is responsible for the transport of membrane to the site of autophagosome formation and thus acts early in the process. ATG9 normally forms puncta at a perinuclear location (the site of autophagosome formation) and at the*trans*-Golgi network in mammalian cells. When α-synuclein is overexpressed, ATG9 is mislocalized and is diffuse throughout the cytoplasm of the cell. The same phenotype is seen with the knockdown of RAB1A. One preautophagosome structure that branches off of the ER is the omegasome, which generates an autophagosome, at least under some circumstances. Omegasome formation is reduced in cells that overexpress α-synuclein and in cells that have reduced RAB1A protein levels. α-Synuclein blocks autophagy by inhibiting the activity of RAB1A, which results in the mislocalization of ATG9 and inhibition of autophagosome formation [32].

α-Synuclein and Mitophagy

More recent studies of α-synuclein in PD have shown a relationship between its aberrant expression and mitophagy. Mitochondrial dysfunction is another characteristic of PD and will be described in more detail later in this article. However, a connection has been made between the activation of autophagy by aberrant α-synuclein expression and mitochondrial dysfunction. In cells expressing the A53T α-synuclein mutant, there is an

observed increase in colocalization between autophagosomes and normal, polarized mitochondria. In addition, there is a decrease in the number and length of mitochondria in these cells. Similar results are seen when wild-type α-synuclein is overexpressed; however, the phenotype is not as severe. The increase in mitochondria clearance in these cell lines is dependent on mitochondrial fragmentation and on the protein PARKIN [35]. PARKIN, currently another large area of focus for autophagy and PD research, will be discussed in the next section of this article. However, the role of α-synuclein in the promotion of mitophagy of polarized mitochondria suggests that there may be a connection between it and PARKIN in the promotion of the disease.

Recent Studies: Controversies Abound

In this section, we will discuss new yet controversial areas of research with regard to PD and autophagy. Recent studies have focused on the hypothesis of mitochondrial dysfunction as a cause of the disease. These studies have resulted in some interesting data, but to date there is no clear indication as to whether mitochondrial dysfunction is a cause of Parkinson or is rather correlated with the progression of the disease.

The Hypothesis: Mitochondria Dysfunction in PD

Mitochondria are essential organelles that provide >90% of the energy in all eukaryotic cells through oxidative phosphorylation [36]. Mitochondria are also involved in various other processes such as calcium homeostasis [37] and regulation of apoptosis [38]. However, mitochondria are also the major source of cellular reactive oxygen species (ROS). Normal levels of ROS can be tolerated because of cellular antioxidants, whereas in pathological situations of mitochondrial respiratory defect, dramatic ROS production exceeds the capability of antioxidant protection and causes severe damage to a wide range of cellular components including mitochondria. Accumulation of this damage is related to aging, cancer, and recently to neurodegenerative diseases such as PD [39].

PD is characterized primarily by the selective loss of dopaminergic neurons in the substantia nigra pars compacta leading to a dopamine deficit in the striatum. Recent evidence suggests that mitochondria dysfunction may play a role in the pathogenesis of both sporadic PD and familial Parkinsonism. One current model suggests that mitochondrial dysfunction results from damage to complex I of the mitochondrial electron transport chain [40]. Indeed, some studies have shown complex I activities to be

significantly reduced in post-mortem substantia nigra of PD patients [41,42]. There are several lines of evidence that suggest that increased oxidative damage and ATP depletion may cause dopaminergic neuronal cell death, but the hypothesis linking PD and complex I deficiency is still highly debatable, and the question of causation versus correlation remains to be answered.

Familial variants of PD account for up to 10% of all cases [43]. In familial PD, several genes have been linked to autosomal recessive (*PARK2*, *PARK6*, *PARK7*) or dominant (*LRRK2*) Parkinson [44]. These genes have been linked to mitochondrial function and several very recent studies have demonstrated that the corresponding gene products are involved in the selective removal of damaged mitochondria through autophagy [45,46]. Thus, these proteins may provide a link between mitophagy and PD.

Mitophagy: Autophagic Mitochondrial Removal

As discussed above, autophagy can be highly specific. During autophagy, the phagophore gradually expands and engulfs a portion of the cytoplasm, or specific cargos, to form the double-membrane autophagosome [47]. The diameter of a typical autophagosome is approximately 500 nm [14]; however, the mechanism of autophagosome formation, involving the sequential expansion of the phagophore, provides autophagy with the capacity to sequester essentially any cellular components, including entire organelles, and deliver them into the lysosome for degradation.

Pioneering studies in yeast have demonstrated that autophagic degradation of mitochondria, mitophagy, can be a highly selective and tightly regulated process [4,48]. In yeast cells, mitophagy fits with the common model of a receptor-adaptor system for the selective degradation of a specific cargo by autophagy; a tag on the cargo is

recognized by a receptor and/or adapter, which links the cargo with the autophagy machinery via interaction with Atg8 [5,49]. In the case of mitophagy, yeast genetic screens discovered a mitochondrial outer membrane resident protein, Atg32, which functions as the receptor for the sequestration of mitochondria into an autophagosome [4,15]. During mitophagy, Atg32 is recognized by an adaptor protein, Atg11, which is proposed to play a role in mediating cargo recognition and transport to the phagophore assembly site (PAS), the nucleating structure for generation of the phagophore [50]. Mitochondrial fragments containing Atg32 are then enwrapped by the expanding phagophore, ultimately being incorporated into an autophagosome. The detailed mechanism of this process is still under study.

In higher eukaryotes, autophagy also plays a critical role in degrading mitochondria. In fact, mitochondria were first detected inside an autophagosome in the 1950s [51]; however, a molecular understanding of this process is occurring only now. Studies suggest that the selective removal of mitochondria, especially damaged mitochondria, is part of an important homeostatic pathway for organelle quality control. Since mitochondria function is compromised in some PD models, a defect in mitochondria quality control may play a critical role in the pathogenesis of PD.

Mitophagy and PD

As mentioned above, several genes related to PD have been recently reported to participate in the removal of damaged mitochondria through autophagy. The *PARK2* gene has been reported to be mutated in nearly 50% of autosomal recessive, and 10%–15% of sporadic early-onset PD. PARKIN, the gene product of *PARK2* is a primarily cytosolic ubiquitin E3 ligase that contains a ubiquitin-like domain, two RING finger domains, and

a conserved region between the RING domains [52]. PARKIN has been previously reported to function in the cytosol, in the ER, on mitochondrial targets, and at the plasma membrane; however, no clear evidence had linked PARKIN function to the pathogenesis of PD. Recent studies from Richard Youle's group and others, however, have provided a model for PARKIN's role in eliminating impaired mitochondria [45]: PARKIN is specifically recruited to damaged mitochondria and promotes their autophagic degradation [43]. At steady state, PARKIN is cytosolic. However, treatment of PARKIN-overexpessing cells with the mitochondrial uncoupler carbonyl cyanide m-chlorophenylhydrazone (CCCP) leads to a rapid and significant relocation of PARKIN to mitochondria, followed by substantial mitochondria loss from the treated cells. The loss of mitochondria is dependent on the expression of PARKIN and the presence of autophagic proteins, demonstrating that degradation of mitochondria is through autophagy. Extensive mitochondria fragmentation is observed following CCCP treatment, in a PARKIN-independent manner. Microscopy studies show that PARKIN is selectively recruited to mitochondria fragments that have decreased or no membrane potential, suggesting a role for PARKIN in distinguishing between healthy and damaged mitochondria. Further observation shows that these PARKIN-marked mitochondrial fragments are LC3 (a mammalian homolog of yeast Atg8) positive, further demonstrating that clearance of damaged mitochondria occurs through autophagy. Overexpressed PARKIN is also recruited to mitochondria upon an increase in complex one-dependent ROS, which follows treatment with the herbicide paraquat, a toxin frequently used to induce a PD phenotype in some animal and cell culture models [53].

Mitochondrial Targets of PARKIN

The translocation of PARKIN to mitochondria is an indispensable step in PARKIN-dependent mitophagy. Therefore, the identification of mitochondrial targets of PARKIN is significant for elucidating the underlying mechanism of this cellular activity. Although the mitochondrial voltage-dependent anion channel 1 (VDAC1) was reported to be ubquitinated by PARKIN in HeLa cells, this ubquitination does not seem to be required for mitochondrial clustering or mitophagy [46,54,55]. The other putative mitochondrial targets of PARKIN include the mitochondrial fusion proteins MFN1 and MFN2 [56,57]. After translocation to mitochondria, PARKIN ubquitinates MFN1/2 causing their degradation, which facilitates mitochondrial fission; normal fission may be necessary for efficient mitophagy. However, if MFN1/2 are the only substrates of PARKIN, the latter might play a role in facilitating, but not activating mitophagy; it is thought that mitochondrial fission is required, but not sufficient to initiate mitophagy. Therefore, to determine the real role of PARKIN in mitophagy, some other specific substrates of PARKIN, if they exist, have to be identified. Along these lines, a recent study from David Chan's group suggests that PARKIN activates the ubiquitin-proteasome system, which results in the ubiquitination of a large number of mitochondrial proteins [58].

The Role of p62 in PARKIN-Dependent Mitophagy

p62 connects ubiquitinated proteins to LC3 for autophagic degradation [59]. As accumulation of p62 is strikingly elevated when autophagy is blocked, it is widely used as an autophagy marker. The loss of mitochondrial membrane potential promotes the

accumulation of p62 on clustered mitochondria in a PARKIN-dependent manner. Whether p62 is required for mitophagy, however, is controversial and further studies are needed to determine its role [54,55].

PINK1

PARKIN interacts with another PD-related protein, PTEN-induced kinase 1 (PINK1), a mitochondrial membrane-anchored kinase. In *Drosophila melanogaster*, the phenotype resulting from the loss of PINK1 is rescued on overexpression of PARKIN; however, loss of PARKIN is not rescued by the overexpression of PINK1 [60,61], suggesting that PINK1 acts upstream of PARKIN. Subsequent studies show that PINK1 plays a role in the recruitment of PARKIN [46,54,62,63]. Expression of PINK1 on individual mitochondria is regulated by voltage-dependent proteolysis; thus, low levels of PINK1 are maintained on healthy, polarized mitochondria. In steady-state cells, PINK1 is imported into the mitochondrial inner membrane in a membrane potential-dependent manner. When imported into the inner membrane, the mitochondrial inner membrane rhomboid protease presenilin-associated rhomboidlike protein (PARL) mediates the cleavage of PINK1 [64]. Upon mitochondria depolarization, PINK1 import into the inner membrane is impaired, leading to a rapid PINK1 accumulation on the outer membrane of damaged mitochondria. PINK1 accumulation on mitochondria is both necessary and sufficient for PARKIN recruitment to mitochondria. How recruited PARKIN on damaged mitochondria can promote their degradation is still under extensive investigation. An intriguing possibility is that PARKIN may mediate the ubiquitination of certain substrates on mitochondria, and the ubiquitinated substrates may serve as a recognition target for p62/SQSTM1, a ubiquitin-binding protein that interacts with LC3 and is proposed to play

a role in cargo recruitment to the phagophore [54,56]. Importantly, several follow-up studies show that disease-associated *PARK2* and *PARK6* mutations result in defective mitophagy, thereby implicating mitophagy defects in the development of PD [46,62,65].

Functions of Different Isoforms of PINK1

PINK1 has at least two isoforms: a full-length form and an N-terminally truncated form [66,67]. PINK1 cleavage is mediated by the mitochondrial protease rhomboid-7/PARL in flies and mammalian cells [64,68,69]. However, which is the functional isoform of PINK1 remains unclear. Early work indicated the cleaved PINK1 might be the functional form, as the expression of a cytoplasmic, cleaved PINK1 is sufficient to protect neurons from mitochondrial stress by MPTP (1-methyl-4-phenyl-1,2,3,6-tetrahydropyridine) [70]. In contrast, recent work suggests that full-length PINK1 is the only functional form. Full-length PINK1 is rapidly degraded in normal conditions, but accumulates in dysfunctional mitochondria to activate mitophagy when mitochondria lose their membrane potential [46,55,62]. These latter results imply that truncated PINK1 is an intermediate product destined for degradation. As different isoforms of PINK1 are related to different cellular locations and functions and might respond to different stresses, further studies are still needed to elucidate this issue.

Protective Function of PINK1 in Different Animal Models

Although the significant role of PINK1 in neuron protection is clear, an apparent difference of displayed phenotypes is observed between fly and mouse models when PINK1 is depleted. In *Pink1* mutant*Drosophila*, the obvious phenotypes, including loss of dopaminergic neurons, reduced life span, mitochondrial impairment, and mobility

abnormalities, are strikingly similar to the PD pathology in humans [60,71]. However, dopaminergic neurons remain normal in the*park6*$^{-/-}$ mouse, which implies an even more complicated mechanism of PINK1 function in PD [72].

Other PD Related Genes and Autophagy

Although 95% of PD cases are sporadic, identification of genes responsible for monogenic forms has improved our knowledge of this neurodegenerative disease. In addition to *SNCA* (encoding α-synuclein),*PARK2*, and *PARK6*, two other monogenic PD-related genes, encoding the leucine-rich repeat kinase 2 (LRRK2) and DJ-1, also play a role in autophagy or mitochondrial dynamics.

Mutation of the gene encoding LRRK2 is responsible for an autosomal dominant form of PD. LRRK2 is mainly localized in membrane microdomains, multivesicular bodies, and autophagic vesicles. Mutation or depletion of LRRK2 results in autophagy impairment and the accumulation of the autophagy marker proteins LC3 and p62 [18,73]. In contrast, DJ-1 was identified as mediating autosomal recessive PD. Recent studies also made a link between autophagy and DJ-1, as depletion of DJ-1 in both human neuroblastoma cells and *Drosophila* results in mitochondrial dysfunction and impaired autophagy [74,75].

These findings imply that mitochondria and autophagy might play a significant role or even be the convergence points for different monogenic PD-related mutations that give rise to similar symptoms. An alternative possibility is that these PD-related gene products might function together. However, to date, only PINK1 and PARKIN have been shown to genetically and physically interact, especially in modulating neuron protection,

mitochondrial function, and mitophagy. Thus, even though many studies have begun to uncover the connections among PINK1, PARKIN, and mitochondria, several controversies remain to be resolved.

Basic Science Research and Clinical Treatment

Based on the significant roles of mitochondria and autophagy in PD, maintaining and stabilizing mitochondrial function or promoting the degradation of damaged mitochondria might benefit the protection of dopaminergic neurons. Data on the possible connection between defects in mitophagy and PD suggest that modulation of autophagy might be one avenue for treating some types of this disease. However, autophagy is described as a double-edged sword, because both reduced and excessive autophagy can be detrimental; therefore, simply upregulating autophagy is not a practical course of action, and the application of autophagy-inducing drugs must be undertaken with extreme caution.

Concluding Remarks

The turnover of proteins has been the focus of attention across neurodegenerative diseases, given that many, if not all, of these diseases show characteristic protein aggregation as part of their cellular pathology. There have been tremendous advances in our understanding of the causes of PD. Novel genes causing familial PD have been discovered, and have been shown to be involved in the autophagy pathway, one of the major proteolytic systems that maintain cellular protein homeostasis. Because autophagy is part of the cell's homeostatic machinery, maintaining a proper level of autophagy is important for minimizing abnormal protein aggregates and for facilitating organelle turnover. Discovery of therapeutic agents that boost autophagic activity or that directly maintain mitochondrial homeostasis, could potentially reduce neuronal loss and slow down disease progression. A better understanding of the regulatory mechanism of autophagy in the pathogenesis of PD will enable the identification of possible methods for clinical intervention.

References

[1] Majeski, A.E. and Dice, J.F. (2004) Int J Biochem Cell Biol 36, 2435-44.

[2] Kunz, J.B., Schwarz, H. and Mayer, A. (2004) J Biol Chem 279, 9987-96.

[3] Klionsky, D.J. (2005) J Cell Sci 118, 7-18.

[4] Kanki, T., Wang, K., Cao, Y., Baba, M. and Klionsky, D.J. (2009) Dev Cell 17, 98-109.

[5] Shintani, T., Huang, W.P., Stromhaug, P.E. and Klionsky, D.J. (2002) Dev Cell 3, 825-37.

[6] Hutchins, M.U. and Klionsky, D.J. (2001) J Biol Chem 276, 20491-8.

[7] Klionsky, D.J., Cueva, R. and Yaver, D.S. (1992) J Cell Biol 119, 287-99.

[8] Yuga, M., Gomi, K., Klionsky, D.J. and Shintani, T. (2011) J Biol Chem 286, 13704-13.

[9] Klionsky, D.J., Cuervo, A.M., Dunn, W.A., Jr., Levine, B., van der Klei, I. and Seglen, P.O. (2007) Autophagy 3, 413-6.

[10] Xie, Z. and Klionsky, D.J. (2007) Nat Cell Biol 9, 1102-9.

[11] He, C. and Klionsky, D.J. (2009) Annu Rev Genet 43, 67-93.

[12] Reggiori, F., Tucker, K.A., Stromhaug, P.E. and Klionsky, D.J. (2004) Dev Cell 6, 79-90.

[13] Geng, J. and Klionsky, D.J. (2008) EMBO Rep 9, 859-64.

[14] Xie, Z., Nair, U. and Klionsky, D.J. (2008) Mol Biol Cell 19, 3290-8.

[15] Okamoto, K., Kondo-Okamoto, N. and Ohsumi, Y. (2009) Dev Cell 17, 87-97.

[16] Huang, J. and Klionsky, D.J. (2007) Cell Cycle 6, 1837-49.

[17] Banerjee, R., Beal, M.F. and Thomas, B. (2010) Trends Neurosci 33, 541-9.

[18] Alegre-Abarrategui, J. and Wade-Martins, R. (2009) Autophagy 5, 1208-10.

[19] Bandyopadhyay, U. and Cuervo, A.M. (2007) Exp Gerontol 42, 120-8.

[20] Clayton, D.F. and George, J.M. (1998) Trends Neurosci 21, 249-54.

[21] Clayton, D.F. and George, J.M. (1999) J Neurosci Res 58, 120-9.

[22] Spencer, B. et al. (2009) J Neurosci 29, 13578-88.

[23] Martinez-Vicente, M. et al. (2008) J Clin Invest 118, 777-88.

[24] Spillantini, M.G., Crowther, R.A., Jakes, R., Hasegawa, M. and Goedert, M. (1998) Proc Natl Acad Sci U S A 95, 6469-73.

[25] Spillantini, M.G., Schmidt, M.L., Lee, V.M., Trojanowski, J.Q., Jakes, R. and Goedert, M. (1997) Nature 388, 839-40.

[26] Polymeropoulos, M.H. et al. (1997) Science 276, 2045-7.

[27] Cuervo, A.M., Stefanis, L., Fredenburg, R., Lansbury, P.T. and Sulzer, D. (2004) Science 305, 1292-5.

[28] Stefanis, L., Larsen, K.E., Rideout, H.J., Sulzer, D. and Greene, L.A. (2001) J Neurosci 21, 9549-60.

[29] Vogiatzi, T., Xilouri, M., Vekrellis, K. and Stefanis, L. (2008) J Biol Chem 283, 23542-56.

[30] Xilouri, M., Vogiatzi, T., Vekrellis, K., Park, D. and Stefanis, L. (2009) PLoS One 4, e5515.

[31] Yang, Q., She, H., Gearing, M., Colla, E., Lee, M., Shacka, J.J. and Mao, Z. (2009) Science 323, 124-7.

[32] Winslow, A.R. et al. (2010) J Cell Biol 190, 1023-37.

[33] Lynch-Day, M.A. et al. (2010) Proc Natl Acad Sci U S A 107, 7811-6.

[34] Huang, J. et al. (2011) Autophagy 7, 17-26.

[35] Choubey, V., Safiulina, D., Vaarmann, A., Cagalinec, M., Wareski, P., Kuum, M., Zharkovsky, A. and Kaasik, A. (2011) J Biol Chem 286, 10814-24.

[36] McBride, H.M., Neuspiel, M. and Wasiak, S. (2006) Curr Biol 16, R551-60.

[37] Celsi, F., Pizzo, P., Brini, M., Leo, S., Fotino, C., Pinton, P. and Rizzuto, R. (2009) Biochim Biophys Acta 1787, 335-44.

[38] Keeble, J.A. and Gilmore, A.P. (2007) Cell Res 17, 976-84.

[39] Wallace, D.C. (2005) Annu Rev Genet 39, 359-407.

[40] Schuler, F. and Casida, J.E. (2001) Biochim Biophys Acta 1506, 79-87.

[41] Schapira, A.H. (1993) Adv Neurol 60, 288-91.

[42] Schapira, A.H., Cooper, J.M., Dexter, D., Jenner, P., Clark, J.B. and Marsden, C.D. (1989) Lancet 1, 1269.

[43] Gasser, T. (2009) Biochim Biophys Acta 1792, 587-96.

[44] Hardy, J., Lewis, P., Revesz, T., Lees, A. and Paisan-Ruiz, C. (2009) Curr Opin Genet Dev 19, 254-65.

[45] Narendra, D., Tanaka, A., Suen, D.F. and Youle, R.J. (2008) J Cell Biol 183, 795-803.

[46] Narendra, D.P., Jin, S.M., Tanaka, A., Suen, D.F., Gautier, C.A., Shen, J., Cookson, M.R. and Youle, R.J. (2010) PLoS Biol 8, e1000298.

[47] Nair, U. and Klionsky, D.J. (2005) J Biol Chem 280, 41785-8.

[48] Mao, K., Wang, K., Zhao, M., Xu, T. and Klionsky, D.J. (2011) J Cell Biol 193, 755-67.

[49] Wang, K. and Klionsky, D.J. (2011) Autophagy 7, 297-300.

[50] Yorimitsu, T. and Klionsky, D.J. (2005) Mol Biol Cell 16, 1593-605.

[51] Eskelinen, E.L., Reggiori, F., Baba, M., Kovacs, A.L. and Seglen, P.O. (2011) Autophagy 7, 935-56.

[52] Schapira, A.H. (2008) Lancet Neurol 7, 97-109.

[53] Terzioglu, M. and Galter, D. (2008) FEBS J 275, 1384-91.

[54] Geisler, S., Holmstrom, K.M., Skujat, D., Fiesel, F.C., Rothfuss, O.C., Kahle, P.J. and Springer, W. (2010) Nat Cell Biol 12, 119-31.

[55] Narendra, D., Kane, L.A., Hauser, D.N., Fearnley, I.M. and Youle, R.J. (2010) Autophagy 6, 1090-106.

[56] Gegg, M.E., Cooper, J.M., Chau, K.Y., Rojo, M., Schapira, A.H. and Taanman, J.W. (2010) Hum Mol Genet 19, 4861-70.

[57] Ziviani, E., Tao, R.N. and Whitworth, A.J. (2010) Proc Natl Acad Sci U S A 107, 5018-23.

[58] Chan, N.C., Salazar, A.M., Pham, A.H., Sweredoski, M.J., Kolawa, N.J., Graham, R.L., Hess, S. and Chan, D.C. (2011) Hum Mol Genet 20, 1726-37.

[59] Pankiv, S. et al. (2007) J Biol Chem 282, 24131-45.

[60] Clark, I.E. et al. (2006) Nature 441, 1162-6.

[61] Yang, Y. et al. (2006) Proc Natl Acad Sci U S A 103, 10793-8.

[62] Matsuda, N. et al. (2010) J Cell Biol 189, 211-21.

[63] Vives-Bauza, C. et al. (2010) Proc Natl Acad Sci U S A 107, 378-83.

[64] Jin, S.M., Lazarou, M., Wang, C., Kane, L.A., Narendra, D.P. and Youle, R.J. (2010) J Cell Biol 191, 933-42.

[65] Lee, J.Y., Nagano, Y., Taylor, J.P., Lim, K.L. and Yao, T.P. (2010) J Cell Biol 189, 671-9.

[66] Beilina, A., Van Der Brug, M., Ahmad, R., Kesavapany, S., Miller, D.W., Petsko, G.A. and Cookson, M.R. (2005) Proc Natl Acad Sci U S A 102, 5703-8.

[67] Silvestri, L., Caputo, V., Bellacchio, E., Atorino, L., Dallapiccola, B., Valente, E.M. and Casari, G. (2005) Hum Mol Genet 14, 3477-92.

[68] Deas, E. et al. (2010) Hum Mol Genet 20, 867-79.

[69] Whitworth, A.J., Lee, J.R., Ho, V.M., Flick, R., Chowdhury, R. and McQuibban, G.A. (2008) Dis Model Mech 1, 168-74; discussion 173.

[70] Haque, M.E. et al. (2008) Proc Natl Acad Sci U S A 105, 1716-21.

[71] Park, J. et al. (2006) Nature 441, 1157-61.

[72] Kitada, T. et al. (2007) Proc Natl Acad Sci U S A 104, 11441-6.

[73] Tong, Y., Yamaguchi, H., Giaime, E., Boyle, S., Kopan, R., Kelleher, R.J., 3rd and Shen, J. (2010) Proc Natl Acad Sci U S A 107, 9879-84.

[74] Hao, L.Y., Giasson, B.I. and Bonini, N.M. (2010) Proc Natl Acad Sci U S A 107, 9747-52.

[75] Thomas, K.J. et al. (2010) Hum Mol Genet 20, 40-50.

APPENDIX B

A Genomic Screen for Yeast Mutants Defective in Selective Mitochondria Autophagy

Abstract

Mitophagy is the process of selective mitochondrial degradation via autophagy, which has an important role in mitochondrial quality control. Very little is known, however, about the molecular mechanism of mitophagy. A genome-wide yeast mutant screen for mitophagy-defective strains identified 32 mutants with a block in mitophagy, in addition to the known autophagy-related (*ATG*) gene mutants. We further characterized one of these mutants, *ylr356w_* that corresponds to a gene whose function has not been identified. *YLR356W* is a mitophagy-specific gene that was not required for other types of selective autophagy or macroautophagy. The deletion of *YLR356W* partially inhibited mitophagy during starvation, whereas there was an almost complete inhibition at post-log phase. Accordingly, we have named this gene *ATG33*. The new mutants identified in this analysis will provide a useful foundation for researchers interested in the study of mitochondrial homeostasis and quality control.

Introduction

The mitochondrion is an organelle that carries out a number of important metabolic processes such as fatty acid oxidation, the citric acid cycle, and oxidative phosphorylation. Mitochondrial oxidative phosphorylation supplies a large amount of energy that contributes to a range of cellular activities. However, this organelle is also the major source of cellular reactive oxygen species (ROS) that cause damage to mitochondrial lipid, DNA and proteins, and the accumulation of these types of damage are related to aging, cancer, and neurodegenerative diseases [1]. Thus, intensive analyses of mitochondrial DNA repair and damaged protein degradation mechanisms have been carried out [2-4]. In addition, it has long been assumed that autophagy is the pathway for mitochondrial recycling, and various theories suggest that a specific targeting of damaged mitochondria to vacuoles or lysosomes occurs by autophagy [5]. Very recently, several studies suggest that selective mitochondrial degradation via autophagy (mitophagy) might play an important role for mitochondrial quality control [6-10]. However, the molecular mechanism of mitophagy is poorly understood.

Macroautophagy is the bulk (i.e., nonspecific) degradation of cytoplasmic components that allows cells to respond to various types of stress and to adapt to changing nutrient conditions [11,12]. In contrast to macroautophagy, the cytoplasm-to-vacuole targeting (Cvt) pathway, pexophagy (specific autophagy of peroxisomes), and mitophagy are categorized as selective types of autophagy. These processes have specific cargos comprised of the Cvt complex (precursor aminopeptidase I (prApe1) and α-mannosidase (Ams1), along with receptor and adaptor proteins), peroxisomes and mitochondria, respectively [13-16]. Studies in the yeast Saccharomyces cerevisiae and

other fungi have enabled the identification of several molecular factors essential for autophagy [17]. At present, there are 32 genes that are primarily involved in autophagy-related (Atg) pathways. Most of the *ATG* genes are required for both macroautophagy and selective autophagy, but some are required only for specific types of autophagy [15]. For example, Atg19, a receptor protein for the Cvt pathway, binds the Cvt complex, and then interacts with Atg11, an adaptor protein for selective autophagy, and recruits them to the phagophore assembly site (PAS), where the sequestering cytosolic vesicles are generated [16]. Similarly, during pexophagy in *Pichia pastoris*, Atg30 localizes to peroxisomes, where it is bound by Atg11, allowing recruitment of the peroxisomes to the PAS [14]. Atg11 is also required for mitochondrial degradation during starvation or in post-log phase, suggesting that mitochondria are selected by Atg11 for autophagic degradation [15]. Recently, we identified Atg32 as a mitochondrial protein that interacts with Atg11 and is required specifically for mitophagy [18,19]; however, the detailed mechanism of mitophagy has not been determined.

To figure out the molecular mechanism of selective mitochondria autophagy, we recently established a method to monitor this process [15]. Using this method, we screened a yeast knockout library for strains that are deficient in mitophagy. Among 4667 strains, we found 32 strains that showed a complete or partial block of mitophagy, in addition to the *ATG* gene knockout strains. We also screened these mutants to ascertain the functionality of macroautophagy and the Cvt pathway. Nine of the strains showed defects in all autophagic pathways, whereas the other 23 strains were normal for the Cvt pathway, but defective to varying extents for macroautophagy and mitophagy. We further characterized the product of one of the genes, *YLR356W*, whose function has not been

previously identified. The Ylr356w protein localized to mitochondria, and the deletion of *YLR356W* resulted in an almost complete inhibition of mitophagy at post-log phase.

Results

A Genome-Wide Screen for Yeast Mitophagy Mutants

Mitophagy can be induced by culturing yeast strains in a medium with a nonfermentable carbon source such as lactate (i.e., YPL; [15,20] or ethanol and glycerol to post-log phase. The GFP-tagged on the C terminus of the mitochondrial outer membrane protein Om45 (Om45-GFP) accumulates in the vacuole, when mitophagy is induced [15]. To identify mitochondrial autophagy-related genes, we used a *MAT*α yeast knockout library and chromosomally tagged the C terminus of Om45 with GFP in each strain (Table SB.1). After the strains were cultured in YPL medium for 3 d to allow growth to the post-log phase, they were observed for vacuolar GFP fluorescence. Among 4667 strains examined (Fig. B.1), 4142 strains showed a clear level of vacuolar GFP, and 400 strains showed either no, or a very weak, vacuolar GFP signal (some examples are shown in Figure SB1A). We could not examine 125 strains because of their displaying a growth defect in YPD medium (some of the library strains grew poorly even in YPD) or because of a difficulty in the Om45-GFP tagging.

Table SB.1. Strains used in this study.

Strain	Genotype	Source
KWY20	SEY6210 *pho8Δ::TRP1 pho13Δ::LEU2* pRS406-*ADH1-COX4-pho8Δ60*	This study
KWY21	SEY6210 *pho8Δ::TRP1 pho13Δ::LEU2* pRS406-*ADH1-COX4-pho8Δ60 atg1Δ::ble*	This study
KWY22	SEY6210 *pho8Δ::TRP1 pho13Δ::LEU2* pRS406-*ADH1-COX4-pho8Δ60 atg32Δ::KAN*	This study
KWY23	SEY6210 *pho8Δ::TRP1 pho13Δ::LEU2* pRS406-*ADH1-COX4-pho8Δ60 aim26Δ::KAN*	This study
KWY24	SEY6210 *pho8Δ::TRP1 pho13Δ::LEU2* pRS406-*ADH1-COX4-pho8Δ60 aim28Δ::KAN*	This study
KWY25	SEY6210 *pho8Δ::TRP1 pho13Δ::LEU2* pRS406-*ADH1-COX4-pho8Δ60 dnm1Δ::KAN*	This study
KWY26	SEY6210 *pho8Δ::TRP1 pho13Δ::LEU2* pRS406-*ADH1-COX4-pho8Δ60 fmc1Δ::KAN*	This study
KWY27	SEY6210 *pho8Δ::TRP1 pho13Δ::LEU2*	This study

	pRS406-*ADH1-COX4-pho8Δ60 lpe10Δ::KAN*	
KWY28	SEY6210 *pho8Δ::TRP1 pho13Δ::LEU2*	This study
	pRS406-*ADH1-COX4-pho8Δ60 ypr146cΔ::KAN*	
KWY29	SEY6210 *pho8Δ::TRP1 pho13Δ::LEU2*	This study
	pRS406-*ADH1-COX4-pho8Δ60 ylr356wΔ::KAN*	
KWY30	SEY6210 *pho8Δ::TRP1 pho13Δ::LEU2*	This study
	pRS406-*ADH1-COX4-pho8Δ60 rpl13bΔ::KAN*	
KWY31	SEY6210 *pho8Δ::TRP1 pho13Δ::LEU2*	This study
	pRS406-*ADH1-COX4-pho8Δ60 rpl15bΔ::KAN*	
KWY32	SEY6210 *pho8Δ::TRP1 pho13Δ::LEU2*	This study
	pRS406-*ADH1-COX4-pho8Δ60 aro2Δ::KAN*	
KWY33	SEY6210 *pho8Δ::TRP1 pho13Δ::LEU2*	This study
	pRS406-*ADH1-COX4-pho8Δ60 bck1Δ::KAN*	
KWY34	SEY6210 *pho8Δ::TRP1 pho13Δ::LEU2*	This study
	pRS406-*ADH1-COX4-pho8Δ60 bub1Δ::KAN*	
KWY35	SEY6210 *pho8Δ::TRP1 pho13Δ::LEU2*	This study
	pRS406-*ADH1-COX4-pho8Δ60 egd1Δ::KAN*	

KWY36	SEY6210 *pho8Δ::TRP1 pho13Δ::LEU2* pRS406-*ADH1-COX4-pho8Δ60 icy2Δ::HIS5*	This study
KWY37	SEY6210 *pho8Δ::TRP1 pho13Δ::LEU2* pRS406-*ADH1-COX4-pho8Δ60 mak10Δ::KAN*	This study
KWY38	SEY6210 *pho8Δ::TRP1 pho13Δ::LEU2* pRS406-*ADH1-COX4-pho8Δ60 nft1Δ::KAN*	This study
KWY39	SEY6210 *pho8Δ::TRP1 pho13Δ::LEU2* pRS406-*ADH1-COX4-pho8Δ60 yil165cΔ::KAN*	This study
KWY40	SEY6210 *pho8Δ::TRP1 pho13Δ::LEU2* pRS406-*ADH1-COX4-pho8Δ60 yor019wΔ::KAN*	This study
KWY41	SEY6210 *OM45-GFP::TRP1 aim26Δ::KAN*	This study
KWY42	SEY6210 *OM45-GFP::TRP1 aim28Δ::KAN*	This study
KWY43	SEY6210 *OM45-GFP::TRP1 dnm1Δ::KAN*	This study
KWY44	SEY6210 *OM45-GFP::TRP1 fmc1Δ::KAN*	This study
KWY45	SEY6210 *OM45-GFP::TRP1 lpe10Δ::KAN*	This study
KWY46	SEY6210 *OM45-GFP::TRP1 ypr146cΔ::KAN*	This study
KWY47	SEY6210 *OM45-GFP::TRP1 ylr356wΔ::KAN*	This study

KWY48	SEY6210 *OM45-GFP::TRP1 rpl13bΔ::KAN*	This study
KWY49	SEY6210 *OM45-GFP::TRP1 rpl15bΔ::KAN*	This study
KWY50	SEY6210 *OM45-GFP::TRP1 aro2Δ::KAN*	This study
KWY51	SEY6210 *OM45-GFP::TRP1 bck1ΔΔ::KAN*	This study
KWY52	SEY6210 *OM45-GFP::TRP1 bub1Δ::KAN*	This study
KWY53	SEY6210 *OM45-GFP::TRP1 egd1Δ::KAN*	This study
KWY54	SEY6210 *OM45-GFP::TRP1 icy2Δ::KAN*	This study
KWY55	SEY6210 *OM45-GFP::TRP1 mak10Δ::KAN*	This study
KWY56	SEY6210 *OM45-GFP::TRP1 nft1Δ::KAN*	This study
KWY57	SEY6210 *OM45-GFP::TRP1 pmr1Δ::KAN*	This study
KWY58	SEY6210 *OM45-GFP::TRP1 hur1Δ::KAN*	This study
KWY59	SEY6210 *OM45-GFP::TRP1 yil165cΔ::KAN*	This study
KWY60	SEY6210 *OM45-GFP::TRP1 yor019wΔ::KAN*	This study
KWY61	SEY6210 *AIM26-GFP::TRP1*	This study
KWY62	SEY6210 *AIM28-GFP::TRP1*	This study
KWY63	SEY6210 *DNM1-GFP::TRP1*	This study
KWY64	SEY6210 *FMC1-GFP::TRP1*	This study

KWY65	SEY6210 *LPE10-GFP::TRP1*	This study
KWY66	SEY6210 *YPR146C-GFP::TRP1*	This study
KWY67	SEY6210 *RPL13B-GFP::TRP1*	This study
KWY68	SEY6210 *RPL15B-GFP::TRP1*	This study
KWY69	SEY6210 *ARG82-GFP::TRP1*	This study
KWY70	SEY6210 *ARO2-GFP::TRP1*	This study
KWY71	SEY6210 *BCK1-GFP::TRP1*	This study
KWY72	SEY6210 *BUB1-GFP::TRP1*	This study
KWY73	SEY6210 *EGD1-GFP::TRP1*	This study
SEY6210	MATα *his3-Δ200 leu2-3,112 lys2-801*	(Robinson et al., 1988)
	trp1-Δ901 ura3-52 suc2-Δ9 GAL	
TKY28	SEY6210 *pep4Δ::LEU2*	This study
TKYM22	SEY6210 *OM45-GFP::TRP1*	(Kanki and Klionsky, 2008)
TKYM25	SEY6210 *atg1Δ::KanMX6 OM45-GFP::TRP1*	This study
TKYM36	SEY6210 *atg8Δ::HIS5 S.p. OM45-GFP::TRP1*	This study
TKYM37	SEY6210 *atg5Δ::LEU2 OM45-GFP::HIS3MX6*	This study
TKYM38	SEY6210 *atg9Δ::HIS5 S.p. OM45-GFP::TRP1*	This study

TKYM39	SEY6210 *atg11Δ::LEU2 OM45-GFP::TRP1*	This study
TKYM44	SEY6210 *atg27Δ::TRP1 OM45-GFP::HIS3MX6*	This study
TKYM45	SEY6210 *atg31Δ::HIS5 S.p.* *OM45-GFP::KanMX6*	This study
TKYM47	SEY6210 *atg17Δ::KanMX6* *OM45-GFP::HIS3MX6*	This study
TKYM49	SEY6210 *atg29Δ::KanMX6* *OM45-GFP::HIS3MX6*	This study
TKYM50	SEY6210 *IDH1-GFP::KanMX6*	(Kanki and Klionsky, 2008)
TKYM53	SEY6210 *atg20Δ::HIS5 S.p.* *OM45-GFP::KanMX6*	This study
TKYM54	SEY6210 *atg24Δ::HIS5 S.p.* *OM45-GFP::KanMX6*	This study
TKYM57	SEY6210 *atg23Δ::KanMX6 OM45-GFP::TRP1*	This study
TKYM62	SEY6210 *atg19Δ::HIS5 S.p. OM45-GFP::TRP1*	This study
TKYM67	SEY6210 *PEX14-GFP::KanMX6*	(Kanki and Klionsky, 2008)
TKYM72	SEY6210 *atg1Δ::HIS5 S.p.*	(Kanki and Klionsky, 2008)

	PEX14-GFP::KanMX6	
TKYM80	SEY6210 *atg1Δ::HIS5 S.p. IDH1-GFP::TRP1*	This study
TKYM167	SEY6210 *ylr356wΔ::HIS5 S.p.*	This study
	OM45-GFP::TRP1	
TKYM170	SEY6210 *atg2Δ::HIS5 S.p. OM45-GFP::TRP1*	This study
TKYM171	SEY6210 *atg3Δ::HIS5 S.p.*	This study
	OM45-GFP::KanMX6	
TKYM172	SEY6210 *atg4Δ::LEU2*	This study
	OM45-GFP::HIS3MX6	
TKYM173	SEY6210 *atg6Δ::LEU2 OM45-GFP::HIS3MX6*	This study
TKYM174	SEY6210 *atg7Δ::HIS5 S.p. OM45-GFP::TRP1*	This study
TKYM175	SEY6210 *atg10Δ::HIS5 S.p. OM45-GFP::TRP1*	This study
TKYM176	SEY6210 *atg12Δ::KanMX6*	This study
	OM45-GFP::HIS3MX6	
TKYM177	SEY6210 *atg13Δ::KanMX6*	This study
	OM45-GFP::HIS3MX6	
TKYM178	SEY6210 *atg14Δ::LEU2 OM45-GFP::HIS3MX6*	This study

TKYM179	SEY6210 *atg15Δ::KanMX6 OM45-GFP::HIS3MX6*	This study
TKYM180	SEY6210 *atg16Δ::KanMX6 OM45-GFP::URA3*	This study
TKYM181	SEY6210 *atg18Δ::KanMX6 OM45-GFP::HIS3MX6*	This study
TKYM182	SEY6210 *atg21Δ::HIS5 S.p. OM45-GFP::TRP1*	This study
TKYM183	SEY6210 *atg22Δ::TRP1 OM45-GFP::HIS3MX6*	This study
TKYM184	SEY6210 *atg26Δ::URA3 OM45-GFP::HIS3MX6*	This study
TKYM186	SEY6210 *icy2Δ::HIS5 S.p. OM45-GFP::TRP1*	This study
TKYM187	SEY6210 *icy2Δ::HIS5 S.p. PEX14-GFP::TRP1*	This study
TKYM188	SEY6210 *ylr356wΔ::HIS5 S.p. PEX14-GFP:: TRP1*	This study
TKYM194	SEY6210 *ylr356wΔ::HIS5 S.p. IDH1-GFP::TRP1*	This study
TKYM195	SEY6210 *icy2Δ::HIS5 S.p. IDH1-GFP::TRP1*	This study
KWY007	SEY6210 *atg1Δ::HIS5 S.p. ICY2-GFP::TRP1*	This study
TKYM196	SEY6210 *ylr356wΔ::HIS5 S.p.*	This study
TKYM197	SEY6210 *icy2Δ::HIS5 S.p.*	This study

TKYM199	TN124 *ylr356wΔ::URA3*	This study
TKYM200	TN124 *icy2Δ::URA3*	This study
TKYM201	SEY6210 *KanMX6::GAL-YLR356W-GFP::TRP1*	This study
TKYM205	SEY6210 *YLR356W-PA:: TRP1* *OM45-GFP::URA3*	This study
TKYM206	SEY6210 *YLR356W-PA:: TRP1* *TIM23-13myc:: HIS5 S.p.*	This study
TN124	MATa *leu2-3,112 ura3-52 trp1* *pho8::pho8Δ60 pho13Δ::LEU2*	(Noda et al., 1995)
WLY176	SEY6210 *pho13Δ pho8Δ60::HIS3*	This study
WLY192	SEY6210 *pho13Δ::KAN pho8Δ60::URA3 atg1Δ::HIS5*	This study
WLY233	SEY6210 *pho13Δ pho8Δ60::HIS3 arg82Δ::KAN*	This study
WLY234	SEY6210 *pho13Δ pho8Δ60::HIS3 aim28Δ::KAN*	This study
WLY235	SEY6210 *pho13Δ pho8Δ60::HIS3 rpl14aΔ::KAN*	This study
WLY236	SEY6210 *pho13Δ pho8Δ60::HIS3 yor019wΔ::KAN*	This study
WLY237	SEY6210 *pho13Δ pho8Δ60::HIS3 icy2Δ::KAN*	This study
WLY238	SEY6210 *pho13Δ pho8Δ60::HIS3 hur1Δ::LEU2*	This study

WLY239	SEY6210 *pho13Δ pho8Δ60::HIS3 fmc1Δ::KAN*	This study
WLY240	SEY6210 *pho13Δ pho8Δ60::HIS3 yil165cΔ::KAN*	This study
WLY241	SEY6210 *pho13Δ pho8Δ60::HIS3 rpl15bΔ::KAN*	This study
WLY242	SEY6210 *pho13Δ pho8Δ60::HIS3 ylr356wΔ::KAN*	This study
WLY243	SEY6210 *pho13Δ pho8Δ60::HIS3 atg32Δ::KAN*	This study
WLY244	SEY6210 *pho13Δ pho8Δ60::HIS3 bck1Δ::KAN*	This study
WLY245	SEY6210 *pho13Δ pho8Δ60::HIS3 aim26Δ::KAN*	This study
WLY246	SEY6210 *pho13Δ pho8Δ60::HIS3 nft1Δ::KAN*	This study
WLY247	SEY6210 *pho13Δ pho8Δ60::HIS3 ypr146cΔ::KAN*	This study
WLY248	SEY6210 *pho13Δ pho8Δ60::HIS3 mak10Δ::KAN*	This study
WLY249	SEY6210 *pho13Δ pho8Δ60::HIS3 egd1Δ::KAN*	This study
WLY250	SEY6210 *pho13Δ pho8Δ60::HIS3 dnm1Δ::KAN*	This study
WLY251	SEY6210 *pho13Δ pho8Δ60::HIS3 aro2Δ::KAN*	This study
WLY252	SEY6210 *pho13Δ pho8Δ60::HIS3 bub1Δ::KAN*	This study
WLY253	SEY6210 *pho13Δ pho8Δ60::HIS3 lpe10Δ::KAN*	This study
WLY254	SEY6210 *pho13Δ pho8Δ60::HIS3 pmr1Δ::KAN*	This study

Kanki, T., and Klionsky, D.J. (2008) J Biol Chem 283:32386-93.
Noda, T., Matsuura, A., Wada, Y., and Ohsumi, Y. (1995) Biochem Biophys Res Commun 210:126-32.
Robinson, J.S., Klionsky, D.J., Banta, L.M., and Emr, S.D. (1988) Mol Cell Biol 8:1936-48.

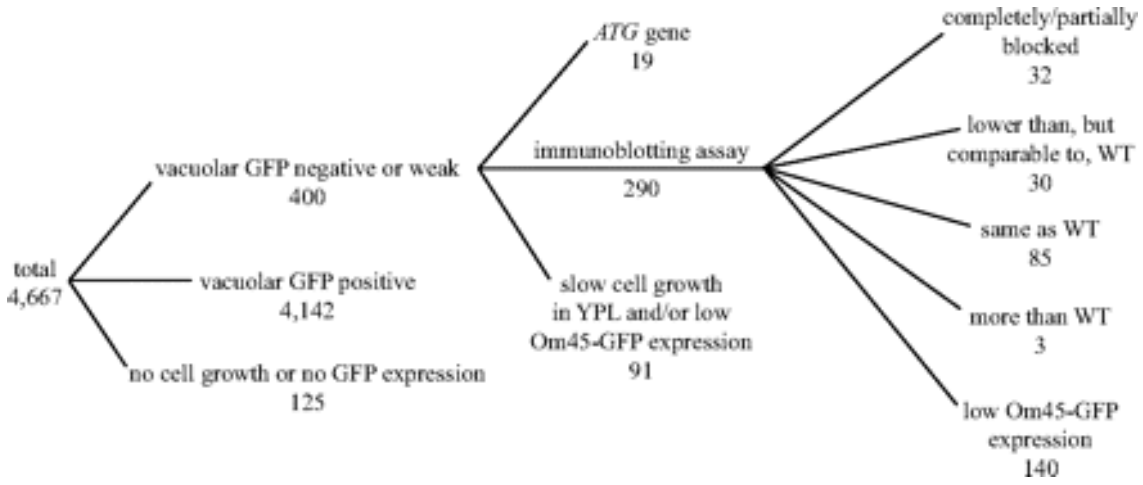

Figure B.1. Schematic diagram of the mitophagy screen and the resulting number of mutants.

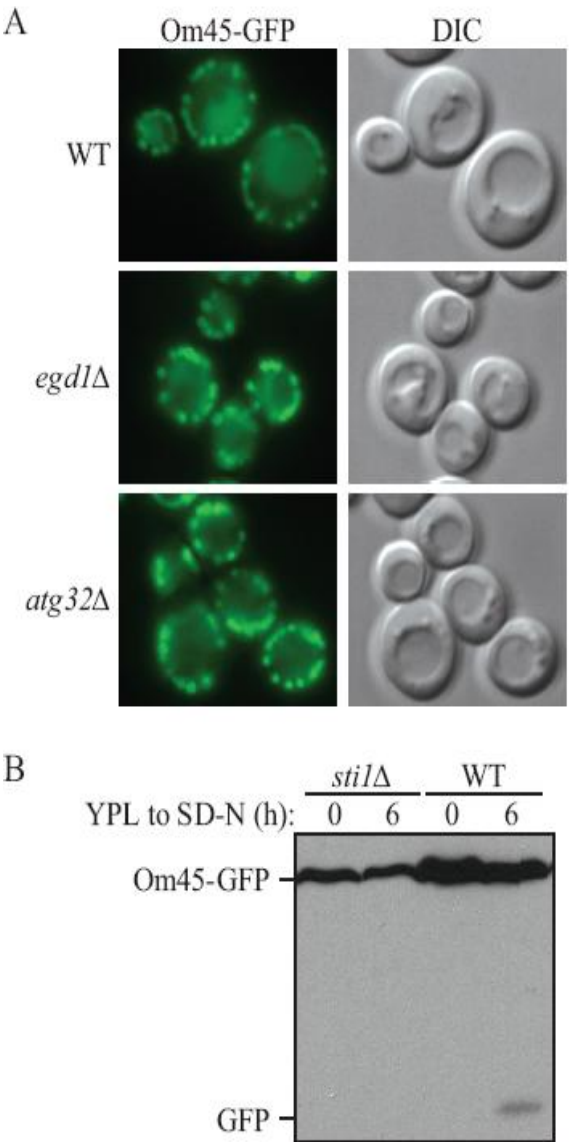

Figure SB.1. Examples of fluorescence microscopy and Om45-GFP processing from the mitophagy screen. (A) Wild-type (WT; BY4742) and knockout strains expressing Om45-GFP were cultured in YPL medium for three days to allow growth to the post-log phase, and were then observed for vacuolar GFP fluorescence. The wild-type strain showed a clear level of vacuolar GFP, *egd1Δ* showed a very weak vacuolar GFP signal and *atg32Δ* showed no vacuolar GFP signal. (B) Wild-type and *sti1Δ* strains expressing Om45- GFP were cultured in YPL medium for 12 h and then starved in SD-N for 6 h. The cell lysates equivalent to A600 = 0.2 units of cells were subjected to immunoblot analysis with anti-YFP antibody. Although no processed GFP was observed in the *sti1Δ* strain after 6 h starvation, we cannot conclude whether it is the result of a defect in mitophagy or a low level of Om45-GFP expression.

The vacuolar GFP-negative or weak strains included 19 autophagy-related (*ATG*) gene knockout strains. We screened all *ATG* gene knockout strains for mitophagy separately (see below); these strains were examined apart from the other mutants uncovered in the present screen. In addition to post-logarithmic-phase growth in lactate medium, mitophagy can be induced when cells are shifted from YPL to nitrogen starvation medium (SD-N), and the level of mitophagy can be semiquantitatively monitored by measuring the amount of GFP processed from Om45-GFP in the vacuole using immunoblotting [15]. For this GFP processing analysis, we required a certain volume of cells and an adequate level of Om45-GFP expression; we excluded 91 strains that showed very slow growth in YPL or very low Om45-GFP expression based on fluorescence microscopy. Among the remaining 290 strains that we screened by GFP processing, 32 strains showed a complete or partial block of mitophagy (Fig. B.2), 30 strains showed lower, but substantial, GFP processing compared with the wild-type strain, 85 strains showed the same level of GFP processing as the wild type, and 140 strains showed lower Om45-GFP expression; in these latter strains we could not determine from this analysis whether the lower amount of GFP processing was a result of a block in mitophagy or was due to a low level of Om45-GFP (an example is shown in Fig. SB.1B). Three strains, with deletions of *VMA13*, *TFP1* (*VMA1*), or *YOR331C* (which overlaps with *VMA4*) showed more than a twofold increase in GFP processing compared with the wild type (our unpublished results). The results for all 4667 strains are listed in Table SB.2 and summarized in Fig. B.1.

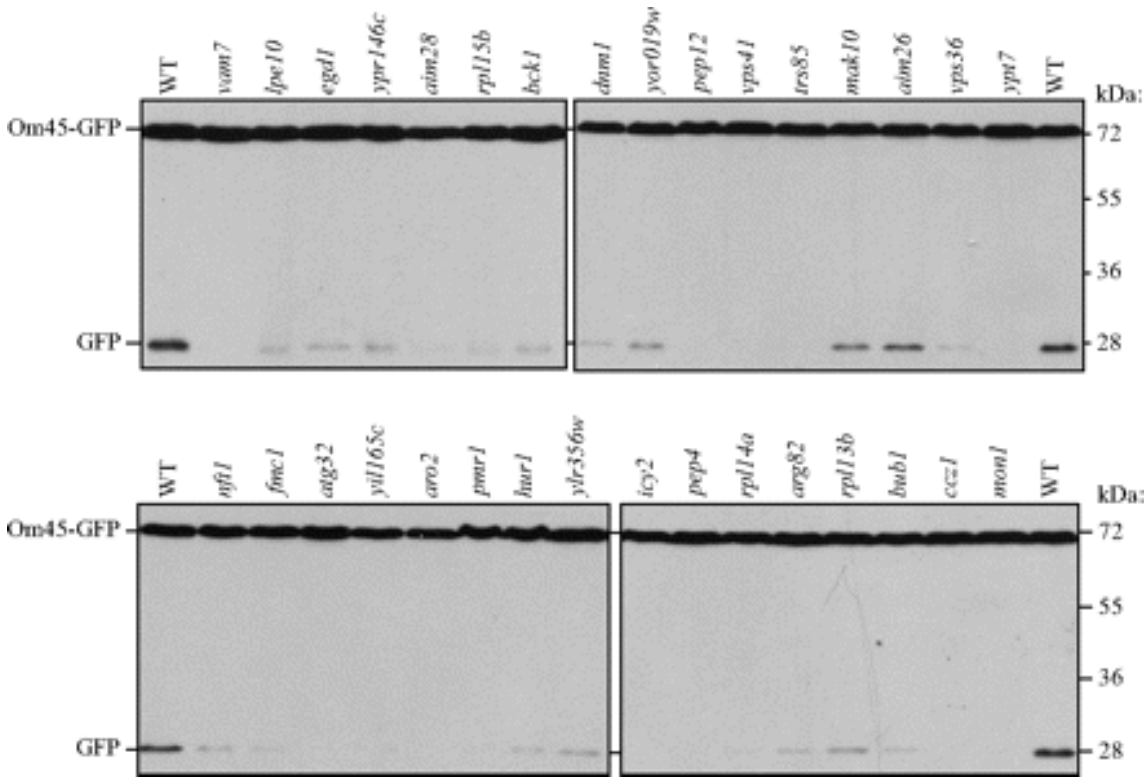

Figure B.2. Screen for defects in mitophagy. Wild-type (WT; BY4742) and the indicated mutant strains expressing Om45-GFP (top and bottom) were cultured in YPL medium for 12 h and then starved in SD-N for 6 h. The cell lysates equivalent to A_{600} = 0.2 U of cells were subjected to immunoblot analysis with anti-YFP antibody. The position of full-length Om45-GFP and free GFP are indicated.

Table SB.2. Initial screen results for all strains tested.

ORF name	Vacuolar GFP	Growth in YPL	OM45-GFP signal	Western blot	Gene
YMR158W-A	No			Fig. S2	Overlap with *ATG16*
YMR159C	No			Fig. S2	*atg16*
YPL166W	No			Fig. S2	*atg29*
YPL149W	No	Slow	Weak signal	Fig. S2	*atg5*
YPL120W	No			Fig. S2	*atg6/vps30*
YPL100W	No			Fig. S2	*atg21*
YBR217W	No			Fig. S2	*atg12*
YJL178C	No			Fig. S2	*atg27*
YPR185W	No			Fig. S2	*atg13*
YBL078C	No			Fig. S2	*atg8*
YFR021W	No			Fig. S2	*atg18*
YPR049C	No			Fig. S2	*atg11*
YLR431C	No			Fig. S2	*atg23*
YCR068W	No			Fig. S2	*atg15*
YDL113C	No			Fig. S2	*atg20*
YDL149W	No			Fig. S2	*atg9*
YNR007C	No	Slow	Weak signal	Fig. S2	*atg3*
YHR171W	No			Fig. S2	*atg7*
YGL180W	No			Fig. S2	*atg1*
YLL001W	No			Fig. 1	*dnm1*
YOR019W	No			Fig. 1	*yor019w*
YOR036W	No			Fig. 1	*pep12*
YPL250C	No			Fig. 1	*icy2*
YPL154C	No			Fig. 1	*pep4*
YDR080W	No			Fig. 1	*vps41*
YDR108W	No			Fig. 1	*trs85/gsg1*
YEL053C	No			Fig. 1	*mak10*
YKL006W	No			Fig. 1	*rpl14a*
YKL037W	No			Fig. 1	*aim26*
YLR417W	No			Fig. 1	*vps36*
YML001W	No			Fig. 1	*ypt7*
YDR173C	No			Fig. 1	*arg82*
YGL212W	No			Fig. 1	*vam7*
YPL060W	No			Fig. 1	*lep10*
YPL037C	No			Fig. 1	*egd1*

YPR146C	No		Fig. 1	*ypr146c*
YKR016W	No		Fig. 1	*aim28*
YMR142C	No		Fig. 1	*rpl13b*
YMR121C	No		Fig. 1	*rpl15b*
YJL095W	No		Fig. 1	*bck1*
YGR188C	No	Slow	Fig. 1	*bub1*
YKR103W	No		Fig. 1	*nft1*
YIL098C	No		Fig. 1	*fmc1*
YIL146C	No		Fig. 1	*atg32*
YIL165C	No		Fig. 1	*yil165c*
YBR131W	No		Fig. 1	*ccz1*
YGL124C	No		Fig. 1	*mon1*
YGL148W	No		Fig. 1	*aro2*
YGL167C	No	Slow	Fig. 1	*pmr1*
YGL168W	No	Slow	Fig. 1	*hur1*
YLR356W	No		Fig. 1	*ylr356w*

*This is only part of the table. The rest of the table can be found at:
http://www.molbiolcell.org/content/20/22/4730/suppl/DC1

Analysis for Defects in Macroautophagy and the Cvt Pathway

To further characterize the 32 newly identified mutant strains that showed a clear defect in mitochondrial degradation, we decided to monitor the nonspecific macroautophagy activity using the Pho8Δ60 alkaline phosphatase assay [21]. Pho8Δ60 is a truncated form of the vacuolar alkaline phosphatase. Deletion of the native signal sequence causes the precursor protein to remain in the cytosol, and it is only delivered to the vacuole by an autophagic mechanism. On delivery, the C-terminal propeptide is removed, resulting in activation of the zymogen, which can be measured enzymatically. We introduced Pho8Δ60 into these 32 knockout strains and measured the Pho8Δ60-dependent alkaline phosphatase activity in both growing and 4-h starvation conditions (Fig. SB.2A). For the initial analysis, to simplify the strain construction, we did not delete the *PHO13* gene, which encodes a cytosolic alkaline phosphatase. This resulted in a higher level of background activity during growing conditions; however, after 4-h starvation the alkaline phosphatase activity was significantly increased in wild-type cells relative to growing conditions, so there was an adequate signal-to-noise ratio. We found eight strains that showed a complete block of nonspecific autophagy and four strains that showed a partial block. We also screened these mutants for defects in the biosynthetic Cvt pathway, a selective type of autophagy used for delivery of the resident hydrolase Ape1 to the vacuole [22], by monitoring the processing of prApe1 (Fig. SB.2B). Eight strains showed a complete block of the Cvt pathway and one strain showed a partial block. We summarized the results for macroautophagy, the Cvt pathway and mitophagy in Table SB.3.

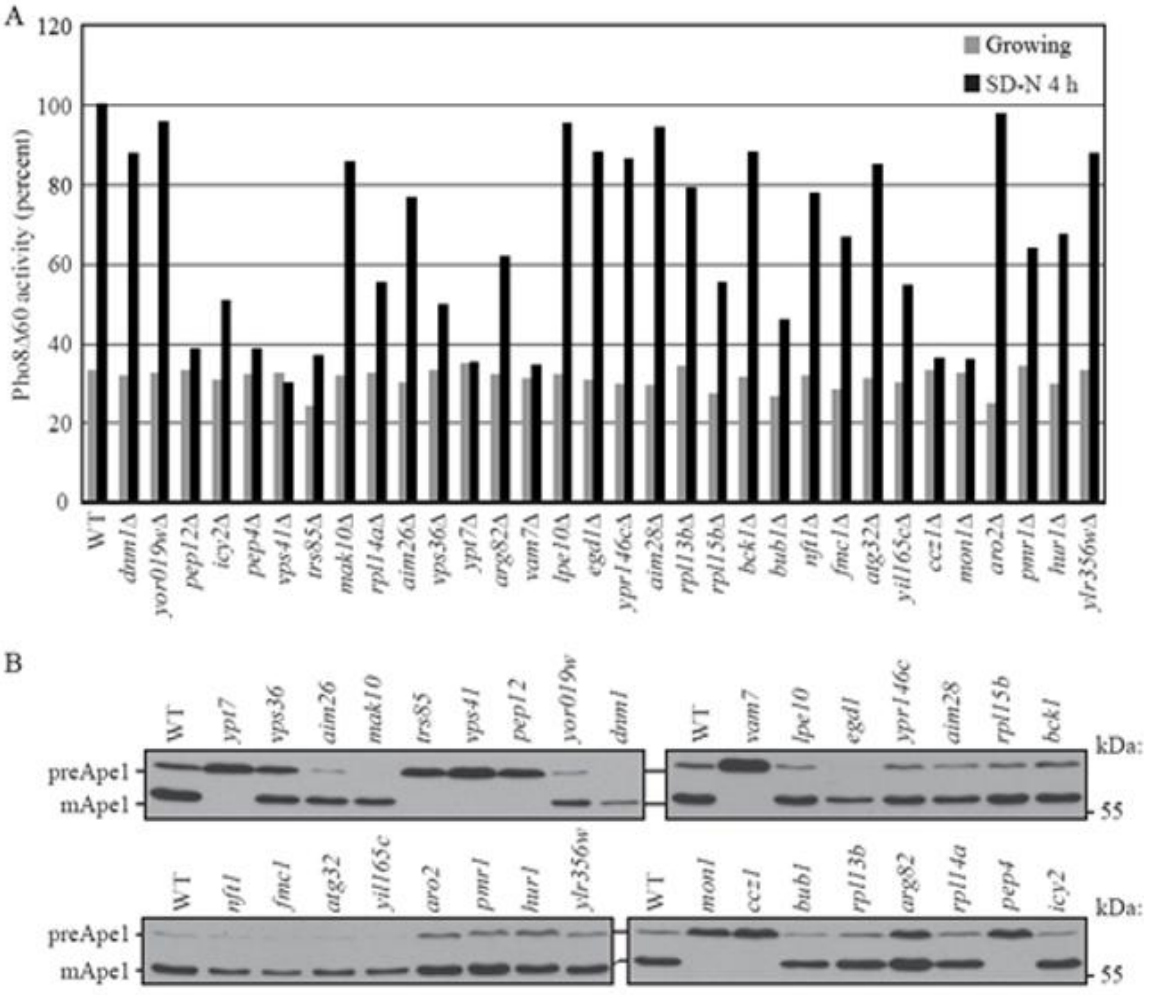

Figure SB.2. Screen for defects in macroautophagy and the Cvt pathway. (A) Wild-type (WT; BY4742) and the indicated mutant strains expressing Pho8Δ60 were grown in YPD and shifted to SD-N for 4 h. Samples were collected and protein extracts assayed for Pho8Δ60 activity. The value for the wild-type strain was set to 100% and the other values were normalized. (B) Wild-type and the indicated mutant strains were cultured in YPD medium and analyzed for prApe1 maturation by immunoblotting to monitor the Cvt pathway during vegetative growth. The positions of precursor and mature Ape1 are indicated.

Table SB.3. Summary of autophagy analyses

		Mitophagy			
		Om45-GFP	Om45-GFP	mitoPho8Δ60	Idh1-GFP
Systematic		BY4742	SEY6210	SEY6210	BY4742
Name	Gene	Fig. 2	Fig. 3	Fig. 4	Fig. S3
YKL037W	*AIM26*	++	+	+	++
YKR016W	*AIM28*	-	-	No defect	No defect
YLL001W	*DNM1*	-	++	++	+
YIL146C	*ATG32*	-	-	-	-
YIL098C	*FMC1*	-	-	-	++
YPL060W	*LPE10*	+	++	No defect	N.D.
YLR356W	*YLR356W/ATG33*	++	-	++	+
YPR146C	*YPR146C*	+	-	No defect	N.D.
YMR142C	*RPL13B*	++	++	+	+
YKL006W	*RPL14A*	-	N.D.	N.D.	-
YMR121C	*RPL15B*	-	No defect	No defect	No defect
YDR173C	*ARG82*	+	N.D.	N.D.	-
YGL148W	*ARO2*	-	-	-	-
YJL095W	*BCK1*	+	-	-	+
YGR188C	*BUB1*	+	+	++	-
YPL037C	*EGD1*	+	-	No defect	-
YPL250C	*ICY2*	-	-	No defect	-
YEL053C	*MAK10*	++	+	+	-
YKR103W	*NFT1*	+	-	No defect	-
*YGL167C**	*PMR1*	-	+	N.D.	+
*YGL168W**	*HUR1*	+	++	N.D.	+
YIL165C	*YIL165C*	-	No defect	No defect	+
YOR019W	*YOR019W*	+	++	++	-
YOR036W	*PEP12*	-	N.D.	N.D.	N.D.
YPL154C	*PEP4*	-	N.D.	N.D.	N.D.
YDR080W	*VPS41*	-	N.D.	N.D.	N.D.
YDR108W	*TRS85/GSG1*	-	N.D.	N.D.	N.D.
YLR417W	*VPS36*	+	N.D.	N.D.	N.D.
YML001W	*YPT7*	-	N.D.	N.D.	N.D.
YGL212W	*VAM7*	-	N.D.	N.D.	N.D.
YBR131W	*CCZ1*	-	N.D.	N.D.	N.D.
YGL124C	*MON1*	-	N.D.	N.D.	N.D.

++: slight defect
+: severe defect
-: complete defect
N.D.: not determined

**YGL167C* and *YGL168W* partially overlap

Table SB.3. Summary of autophagy analyses (Continued)

	Macroautophagy Cvt			
	Pho8Δ60	Pho8Δ60	GFP-Atg8	Ape1
	SEY6210	BY4742	BY4742	BY4742
Gene	Fig. 5	Fig. S2	Fig. S4	Fig. S2
AIM26	++	++	No defect	No defect
AIM28	No defect	No defect	No defect	No defect
DNM1	No defect	No defect	No defect	No defect
ATG32	No defect	No defect	No defect	No defect
FMC1	++	++	No defect	No defect
LPE10	No defect	No defect	No defect	No defect
YLR356W/ATG33	No defect	No defect	No defect	No defect
YPR146C	No defect	No defect	No defect	No defect
RPL13B	N.D.	No defect	No defect	No defect
RPL14A	+	++	No defect	No defect
RPL15B	No defect	++	No defect	No defect
ARG82	No defect	++	N.D.	No defect
ARO2	No defect	No defect	N.D.	No defect
BCK1	++	No defect	No defect	No defect
BUB1	++	+	No defect	No defect
EGD1	++	No defect	No defect	No defect
ICY2	+	+	No defect	No defect
MAK10	No defect	No defect	No defect	No defect
NFT1	++	No defect	No defect	No defect
PMR1	No defect	++	No defect	No defect
HUR1	No defect	++	No defect	No defect
YIL165C	++	++	No defect	No defect
YOR019W	No defect	No defect	N.D.	No defect
PEP12	N.D.	-	N.D.	-
PEP4	N.D.	-	N.D.	-
VPS41	N.D.	-	N.D.	-
TRS85/GSG1	N.D.	-	N.D.	-
VPS36	N.D.	+	N.D.	+
YPT7	N.D.	-	N.D.	-
VAM7	N.D.	-	N.D.	-
CCZ1	N.D.	-	N.D.	-
MON1	N.D.	-	N.D.	-

Analysis of 23 Novel Mutants

Among these 32 mitophagy-related genes identified from the screen, nine of them are related with vacuolar protein sorting, membrane fusion machinery, or normal vacuolar function. As expected based on published data, deletion of these genes resulted in a partial or complete block in all autophagy-related pathways, and we did not pursue a further analysis of the associated gene products. The remaining 23 gene products are involved in diverse cellular processes. In particular, Atg32 is a mitochondrially-localized receptor required for starvation-dependent and post-log phase growth mitophagy [18,19]. In addition, eight of these 23 genes encode mitochondrially-related proteins. Accordingly, we decided to extend our analysis of these 23 mutants.

First, to verify the screen results, we decided to delete these 23 genes in another yeast strain background to eliminate potential strain-dependent phenotypes and to verify that the mitophagy defect was due to the correct gene deletion. We used the SEY6210 strain that had the integrated Om45-GFP tag, and conducted the same processing assay (Fig. B.3). Two mutants, *rpl15b*Δ and *yil165c*Δ, showed comparable GFP processing with the wild type, whereas other mutants showed partial or no GFP processing, consistent with the previous screen result. In two cases, for *rpl14a* and *arg82*, we were unable to generate the appropriate strains.

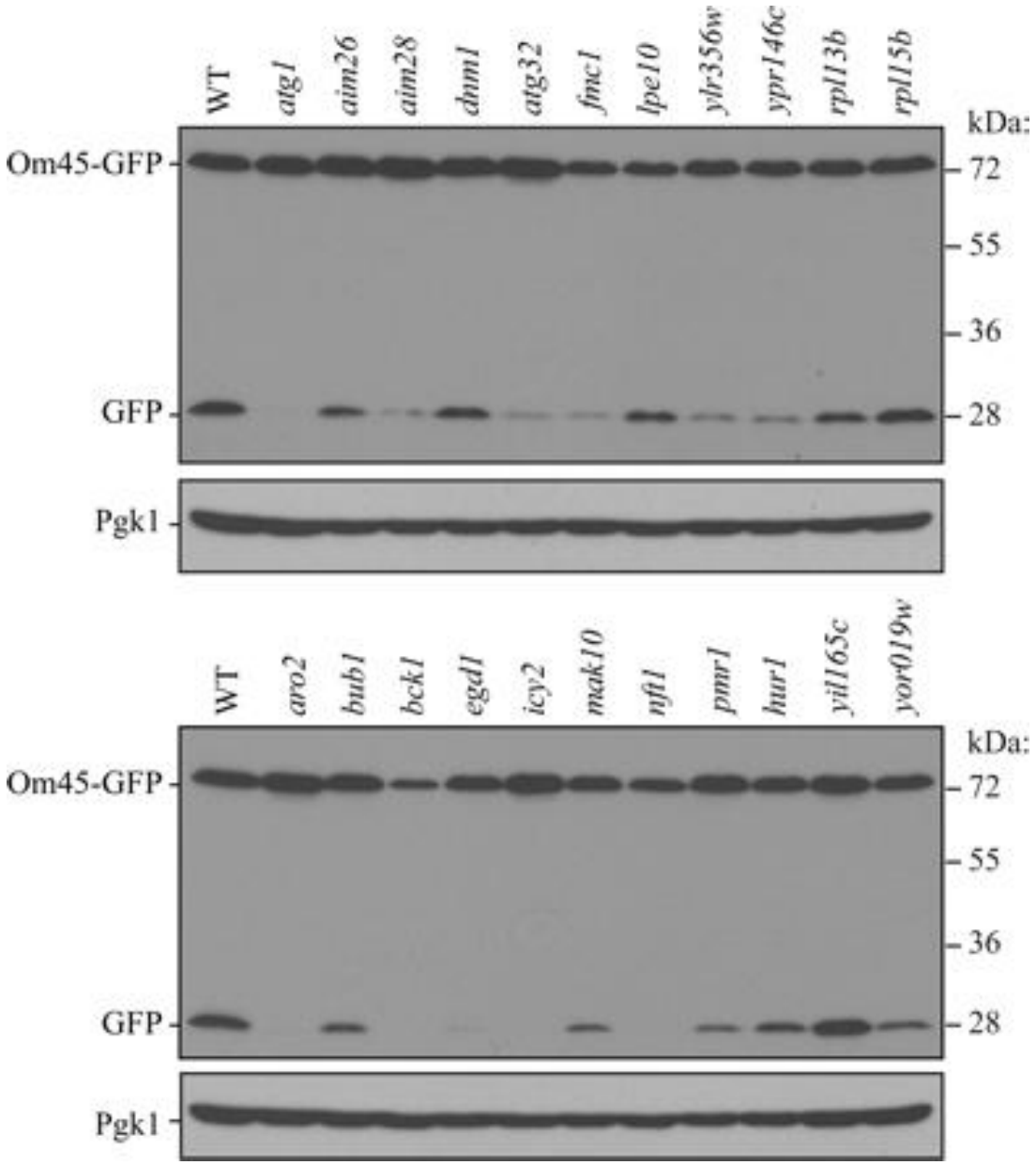

Figure B.3. Om45-GFP processing analysis of novel mutants. Wild-type (WT; TKYM22) and the indicated mutant strains expressing Om45-GFP (top and bottom) were cultured in YPL medium for 12 h and then starved in SD-N for 6 h. The cell lysates equivalent to A_{600} = 0.2 U of cells were subjected to immunoblot analysis with anti-YFP or anti-Pgk1 (loading control) antibodies or antiserum, respectively.

To provide a second method of mitophagy analysis, we also integrated GFP at the 3′ end of the *IDH1* locus of the corresponding deletion strains and carried out an Idh1-GFP processing assay; Idh1 is a mitochondrial matrix protein, and its delivery to the vacuole should mirror that of Om45-GFP (Fig. SB.3). We found that the *rpl15b*Δ and *aim28*Δ mutant strains showed normal GFP-processing compared with the wild type, whereas the other mutant strains displayed reduced or no GFP-processing. In two cases, for *ypr146c*Δ and *lpe10*Δ, we were unable to generate the appropriate strains. In some cases, we noted discrepancies between the results for the Om45-GFP and Idh1-GFP processing assays. In addition, neither of these assays is quantitative. Therefore, we modified a previously described alkaline phosphatase assay that uses a mitochondrially-targeted Pho8Δ60 (mitoPho8Δ60) construct [23] and assayed the deletion mutants for mitophagy activity. The mitoPho8Δ60 can only be delivered into the vacuole after the autophagic degradation of mitochondria. Cells expressing mitoPho8Δ60 were cultured in YPL to midlog phase and shifted to SD-N or SL-N for 4 h, and mitoPho8Δ60-dependent alkaline phosphatase activity was measured. The YPL to SD-N shift will induce selective autophagic mitochondria degradation as well as nonselective autophagy, whereas the YPL to SL-N shift will only induce bulk autophagy [15]; thus, the SD-N minus SL-N value represents the activity of selective autophagic mitochondrial degradation. For the wild-type strain, we observed 36% higher alkaline phosphatase activity during the SD-N shift than was seen after the shift to SL-N (Fig. B.4). In the *atg1*Δ strain, the alkaline phosphatase activities during both starvation conditions represent the background level. In the *atg32*Δ strain, we observed a significant decrease (75%) of mitoPho8Δ60 activity during the SD-N shift compared with the wild type, which showed that Atg32 is required

for efficient selective autophagic mitochondria degradation. We also observed a 63% decrease of alkaline phosphatase activity during the SL-N shift compared with the wild type, possibly because of the absence of Atg32-dependent mitochondrial degradation that occurs through nonspecific autophagy (which is likely to still require Atg32 to be efficient). We were unable to generate the mitoPho8Δ60 strains for deletions of *ARG82*, *RPL14A*, *PMR1*, and*HUR1*. For the remaining 19 mutants, eight strains (*icy2*Δ, *rpl15b*Δ, *nft1*Δ, *yil165c*Δ, *lpe10*Δ, *egd1*Δ, *aim28*Δ, and *ypr146c*Δ) showed mitophagy activity comparable to that of the wild type, whereas the 11 other strains displayed a significant to complete mitophagy defect (Fig. B.4). The potential reasons for the differences between the Om45-GFP processing assay results and those of the mitoPho8Δ60 assay are considered in the *Discussion.*

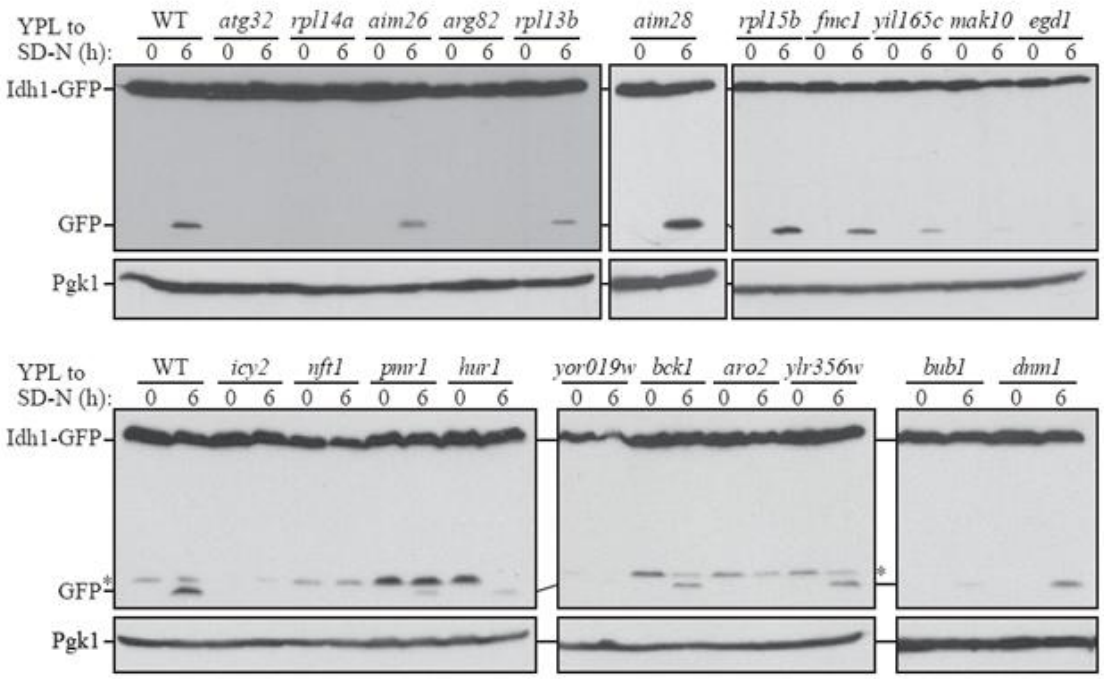

Figure SB.3. Idh1-GFP processing analysis for novel mutants. Wild-type (WT; BY4742) and the indicated mutant strains expressing Idh1-GFP were cultured in YPL medium for 12 h and then starved in SD-N for 6 h. The cell lysates equivalent to A600 = 0.2 units of cells were subjected to immunoblot analysis with anti-YFP antibody and anti-Pgk1 antiserum as a loading control. The asterisks indicate non-specific bands that result from repeated use of the anti-YFP antibody.

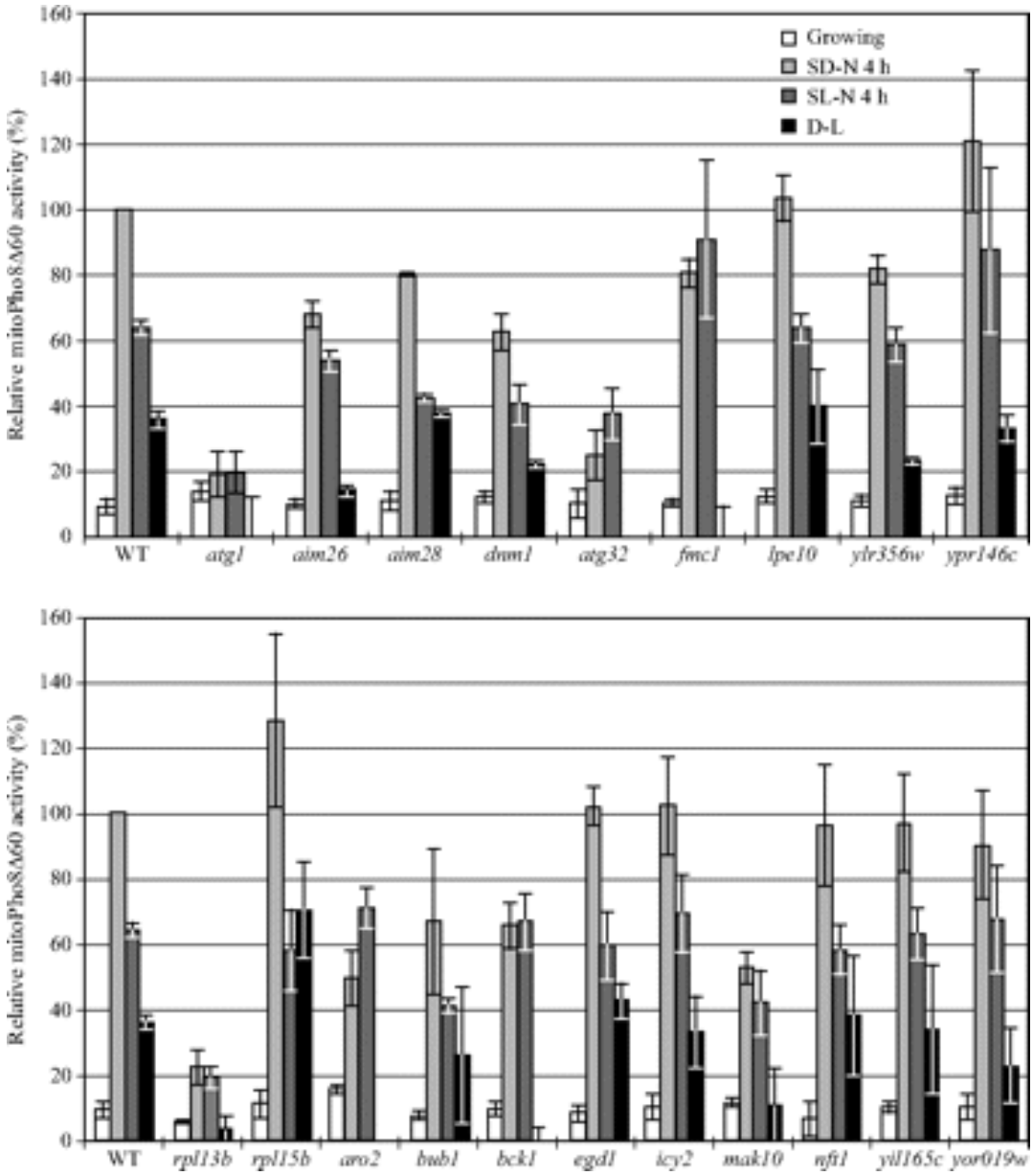

Figure B.4. MitoPho8Δ60 analysis of novel mutants. Wild-type (WT; KWY20) and the indicated mutant strains (top and bottom) expressing mitoPho8Δ60 were grown in YPL and shifted to SD-N and SL-N for 4 h. Samples were collected, and protein extracts were assayed for mitoPho8Δ60 activity. The value for the wild-type strain was set to 100%, and the other values were normalized. Values lower than zero are depicted as zero.

Next, to examine potential effects on nonspecific macroautophagy, we used the GFP-Atg8 processing assay. This assay relies on the same principle as the Om45-GFP processing assay, but the marker protein is a component of the autophagosome; substantial generation of free GFP from GFP-Atg8 is only seen during nonspecific autophagy. All 23 mutant strains essentially showed normal GFP-Atg8 processing (Fig. SB.4), demonstrating they do not have substantial defects in nonspecific macroautophagy. To extend the analysis, we generated *pho8::pho8Δ60 pho13Δ* strains in the SEY6210 background for each mutant and monitored them using the more quantitative Pho8Δ60 activity assay as a second method for analyzing potential macroautophagy defects (Fig. B.5); we were unable to generate the Pho8Δ60 strain for *rpl13bΔ*. Two strains (*rpl14aΔ* and*icy2Δ*) displayed a more than 40% decrease of Pho8Δ60 activity, seven strains (*aim26Δ*, *fmc1Δ*, *bck1Δ*, *bub1Δ*, *egd1Δ*, *nft1Δ*, and *yil165cΔ*) showed a slightly reduced Pho8Δ60 activity (<30% decrease), and the other strains were essentially normal.

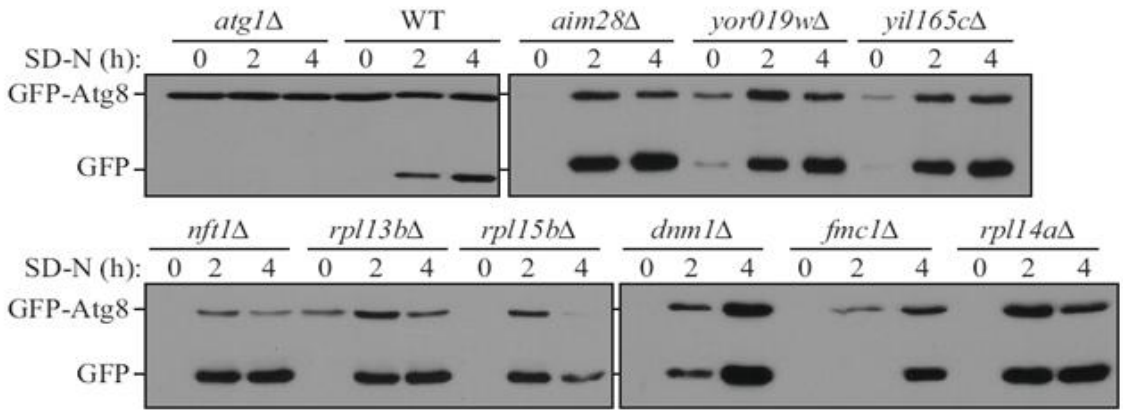

Figure SB.4. GFP-Atg8 processing analysis for novel mutants. Wild-type (WT, BY4742) and the indicated mutant strains expressing GFP-Atg8 were cultured in YPD medium to mid-log phase and then starved in SD-N for 2 and 4 h. The cell lysates equivalent to A600 = 0.2 units of cells were subjected to immunoblot analysis with anti-YFP antibody.

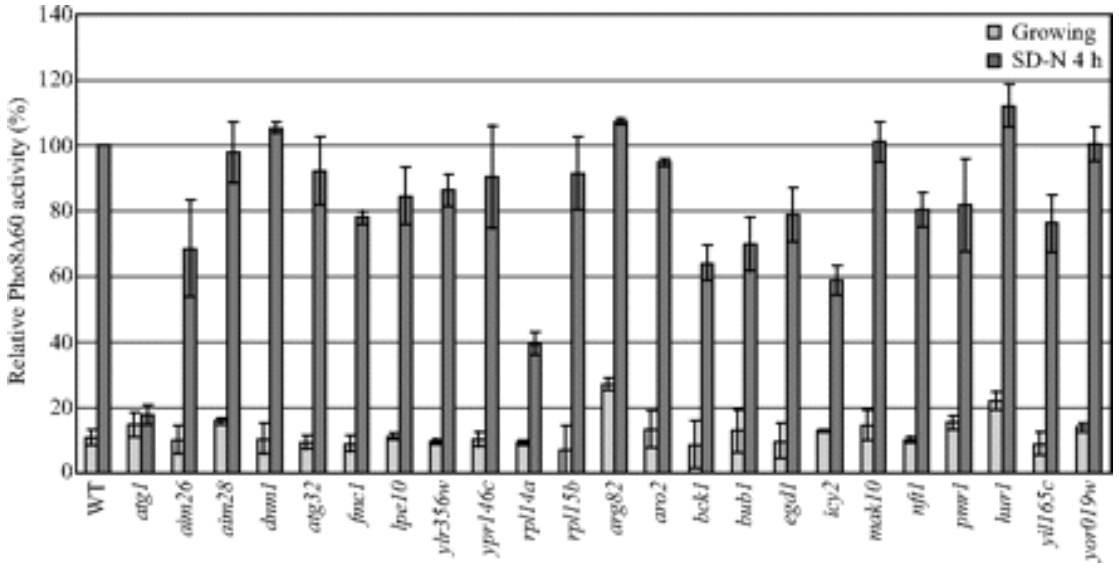

Figure B.5. Wild-type (WT; WLY176) and the indicated mutant strains expressing Pho8Δ60 were grown in YPD and shifted to SD-N for 4 h. Samples were collected, and protein extracts were assayed for Pho8Δ60 activity. The value for the wild-type strain was set to 100%, and the other values were normalized.

Finally, we determined the subcellular localization of these proteins by chromosomally tagging them with GFP and observed them with fluorescence microscopy (Fig. SB.5). Atg32 has already been reported as being localized to the mitochondria. For the other 22 proteins, eight of them (Aim26, Aim28, Dnm1, Fmc1, Lpe10, Ypr146c, and Ylr356w) displayed a mitochondrial localization pattern. The localization of Ylr356w was further studied as described below. The subcellular localization of most proteins under nitrogen starvation condition was basically the same as during vegetative growth (data not show). The localization information is summarized in Table SB.3.

Characterization of Ylr356w

The mitophagy-related genes that we found from the screen include eight genes of unknown function. Among them, we initially focused on *YLR356W*. The Ylr356w protein is reported to localize to mitochondria [24], and we obtained consistent data between our different detection methods for both mitophagy and autophagy. Thus, we decided to characterize this gene as a candidate for a novel*ATG* gene. In agreement with the previous report, we found that Ylr356w tagged with GFP is mitochondrially-localized (Fig. SB.5, Fig. B.6A); however, the overexpressed chimera is not fully functional. We detected a similar mitochondrial localization using a chromosomally tagged GFP construct, but the fluorescence signal was extremely weak (our unpublished data). Accordingly, we further examined the mitochondrial localization of Ylr356w using a biochemical approach. A strain expressing protein A–tagged Ylr356w (Ylr356w-PA) and Myc-tagged Tim23 (inner membrane marker) was fractionated by differential centrifugation. Mitochondrial porin and Tim23-myc were enriched in the mitochondrial (6500 × *g*) fraction, along with Ylr356w-PA (Fig. B.6B), whereas the cytosolic marker

Pgk1 was mostly in the supernatant fraction. Next, the isolated mitochondria were treated with proteinase K before or after hypotonic treatment or in the presence of Triton X-100. Although Tim23-myc was protected from proteinase K before hypotonic treatment or in the absence of detergent, Ylr356w-PA was degraded, suggesting that this protein localizes on the mitochondrial outer membrane (Fig. B.6C). As our data showed, macroautophagy and the Cvt pathway were essentially normal in *ylr356w*Δ strains in both the BY4742 and SEY6210 backgrounds (Fig. B.5, Figs. SB.2, SB.4, and SB.6A). There was a substantial decrease of Om45-GFP processing for starvation-induced mitophagy (Fig. B.3), and the mitoPho8Δ60 assay revealed a 36% decrease of mitophagy activity (Fig. B.4) in the *ylr356w*Δ strain. We also monitored pexophagy, another type of selective autophagy, using the Pex14-GFP processing assay. Pex14 is a peroxisomal membrane protein, and processing of Pex14-GFP to release free GFP can be used for monitoring peroxisome degradation in the vacuole [25]. The *ylr356w*Δ strain displayed processing of Pex14-GFP at a level similar to that of the wild-type strain after shifting cells from oleic acid medium to starvation medium, whereas the *atg1*Δ mutant showed a complete block (Fig. SB.6B). From these findings, we conclude that *YLR356W* is a mitophagy-specific gene that is not required for macroautophagy or other types of selective autophagy.

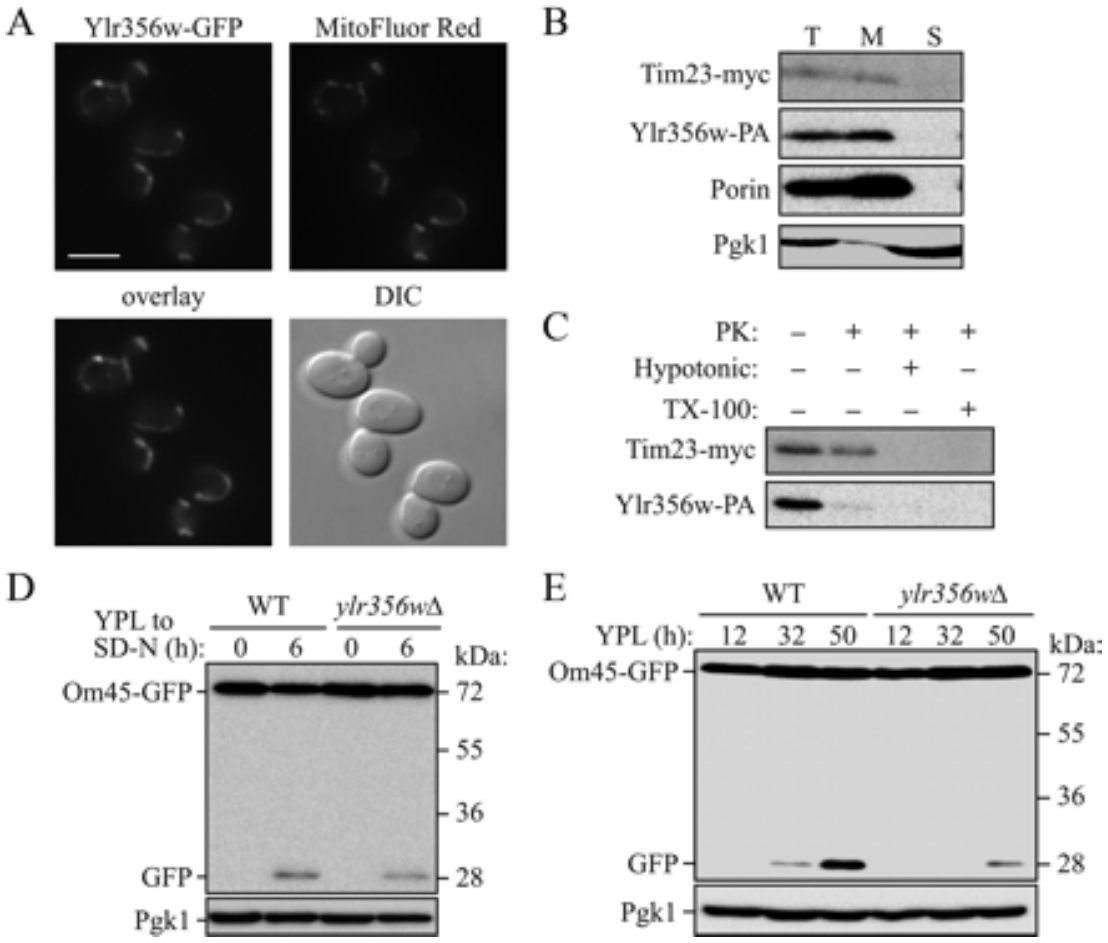

Figure B.6. Characterization of Ylr356w. (A) A strain expressing Ylr356w-GFP under the control of the *GAL1* promoter (TKYM201) was cultured in YPD medium to midlog phase and shifted to YPGal medium for 4 h. Cells were labeled with the mitochondrial marker MitoFluor Red 589. The localization of GFP and MitoFluor Red were visualized by fluorescence microscopy. DIC, differential interference contrast. Bar, 5 μm. (B) Mitochondria were purified from a strain expressing chromosomally tagged Tim23-myc and Ylr356w-PA as described in *Materials and Methods.* Equal amounts of the total cell homogenate (T), mitochondrial (M), and supernatant (S) fractions were loaded and detected with antibodies to myc and porin, a purified antibody that recognizes PA, or with antiserum to Pgk1. (C) Isolated mitochondria were treated with proteinase K (PK) with or without hypotonic or Triton X-100 treatment. Samples were TCA-precipitated and subjected to immunoblotting using the appropriate antibodies. (D) Wild-type (WT; TKYM22) and *ylr356w*Δ strains expressing Om45-GFP were cultured in YPL medium for 12 h and then starved in SD-N for 6 h. The cell lysates equivalent to A_{600} = 0.2 U of cells were subjected to immunoblot analysis with anti-YFP and anti-Pgk1 (loading control) antibody or antiserum, respectively. (E) Wild-type (WT; TKYM22) and *ylr356w*Δ strains expressing Om45-GFP were cultured in YPL medium for the indicated times. Cell lysates equivalent to A_{600} = 0.2 U of cells were subjected to immunoblot analysis with anti-YFP antibodies and anti-Pgk1 antiserum.

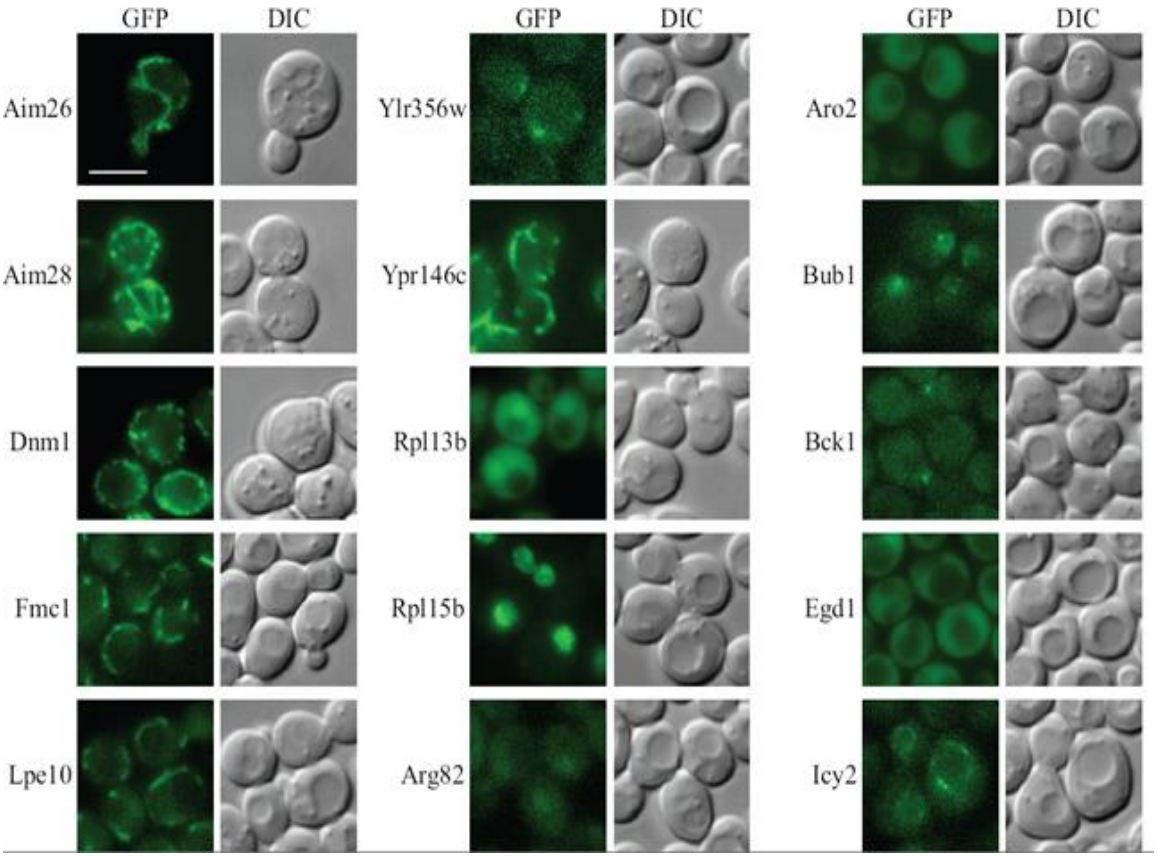

Figure SB.5. Subcellular localization of the mitophagy-related proteins identified from the screen. Each protein was chromosomally tagged with GFP and observed with fluorescence microscopy as described in Materials and Methods. DIC, differential interference contrast.

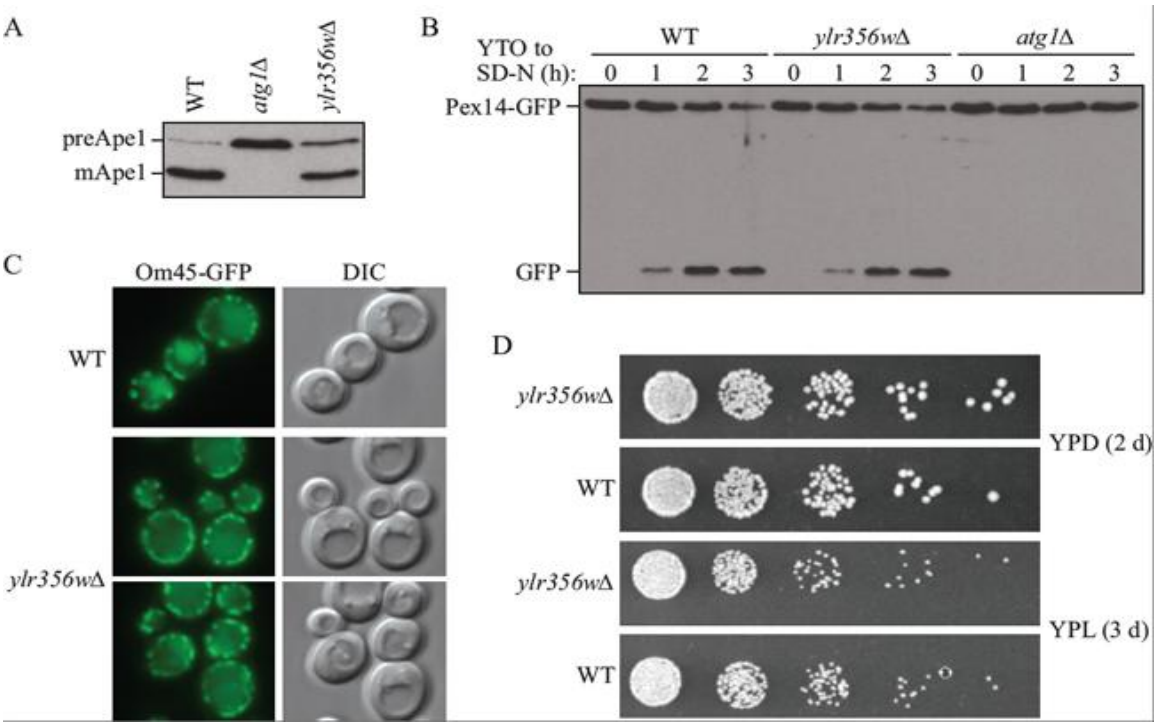

Figure SB.6. The Cvt pathway, pexophagy and cell growth are normal in the *ylr356wΔ* strain. (A) Wild-type (WT; SEY6210), *atg1Δ*, and *ylr356wΔ* strains were cultured in YPD medium and analyzed for prApe1 maturation by immunoblotting to monitor the Cvt pathway during vegetative growth. The positions of precursor and mature Ape1 are indicated. (B) GFP was integrated at the *PEX14* locus in wild-type (SEY6210), *atg1Δ*, and *ylr356wΔ* strains. Cells were grown in oleic acid-containing medium (YTO) for 19 h, then shifted to SD-N for the indicated times. Samples were collected and analyzed by immunoblot with antibody to YFP. (C) Wild-type (SEY6210) and *ylr356wΔ* strains expressing Om45-GFP were cultured in YPL medium for three days. The localization of GFP was visualized by fluorescence microscopy. DIC, differential interference contrast. (D) Wild-type (WT; SEY6210), *ylr356wΔ* and *icy2Δ* strains were cultured in YPD medium to mid-log phase and washed in sterile water. Equal numbers of cells suspended in sterile water were inoculated on YPD and YPL plates. Cells were diluted 1:5 in each step from left to right.

Considering that we observed relatively minor vacuolar GFP fluorescence from the*ylr356w*Δ (BY4742 background) strain expressing Om45-GFP at the post-log phase (day 3 in YPL medium) in our initial screen, although we obtained a relatively slight decrease (36% based on the mitoPho8Δ60 assay [Fig. B.4] and 33% based on the Om45-GFP processing assay [Fig. B.6D]) of mitophagy activity during starvation, we considered the possibility that Ylr356w might play different roles in these two mitophagy-inducing conditions. Thus, we repeated the analysis of Om45-GFP fluorescence of the *ylr356w*Δ strain in the SEY6210 background. After 45 h in YPL medium, the *ylr356w*Δ strain again showed only faint vacuolar GFP fluorescence (Fig. SB.6C), and Om45-GFP processing was mostly blocked (93 and 80% decrease compared with the wild type at 32 and 50 h in YPL, respectively; Fig. B.6E). One possibility to explain the mitophagy defect in the *ylr356w*Δ strain in the post-log phase was that the severe block in Om45-GFP processing was due to a growth defect in YPL medium that prevented the cells from reaching the mitophagy-inducing post-log phase. Accordingly, we checked the growth of the*ylr356w*Δ strain. This strain showed the same growth both on YPD and YPL plates and was similar to the wild-type strain (Fig. SB.6D). Thus, we concluded that Ylr356w was required primarily for mitophagy induced at the post-log phase and played a less significant role during starvation-induced mitophagy. On the basis of the cumulative analyses of the phenotypes of the *ylr356w*Δ strain, we named this gene *ATG33*.

Screen of ATG Knockout Strains for Mitophagy Defects

Several *ATG* genes are required for mitophagy [10,15,20,26,27], and our first mitophagy screen revealed 18 *ATG* genes that may be required for this process (one of

the additional strains with a mitophagy defect is deleted for *YMR158W-A*, a gene that overlaps with *ATG16*, thus implicating 19 *ATG* genes in total). Thus, we decided to screen all 28 *ATG* knockout strains that play a role in autophagy-related processes in S. *cerevisiae* using the Om45-GFP processing analysis. *ATG* genes that play a fundamental role in autophagy such as that encoding the protein kinase Atg1 and its binding partner Atg13, the genes for the ubiquitin-like protein modification systems (*ATG3*, *4*, *5*, *7*, *8*, *10*, *12*, and *16*) and those that encode components that are involved in supplying membrane to the phagophore (*ATG2* and *ATG9*) were essential for mitophagy (Fig. SB.7). Genes that are required for the Cvt pathway but not macroautophagy (*ATG20*, *21* and *24*), or for macroautophagy but not the Cvt pathway (*ATG17*, *29*, and *31*) were also required for efficient mitophagy. Finally, the gene encoding *ATG11*, which is a common adaptor for selective types of autophagy was required for mitophagy as shown previously [15], whereas the genes for the Cvt cargo-specific receptor*ATG19* [16], a vacuolar permease *ATG22* [28], and an autophagy gene that is not required in *S. cerevisiae ATG26* [29] were not required for mitophagy.

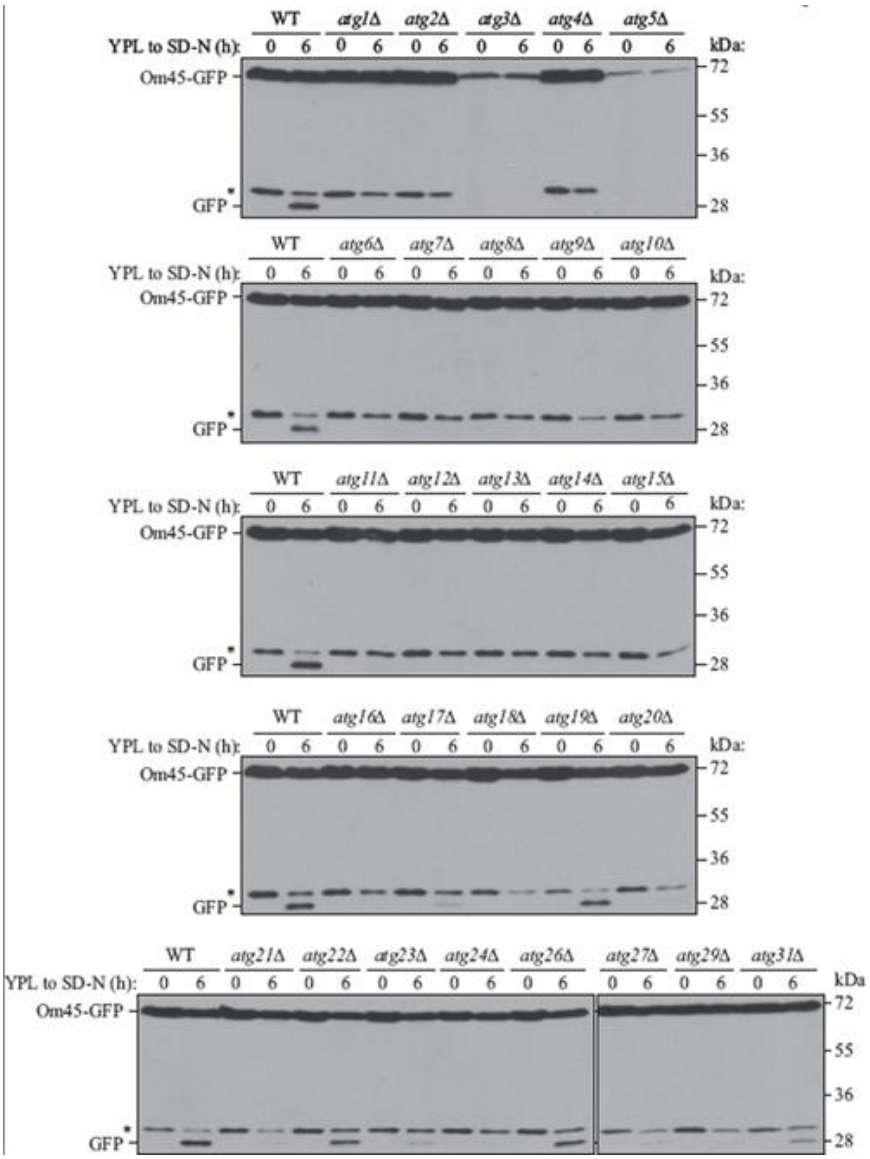

Figure SB.7. Analysis of mitophagy in the *atg* mutant strains. The wild type (WT; TKYM22) and the indicated *atg* mutant strains expressing Om45-GFP were cultured in YPL medium for 12 h and then starved in SD-N for 6 h. The cell lysates equivalent to A600 = 0.2 units of cells were subjected to immunoblot analysis with anti-YFP antibodies.

Discussion

A Mitochondria Degradation Screen Identified 32 Mitophagy-Related Genes

The initial screen for mitophagy was carried out in 96-well plates. Thus, the screen was performed in a blind manner as the gene names of each strain were hidden during the screen. Among 25 *ATG* genes that are required for mitophagy (Fig. SB.7), our knockout library included 21 *ATG* knockout strains (*atg2*Δ, *4*Δ, and *10*Δ were not included in our BY4739 or BY4742 background library, and *atg14*Δ was incorrect). Based on our initial screen, 17 of them (18 if we include the strain where the deletion overlaps with *ATG16*) were identified as positive for a defect in mitophagy, and three of them were negative (*atg17*Δ, *24*Δ, and *31*Δ). If it is assumed that these *ATG* knockout strains serve as positive controls, our initial screen sensitivity was 81–86% (17 or 18/21). In other words, we may have missed 14–19% of the positive strains during our initial screen; however, considering that *atg17*Δ and *atg31*Δ have only partial defects, our detection rate may have been closer to 95%. We cannot calculate the sensitivity of the secondary screen, because the *ATG* genes were screened by the Om45-GFP–processing assay (the secondary screen for the other mutants). The fact that at least one novel*ATG* gene, *YLR356W/ATG33*, was identified from our screen further supports its utility.

Our screen identified eight membrane trafficking-related genes (*CCZ1*, *MON1*, *PEP12*, *TRS85*, *VAM7*, *VPS36*, *VPS41*, and *YPT7*) that are required for mitophagy. All of them are also required for both macroautophagy and the Cvt pathway. The requirement of some of these genes for autophagy has been reported previously [30-35], and the requirement of membrane-trafficking pathways for autophagy has also been

reported [36,37]. It is widely believed that defects in membrane-trafficking pathways affect the lipid supply that is needed for extension of the phagophore, the initial sequestering compartment that generates the autophagosome. The two genes identified here that are involved in membrane trafficking that have not been reported previously as affecting autophagy, *PEP12*and *VPS36*, presumably do so for the same reason.

We identified nine mitophagy-related genes whose functions were not previously known (*AIM26*, *AIM28*, *ATG32*, *HUR1*, *ICY2*, *YIL165C*, *YLR356W*, *YOR019W*, and *YPR146C*). *HUR1* overlaps with*PMR1*, which encodes a cation P-type ATPase in the Golgi complex. Thus, the phenotype of the *hur1*Δ strain may result from a knockout of the *PMR1* gene. The further characterization of the other eight gene products may provide substantial insight into the mechanism of mitophagy. In particular, Ylr356w localized to mitochondria and may play an important role in determining whether a particular mitochondrial segment is destined for degradation by autophagy. Thus, we initially focused on the *YLR356W* gene and the corresponding protein.

DNM1 encodes mitochondrial dynamin-related GTPase that is required for mitochondrial fission. The fragmentation of mitochondria is a prerequisite for mitophagy in mammalian cells [9] and the *dnm1*Δ strain inhibits the mitophagy induced by *mdm38*conditional knockout in yeast [7]. The identification of the*dnm1*Δ strain from our screen further confirmed the importance of mitochondrial fission for mitophagy.

Different Methods to Monitor Mitophagy

In this article, we used the Om45-GFP processing and mitoPho8Δ60 assays to measure mitophagy activity. Importantly, with the mitoPho8Δ60 assay, we can measure

mitophagy in a quantitative manner. Both assays showed the expected results for the wild-type, *atg1*Δ, and *atg32*Δ strains, demonstrating they are adequate for measuring mitophagy. In some cases, however, we obtained different results between these two methods. One potential problem with the mitoPho8Δ60 assay is that the marker protein may not be properly targeted to the mitochondria in each mutant strain, especially in mutants that may have a defect in the mitochondrial protein import system. This would cause an apparent mitophagy defect, and correct localization should be confirmed in each case.

YLR356W/ATG33 Is Required Primarily for Mitophagy Induced at the Post-Log Phase

Although a genome-wide screen for protein localization revealed that Ylr356w localizes to mitochondria [24], there have not been any other reports about this protein. Ylr356w is composed of 197 amino acids and is predicted to have four transmembrane domains. This protein is conserved within fungi, but not in higher eukaryotes. *YLR356W* is a mitophagy-specific gene that is not required for macroautophagy or other types of selective autophagy (Figs. B.5, B.6, SB.2B, SB.4, and SB.6). Although *ylr356w*Δ blocked mitophagy to half the level of the wild type during starvation, it blocked mitophagy almost completely at the post-log phase (Fig. B.6, D and E). This finding suggests that Ylr356w may be required to detect or present aged mitochondria for mitophagy when cells have reached the post-log phase.

The Induction of Mitophagy during Starvation and at the Post-Log Phase in Yeast

Although mitochondria depolarized by an uncoupler such as CCCP (carbonyl cyanide m-chlorophenylhydrazone) are degraded by autophagy in mammalian cells

[38,39], we did not observe mitochondrial degradation in wild-type yeast under similar conditions (our unpublished results). Thus, in our experience, nitrogen starvation or culturing cells to the post-log phase in a nonfermentable carbon source medium are the only reliable methods that can induce mitophagy efficiently in a wild-type yeast strain. A previous study suggests that mitophagy in S. cerevisiae occurs by a microautophagic process when cells are grown under nonfermentable conditions [27]. Thus, we considered the possibility that mitophagy might happen by different mechanisms depending on the inducing conditions. We attempted to examine the mode of autophagic sequestration occurring in SD-N versus post-log phase growth through electron microscopy (Fig. SB.8). In both conditions we could detect mitochondria within double-membrane vesicles, suggesting a macroautophagic mechanism; however, we cannot rule out the possibility of a microautophagic process.

It is thought that mitophagy is induced to adapt the cell to conditions where the cell energy requirement is decreased, and accordingly the cell needs to reduce the amount of mitochondria when reaching the post-log phase in nonfermentable medium [15], although there is little direct evidence for this hypothesis. On the other hand, macroautophagy is induced at the post-log phase [40], presumably because cells are starved at this growing phase. Thus, it has been unclear whether mitophagy is induced at the post-log phase through some specific mechanism or simply as a result of cellular starvation. The specific requirement of Ylr356w for mitophagy primarily at the post-log phase suggests that there are some differences between the pathways of mitophagy induced during starvation versus post-log phase growth. Because only a fraction of the total mitochondrial pool is degraded by mitophagy at the post-log phase (compare full-

length Om45-GFP and the processed GFP band in Fig. B.6E, WT), it is reasonable to propose that aged or damaged mitochondria are selected for degradation. We propose that Ylr356w may contribute to this selection process, although future experiments will be needed to confirm this hypothesis.

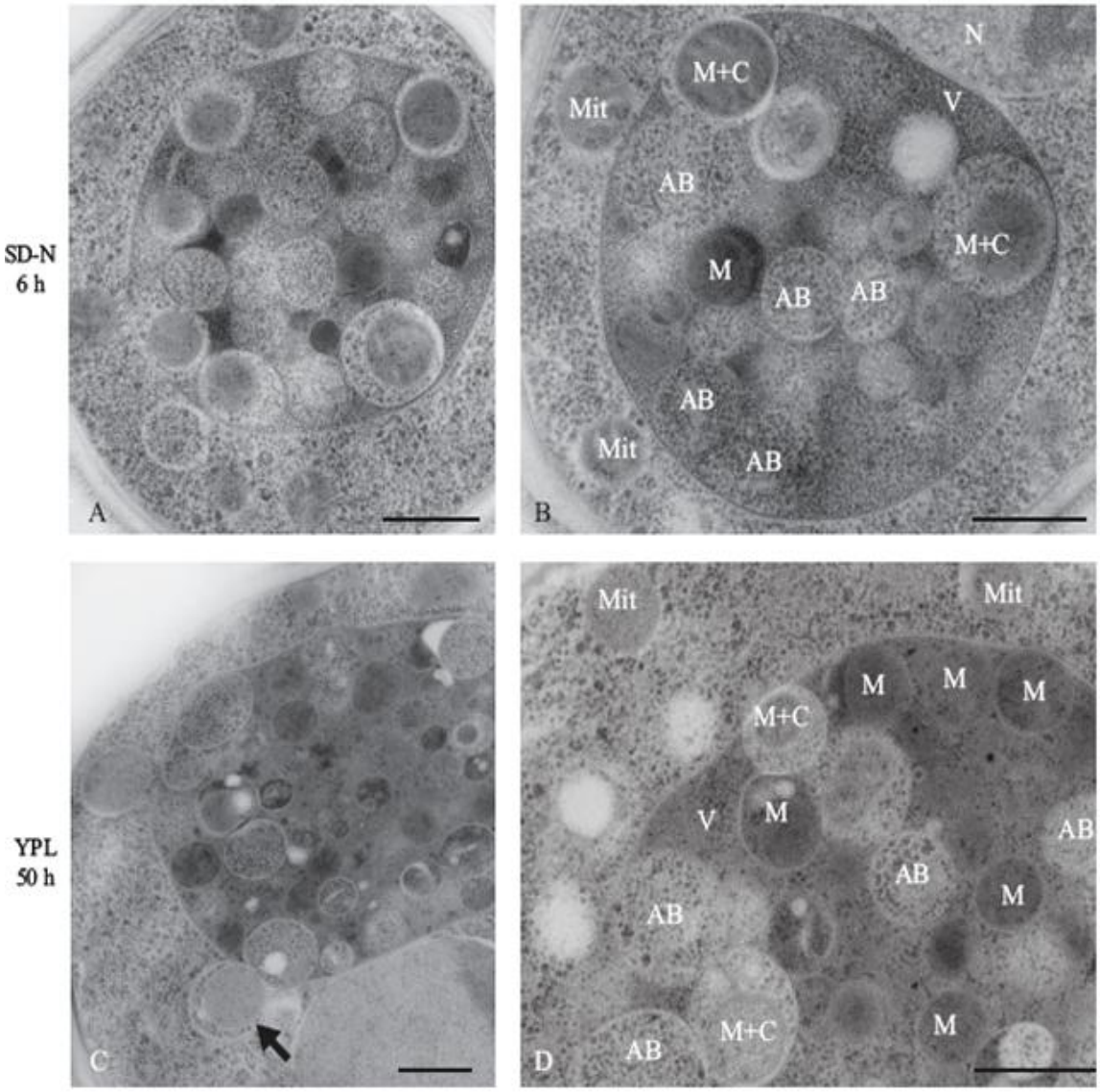

Figure SB.8. EM. Electron microscopy of mitophagy during starvation and at post-log phase. The *pep4Δ* strain was cultured in YPL medium to growing phase, then shifted to SD-N and cultured for 6 h (A and B) or was cultured in YPL medium to stationary phase (for 50 h; C and D). Cells were prepared for electron microscopy using freeze substitution. The arrow marks an example of autophagosome containing a mitochondria and cytosolic components. AB, autophagic body including cytosolic components; M, autophagic body including mitochondria only; M+C, autophagic body including mitochondria and cytosolic components; Mit, mitochondria in cytosol; V, vacuole; N, nucleus. Scale bar, 500 nm.

Materials and Methods

Strains and Media

The yeast strains used in this study are listed in Supplemental Table S1. Yeast cells were grown in rich medium (YPD; 1% yeast extract, 2% peptone, 2% glucose), lactate medium (YPL; 1% yeast extract, 2% peptone, 2% lactate), synthetic minimal medium with glucose (SMD; 0.67% yeast nitrogen base, 2% glucose, amino acids, and vitamins), synthetic minimal medium with lactate (SML; 0.67% yeast nitrogen base, 2% lactate, amino acids, and vitamins), synthetic minimal medium with oleic acid (YTO; 0.67% yeast nitrogen base without amino acids, 0.1% Tween-40, and 0.1% oleic acid), or synthetic minimal medium with galactose (SMGal; 0.67% yeast nitrogen base, 2% galactose, amino acids, and vitamins). Starvation experiments were performed in synthetic minimal medium lacking nitrogen (SD-N: 0.17% yeast nitrogen base without amino acids, 2% glucose; SL-N: 0.17% yeast nitrogen base without amino acids, 2% lactate).

Mitophagy Screening

For the first round of screening, a yeast knockout strain library (BY4739 or BY4742 background) was analyzed. To express Om45-GFP, a DNA fragment encoding green fluorescent protein (GFP) was integrated at the 3′ end of *OM45* by a PCR-based integration method [41]. Cells grown on SMD plates were shifted to YPL medium and cultured for 3 d (50 ± 5 h), and the vacuolar GFP fluorescence was observed by fluorescence microscopy. If there was no vacuolar GFP signal, or a weak signal, the mitochondrial GFP signal and the cell growth were also recorded.

For the secondary screening, the Om45-GFP-expressing strains that showed a weak or absent vacuolar GFP signal were cultured in YPL medium for 12 h and then shifted to SD-N medium. The cells were collected after 6 h, and the cell lysates equivalent to A_{600} = 0.2 U of cells were subjected to immunoblotting analysis.

Plasmids and Antibodies

The mitoPho8Δ60 expressing plasmid [ADH1-COXIV-PHO8Δ60(406)] was derived from ADH1-COXIV-PHO8Δ60(313) described previously [23] by digesting with PvuI and inserting the *ADH1-COXIV-PHO8Δ60* fragment into the pRS406 vector.

Monoclonal anti-YFP antibody clone JL-8 (Clontech, Mountain View, CA) and anti-Ape1 antiserum [16] were used for immunoblotting. Monoclonal anti-myc and anti-porin antibodies were from Molecular Probes/Invitrogen (Eugene, OR), and anti-Pgk1 antiserum was a kind gift of Dr. Jeremy Thorner (University of California, Berkeley).

Assays for Autophagy and Pexophagy

For monitoring bulk autophagy, the alkaline phosphatase activity of Pho8Δ60 was carried out as described previously [21]. The Pex14-GFP processing assay to monitor pexophagy has been described previously [25].

MitoPho8Δ60 Assay

For monitoring mitophagy, the mitochondrially-targeted Pho8Δ60-expressing strains were cultured in YPL medium for 12 h and then shifted to SD-N or SL-N medium. The cells were collected after 4 h, and the alkaline phosphatase activity of Pho8Δ60 was carried out as described previously [21].

Cell Fractionation and Submitochondrial Localization

Cells expressing Tim23-myc and Ylr356w tagged with protein A (PA) were converted to spheroplasts with Zymolyase (Zymo Research, Orange, CA), suspended in homogenization buffer (0.6 M mannitol, 20 mM HEPES, pH 7.4, and proteinase inhibitors) and homogenized in a Potter homogenizer on ice. The cell homogenate was centrifuged at 600 × *g* for 10 min at 4°C to remove the nucleus and unbroken cells. The supernatant fraction was then centrifuged at 6500 × *g* for 10 min at 4°C. The pellet was collected as the mitochondrial fraction. Isolated mitochondria was suspended in ice-cold suspension medium (0.6 M mannitol, 20 mM HEPES, pH 7.4) or hypotonic buffer (10 mM Tris-HCl, pH 7.4, and 1 mM EDTA) and treated with proteinase K (200 μg/ml) for 30 min on ice with or without 0.5% Triton X-100. The proteinase K reaction was stopped by adding 10% trichloroacetic acid (TCA). TCA precipitated proteins were washed with acetone and subjected to immunoblotting.

Fluorescence Microscopy

Yeast cells expressing fluorescent protein–fused chimeras were grown to midlog phase or starved in the indicated media. To label the vacuolar membrane or mitochondria, cells were incubated in medium containing 20 μg/ml *N*-(3-triethylammoniumpropyl)-4-(*p*-diethylaminophenylhexatrienyl) pyridinium dibromide (FM 4-64; Molecular Probes, Eugene, OR) or 1 μM MitoFluor Red 589 (Molecular Probes) at 30°C for 30 min, respectively. After being washed with medium, the cells were incubated in medium at 30°C for 30–60 min. Fluorescence microscopy observation was carried out as described previously [42].

Electron Microscopy

The *pep4*Δ strain (TKY28) was cultured in YPL medium to midlog phase and then shifted to SD-N and cultured for 6 h or was cultured in YPL medium to stationary phase (for 50 h). Cells were frozen in a KF80-freezing device (Reichert-Jung, Vienna, Austria). Transmission electron microscopy was performed according to the procedures described previously [43].

References

[1] Wallace, D.C. (2005) Annu Rev Genet 39, 359-407.

[2] Bogenhagen, D.F. (1999) Am J Hum Genet 64, 1276-81.

[3] Larsson, N.G. and Clayton, D.A. (1995) Annu Rev Genet 29, 151-78.

[4] Rep, M. and Grivell, L.A. (1996) Curr Genet 30, 367-80.

[5] Abeliovich, H. and Klionsky, D.J. (2001) Microbiol Mol Biol Rev 65, 463-79, table of contents.

[6] Mijaljica, D., Prescott, M. and Devenish, R.J. (2007) Autophagy 3, 4-9.

[7] Nowikovsky, K., Reipert, S., Devenish, R.J. and Schweyen, R.J. (2007) Cell Death Differ 14, 1647-56.

[8] Priault, M., Salin, B., Schaeffer, J., Vallette, F.M., di Rago, J.P. and Martinou, J.C. (2005) Cell Death Differ 12, 1613-21.

[9] Twig, G. et al. (2008) EMBO J 27, 433-46.

[10] Zhang, Y., Qi, H., Taylor, R., Xu, W., Liu, L.F. and Jin, S. (2007) Autophagy 3, 337-46.

[11] Klionsky, D.J. (2005) J Cell Sci 118, 7-18.

[12] Yorimitsu, T. and Klionsky, D.J. (2007) Trends Cell Biol 17, 279-85.

[13] Dunn, W.A., Jr. et al. (2005) Autophagy 1, 75-83.

[14] Farre, J.C., Manjithaya, R., Mathewson, R.D. and Subramani, S. (2008) Dev Cell 14, 365-76.

[15] Kanki, T. and Klionsky, D.J. (2008) J Biol Chem 283, 32386-93.

[16] Shintani, T., Huang, W.P., Stromhaug, P.E. and Klionsky, D.J. (2002) Dev Cell 3, 825-37.

[17] Yorimitsu, T. and Klionsky, D.J. (2005) Cell Death Differ 12 Suppl 2, 1542-52.

[18] Kanki, T., Wang, K., Cao, Y., Baba, M. and Klionsky, D.J. (2009) Dev Cell 17, 98-109.

[19] Okamoto, K., Kondo-Okamoto, N. and Ohsumi, Y. (2009) Dev Cell 17, 87-97.

[20] Tal, R., Winter, G., Ecker, N., Klionsky, D.J. and Abeliovich, H. (2007) J Biol Chem 282, 5617-24.

[21] Noda, T., Matsuura, A., Wada, Y. and Ohsumi, Y. (1995) Biochem Biophys Res Commun 210, 126-32.

[22] Klionsky, D.J. and Emr, S.D. (2000) Science 290, 1717-21.

[23] Campbell, C.L. and Thorsness, P.E. (1998) J Cell Sci 111 (Pt 16), 2455-64.

[24] Huh, W.K., Falvo, J.V., Gerke, L.C., Carroll, A.S., Howson, R.W., Weissman, J.S. and O'Shea, E.K. (2003) Nature 425, 686-91.

[25] Reggiori, F., Monastyrska, I., Shintani, T. and Klionsky, D.J. (2005) Mol Biol Cell 16, 5843-56.

[26] Kissova, I., Deffieu, M., Manon, S. and Camougrand, N. (2004) J Biol Chem 279, 39068-74.

[27] Kissova, I., Salin, B., Schaeffer, J., Bhatia, S., Manon, S. and Camougrand, N. (2007) Autophagy 3, 329-36.

[28] Yang, Z., Huang, J., Geng, J., Nair, U. and Klionsky, D.J. (2006) Mol Biol Cell 17, 5094-104.

[29] Cao, Y. and Klionsky, D.J. (2007) Autophagy 3, 17-20.

[30] Meiling-Wesse, K., Barth, H. and Thumm, M. (2002) FEBS Lett 526, 71-6.

[31] Nazarko, T.Y., Huang, J., Nicaud, J.M., Klionsky, D.J. and Sibirny, A.A. (2005) Autophagy 1, 37-45.

[32] Sato, T.K., Darsow, T. and Emr, S.D. (1998) Mol Cell Biol 18, 5308-19.

[33] Wang, C.W., Stromhaug, P.E., Kauffman, E.J., Weisman, L.S. and Klionsky, D.J. (2003) J Cell Biol 163, 973-85.

[34] Wichmann, H., Hengst, L. and Gallwitz, D. (1992) Cell 71, 1131-42.

[35] Wurmser, A.E., Sato, T.K. and Emr, S.D. (2000) J Cell Biol 151, 551-62.

[36] Ishihara, N. et al. (2001) Mol Biol Cell 12, 3690-702.

[37] Reggiori, F., Wang, C.W., Nair, U., Shintani, T., Abeliovich, H. and Klionsky, D.J. (2004) Mol Biol Cell 15, 2189-204.

[38] Narendra, D., Tanaka, A., Suen, D.F. and Youle, R.J. (2008) J Cell Biol 183, 795-803.

[39] Sandoval, H., Thiagarajan, P., Dasgupta, S.K., Schumacher, A., Prchal, J.T., Chen, M. and Wang, J. (2008) Nature 454, 232-5.

[40] Wang, Z., Wilson, W.A., Fujino, M.A. and Roach, P.J. (2001) Mol Cell Biol 21, 5742-52.

[41] Longtine, M.S., McKenzie, A., 3rd, Demarini, D.J., Shah, N.G., Wach, A., Brachat, A., Philippsen, P. and Pringle, J.R. (1998) Yeast 14, 953-61.

[42] Monastyrska, I., He, C., Geng, J., Hoppe, A.D., Li, Z. and Klionsky, D.J. (2008) Mol Biol Cell 19, 1962-75.

[43] Baba, M. (2008) Methods Enzymol 451, 133-49.

APPENDIX C

Ume6 transcription factor is part of a signaling cascade that regulates autophagy

Abstract

Autophagy has been implicated in a number of physiological processes important for human health and disease. Autophagy involves the formation of a double-membrane cytosolic vesicle, an autophagosome. Central to the formation of the autophagosome is the ubiquitin-like protein autophagy-related (Atg)8 (microtubuleassociated protein 1 light chain 3/LC3 inmammalian cells). Following autophagy induction, Atg8 shows the greatest change in expression of any of the proteins required for autophagy. The magnitude of autophagy is, in part, controlled by the amount of Atg8; thus, controlling Atg8 protein levels is one potential mechanism for modulating autophagy activity. We have identified a negative regulator of ATG8 transcription, Ume6, which acts along with a histone deacetylase complex including Sin3 and Rpd3 to regulate Atg8 levels; deletion of any of these components leads to an increase in Atg8 and a concomitant increase in autophagic activity. A similar regulatory mechanism is present in mammalian cells, indicating that this process is highly conserved.

Introduction

Macroautophagy, hereafter referred to as autophagy, is an evolutionarily conserved process used by eukaryotic cells for the bulk degradation of intracellular proteins and organelles [1]. Autophagy is not only vital for cell survival in nutrient-poor conditions [2] but is also linked to various physiological processes, including immune defense, tumor suppression, and prevention of neurodegeneration [3]. Whereas autophagy plays a primarily protective role, it can also contribute to cell death; thus, the magnitude of autophagy must be carefully regulated.

Central to autophagy is the formation of autophagosomes [4], double-membrane–bound structures that engulf and deliver cytoplasmic materials to the vacuole/lysosome for degradation. During autophagosome formation, the autophagy-related ubiquitin-like protein Atg8/microtubule-associated protein 1 light chain 3 (LC3) covalently modifies phosphatidylethanolamine (PE). Almost one-fourth of the characterized autophagy-related (Atg) proteins in yeast are involved in the formation or stability of Atg8–PE, which plays a critical role in controlling expansion of the phagophore (the initial sequestering membrane), and in determining autophagosome size, thereby regulating autophagy activity [5,6]. Upon starvation, the level of ATG8 mRNA sharply increases, leading to a subsequent induction of the Atg8 protein level [7,8]. The increase in the amount of Atg8 during autophagy is critical for supplying a sufficient amount of this protein to maintain normal levels of autophagy; yeast strains deficient inAtg8 induction generate abnormally small autophagosomes [6]. Thus, characterization of how Atg8 protein levels are modulated is of tremendous importance both in understanding the

regulation of autophagy and for the elucidation of potential therapeutic targets. However, little is known about the mechanisms regulating ATG8 transcription.

Results

Ume6-Sin3-Rpd3 Complex Represses Atg8 Expression.

To identify candidate transcriptional regulators of ATG8, we analyzed its promoter region and identified an upstream regulatory sequence, URS1, which is a consensus binding site for the transcription factor Ume6 (Fig. C.1A), which was previously identified during a whole-genome microarray analysis [9-11]. The URS1 consensus site consists of two invariant GGC repeats, which tend to be immediately preceded by a C and several T nucleotides and followed by a T and two A nucleotides, although some variability exists in these positions [11]. We examined the promoter regions of other ATG genes and note that the gene encoding Atg23 also contains a potential URS1 site. Ume6 is a zinc cluster protein that both represses and activates transcription of a diverse set of genes involved in meiosis and metabolism in response to nutritional cues such as glucose, nitrogen, and inositol [11-14]. If Ume6 regulates Atg8, then a *ume6Δ* strain should have altered Atg8 protein levels. We examined the protein level of Atg8 in a *ume6Δ* strain in vegetative (growing) conditions and found that it was substantially induced relative to the wild type (Fig. C.1B). Ume6 exerts control of transcription by forming a complex with the corepressor Sin3 and the histone deacetylase Rpd3 [15]. Accordingly, we extended our analysis by examining the level of Atg8 in *rpd3Δ* and *sin3Δ* strains. Similar to the result with the *ume6Δ* strain, both the *sin3Δ* and *rpd3Δ* strains displayed a substantial induction of Atg8 expression in nutrient-rich conditions (Fig. C.1B). Together, our data suggest that the Ume6-Sin3-Rpd3 complex negatively regulates Atg8 expression and, consequently, the amount of Atg8 available during autophagy.

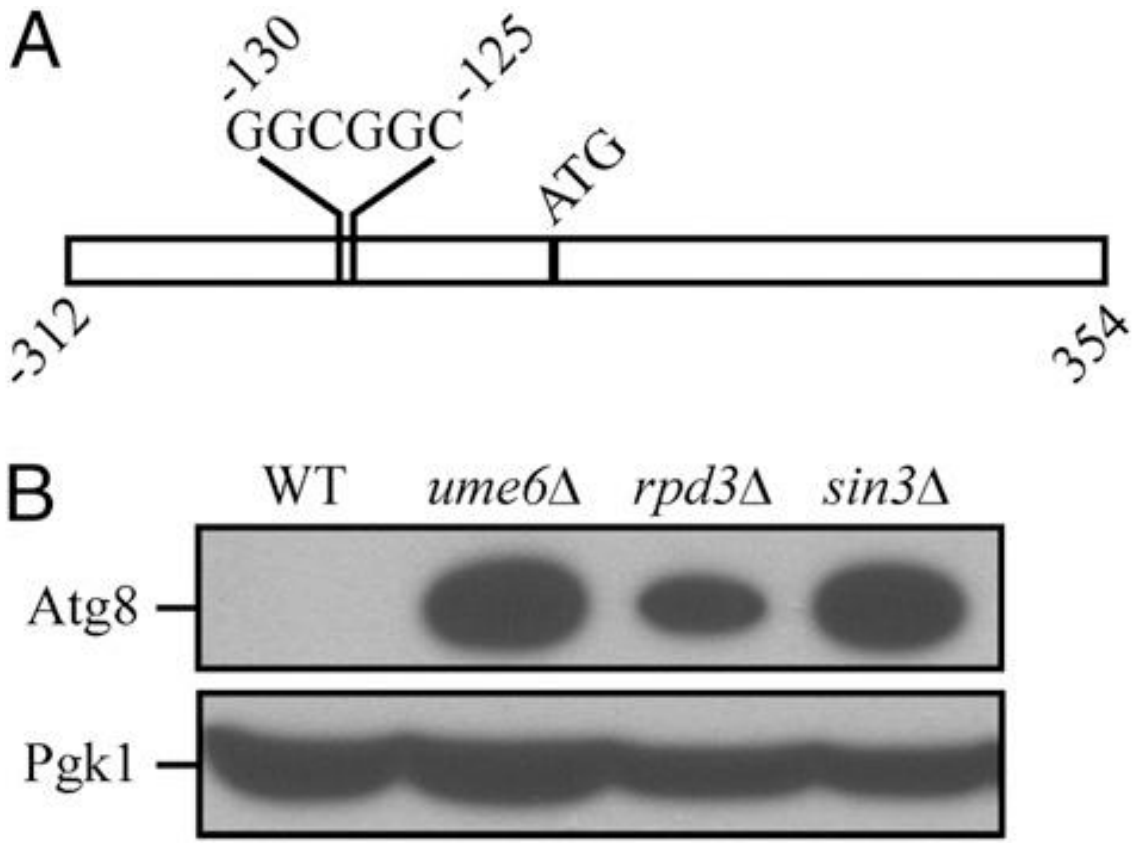

Figure C.1. Ume6-Sin3-Rpd3 Complex Represses Atg8 Expression. (A) Diagram depicting the URS1 site in the ATG8 promoter. (B) The Ume6-Sin3-Rpd3 complex represses Atg8 expression. Wild-type (BY4742), ume6Δ, sin3Δ, and rpd3Δ yeast cells were grown in rich medium to midlog phase. Protein extracts from cells were prepared and subjected to immunoblotting with anti-Atg8 and anti-Pgk1 antiserum(the latter as a loading control).

Ume6 Binds the ATG8 Promoter and Negatively Regulates ATG8 Transcription.

To determine whether Ume6 regulates ATG8 at a transcriptional level, we examined β-galactosidase activity in wild-type and *ume6Δ* strains expressing LacZ under the control of the ATG8 promoter in nutrient-rich and nitrogen starvation conditions. The β-galactosidase activity in the *ume6Δ* strain was substantially higher than that seen in the wild-type strain under growing conditions (Fig. C.2A), suggesting that Ume6 negatively regulates ATG8 transcription, rather than exerting its effect directly on the Atg8 protein. The β-galactosidase activity in the *ume6Δ* strain increased only slightly under starvation conditions, suggesting that the transcription of ATG8 in growing conditions was close to the maximal level seen when fully induced (Fig. C.2A). To further test whether Ume6 binds the ATG8 promoter, we conducted a chromatin immunoprecipitation (ChIP) analysis in a strain expressing Ume6 tagged with protein A (Ume6-PA). We examined the binding of Ume6-PA to the ATG8 URS1 region and a sequence 3 kb upstream of the ATG8 start codon (-3K), which served as a negative control; binding at the promoter of INO1 was examined as a positive control [16]. The quantitative PCR results showed that Ume6-PA binding to the URS1 region was ~19 times higher than that seen in the -3K control and was at a level similar to that detected for the INO1 promoter (Fig. C.2B), suggesting that Ume6 actually bound to the URS1 element of the ATG8 promoter.

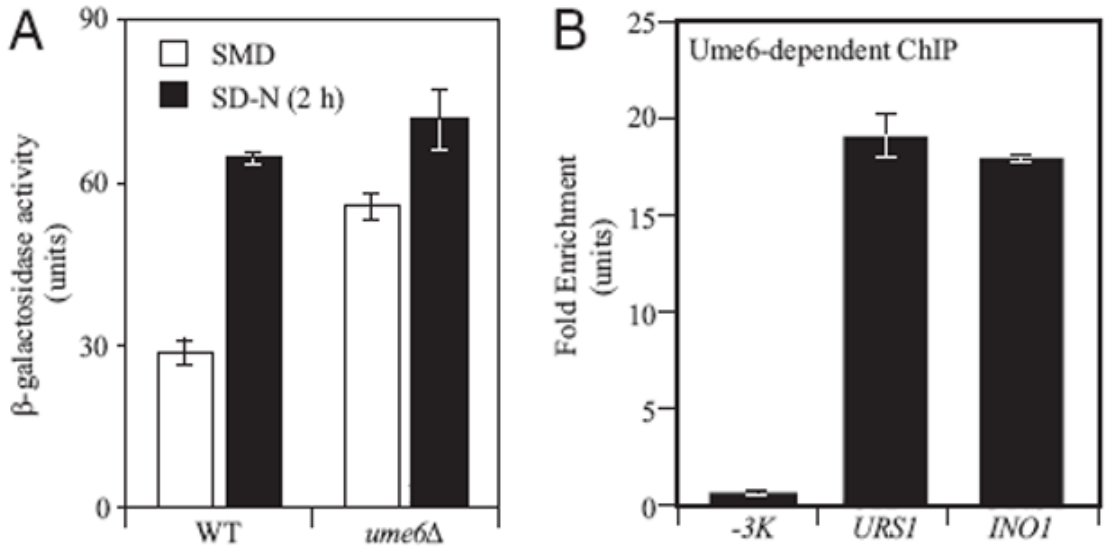

Figure C.2. Ume6 binds the ATG8 promoter and negatively regulates ATG8 transcription. (A) Expression ofATG8p-LacZ in a UME6 deletion strain.Wild-type and *ume6Δ* cells containing LacZ driven by the ATG8 promoter were grown to midlog phase and switched to nitrogen starvation medium (SD-N) for 2 h. β-galactosidase activity was measured from protein extracts. (B) Protein A– tagged Ume6 binds the ATG8 promoter. ChIP analysis was conducted on two regions of the ATG8 promoter: the URS1 region and a region −3 kbupstreamof the ATG8 start codon (-3K), which was used as a negative control. The URS1 region in the INO1 promoter served as a positive control. The ChIP results were normalized to the input DNA and calibrated to the -3K PCR product, which was set to 1.0. Error bars represent the SDof at least three independent experiments.

Rim15 Promotes Ume6 Phosphorylation and Functions As a Positive Regulator of Atg8 Induction.

During meiosis, removal of Sin3 and Rpd3 from the Ume6 complex is regulated by the protein kinase Rim15 in response to nitrogen and glucose limitation. For example, when cells are grown on acetate as the sole carbon source in conditions of nitrogen limitation, Rim15 promotes Ume6 phosphorylation and disrupts the association of Sin3 and Rpd3 with the complex, thus relieving transcriptional repression of the target genes [12]. In addition, we have shown that Rim15 is a positive regulator of autophagy [17,18], although its relevant target(s) had not been identified. Therefore, we decided to investigate a potential role for Rim15 in Ume6-regulated Atg8 induction. Accordingly, we first tested whether Rim15 promotes Ume6 phosphorylation during autophagy. In wild-type cells, upon nitrogen starvation, Ume6 exhibited a slower migration, which is consistent with the previous finding [12] that Ume6 is subject to phosphorylation (Fig. C.3A). However, RIM15 deletion caused a block in Ume6 phosphorylation in starvation conditions, suggesting that Rim15 promotes Ume6 phosphorylation during autophagy (Fig. C.3A).

To further investigate the role of Rim15 in regulating Atg8 induction, we decided to examine Atg8 levels in the presence and absence of this kinase. Accurate measurement of Atg8 levels is complicated by the continuous degradation of Atg8–PE in the vacuole during autophagy. (Atg8 is one of the few Atg proteins that remains associated with the completed autophagosome, and a portion of the protein is delivered into the vacuole lumen where it is degraded.) Thus, we used a *pep4Δ* background strain. The hydrolase

activity of Pep4, a vacuolar aspartyl protease, is required for the breakdown of autophagic bodies (the singlemembrane intralumenal vesicles that result from fusion of autophagosomes with the vacuole) and the subsequent degradation of Atg8–PE. Therefore, we examined Atg8 levels in wildtype, *rim15Δ*, and *rim15Δ ume6Δ* strains in which the PEP4 locus was deleted to prevent the turnover of Atg8–PE. Before nitrogen starvation, wild-type cells displayed a basal level of Atg8, and even after a short 15-min period of nitrogen starvation, an increase in Atg8–PE could be detected (Fig. C.3B). In *rim15Δ* cells, the basal level of Atg8 was clearly lower, and there was a lag in the generation of Atg8–PE, indicating that Rim15 functions as a positive regulator of Atg8 induction. Deletion of UME6 in the *rim15Δ* strain rescued the induction defect in response to nitrogen starvation, suggesting that Rim15 acts upstream of Ume6 to regulate Atg8 synthesis during autophagy.

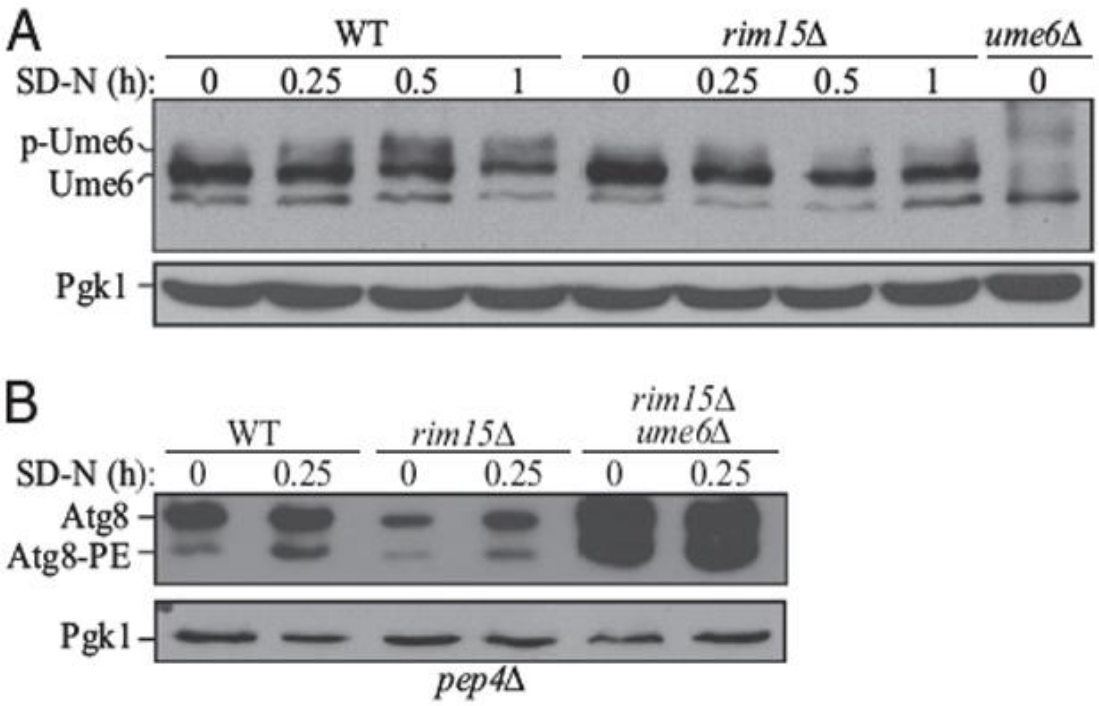

Figure C.3. Rim15 promotes Ume6 phosphorylation and functions as a positive regulator of Atg8 induction. (A) Rim15 is required for Ume6 phosphorylation in starvation conditions. Wild-type (WT, BY4742) and *rim15Δ* cells were grown in rich medium and starved in SD-N for up to 1 h. Cells were collected, and protein extracts were analyzed with anti-Ume6 and anti-Pgk1 (loading control) antisera. (B) Wild-type (WT, YZD005), *rim15Δ* (YZD006), and *rim15Δ ume6Δ* (YZD007) cells in a pep4Δ background were grown in rich medium and shifted to SD-N for starvation. Cells were collected at the indicated time points and subjected to immunoblotting with anti-Atg8 and anti-Pgk1 antisera.

Ume6 Negatively Regulates Autophagy Activity.

To determine whether modulation of Atg8 levels by Ume6 has a physiological effect on autophagy, we measured autophagy activity using the Pho8Δ60 assay [19]. This assay measures the autophagy-dependent alkaline phosphatase activity of Pho8Δ60, a modified vacuolar alkaline phosphatase precursor that remains in the cytosol; Pho8Δ60 can only be delivered to the vacuole via autophagy, in which case, a C-terminal propeptide is subsequently removed, resulting in enzymatic activation. Therefore, the alkaline phosphatase activity of Pho8Δ60 reflects the magnitude of nonselective autophagic cargo delivery.

In growing conditions, the wild-type strain displayed a basal level of Pho8Δ60-dependent alkaline phosphatase activity, whereas the *ume6Δ* strain displayed an increase in the basal level of autophagy consistent with a role for Ume6 in negatively regulating autophagy by limiting the amount of Atg8 [Fig. C.4A; 0 h in nitrogen starvation medium (SD-N)]. Upon nitrogen starvation, Pho8Δ60 activity increased in the wild-type cells but remained at the background level in an *atg1Δ* mutant, which is defective for autophagy. In *ume6Δ* cells, autophagy was induced more rapidly and to a higher level, as indicated by Pho8Δ60 activity compared with that seen in the wild type (Fig. C.4A). Thus, Ume6 acts as a negative regulator of autophagy activity.

We further sought to determine how deletion of UME6 caused an up-regulation of autophagy. An increase in the magnitude of autophagic cargo delivery suggested the possibility that more autophagosomes were being formed and/or the size of the autophagosomes were increased in the *ume6Δ* strain compared with the wild-type cells. After nitrogen starvation for either 1 or 2 h, the number and size of autophagic bodies per

cell was examined by transmission electron microscopy (TEM). The mean number of autophagic bodies per cell section was slightly higher in the *ume6Δ* cells than wild-type at the 1 h (3.1 ± 0.4 and 2.3 ± 0.3, respectively) and 2 h (4.7 ± 0.4 and 4.0 ± 0.4, respectively) time points, but this difference was not statistically significant [P = 0.25 (1 h) and P = 0.19 (2 h)]. A highly significant difference ($P < 5 \times 10^{-8}$), however, was observed in the size of the autophagic bodies. The autophagic bodies of *ume6Δ* cells had an average cross-sectional radius that was 22% and 17% larger than that found in the wild-type cells at the 1 and 2 h time points, respectively (Fig. C.4 B and C and Fig. SC.1). Notably, this translates into a substantial difference in average volume. To estimate the actual volume of the autophagic bodies from the observed crosssectional radii, we used a statistical method previously developed for this purpose [20]. The calculations indicated that the *ume6Δ* cells had autophagosomes that were 68% and 112% larger by volume than wild-type autophagosomes at the 1- and 2-h time points, respectively. This ∼2.1-fold increase in autophagosome volume at the 2-h time point is quite similar to the 1.8-fold increase in Pho8Δ60 activity at the same time point (Fig. C.4 A and B); thus, a small increase in the diameter of autophagosomes has robust effects on the magnitude of bulk autophagy. We also noted that the average cross-sectional area of the wild-type and *ume6Δ* cells was 7.3 and 11.6 μm2, respectively, based on the measurements of over 300 cells each; however, no data suggest that autophagosome or autophagic body size is affected by cell size.

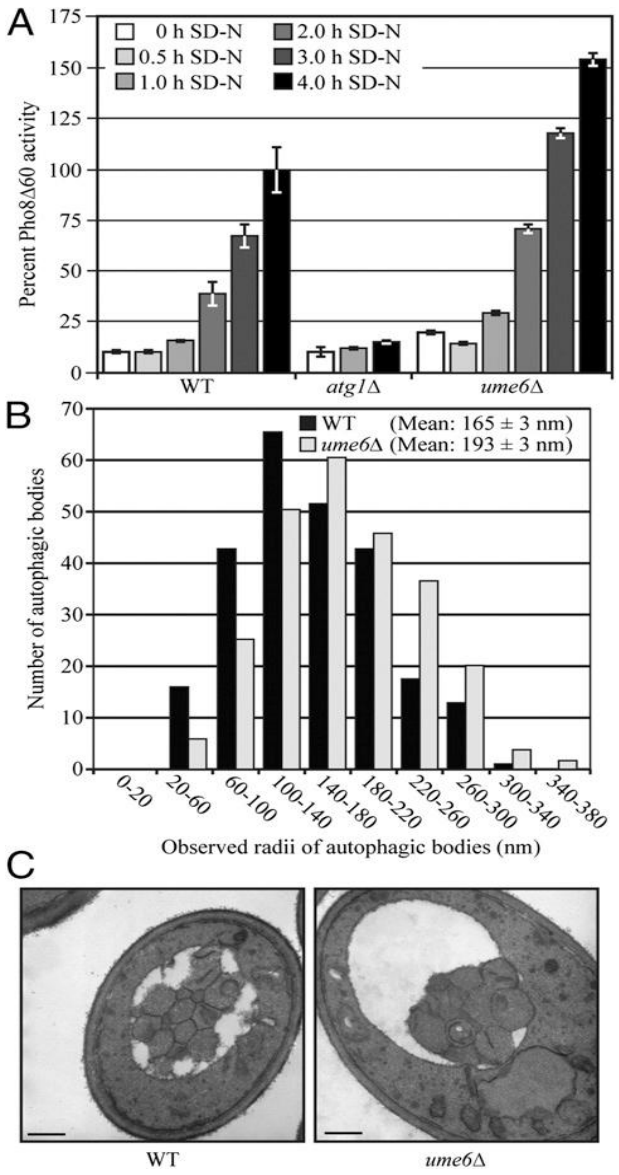

Figure C.4. Ume6 negatively regulates autophagy. (A) Autophagy as measured by the Pho8Δ60 assay is increased in ume6Δ cells. Wild-type (YCB193, SEY6210), atg1Δ (YCB194), and ume6Δ (YCB197) cells were grown in SMD medium and then starved for 0, 0.5, 1, 2, 3, and 4 h. The Pho8Δ60 activity was measured as described in Materials and Methods and normalized to the activity of the wild-type cells, which was set to 100%. Error bars indicate the SEM of three independent experiments. (B) Autophagosome size is increased in ume6Δ cells. Wild-type (FRY143, SEY6210) and ume6Δ (YCB234) strains with deletions of VPS4 and PEP4 to eliminate vesicles generated from the multivesicular body pathway and the breakdown of autophagic bodies, respectively, were grown in rich medium and starved in SD-N for 2 h. Samples were collected, prepared, and examined by TEM as described in Materials and Methods. The radius of each autophagosome was determined as described in Materials and Methods. The error represents the SEM for >400 autophagic bodies. (C) Representative TEM images of the cells in B. (Scale bars: 500 nm.)

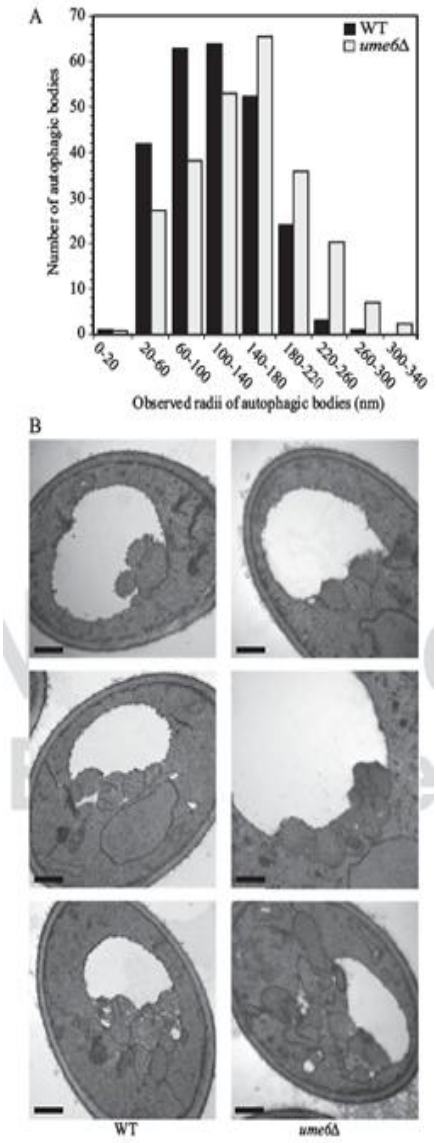

Figure SC.1. Autophagosome volume is increased in *ume6Δ* cells. (A) Wild-type (FRY143, SEY6210) and *ume6Δ* (YCB234) strains with *vps4Δ* and *pep4Δ* deletions to eliminate vesicles generated from the multivesicular body pathway and the breakdown of autophagic bodies, respectively, were grown in rich medium and starved in SD-N for 1 h. Samples were collected, prepared, and examined by TEM as described in Materials and Methods. The radius of each autophagosome was determined as described in Materials and Methods. The error represents the SEM for >225 autophagic bodies. (B) Supplemental images for Fig. 4C. Wildtype (FRY143, SEY6210) and ume6Δ (YCB234) strains were grown as above and starved in SD-N for 2 h. Samples were collected, prepared, and examined by TEM as described in Materials and Methods. (Scale bars: 500 nm.)

SIN3A and SIN3B Play Redundant Roles in Regulating LC3 Expression.

We next explored the possibility that the mechanism of Atg8/LC3 regulation that we discovered here was conserved in higher eukaryotes. The transcription factor Ume6 has no clear homolog in mammalian cells, but 2 homologs of SIN3 (SIN3A and SIN3B) and 11 homologs of RPD3 exist in vertebrates. Accordingly, SIN3 was chosen for further study. SIN3A and SIN3B were knocked down by treating HeLa cells with three individual shRNA targeted to SIN3A and two individual shRNA targeted to SIN3B alone and in combination, with nearly identical results in terms of the degree of knockdown; SIN3A and SIN3B mRNA levels were reduced to ~9–30% and 15–36% of the scrambled control, respectively (Fig. C.5B). Knockdown of SIN3A and SIN3B individually had little or no effect on LC3 levels compared with the scrambled control (Fig. SC.2A). In contrast, when SIN3A and SIN3B were simultaneously knocked down, a robust increase in LC3 levels was readily apparent in various shRNA combinations under nutrient-rich conditions in HeLa cells (Fig. C.5 A and B). The same results were also found for HEK293T and human fibroblast cell lines (Fig. C.5A). The increase in LC3 protein levels was not attributable to indirect effects through protein level or activity of the mechanistic target of rapamycin (MTOR) complex, because the amount of MTOR and its associated protein regulatory associated protein of MTOR, complex 1 (RPTOR) were unchanged (Fig. C.5A), nor was there an effect on the activity of MTORC1 or MTORC2, as determined by the phosphorylation state of their targets ribosomal protein S6 kinase, 70kDa, polypeptide 1 (RPS6KB1/S6K) and eukaryotic translation initiation factor 4E binding protein 1 (EIF4EBP1/4EBP1), or v-akt murine thymoma viral oncogene homolog 1 (AKT1), respectively (Fig. C.5A and Fig. SC.2B). Furthermore, we examined

autophagic flux by exposing the cells to NH4Cl, which raises the lysosomal pH and prevents the turnover of LC3 (similar, in effect, to deleting the PEP4 gene in yeast). The presence of NH4Cl resulted in elevated levels of LC3-II, indicating that the knockdown of SIN3A/B caused an increase in basal autophagy, and not just an increase in the level of LC3. Note that in human fibroblasts, the lack of a clear difference in LC3 levels in the absence, but not the presence, of NH4Cl indicates a rapid rate of lysosomal turnover of this protein [21].

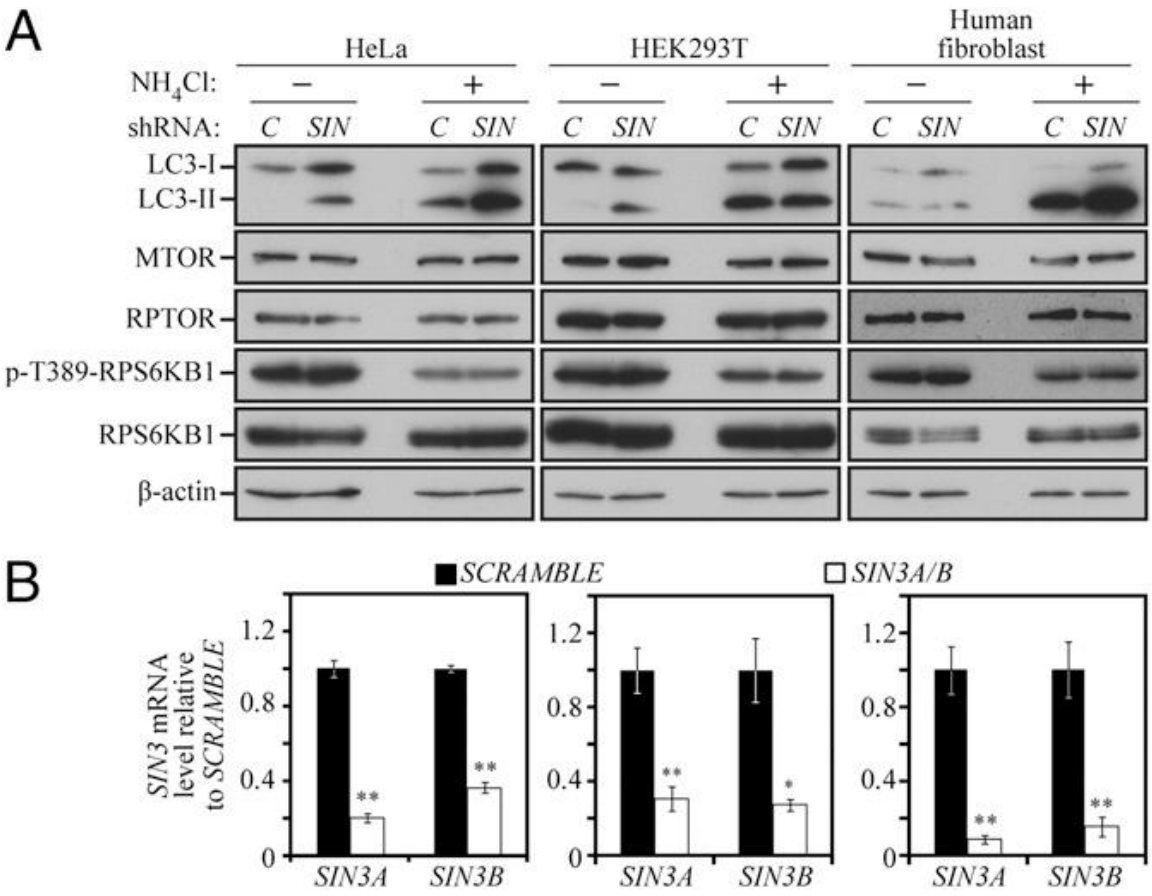

Figure C.5. SIN3A and SIN3B play redundant roles in regulating LC3 expression. (A) SIN3A- and SIN3B-targeted shRNA was prepared and used to generate viruses as described in Materials and Methods. The shRNA-expressing viruses were infected in combination into HeLa, HEK293T, and human fibroblast cells using scrambled DNA as a control (C). Cell lysates were analyzed by immunoblotting with the indicated antibodies. (B) SIN3A and SIN3B mRNA levels were monitored by quantitative PCR in shRNA-treated cells. The values for scrambled DNA were set to 1.0, and the other values were normalized. *P < 0.05; **P < 0.01. Error bars represent the SD.

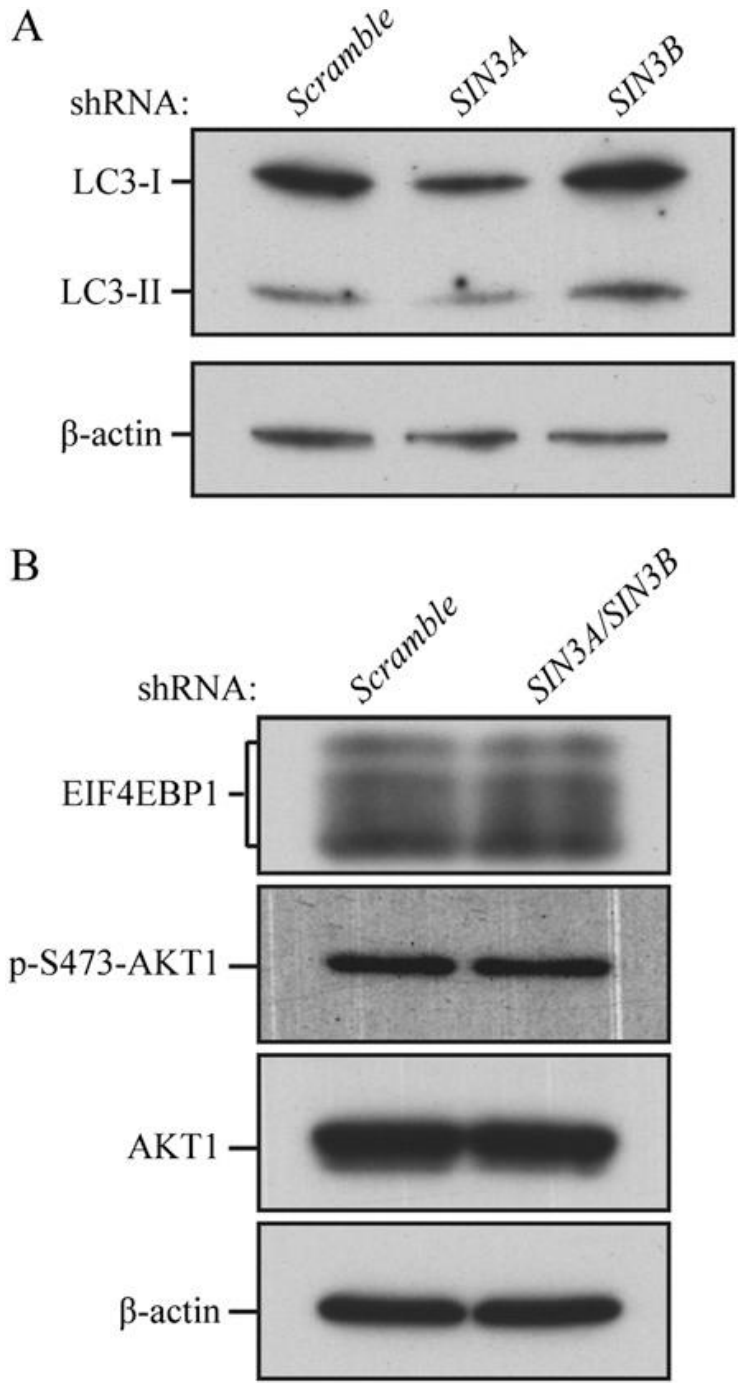

Figure SC.2. SIN3A and SIN3B play redundant roles in regulating LC3 expression. (A) SIN3A- and SIN3B-targeted shRNA was prepared and used to generate viruses as described in Materials and Methods. The shRNA-expressing viruses were singly infected into HeLa cells using scrambled DNA as a control. Cell lysates were analyzed by immunoblotting with anti-LC3 and anti-actin antiserum (the latter as a loading control). (B) SIN3A and SIN3B were knocked down in combination, and cell lysates were analyzed with the indicated antibodies.

Discussion

Our findings suggest that in response to nitrogen starvation, the kinase Rim15 phosphorylates Ume6. During meiosis, this phosphorylation causes the dissociation of Ume6 from Sin3-Rpd3, leading to transcriptional activation [12,14]. Rim15 plays an important role in integrating many nutrient-regulatory signals and, therefore, plays a central role in regulating autophagy [17,22]. Rim15 is negatively regulated through direct phosphorylation by cAMP-dependent protein kinase A (PKA) and Sch9 in the presence of glucose and nitrogen [23,24] and is involved in the autophagy induction that occurs upon PKA-Sch9 inactivation [18]. PKA and Sch9 are upstream sensors that act to negatively regulate autophagy; however, the downstream components in this signaling pathway are unknown, and how PKA and Sch9 signaling affects the autophagy machinery to regulate autophagosome formation has not been elucidated previously. Yeast Sch9 is homologous to mammalian ribosomal protein S6 kinase, 70kDa (RPS6KB/p70S6 kinase) or AKT1 [18]. In mammalian cells, AKT1 phosphorylates and inactivates the forkhead box O (FOXO) family of transcription factors [25]. During muscle atrophy, FOXO3 induces the expression of multiple autophagy genes including Lc3, Gabrapl1 (an Lc3 homolog), unc-51-like kinase 1 (Ulk1), Atg4, Atg12, phosphoinositide-3-kinase, class 3 (Pik3c3/Vps34), and beclin 1, autophagy related (Becn1) [26,27]; and in hepatic tissue, FOXO1 regulates the autophagy genes Gabarapl1, Pik3c2, and Atg12 [28]. Although Ume6 is not conserved in mammalian cells, the regulation of the FOXO family by Sch9 and AKT1 suggests that the pathway regulating Atg8/LC3 may be conserved from yeast to human. Just as the knockdown of SIN3A and

SIN3B promotes an increase in cellular LC3 levels, inhibition of RPD3 promotes a similar increase [29-31], although the detailed mechanism has not been determined.

One frequently overlooked method of regulating the magnitude of autophagy is the regulation of the size of the autophagosome. Research in yeast has shown that the average size of the autophagosome is modulated by the amount of available Atg8 [6]. Our results provide strong evidence that transcriptional repression plays a major role in regulating Atg8/LC3 levels, and this up-regulation results in an increase in the size of the autophagosome. Basal autophagy is especially important in the liver and other cells such as neurons and myocytes, which, after differentiation, cease dividing. Modulation of LC3 levels through inhibition of histone deacetylation at the LC3 locus may be a viable option to increase basal autophagy in nondividing terminally differentiated cells.

Materials and Methods

Yeast.

Gene disruptions and PAtag integrations were performed using a standard method [32]. Yeast cells were grown in rich medium[YPD; 1% yeast extract, 2% peptone, and 2%glucose (allwt/vol)] or syntheticminimalmedium (SMD; 0.67% yeast nitrogen base, 2% glucose, supplemented with the appropriate amino acids and vitamins). Autophagy was induced in starvationmedium(SD-N; 0.17% yeast nitrogen base without amino acids, containing 2% glucose). The yeast strains used in this study are listed in Table SC.1. Protein extraction, immunoblot, GFP-Atg8 processing, and alkaline phosphatase (Pho8Δ60) assays were performed as described previously [18,19,33]. Yeast strains containing the β-galactosidase reporter plasmid ATG8p-LacZ(416) were grown in SMD or shifted to SD-N to induce autophagy and then examined with a β-galactosidase assay as described previously [34]. ChIP was performed as described previously [35]. Samples for TEMwere prepared as described previously [6]. Sections (85 nm) were cut using a Leica Ultracut-E microtome at the University of Michigan Microscopy and Image Analysis Laboratory. Images were acquired on a Philips CM100 BioTwin electron microscope at the University of Michigan Molecular, Cellular and Developmental Biology departmental TEM facility. The observed radii of the autophagic body cross-sections were determined and used to estimate the actual radii as described [20], which were converted to volume. Statistical significance was determined using the Mann–Whitney U test.

Cell Culture.

Knockdown of SIN3 homologs was performed by cloning SIN3A and SIN3B-targeted shRNA into the pLKO1 lentiviral expression vector, and these plasmids were cotransfected together with psPAX2 and pMP2 plasmids into actively growing cells. HeLa, HEK293T, and human fibroblast cells were infected with isolated viruses, selected for puromycin resistance, and analyzed on the seventh day after infection with scrambled DNA as a control. Cell lysates were suspended in Nonidet P-40 buffer and subjected to SDS/PAGE and Western blot analysis.

Table SC.1. Strains used in this study.

Strain	Genotype	Source
BY4742	MAT*α his3Δ1 leu2Δ0 ura3Δ0*	Invitrogen
FRY143	SEY6210 *pep4Δ::LEU2 vps4Δ::TRP1*	1
rim15Δ	BY4742 *rim15Δ::KanMX6*	Invitrogen
rpd3Δ	BY4742 *rpd3Δ::KanMX6*	Invitrogen
SEY6210	MAT*α his3Δ200 leu2-3,112 lys2-801 suc2-Δ9 trp1Δ901 ura3-52*	2
sin3Δ	BY4742 *sin3Δ::KanMX6*	Invitrogen
ume6Δ	BY4742 *ume6Δ::KanMX6*	Invitrogen
W303-1B	MATα *ade2-1 his3-11,15 leu2,3,112 trp1-1 ura3-1 can1-100*	3
YCB193	SEY6210 *pho8::pho8Δ60 pho13Δ*	This Study
YCB194	SEY6210 *atg1Δ::HIS3 pho8::pho8Δ60 pho13Δ*	This Study
YCB197	SEY6210 *ume6Δ::HIS3 pho8::pho8Δ60 pho13Δ*	This Study
YCB234	SEY6210 *pep4Δ::LEU2 vps4Δ::TRP1 ume6Δ::KanMX6*	This Study
YZD005	W303-1B *pep4Δ::URA3 pho13Δ pho8Δ60*	This Study
YZD006	W303-1B *pep4Δ::URA3 pho13Δ pho8Δ60 rim15Δ::BLE*	This Study
YZD007	W303-1B *pep4Δ::URA3 pho13Δ pho8Δ60 rim15Δ::BLE ume6Δ::HIS3*	This Study

1. Cheong H, et al. (2005) Atg17 regulates the magnitude of the autophagic response. Mol Biol Cell 16:3438–3453.
2. Robinson JS, Klionsky DJ, Banta LM, Emr SD (1988) Protein sorting in Saccharomyces cerevisiae: Isolation of mutants defective in the delivery and processing of multiple vacuolar hydrolases. Mol Cell Biol 8:4936–4948.
3. Thomas BJ, Rothstein R (1989) Elevated recombination rates in transcriptionally active DNA. Cell 56:619–630.

References

[1] Xie, Z. and Klionsky, D.J. (2007) Nat Cell Biol 9, 1102-9.

[2] Yorimitsu, T. and Klionsky, D.J. (2005) Cell Death Differ 12 Suppl 2, 1542-52.

[3] Mizushima, N., Levine, B., Cuervo, A.M. and Klionsky, D.J. (2008) Nature 451, 1069-75.

[4] Klionsky, D.J. et al. (2011) Autophagy 7, 1273-94.

[5] Weidberg, H., Shvets, E., Shpilka, T., Shimron, F., Shinder, V. and Elazar, Z. (2010) EMBO J 29, 1792-802.

[6] Xie, Z., Nair, U. and Klionsky, D.J. (2008) Mol Biol Cell 19, 3290-8.

[7] Huang, W.P., Scott, S.V., Kim, J. and Klionsky, D.J. (2000) J Biol Chem 275, 5845-51.

[8] Kirisako, T., Baba, M., Ishihara, N., Miyazawa, K., Ohsumi, M., Yoshimori, T., Noda, T. and Ohsumi, Y. (1999) J Cell Biol 147, 435-46.

[9] Park, H.D., Luche, R.M. and Cooper, T.G. (1992) Nucleic Acids Res 20, 1909-15.

[10] Strich, R., Surosky, R.T., Steber, C., Dubois, E., Messenguy, F. and Esposito, R.E. (1994) Genes Dev 8, 796-810.

[11] Williams, R.M., Primig, M., Washburn, B.K., Winzeler, E.A., Bellis, M., Sarrauste de Menthiere, C., Davis, R.W. and Esposito, R.E. (2002) Proc Natl Acad Sci U S A 99, 13431-6.

[12] Pnueli, L., Edry, I., Cohen, M. and Kassir, Y. (2004) Mol Cell Biol 24, 5197-208.

[13] Washburn, B.K. and Esposito, R.E. (2001) Mol Cell Biol 21, 2057-69.

[14] Xiao, Y. and Mitchell, A.P. (2000) Mol Cell Biol 20, 5447-53.

[15] Kadosh, D. and Struhl, K. (1997) Cell 89, 365-71.

[16] Jackson, J.C. and Lopes, J.M. (1996) Nucleic Acids Res 24, 1322-9.

[17] Yang, Z., Geng, J., Yen, W.L., Wang, K. and Klionsky, D.J. (2010) Mol Cell 38, 250-64.

[18] Yorimitsu, T., Zaman, S., Broach, J.R. and Klionsky, D.J. (2007) Mol Biol Cell 18, 4180-9.

[19] Noda, T., Matsuura, A., Wada, Y. and Ohsumi, Y. (1995) Biochem Biophys Res Commun 210, 126-32.

[20] Xie, Z., Nair, U., Geng, J., Szefler, M.B., Rothman, E.D. and Klionsky, D.J. (2009) Autophagy 5, 217-20.

[21] Klionsky, D.J., Abdalla, Abeliovich, Abraham, Acevedo-Arozena, Adeli, Agholme, Agnello, Agostinis, Aguirre-Ghiso (2012) Autophagy 8, 445-544.

[22] Swinnen, E. et al. (2006) Cell Div 1, 3.

[23] Pedruzzi, I., Dubouloz, F., Cameroni, E., Wanke, V., Roosen, J., Winderickx, J. and De Virgilio, C. (2003) Mol Cell 12, 1607-13.

[24] Reinders, A., Burckert, N., Boller, T., Wiemken, A. and De Virgilio, C. (1998) Genes Dev 12, 2943-55.

[25] Salih, D.A. and Brunet, A. (2008) Curr Opin Cell Biol 20, 126-36.

[26] Mammucari, C. et al. (2007) Cell Metab 6, 458-71.

[27] Zhao, J., Brault, J.J., Schild, A., Cao, P., Sandri, M., Schiaffino, S., Lecker, S.H. and Goldberg, A.L. (2007) Cell Metab 6, 472-83.

[28] Liu, H.Y., Han, J., Cao, S.Y., Hong, T., Zhuo, D., Shi, J., Liu, Z. and Cao, W. (2009) J Biol Chem 284, 31484-92.

[29] Ahn, M.Y., Ahn, S.G. and Yoon, J.H. (2011) Oral Oncol 47, 1032-8.

[30] Chen, M.Y. et al. (2011) Cancer 117, 4424-38.

[31] Park, J.H. et al. (2010) Invest New Drugs.

[32] Longtine, M.S., McKenzie, A., 3rd, Demarini, D.J., Shah, N.G., Wach, A., Brachat, A., Philippsen, P. and Pringle, J.R. (1998) Yeast 14, 953-61.

[33] Shintani, T. and Klionsky, D.J. (2004) J Biol Chem 279, 29889-94.

[34] Rose, M. and Botstein, D. (1983) Methods Enzymol 101, 167-80.

[35] Aparicio, O., Geisberg, J.V., Sekinger, E., Yang, A., Moqtaderi, Z. and Struhl, K. (2005) Curr Protoc Mol Biol Chapter 21, Unit 21 3.